

**Palladium-Catalyzed Ligand-Directed C–H and C=C Bond  
Functionalization**

by

Sharon Rose Neufeldt

A dissertation submitted in partial fulfillment  
of the requirements for the degree of  
Doctor of Philosophy  
(Chemistry)  
in the University of Michigan  
2013

Doctoral Committee:

Professor Melanie S. Sanford, Chair  
Assistant Professor Anne J. McNeil  
Professor John Montgomery  
Professor Phillip E. Savage

© Sharon R. Neufeldt 2013

To my parents

## ACKNOWLEDGMENTS

I am so blessed to have had the opportunities, the mentors, and the friends that have gotten me this far. Melanie, as excited as I am to graduate, I am genuinely sad to be leaving you. When I was applying for grad school, I was completely clueless about the chemistry world, so I didn't really know who you (or anyone) was at the time. But soon after getting my acceptance letter from Michigan, I got a phone call from a woman talking really fast and sounding super excited about something, and I couldn't help but feel excited myself to visit Michigan and meet this Dr. Sanford. And now I still can't believe my good fortune of ending up with you as my advisor. Your excitement and energy are contagious, and the world always seems brighter after talking with you. You have to be one of the smartest people on the planet, and if I can ever be even half as logical, meticulous, creative, and quick-thinking as you I will be content. I have learned so much from your example – about chemistry, writing, and presentation – but also about diplomacy, balancing priorities, and having a positive outlook. I am so grateful for your unwavering support the past 5+ years – I would not have made it without you. You work unbelievably hard for all of us, and I thank you so much for everything.

I want to acknowledge a number of other members of the faculty and staff here at Michigan as well. I am grateful to my committee members for their support and ideas. Dr. Montgomery and Dr. McNeil – I learned a lot from you both in the spectroscopy and physical organic classes you taught. Both of you, as well as Dr. Savage, have asked insightful questions and made useful suggestions over the past few years, which I really appreciate. I also want to thank Dr. Matzger for letting me rotate in his group, for giving me advice about analytical techniques, and for usually having something funny to say. Dr. Vedejs and Dr. Wolfe – I really enjoyed taking mechanisms, synthesis, and organometallics classes from you. I have learned a lot about NMR from Eugenio Alvarado and Chris Kojiro, and I especially want to thank Eugenio for taking so much



time to help me try to analyze my diastereomers with some weird pulse sequences. Jim Windak and Paul Lennon have been extremely fast with getting HRMS results to me, so I thank you both for that. I am grateful to Tracy Stevenson, Rich Giszczak, Laurie MacDonald, and Jon Boyd for their hard work to keep the chemistry building and department running smoothly. I also thank all the administrative staff that have helped me with assorted problems over the years, especially Margarita Bekiaries, Jennifer Rieger, and Beverly Lange. Antek, I'm not sure where to put you under my acknowledgments organizational strategy, but I appreciate your efforts at helping me try to analyze my diastereomers by GC and the funny conversations we've had, and also thanks for the delicious stir fry that has gotten me through finishing my thesis.

The Sanford group, present and past, has truly been my support here in Michigan. Although I can't possibly thank everyone, I do want to acknowledge several members in particular, starting with Chelsea. Chelsea, you have made lab so much fun for me with our frosty and fro-yo runs, squash anthropomorphizing (Patrick and Sinnamon Sally), vandalizing houses with balloons late at night, and baking parties. I've learned a lot from you and with you – mostly made-up words like fig, butternub, chitter, and worb – but also some useful things like how to dry solvents and use glovebox snorkels to make cookies disappear and how to squish freshly baked cake with my bare hands. I will really miss you. (But we can still chitter.) Cydney, I am so happy I got to work with you the past several months! You *are* the Michigan difference, and I've really valued your smart insights, your hard work, and your friendship. Tiffany, it has been so fun getting to know you, and you are a great deskmate. I admire your hard work and positive energy. Kate, I really enjoyed working with you on photocatalysis stuff, and your friendliness makes lab a cheerier place. Yingda, you are a brilliant amazing fantastic scientist and you've also been a good friend, so thank you and keep running even when it snows – how hard could it possibly be? Anna and Amanda, I appreciate your friendliness and hard work, and good luck with the GCs and GCMS. Doug and Laura, thank you both for editing thesis chapters for me along with Chelsea, Kate, and Tiffany. All the other current group members, thank you so much for all your contributions that make the lab the busy, fun, and productive place that it is. Several past group members have also been really meaningful to me, like Dipa. Deeps, you have become one of my dearest friends and I

can't even list all the ways you have been there for me throughout grad school. You are always willing to talk about chemistry or anything, and you have such good ideas and suggestions. But even more, you have such a big heart, and you have been an invaluable emotional support for me. You always make me feel unconditionally accepted, and that has given me so much strength. Andrew, I am completely indebted to you for reaching out to befriend me early on in grad school. I was grateful for your ability to talk when I had nothing to say, and I am grateful now for both the deep and shallow (coughprojectrunwaycough) conversations that we have. Over the years I've watched you transform from a clean-shaven buzzcut chicken-finger-eating foul-mouthed graduate student to a shaggy bearded vegetarian/vegan foul-mouthed professor. I don't know what the next metamorphosis will be, but I'll be there for you no matter what. Tom, you were also a big support to me during a lot of grad school and I am truly grateful for all the fun times we've had. Deprez (desk buddy), Lopa (my mentor :), Kami, and Kara, I thank all of you for welcoming me into the group and for creating such a positive atmosphere.

Prior to coming to Michigan, a number of other mentors have been influential in my life. I am honored to have had the opportunity to be Dr. Clint Lane's first (and only) student. He exemplified a happy scientist – one who was excited to come to lab every day and explore. I learned so much from him about chemistry and lab techniques, and I appreciate his patience and compassion. Dr. Lane, thank you, and you are missed. I was lucky to also work in Dr. Gary Molander's lab for a summer, where I learned how to run columns and what grad school would be like. Dr. Molander, I thank you so much for believing in me. Dr. Marin Robinson, your class was the one that made me realize how awesome organic chemistry is. Thank you for being such a clear, articulate teacher, and for then being my advisor, letting me work with you on Write Like a Chemist, and for supporting me all of this time. Finally, I thank Mr. Woon, my high school AP Chemistry teacher. He intimidated me at first by telling us all to memorize a giant list of polyatomic ions for a quiz the first week, but ultimately Mr. Woon made the class really fun and made me want to be a chemistry major in college.

Last but not most, I thank my family – my genius/creative siblings Dan and Ruth, and especially my parents John and Diane. When I look back on my childhood, I remember it as a time of wonder and exploring and creating. I'm grateful for that experience, because

this perspective has stuck with me. Thank you Mōme for teaching me to create, to obsess (in a hopefully good way), and to not see work as work. Thank you for dedicating so many years to homeschooling me and Dan and Ruth. Your efforts made my childhood such a richer experience than I can imagine otherwise. You are someone that feels deeply, cares completely, and gives selflessly. I thank you for being that person to me. And thank you for teaching me how to write and spell real good to just like you. Dada, thank you for working so hard for all of us all these years – you allowed us to grow up feeling safe and secure. Your approach to solving problems has modeled a rational, scientific way of thinking for me that has probably come in handy a time or two. I'd like to think that playing chess against you has taught me to think logically, but I'm pretty sure I still can't beat you. To both of you, it really does mean so much to me to know you're there, so thank you.

## TABLE OF CONTENTS

DEDICATION . . . . .	ii
ACKNOWLEDGMENTS . . . . .	iii
LIST OF SCHEMES . . . . .	x
LIST OF FIGURES . . . . .	xvii
LIST OF TABLES . . . . .	xix
LIST OF ABBREVIATIONS . . . . .	xxii
ABSTRACT . . . . .	xxiv

### CHAPTER

<b>1. Introduction . . . . .</b>	<b>1</b>
1.1 C–H Functionalization . . . . .	1
1.2 Controlling the Site Selectivity of C–H Functionalization . . . . .	3
1.3 Pd Catalysis for C–H Functionalization . . . . .	4
1.4 Challenges . . . . .	6
1.5 References . . . . .	11
<b>2. Room-Temperature Photoredox Pd/Ir-Catalyzed C–H Arylation with Ph<sub>2</sub>I<sup>+</sup> . . . . .</b>	<b>13</b>
2.1 Background and Significance . . . . .	13
2.2 Reaction Optimization . . . . .	23
2.3 Substrate Scope . . . . .	29
2.4 Scope of Diaryliodonium Oxidants . . . . .	31
2.5 Inhibition by Radical Scavengers and Chemoselectivity Studies . . . . .	32
2.6 Proposed Reaction Mechanism. . . . .	36

2.7	Comparison of Ph <sub>2</sub> I <sup>+</sup> vs PhN <sub>2</sub> <sup>+</sup> Reagents	38
2.8	Conclusions	39
2.9	Experimental Procedures and Characterization Data	40
2.10	References	53
<b>3.</b>	<b>Pd-Catalyzed Radical-Mediated C–H Alkylation Using Potassium Alkyltrifluoroborates</b>	<b>59</b>
3.1	Background and Significance	59
3.2	Reaction Optimization	67
3.3	Methylation Scope	70
3.4	Alkyl Scope	73
3.5	Proposed Radical-Mediated Reaction Mechanism	76
3.6	Evidence for an Alkyl Radical-Mediated Mechanism: Molander-Type Side Products	77
3.7	Evidence for an Alkyl Radical-Mediated Mechanism: Reactivity Trends of Alkyltrifluoroborates	79
3.8	Evidence for an Alkyl Radical-Mediated Mechanism: Results of Screening Alternative Oxidants	82
3.9	Discussion of the Roles of Acetic Acid and Water	83
3.10	C–H Arylation with Potassium Aryltrifluoroborates	86
3.11	Conclusions and Outlook	86
3.12	Experimental Procedures and Characterization Data	87
3.13	References	98
<b>4.</b>	<b>Asymmetric Pd-Catalyzed Chiral Ligand-Directed Alkene Dioxygenation</b>	<b>103</b>
4.1	Background and Significance	103
4.2	Reaction Optimization	109
4.3	Control Reactions	110
4.4	<i>Syn</i> Diastereoselectivity and Reaction Mechanism	112

4.5	Use of Chiral Auxiliaries Derived from Commercial Ketones . . . . .	114
4.6	Use of Auxiliaries Derived from 8-Substituted Menthone. . . . .	116
4.7	<i>E/Z</i> Stereochemical Assignment of Oxime Ether Substrates . . . . .	118
4.8	Quantification of Diastereomeric Ratios . . . . .	119
4.9	Identification of Side Products . . . . .	120
4.10	Preliminary Results with Additional Directing Groups . . . . .	121
4.11	Substituted Alkene Substrates . . . . .	124
4.12	Conclusions and Outlook . . . . .	126
4.13	Experimental Procedures and Characterization Data . . . . .	126
4.14	References . . . . .	153
<b>5.</b>	<b>A Transformable Directing Group for Pd-Catalyzed C–H Oxygenation . . . . .</b>	<b>158</b>
5.1	Background and Significance . . . . .	158
5.2	Directing Group Optimization . . . . .	163
5.3	Scope of <i>O</i> -Acetyl Oxime-Directed Acetoxylation . . . . .	166
5.4	Deprotection to $\beta$ - and <i>ortho</i> -Hydroxyketones . . . . .	171
5.5	Diverse Transformations of the <i>O</i> -Acetyl Oxime Directing Group . . . . .	174
5.6	Other C–H Functionalizations of <i>O</i> -Acetyl Oximes . . . . .	174
5.7	Subsequent Examples of Transformable Directing Groups . . . . .	176
5.8	Conclusions and Outlook . . . . .	178
5.9	Experimental Procedures and Characterization Data . . . . .	181
5.10	References . . . . .	209

## LIST OF SCHEMES

### CHAPTER 1

#### Introduction

<b>Scheme 1.1:</b> Example of a Functional Group Interconversion Strategy. . . . .	1
<b>Scheme 1.2:</b> Transition Metal-Catalyzed C–H Activation/Functionalization. . . . .	3
<b>Scheme 1.3:</b> Intramolecular C–H Functionalization. . . . .	3
<b>Scheme 1.4:</b> Ligand-Directed Transition Metal-Catalyzed C–H Functionalization. . . . .	4
<b>Scheme 1.5:</b> Electrophilic Mechanism for Ligand-Directed C–H Activation at Pd <sup>II</sup> . . . . .	5
<b>Scheme 1.6:</b> Oxidative Addition Mechanism for C–H Activation at Ir <sup>I</sup> . . . . .	5
<b>Scheme 1.7:</b> Ligand-Directed Pd <sup>II</sup> /Pd <sup>IV</sup> -Catalyzed C–H Functionalization . . . . .	6
<b>Scheme 1.8:</b> Rerouting C–H Arylation with Ph <sub>2</sub> I <sup>+</sup> Through a Radical-Mediated Pathway . . . . .	8
<b>Scheme 1.9:</b> Ligand-Directed Pd-Catalyzed C–H Alkylation with Alkyltrifluoroborates and Mn <sup>III</sup> . . . . .	9
<b>Scheme 1.10:</b> Chiral Directing Group Strategy for Pd-Catalyzed Alkene Difunctionalization . . . . .	9
<b>Scheme 1.11:</b> Transformable Directing Group Strategy for C–H Functionalization . . . . .	10

### CHAPTER 2

#### Room-Temperature Photoredox Pd/Ir-Catalyzed C–H Arylation with Ph<sub>2</sub>I<sup>+</sup>

<b>Scheme 2.1:</b> Pd- and Ni-Catalyzed Aryl–Aryl Cross-Coupling Reactions. . . . .	14
<b>Scheme 2.2:</b> Biaryl Formation by C–H Arylation . . . . .	14
<b>Scheme 2.3:</b> Biaryl Formation at an Early Stage in the Synthesis of <b>5</b> . . . . .	15
<b>Scheme 2.4:</b> Biaryl Formation at a Late Stage in the Synthesis of <b>5</b> via C–H	

Arylation .....	15
<b>Scheme 2.5:</b> Common Mechanistic Manifolds for Pd-Catalyzed C–H Arylation Reactions .....	16
<b>Scheme 2.6:</b> Intramolecular C–H Arylation to Form Dibenzofurans .....	16
<b>Scheme 2.7:</b> Directed C–H Arylation of 2-Phenylphenol .....	17
<b>Scheme 2.8:</b> Directed C–H Arylation of 1-Naphthol .....	17
<b>Scheme 2.9:</b> Directed C–H Phenylation of <b>7</b> with Ar <sub>2</sub> I <sup>+</sup> Salts under Thermal/Ionic Conditions .....	17
<b>Scheme 2.10:</b> Directed C–H Arylation with Aryl Iodides .....	18
<b>Scheme 2.11:</b> Directed C–H Arylation with Aryl Chlorides .....	18
<b>Scheme 2.12:</b> Directed C–H Arylation with Arylboronic Acids .....	18
<b>Scheme 2.13:</b> Directed C–H Arylation with Trialkoxysilanes .....	19
<b>Scheme 2.14:</b> Room-Temperature C–H Arylation of Phenol Esters with Diaryliodonium Oxidants .....	19
<b>Scheme 2.15:</b> Thermal C–H Arylation with Ar <sub>2</sub> I <sup>+</sup> is Limited by the Oxidation Step ...	20
<b>Scheme 2.16:</b> Radical-Accelerated Kumada Cross-Coupling .....	21
<b>Scheme 2.17:</b> Generation of Ph• from Ph <sub>2</sub> I <sup>+</sup> by Photoredox Catalysis .....	21
<b>Scheme 2.18:</b> Ar•-Mediated Pd-Catalyzed C–H Arylation using Aryl Acylperoxides .	22
<b>Scheme 2.19:</b> Pd-Catalyzed C–H Arylation with ArN <sub>2</sub> <sup>+</sup> using Visible-Light Photoredox Catalysis .....	22
<b>Scheme 2.20:</b> Two Different Pathways for Pd-Catalyzed C–H Arylation using Ph <sub>2</sub> I <sup>+</sup> ..	23
<b>Scheme 2.21:</b> Unsuccessful C–H Arylation of Oxime Ether <b>27</b> with Ph <sub>2</sub> I <sup>+</sup> Under Thermal Conditions .....	31
<b>Scheme 2.22:</b> Attenuation of Chemoselectivity Differences Between Thermal and Photocatalytic Reaction Conditions for Intermolecular Competition ...	36
<b>Scheme 2.23:</b> Possible Pd <sup>II</sup> /Pd <sup>IV</sup> Mechanism for the Pd/Ir-Catalyzed C–H Arylation with Ar <sub>2</sub> I <sup>+</sup> .....	37
<b>Scheme 2.24:</b> Alternative Pd <sup>I</sup> /Pd <sup>III</sup> Mechanism for the Pd/Ir-Catalyzed C–H Arylation with Ar <sub>2</sub> I <sup>+</sup> .....	37



## CHAPTER 3

### Pd-Catalyzed Radical-Mediated C–H Alkylation Using Potassium Alkyltrifluoroborates

<b>Scheme 3.1:</b> Suzuki-Miyaura Cross-Coupling with Alkylboron Reagents . . . . .	59
<b>Scheme 3.2:</b> Pd <sup>II</sup> /Pd <sup>0</sup> -Catalyzed Ligand-Directed C–H Alkylation with Alkyl–BX <sub>n</sub> Reagents. . . . .	60
<b>Scheme 3.3:</b> Pyridine- and Pyrazole-Directed C–H Methylation with Methylboroxine and Cu(OAc) <sub>2</sub> . . . . .	61
<b>Scheme 3.4:</b> Carboxylic Acid-Directed C–H Methylation with Methylboronic Acid and Ag <sub>2</sub> CO <sub>3</sub> . . . . .	61
<b>Scheme 3.5:</b> 2-Pyridylsulfonyl-Directed C–H Methylation with Methylboronic Acid and AgOAc. . . . .	61
<b>Scheme 3.6:</b> Pyridine-Directed C–H Alkylation with Alkylboronic Acids and Ag <sub>2</sub> O . . . . .	62
<b>Scheme 3.7:</b> Methyl Hydroxamic-Directed sp <sup>3</sup> -C–H Alkylation with Alkylboronic Acids and Ag <sub>2</sub> O . . . . .	62
<b>Scheme 3.8:</b> <i>N</i> -(Perfluoroaryl)benzamide-Directed C–H Alkylation of Cyclopropanes with Alkyltrifluoroborates and Ag <sub>2</sub> CO <sub>3</sub> . . . . .	63
<b>Scheme 3.9:</b> Competing Unproductive Processes in Pd-Catalyzed C–H Alkylation Reactions . . . . .	63
<b>Scheme 3.10:</b> Envisioned Alkyl Radical-Mediated Pd-Catalyzed C–H Alkylation . . . . .	65
<b>Scheme 3.11:</b> Alkylation of Electron-Deficient Heteroarenes with Alkyl Radicals Generated from Alkyltrifluoroborates and Mn(OAc) <sub>3</sub> . . . . .	66
<b>Scheme 3.12:</b> Ligand-Directed Pd-Catalyzed C–H Alkylation with Alkyltrifluoroborates and Mn <sup>III</sup> . . . . .	66
<b>Scheme 3.13:</b> Reaction of Cyclopalladated Complex <b>4</b> With MeBF <sub>3</sub> K and Mn(OAc) <sub>3</sub> . . . . .	67
<b>Scheme 3.14:</b> Reactivity of 3'-Methoxyphenylpyridine <b>25</b> Under the Radical-Mediated Methylation Conditions . . . . .	72
<b>Scheme 3.15:</b> Reaction of BnOCH <sub>2</sub> BF <sub>3</sub> K with <b>6</b> Under the Pd-Catalyzed C–H Alkylation Conditions. . . . .	76
<b>Scheme 3.16:</b> Proposed Pd <sup>II</sup> /Pd <sup>III</sup> /Pd <sup>IV</sup> Mechanism for the Alkylation Reaction. . . . .	77

<b>Scheme 3.17:</b> Control Reactions for Yu's Pd <sup>II</sup> /Pd <sup>0</sup> -Catalyzed C–H Arylation . . . . .	78
<b>Scheme 3.18:</b> Examples of Side Reactions of Alkyl• that Could Compete with Step <i>ii</i> of the Proposed Catalytic Cycle. . . . .	80
<b>Scheme 3.19:</b> Reaction of Cyclopropyl–BF <sub>3</sub> K with <b>6</b> Under the Pd-Catalyzed C–H Alkylation Conditions. . . . .	81
<b>Scheme 3.20:</b> Possible Mechanism for Formation of Acetoxyated Product <b>8</b> . . . . .	81
<b>Scheme 3.21:</b> Pd-Catalyzed C–H Arylation with Aryltrifluoroborates and Mn(OAc). . . . .	86

## CHAPTER 4

### Asymmetric Pd-Catalyzed Ligand-Directed Alkene Dioxygenation

<b>Scheme 4.1:</b> Strategies for Alkene Dioxygenation . . . . .	103
<b>Scheme 4.2:</b> Sharpless Asymmetric Dihydroxylation . . . . .	104
<b>Scheme 4.3:</b> Sharpless Osmium-Catalyzed Aminohydroxylation . . . . .	104
<b>Scheme 4.4:</b> General Mechanism of Pd-Catalyzed Alkene Difunctionalization. . . . .	105
<b>Scheme 4.5:</b> Alkene Difunctionalization by High-Oxidation-State Palladium Catalysis . . . . .	105
<b>Scheme 4.6:</b> Asymmetric Pd <sup>II</sup> /Pd <sup>IV</sup> -Catalyzed Oxidative Cyclization of Enynes . . . . .	106
<b>Scheme 4.7:</b> Pd-Catalyzed Asymmetric C–H Iodination using a Chiral Directing Group Strategy . . . . .	106
<b>Scheme 4.8:</b> Chiral Directing Group Strategy for Pd-Catalyzed Asymmetric Alkene Difunctionalization . . . . .	107
<b>Scheme 4.9:</b> Diacetoxylation of an Undirected Substrate with PhI(OAc) <sub>2</sub> Using a Cationic Pd Triflate Salt vs Pd(OAc) <sub>2</sub> . . . . .	107
<b>Scheme 4.10:</b> Diacetoxylation of an Undirected Substrate with PhI(OAc) <sub>2</sub> Using a Cationic Pd(NHC) Triflate Salt . . . . .	108
<b>Scheme 4.11:</b> Chiral Oxime Ethers as Directing Groups for Asymmetric Alkene Dioxygenation . . . . .	108
<b>Scheme 4.12:</b> Dibenzoylation of <b>16</b> with PhI(OBz) <sub>2</sub> and PdCl <sub>2</sub> (PhCN) <sub>2</sub> . . . . .	110
<b>Scheme 4.13:</b> Metal-Free TfOH-Catalyzed Alkene Diacetoxylation with PhI(OAc) <sub>2</sub> . . . . .	111

<b>Scheme 4.14:</b> No Observed Reactivity in a Substrate Lacking a Directing Group. . . .	112
<b>Scheme 4.15:</b> Possible Mechanistic Pathways for the Oxime-Directed Dibenzoylation . . . . .	112
<b>Scheme 4.16:</b> <i>Syn</i> Selective Dibenzoylation of <i>cis</i> Alkene Substrate <b>19</b> . . . . .	113
<b>Scheme 4.17:</b> <i>Syn</i> Selective Dibenzoylation of <i>trans</i> Alkene Substrate <b>22</b> . . . . .	113
<b>Scheme 4.18:</b> Preparation of <i>Erythro</i> Diol <b>23</b> By Deprotection of <b>21</b> . . . . .	114
<b>Scheme 4.19:</b> Preparation of Authentic <i>Erythro</i> Diol <b>23</b> by Os-Catalyzed <i>Syn</i> Dihydroxylation of <b>19</b> . . . . .	114
<b>Scheme 4.20:</b> Side Products Isolated from the Diacetoxylation Reaction of <b>16</b> . . . . .	121
<b>Scheme 4.21:</b> Diacetoxylation of Aldoxime <b>54</b> to Afford Four Diastereomeric Products . . . . .	122
<b>Scheme 4.22:</b> Diacetoxylation of Aldoxime <b>55</b> to Afford Four Diastereomeric Products . . . . .	122
<b>Scheme 4.23:</b> Diacetoxylation of C2-Symmetric Substrate <b>57</b> . . . . .	124
<b>Scheme 4.24:</b> Resubjection of <b>58</b> to the Dibenzoylation Conditions . . . . .	125
<b>Scheme 4.25:</b> Site Selective Functionalization of Diene <b>60</b> . . . . .	126
<b>Scheme 4.26:</b> Synthesis of <i>cis</i> -Crotyl Oxime Ether <b>21</b> . . . . .	132
<b>Scheme 4.27:</b> Synthesis of <i>trans</i> -Crotyl Oxime Ether <b>22</b> . . . . .	133
<b>Scheme 4.28:</b> Synthesis of 8-Substituted Menthone Derivatives <b>62</b> , <b>63</b> , <b>64</b> , and <b>65</b> . .	134
<b>Scheme 4.29:</b> Synthesis 8-Isopropyl Menthone <b>66</b> . . . . .	134
<b>Scheme 4.30:</b> Synthesis of <i>trans</i> -Crotyl Oxime Ether <b>22</b> . . . . .	133

## CHAPTER 5

### A Transformable Directing Group for Pd-Catalyzed C–H Oxygenation

<b>Scheme 5.1:</b> Indirect <i>ortho</i> -C–H Alkylation of Toluenes via Alkenylation of <i>N,N</i> - Dimethylbenzylamines . . . . .	159
<b>Scheme 5.2:</b> Triflamide-Directed C–H Fluorination Followed by Nucleophilic Displacement of Directing Group . . . . .	159
<b>Scheme 5.3:</b> Oxazoline-Directed C–H Iodination Followed by Directing Group	

Hydrolysis .....	160
<b>Scheme 5.4:</b> Carboxylic Acid-Directed C–H Arylation Followed by Decarboxylation .....	160
<b>Scheme 5.5:</b> Amide-Directed C–H Arylation Followed by Conversion to a Nitrile ...	160
<b>Scheme 5.6:</b> Amide-Directed C–H Arylation Followed by Conversion to a Carboxylic Acid .....	161
<b>Scheme 5.7:</b> Ketone-Directed C–H Amidation .....	161
<b>Scheme 5.8:</b> <i>Ortho</i> -C–H Arylation of Benzaldehydes. ....	162
<b>Scheme 5.9:</b> Ketones as Synthons for Diverse $\beta$ -Oxygenated Motifs. ....	162
<b>Scheme 5.10:</b> Approach to $\beta$ -C–H Functionalization of Ketones .....	163
<b>Scheme 5.11:</b> Methyl Oxime Ether-Directed C–H Acetoxylation .....	164
<b>Scheme 5.12:</b> Elimination During Acid-Catalyzed Hydrolysis of $\beta$ -Acetoxyated Oxime Ethers .....	164
<b>Scheme 5.13:</b> Lability of Alkyl Imines Under C–H Acetoxylation Conditions .....	164
<b>Scheme 5.14:</b> Oxidative Cleavage of Hydroxyl Oximes by $\text{PhI}(\text{OAc})_2$ .....	165
<b>Scheme 5.15:</b> Oxidative Cleavage of Hydroxyl Oxime <b>7</b> Under C–H Acetoxylation Conditions .....	165
<b>Scheme 5.16:</b> Mechanism of Oxidative Cleavage of Hydroxyl Oximes by $\text{PhI}(\text{OAc})_2$ .....	165
<b>Scheme 5.17:</b> <i>O</i> -Acetylation and C–H Acetoxylation of Hydroxyl Oximes in the Presence of $\text{Ac}_2\text{O}$ .....	166
<b>Scheme 5.18:</b> <i>O</i> -Acetyl Oxime-Directed Acetoxylation from Hydroxyl Oxime <b>7</b> ...	166
<b>Scheme 5.19:</b> Nitrile Formation From an <i>O</i> -Acetyl Aldoxime Under C–H Acetoxylation Conditions .....	171
<b>Scheme 5.20:</b> Nitrile Formation via Elimination of AcOH from an <i>O</i> -Acetyl Aldoxime. ....	171
<b>Scheme 5.21:</b> Methanolysis of Acetate Groups in <b>10</b> .....	172
<b>Scheme 5.22:</b> Cleavage of Oxime <b>37</b> by $\text{NaHSO}_3$ to Afford $\beta$ -Hydroxy Ketone <b>38</b> . ...	172
<b>Scheme 5.23:</b> One Pot Deprotection of $\beta$ -Acetoxy Acetyl Oxime <b>10</b> to $\beta$ -Hydroxy Ketone <b>38</b> .....	173
<b>Scheme 5.24:</b> Diverse Transformations of C–H Functionalization Product <b>32</b> .....	174

<b>Scheme 5.25:</b> <i>O</i> -Acetyl Oxime-Directed C–H Iodination . . . . .	175
<b>Scheme 5.26:</b> <i>O</i> -Acetyl Oxime-Directed C–H Chlorination . . . . .	175
<b>Scheme 5.27:</b> Rearrangement of an <i>O</i> -Acetyl Oxime to an Anilide Under C–H Arylation Conditions . . . . .	175
<b>Scheme 5.28:</b> <i>Ortho</i> Bromination and Hydrolysis of Methyl Benzaldoxime Ethers . .	176
<b>Scheme 5.29:</b> <i>Exo</i> -Aldoxime Ether-Directed C–H Acetoxylation Followed by Conversion to a Diol . . . . .	176
<b>Scheme 5.30:</b> Pyridyldiisopropylsilyl as a Traceless Directing Group for C–H Acyloxylation . . . . .	177
<b>Scheme 5.31:</b> Pyrimidinyldiisopropylsilyl as a Traceless Directing Group for Double- Fold C–H Acyloxylation . . . . .	177
<b>Scheme 5.32:</b> Silanol-Directed <i>ortho</i> C–H Olefination of Arenes with Subsequent Deprotection to a Phenol . . . . .	178
<b>Scheme 5.33:</b> Rh-Catalyzed <i>ortho</i> Arylation of Phenols Using a Catalytic Directing Group . . . . .	181
<b>Scheme 5.34:</b> Synthetic Route to Ketone <b>6</b> and Related Ketones. . . . .	182
<b>Scheme 5.35:</b> <i>O</i> -Acetyl Oxime-Directed C–H Iodination . . . . .	175

## LIST OF FIGURES

### CHAPTER 1

#### Introduction

**Figure 1.1:** Homolytic and Heterolytic Bond Strengths of C–H Bonds . . . . . 2

**Figure 1.2:** Examples of Bond Constructions Achieved by Ligand-Directed High-Valent Pd-Catalyzed C–H Functionalization . . . . . 6

### CHAPTER 2

#### Room-Temperature Photoredox Pd/Ir-Catalyzed C–H Arylation with $\text{Ph}_2\text{I}^+$

**Figure 2.1:** Examples of Biphenyl Motifs in Bioactive Molecules . . . . . 13

**Figure 2.2:** Comparison of Dry/Degassed, Wet/Degassed, and Wet/Non-Degassed MeOH for the Pd/Ir-Catalyzed C–H Arylation of **9** . . . . . 26

**Figure 2.3:** Comparison of Dry/Degassed and Wet/Degassed MeOH for the Pd/Ir-Catalyzed C–H Arylation of **7** . . . . . 27

**Figure 2.4:** Typical Gas Chromatogram of the Pd/Ir-Catalyzed Arylation of **7** . . . . . 28

**Figure 2.5:** Oxidant Counterion Screen for the Pd/Ir-Catalyzed C–H Arylation of **7** . . 29

**Figure 2.6:** Structures of Radical Scavengers TEMPO and Galvinoxyl. . . . . 33

**Figure 2.6:** Structures of Radical Scavengers TEMPO and Galvinoxyl. . . . . 33

### CHAPTER 3

#### Pd-Catalyzed Radical-Mediated C–H Alkylation Using Potassium Alkyltrifluoroborates

**Figure 3.1:** Substrates Screened That Provided <10% Yield of Methylated Product by

GC Under the C–H Methylation Conditions . . . . .	72
<b>Figure 3.2</b> Alkyltrifluoroborate Reagents that Afforded no Detectable C–H Alkylation Products. . . . .	76
<b>Figure 3.3:</b> Yield of Methylated Product <b>20</b> in the Presence of Varying Equivalents of Water . . . . .	84
<b>Figure 3.4:</b> Yield of Methylated Product <b>5</b> in the Presence of Varying Equivalents of Acetic Acid . . . . .	85
<b>Figure 3.5:</b> Yield of Methylated Product <b>20</b> in the Presence of Varying Equivalents of Acetic Acid. . . . .	85

## CHAPTER 4

### Asymmetric Pd-Catalyzed Ligand-Directed Alkene Dioxygenation

**Figure 4.1:** Relative Chemical Shifts of  $\alpha$  Protons and Carbons of *E* and *Z* Oximes . . 118

**Figure 4.2:** Chemical Shifts of  $\alpha$  Carbons and Protons of **24**, **25**, **27**, and **28**. . . . . 119

## CHAPTER 5

### A Transformable Directing Group for Pd-Catalyzed C–H Oxygenation

**Figure 5.1:** Examples of Substrates With Nitrogen-Containing Directing Groups for Pd- Catalyzed C–H Functionalization. . . . . 158

## LIST OF TABLES

### CHAPTER 2

#### Room-Temperature Photoredox Pd/Ir-Catalyzed C–H Arylation with Ph<sub>2</sub>I<sup>+</sup>

<b>Table 2.1:</b> Optimization of the Room-Temperature C–H Phenylation of <b>9</b> with Ph <sub>2</sub> I <sup>+</sup> . . . . .	24
<b>Table 2.2:</b> Control Reactions for the Pd/Ir-Catalyzed C–H Phenylation of <b>9</b> with Ph <sub>2</sub> I <sup>+</sup> . . . . .	25
<b>Table 2.3:</b> Substrate Scope for the Pd/Ir-Catalyzed C–H Phenylation with Ph <sub>2</sub> I <sup>+</sup> . . . . .	30
<b>Table 2.4:</b> Scope of Ar <sub>2</sub> I <sup>+</sup> Salts for the Pd/Ir-Catalyzed C–H Arylation of <b>9</b> . . . . .	32
<b>Table 2.5:</b> Effect of Radical Scavengers on the Pd/Ir-Catalyzed C–H Arylation of <b>23</b> . . . . .	33
<b>Table 2.6:</b> Comparison of Chemoselectivity for Pd-Catalyzed C–H Arylation with Mixed Diaryliodonium Oxidants for Thermal and Photocatalytic Reaction Conditions . . . . .	35
<b>Table 2.7:</b> Comparison of Pd/Ir-Catalyzed C–H Phenylation with Ph <sub>2</sub> I <sup>+</sup> vs Pd/Ru-Catalyzed C–H Phenylation with PhN <sub>2</sub> <sup>+</sup> . . . . .	39
<b>Table 2.8:</b> Scope of Ar <sub>2</sub> I <sup>+</sup> Salts for the Pd/Ir-Catalyzed C–H Arylation of <b>9</b> . . . . .	32

### CHAPTER 3

#### Pd-Catalyzed Radical-Mediated C–H Alkylation Using Potassium Alkyltrifluoroborates

<b>Table 3.1:</b> Optimization of the Pd-Catalyzed C–H Methylation with MeBF <sub>3</sub> K and Mn <sup>III</sup> . . . . .	68
<b>Table 3.2:</b> Control Reactions for the Pd-Catalyzed Radical-Mediated C–H Methylation of Substrate <b>6</b> . . . . .	69
<b>Table 3.3:</b> Substrate Scope for the Pd-Catalyzed Radical Mediated Methylation . . . . .	70
<b>Table 3.4:</b> Reactivity of Substituted Arylpyridine Substrates Under the Radical-	



Mediated Methylation Conditions . . . . .	71
<b>Table 3.5:</b> Alkyl Scope of the Radical-Mediated Pd-Catalyzed C–H Alkylation . . . . .	74
<b>Table 3.6:</b> Reaction of Cyclohexyltrifluoroborate with <b>6</b> Under the Pd-Catalyzed C–H Alkylation Conditions . . . . .	75
<b>Table 3.7:</b> Observation of Undirected Pyridine-Alkylated Products with Phenethyl–BF <sub>3</sub> K . . . . .	78
<b>Table 3.8:</b> Comparison of Alkylation Yields vs Redox Potentials of Alkyl• . . . . .	79
<b>Table 3.9:</b> Oxidant Screen for the Pd-Catalyzed C–H Alkylation Reaction . . . . .	83

## CHAPTER 4

### Asymmetric Pd-Catalyzed Ligand-Directed Alkene Dioxygenation

<b>Table 4.1:</b> Solvent and Catalyst Optimization for Pd-Catalyzed Ligand Directed Diacetoxylation of <b>14</b> . . . . .	109
<b>Table 4.2:</b> Control Reactions for the Dibenzoylation of <b>16</b> . . . . .	111
<b>Table 4.3:</b> Dibenzoylation with Chiral Auxiliaries Derived from Commercial Ketones . . . . .	114
<b>Table 4.4:</b> Dibenzoylation with Chiral Auxiliaries Derived from 8-Substituted Menthone . . . . .	117
<b>Table 4.5:</b> Diacetoxylation of Derivatives of Oxime Ether <b>56</b> . . . . .	123
<b>Table 4.6:</b> Efforts Toward Dioxygenation of Substituted Alkene Substrates . . . . .	125
<b>Table 4.7:</b> Subjection of <b>16</b> to TfOH or BF <sub>3</sub> •OEt <sub>2</sub> with PhI(OAc) <sub>2</sub> . . . . .	149
<b>Table 4.8:</b> Stereoselectivity of Dioxygenation of <b>30</b> as a Function of Pd Catalyst . . . . .	152

## CHAPTER 5

### A Transformable Directing Group for Pd-Catalyzed C–H Oxygenation

<b>Table 5.1:</b> <i>O</i> -Acetyl Oxime-Directed Acetoxylation of sp <sup>3</sup> C–H Bonds . . . . .	168
<b>Table 5.2:</b> <i>O</i> -Acetyl Oxime-Directed Acetoxylation of sp <sup>2</sup> C–H Bonds . . . . .	170
<b>Table 5.3:</b> Deprotection of β- and <i>ortho</i> -Acetoxy Acetyl Oximes to β- and <i>ortho</i> -	

Hydroxy Ketones .....	173
<b>Table 5.4:</b> Transformable Directing Groups for Pd-Catalyzed C–H	
Functionalization .....	180

## LIST OF ABBREVIATIONS

Ac	acetyl
Ad	adamantyl
Ar	aryl
atm	standard atmosphere
BINAP	2,2'-bis(diphenylphosphino)-1,1'-binaphthyl
Bn	benzyl
bpy	bipyridine
<sup>n</sup> Bu	butyl
<sup>i</sup> Bu	<i>iso</i> -butyl
<sup>s</sup> Bu	<i>sec</i> -butyl
Bz	benzoyl
Cy	cyclohexyl
DCE	1,2-dichloroethane
DG	directing group
DMA	<i>N,N</i> -dimethylacetamide
DMF	<i>N,N</i> -dimethylformamide
dppp	1,3-bis(diphenylphosphino)propane
dtbbpy	4,4'-di- <i>tert</i> -butyl-2,2'-bipyridine
Et	ethyl
FG	functional group
GC	gas chromatography
GCMS	gas chromatography–mass spectrometry
<sup>n</sup> Hex	hexyl
L	ligand
Me	methyl

Mes	mesityl (2,4,6-trimethylphenyl)
NBS	<i>N</i> -bromosuccinimide
NCS	<i>N</i> -chlorosuccinimide
NHC	<i>N</i> -heterocyclic carbene
NHE	normal hydrogen electrode
NIS	<i>N</i> -iodosuccinimide
NMP	<i>N</i> -methylpyrrolidone
NMR	nuclear magnetic resonance
Nu	nucleophile
[ <i>O</i> ]	oxidant
PCC	pyridinium chlorochromate
Ph	phenyl
Phth–OH	<i>N</i> -hydroxyphthalimide
Piv	pivaloyl
ppy	phenylpyridine
Pr	propyl
rt	room temperature (~25 °C)
SCE	saturated calomel electrode
SPRIX	spiro bis(isoxazoline)
TBDPS	<i>tert</i> -butyldiphenylsilyl
TEMPO	(2,2,6,6-tetramethylpiperidin-1-yl)oxyl
Tf	trifluoromethanesulfonyl
TFA	trifluoroacetic acid
TFE	2,2,2-trifluoroethanol
THF	tetrahydrofuran
TMS	tetramethylsilane
Ts	<i>p</i> -toluenesulfonyl

## Abstract

Because of their abundance, C–H bonds are highly attractive starting materials for the elaboration of complex molecules. Transition metal catalysis can enable these typically inert bonds to undergo functionalization via a metal-catalyzed C–H activation step. In particular, ligand-directed Pd<sup>II</sup>/Pd<sup>IV</sup>-catalyzed C–H functionalization reactions have emerged as powerful techniques for diverse bond constructions. Nevertheless, these methodologies face a number of challenges that limit their applicability. These challenges include the common requirement for harsh reaction conditions, the shortage of examples of asymmetric functionalization reactions, and the poor transformability of most directing groups. This thesis describes the development of new methodologies that aim to address these challenges.

Chapter 2 describes a new photoredox Pd/Ir-catalyzed C–H arylation reaction that reroutes the mechanism of Pd-catalyzed C–H arylation with diaryliodonium salts from an ionic pathway through a radical-mediated pathway. This radical-mediated transformation proceeds at room temperature in a non-acidic solvent, conditions that are considerably milder than those required for C–H arylation with diaryliodonium salts via a traditional Pd<sup>II</sup>/Pd<sup>IV</sup> mechanism (100 °C in acetic acid).

Chapter 3 details the development of a Pd-catalyzed C–H alkylation reaction that utilizes convenient potassium alkyltrifluoroborate salts in combination with a 1 e<sup>-</sup> oxidant (Mn<sup>III</sup>). Several pieces of evidence support an alkyl radical-mediated mechanism for this transformation. The alkylation reaction requires only mild temperatures (25–40 °C), in contrast to the significantly higher temperatures (70–110 °C) needed for previous examples of analogous transformations.

Chapter 4 describes efforts toward understanding the interplay of chiral directing groups with Pd in the context of high oxidation state Pd catalysis. In this work, we

developed a chiral ligand-directed Pd-catalyzed asymmetric alkene dioxygenation reaction.

Chapter 5 describes the identification of a transformable directing ligand for Pd-catalyzed C–H functionalization reactions. *In situ* generated *O*-acetyl oxime ethers were shown to be effective directing groups that are stable under the reaction conditions required for Pd-catalyzed C–H oxygenation, but can then be readily manipulated to afford ketones, alcohols, amines, and heterocycles.

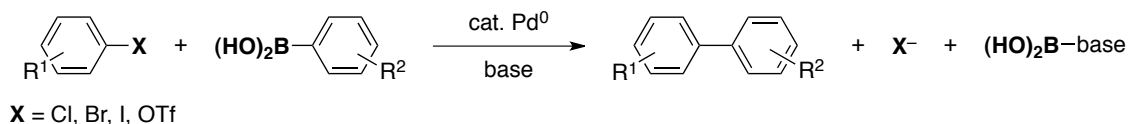
# CHAPTER 1

## Introduction

### 1.1 C–H Functionalization

Most synthetic organic transformations involve conversion of one preexisting functional group into another. This functional group interconversion strategy is well illustrated by transition metal-catalyzed cross-coupling reactions that join two prefunctionalized hydrocarbon fragments. For instance, biaryls can be synthesized by a palladium-catalyzed Suzuki-Miyaura coupling of an aryl halide and an aryl boronic acid (Scheme 1.1).

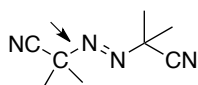
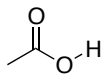
**Scheme 1.1.** Example of a Functional Group Interconversion Strategy



Although transformations like these are extremely powerful, they have a number of drawbacks. First, as illustrated in Scheme 1.1, functional group interconversion reactions necessarily generate stoichiometric waste – the unwanted byproducts of preexisting functional groups. Second, it is not always feasible (or desirable) to carry the necessary functional groups through several steps of a synthesis, or to regioselectively install the ‘prefunctionalization’ into an advanced intermediate. As such, functional group interconversion strategies are often non-ideal for the derivatization of complex molecules at a late stage.

An efficient strategy that avoids the requirement for at least one prefunctionalized starting material is the direct conversion of C–H bonds into the target C–X bonds. This

strategy is not usually feasible using traditional organic reaction methodology because unactivated C–H bonds are inert to both homolytic and heterolytic cleavage under most conditions. As illustrated by Figure 1.1A, typical C–H bonds have large bond dissociation energies (BDE) that range from ~90–115 kcal mol<sup>-1</sup>. Similarly, unactivated C–H bonds have very high pK<sub>a</sub> values relative to bonds that can be deprotonated by moderate bases (Figure 1.1B).

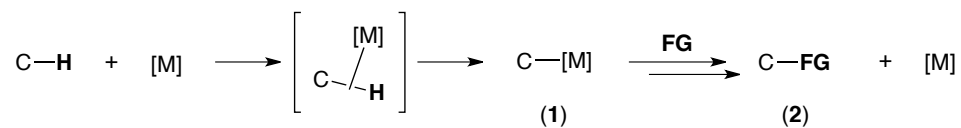
<b>A Homolytic Bond Strength (BDE, kcal/mol):</b>			
<chem>H3C-H</chem>	105		72
<chem>CC(C)C-H</chem>	97	<chem>HO-OH</chem>	50
<chem>c1ccccc1-H</chem>	113	<chem>I-I</chem>	36
<i>no homolysis under normal conditions</i>		<i>homolysis is common</i>	
-----			
<b>B Heterolytic Bond Strength (pK<sub>a</sub>):</b>			
<chem>H3C-H</chem>	48	<chem>HO-H</chem>	15.7
<chem>CC(C)C-H</chem>	51		4.8
<chem>c1ccccc1-H</chem>	43	<chem>Cl-H</chem>	-8.0
<i>not acidic</i>		<i>weakly to strongly acidic</i>	

**Figure 1.1.** Homolytic and Heterolytic Bond Strengths of C–H Bonds<sup>1</sup>

However, a number of transition metals (*e.g.*, Pt, Pd, Ni, Ir, Rh, Ru) have been demonstrated to ‘activate’ C–H bonds by converting them into reactive carbon–metal species **1** (Scheme 1.2).<sup>2</sup> These intermediate organometallic complexes are typically unstable and readily participate in subsequent steps to afford products in which a C–H bond has been replaced by a new functional group (**2**). This unique reactivity of transition metals, in combination with the ubiquity of C–H bonds in organic molecules, makes transition-metal catalyzed C–H functionalization a powerful alternative to traditional functional group interconversion strategies.



**Scheme 1.2.** Transition Metal-Catalyzed C–H Activation/Functionalization

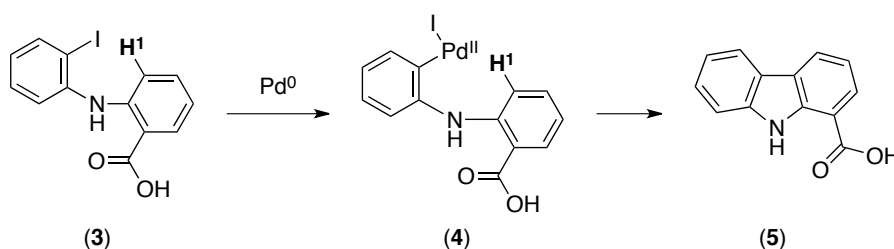


### 1.2 Controlling the Site Selectivity of C–H Functionalization

The great abundance of C–H bonds relative to any other functional group makes them attractive starting materials for the elaboration of complex molecules. However, this same characteristic also presents a major challenge to developing practical methods for C–H bond functionalization. To achieve useful yields of a single product, functionalization must occur with high site selectivity for one C–H bond over all the others within a substrate.

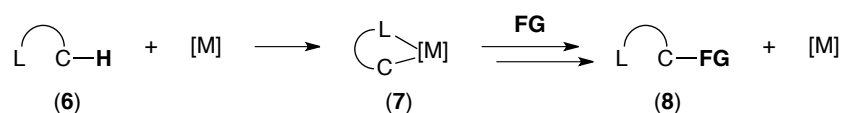
One approach to targeting just a single C–H bond is to engineer an intramolecular C–H functionalization reaction. For instance, molecule **3** in Scheme 1.3 contains 8 different C–H bonds, but complete selectivity was observed for activation of **H<sup>1</sup>** in the presence of a palladium catalyst, affording carbazole product **5**.<sup>3</sup> This exquisite selectivity can be explained by the structure of Pd<sup>II</sup> intermediate **4**, formed by oxidative addition of Pd<sup>0</sup> into the carbon–iodine bond of **3**. In intermediate **4**, a single C–H bond (**H<sup>1</sup>**) is geometrically accessible to the Pd center, thereby facilitating selective activation of C–**H<sup>1</sup>** over all of the other C–H bonds. While effective, this intramolecular approach to controlling site selectivity is inherently limited to a small subset of target molecules and is only useful for forming cyclic products.

**Scheme 1.3.** Intramolecular C–H Functionalization<sup>3</sup>



An alternative approach for controlling site selectivity is to employ substrates **(6)** containing coordinating ligands (L) that can reversibly bind to a metal center and direct C–H activation at a proximal site (Scheme 1.4). Directed C–H activation results in a metallacycle intermediate **7** that undergoes further functionalization with external nucleophiles or oxidants. The overall transformation affords products of a net intermolecular C–H functionalization **(8)**, and both the metal and the directing ligand undergo no net change. As such, this ligand-directed strategy for C–H functionalization exploits the kinetic advantages of intramolecular transformations without being limited to the formation of cyclic products. This strategy has proven particularly powerful for C–H functionalization reactions catalyzed by palladium.

**Scheme 1.4.** Ligand-Directed Transition Metal-Catalyzed C–H Functionalization



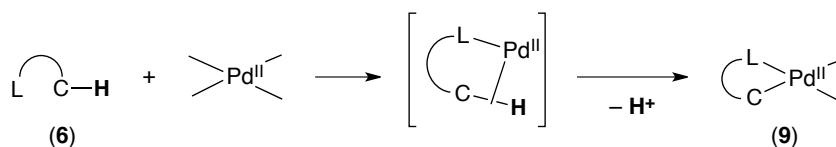
### 1.3 Pd Catalysis for C–H Functionalization

Palladium provides several advantages over other transition metals for C–H functionalization.<sup>4</sup> Many of these advantages relate to (1) the +2 oxidation state of the metal species that undergoes C–H activation, (2) the square planar geometry of the Pd<sup>II</sup> intermediate that is produced upon C–H activation, and (3) the accessibility of a +4 oxidation state under oxidizing conditions.

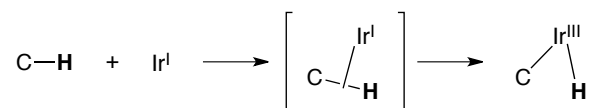
Palladium activates C–H bonds from its +2 oxidation state by an ‘electrophilic’ mechanism that results in no net change in oxidation state (Scheme 1.5). In contrast, several other metals activate C–H bonds by an oxidative addition pathway (Scheme 1.6), requiring that catalysis is initiated by a low-valent metal species (Ir<sup>I</sup>, Rh<sup>I</sup>, and Ru<sup>0</sup>).<sup>2</sup> Metals in low oxidation states such as these tend to be unstable to oxygen; therefore, care must be taken to exclude ambient air from reactions involving these metal species (*i.e.*, glovebox or Schlenk techniques are required). However, Pd<sup>II</sup> species are stable to air under most conditions, and most Pd-catalyzed C–H functionalization reactions are conveniently run on the benchtop. Additionally, Pd<sup>II</sup> is compatible with oxidants that are

needed to effect functionalization, unlike most low valent metal species. Finally, although low valent metal species – including Pd<sup>0</sup> – often undergo facile oxidative addition into bonds such as C–halogen, Pd<sup>II</sup> does not usually react with these types of functional groups. As such, Pd<sup>II</sup>-catalyzed reactions are often characterized by a broader functional group tolerance than transformations catalyzed by other metals.

**Scheme 1.5.** Electrophilic Mechanism for Ligand-Directed C–H Activation at Pd<sup>II</sup>



**Scheme 1.6.** Oxidative Addition Mechanism for C–H Activation at Ir<sup>I</sup>

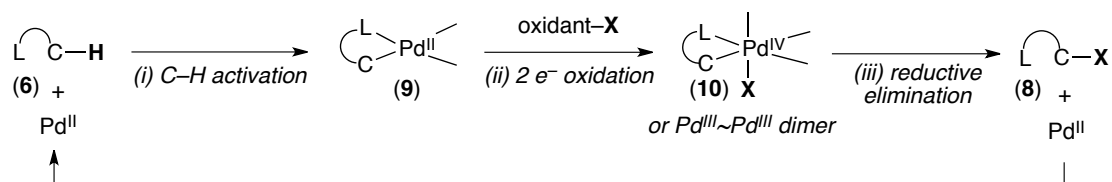


The product of electrophilic C–H activation at Pd<sup>II</sup> is a square planar Pd<sup>II</sup> species (**9**, Scheme 1.5) that is coordinatively unsaturated, allowing for relatively facile further functionalization to occur. Other metal species that also undergo C–H activation through an electrophilic mechanism (Rh<sup>III</sup>, Ir<sup>III</sup>) often result in coordinatively saturated octahedral complexes that do not easily participate in subsequent reactions. Thus, the square planar geometry of Pd<sup>II</sup> contributes to its relative versatility compared to other metals for the construction of diverse C–X bonds.

In addition to Pd<sup>0</sup> and Pd<sup>II</sup>, higher oxidation states of Pd (+3 and +4) can be accessed under oxidizing conditions. Because carbon ligands (especially alkyl and aryl) are electron-donating toward metal centers, the Pd<sup>II</sup>–carbon species generated upon C–H activation is more susceptible to oxidation than simple Pd<sup>II</sup> salt precursors. As such, C–H activation can be followed by oxidative interception of the resultant Pd<sup>II</sup> complex to afford a high valent Pd<sup>IV</sup>–carbon intermediate **10** (Scheme 1.7). Such species are typically unstable, and reductive elimination from high valent Pd is relatively facile and can provide for diverse bond constructions that are often not accessible by reductive

elimination at Pd<sup>II</sup> (e.g., C–O, C–N, C–Cl). Furthermore, high valent Pd catalysis can be used to install C–Br and C–I bonds that are typically unfeasible by reductive elimination at Pd<sup>II</sup> because the resultant Pd<sup>0</sup> species readily reinserts into C–X. Together, all of these attributes make high valent Pd catalysis particularly appealing for C–H functionalization reactions.

**Scheme 1.7.** Ligand-Directed Pd<sup>II</sup>/Pd<sup>IV</sup>-Catalyzed C–H Functionalization



## 1.4 Challenges

Over the past decade, an enormous number of transformations have been reported that combine the advantages of a ligand-directed approach (site selectivity) with those of high valent Pd catalysis (convenient reaction protocols, access to diverse bond constructions). Figure 1.2 presents a sampling of the types of products that can be formed by ligand-directed Pd-catalyzed oxidative C–H functionalization, demonstrated by our group<sup>5</sup> and others.<sup>4f</sup>

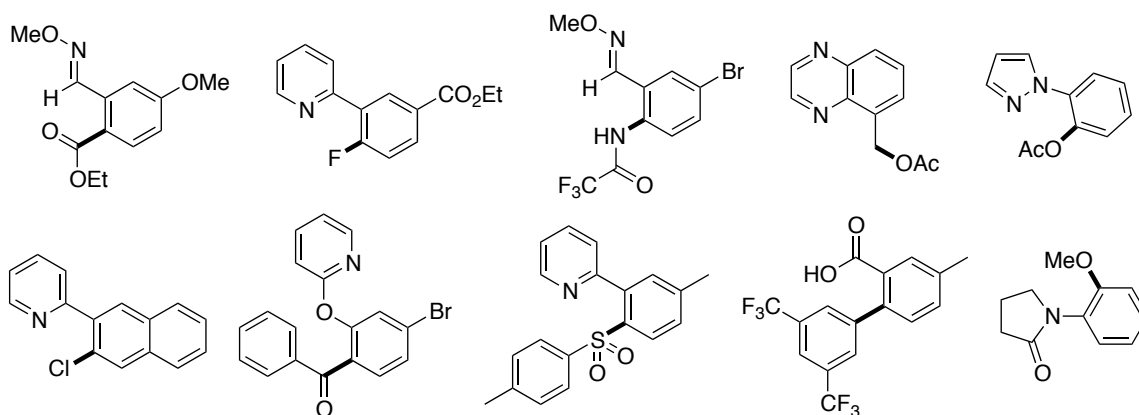


**Figure 1.2.** Examples of Bond Constructions Achieved by Ligand-Directed High-Valent Pd-Catalyzed C–H Functionalization

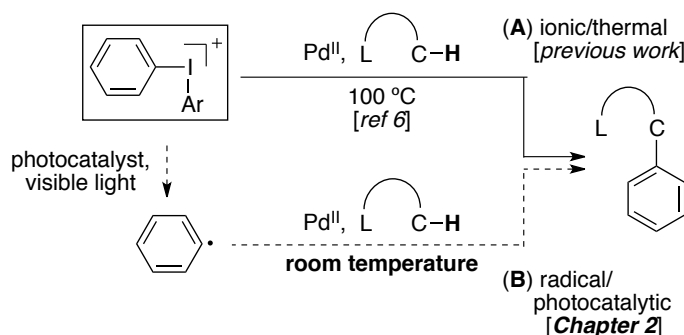
While great strides have been made over the past decade, these transformations still face a number of key challenges including the following: First, they are frequently sluggish and require relatively high temperatures, often in conjunction with strong acids or bases, to proceed efficiently (*Challenge 1*). Second, *asymmetric* examples of Pd-catalyzed oxidative C–H functionalization reactions remain relatively rare (*Challenge 2*). Third, removal or transformation of the directing ligand is often desirable to access a final target molecule; however, most directing groups commonly used for C–H functionalizations are difficult to transform (*Challenge 3*). The work described in this thesis aims to address each of these three challenges.

*Challenge 1.* The majority of examples of Pd-catalyzed C–H activation/C–C bond forming reactions proceed through either a Pd<sup>II</sup>/Pd<sup>IV</sup> or a Pd<sup>II</sup>/Pd<sup>0</sup> mechanistic pathway. C–H arylation has been demonstrated using Pd<sup>II</sup>/Pd<sup>IV</sup> catalysis in conjunction with 2 e<sup>-</sup> oxidants such as diaryliodonium salts (Scheme 1.8A).<sup>6</sup> Alternatively, several examples of C–H arylation and C–H alkylation utilize carbon–[M] reagents (*e.g.*, alkyl–B(OH)<sub>2</sub>) and proceed through a Pd<sup>II</sup>/Pd<sup>0</sup> catalytic cycle involving transmetalation. These transformations usually require high reaction temperatures (~100 °C) and/or strongly acidic or basic conditions to proceed efficiently. Consequently, these methodologies have limited applicability for the derivatization of complex molecules containing sensitive functional groups. Mechanistic studies on Pd-catalyzed C–H arylation with diaryliodonium oxidants have shown that the rate-limiting step of this transformation is oxidation of Pd<sup>II</sup> to Pd<sup>IV</sup>.<sup>6b</sup> As such, it is likely that a more facile oxidation step would enable C–H arylation and alkylation reactions to take place under milder conditions. Our group has been interested in developing strategies to accelerate the rate of oxidation, with the goal of developing novel transformations that can proceed under less forcing reaction conditions. Recently, we initiated investigations into the use of carbon-centered radicals as 1 e<sup>-</sup> oxidants for Pd.<sup>7a</sup> The high kinetic reactivity of radicals makes this oxidation step fast relative to a 2 e<sup>-</sup> oxidation step using traditional reagents.

To this end, **Chapter 2** describes a new photoredox Pd/Ir-catalyzed C–H arylation reaction that reroutes the mechanism of Pd-catalyzed C–H arylation with diaryliodonium salts from an ionic pathway through a radical-mediated pathway (Scheme 1.8B).<sup>8</sup> Importantly, this transformation uses reagents that are identical to those used in

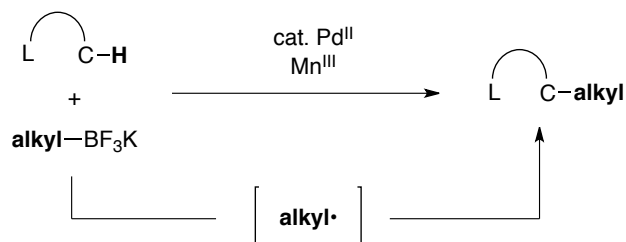
previously reported thermal C–H arylation reactions – namely, diaryliodonium salts. Unlike previous examples, however, this transformation proceeds efficiently at room temperature.

**Scheme 1.8.** Rerouting C–H Arylation with  $\text{Ph}_2\text{I}^+$  Through a Radical-Mediated Pathway



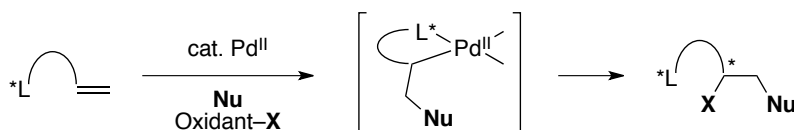
**Chapter 3** describes the development of a Pd-catalyzed C–H alkylation reaction that utilizes convenient potassium alkyltrifluoroborate salts in combination with a  $1\text{ }e^-$  oxidant (Scheme 1.9). This transformation is effective for the installation of methyl and  $1^\circ$  alkyl groups into aryl substrates containing pyridine and amide directing ligands. Though relatively rare, previous examples of Pd-catalyzed C–H alkylation with boronic acid derivatives proceed through a  $\text{Pd}^{\text{II}}/\text{Pd}^0$  catalytic cycle involving transmetalation from boron to palladium. In contrast, several pieces of evidence support an alkyl radical-mediated reaction mechanism for the alkylation reaction described in Chapter 3. Notably, this transformation proceeds at mild temperatures ( $25\text{--}40\text{ }^\circ\text{C}$ ), unlike the significantly higher temperatures ( $70\text{--}110\text{ }^\circ\text{C}$ ) required for all previous examples of analogous transformations in the literature.

**Scheme 1.9.** Ligand-Directed Pd-Catalyzed C–H Alkylation with Alkyltrifluoroborates and Mn<sup>III</sup>



*Challenge 2.* A large number of examples of Pd-catalyzed transformations exist that employ chiral ancillary ligands to construct bonds asymmetrically using Pd<sup>0</sup>/Pd<sup>II</sup> catalysis. However, examples of asymmetric transformations that proceed through high valent Pd are extremely rare. Most of the ancillary ligands that are well-studied for Pd<sup>0</sup>/Pd<sup>II</sup> catalysis are not stable to oxidative conditions (*e.g.*, phosphines), an attribute that may contribute to the dearth of examples of asymmetric transformations at high oxidation-state Pd. One promising approach to asymmetric oxidative C–H functionalization reactions is to use substrates containing chiral directing ligands. **Chapter 4** describes efforts toward understanding the interplay of chiral directing groups with Pd in the context of high oxidation state Pd catalysis. For this work, we focused on a different type of oxidative transformation – a Pd-catalyzed alkene difunctionalization (Scheme 1.10). This asymmetric reaction is directed by a chiral oxime ether auxiliary, and the best auxiliary identified provides dioxygenated products with diastereomeric ratios up to 90:10.<sup>9</sup>

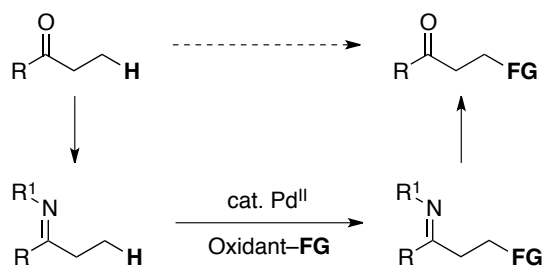
**Scheme 1.10.** Chiral Directing Group Strategy for Pd-Catalyzed Alkene Difunctionalization



*Challenge 3.* The synthetic utility of most Pd-catalyzed ligand-directed transformations (like those presented in Chapters 2–4) would be significantly enhanced if they provided products that could be more easily derivatized. As such, we have been

interested in identifying general and efficient directing ligands that can be removed or otherwise transformed after they are no longer needed to direct functionalization (Scheme 1.11). To this end, we have demonstrated the use of *in situ* generated *O*-acetyl oxime ethers as effective directing groups in Pd-catalyzed C–H oxygenation reactions.<sup>10</sup> These directing groups are stable under the reaction conditions, but can then be readily manipulated to afford ketones, alcohols, amines, and heterocycles.

**Scheme 1.11.** Transformable Directing Group Strategy for C–H Functionalization





## 1.5 References

1. (a) Mishra, M. K.; Yagci, Y. *Handbook of Radical Vinyl Polymerization*. Marcel Dekker: New York, 1998; p 32. (b) Blanksby, S. J.; Ellison, G. B. Bond Dissociation Energies of Organic Molecules. *Acc. Chem. Res.* **2003**, *36*, 255. (c) Evans pKa Table. Downloaded from <http://www2.lsddiv.harvard.edu/labs/evans/> on June 11, 2010. (c) Anslyn, E. V; Dougherty, D. A. *Modern Physical Organic Chemistry*. University Science Books: Sausalito, CA, 2006.
2. For a comprehensive review see: Hartwig, J. F. *Organotransition Metal Chemistry, from Bonding to Catalysis*. University Science Books: Sausalito, CA, 2010.
3. Ames, D. E.; Opalko, A. Palladium-Catalyzed Cyclization of 2-Substituted Halogenoarenes by Dehydrohalogenation. *Tetrahedron* **1984**, *40*, 1919.
4. (a) Alberico, D.; Scott, M. E.; Lautens, M. Aryl–Aryl Bond Formation by Transition-Metal-Catalyzed Direct Arylation. *Chem. Rev.* **2007**, *107*, 174. (b) Chen, X.; Engle, K. M.; Wang, D.-H.; Yu, J.-Q. Palladium(II)-Catalyzed C–H Activation/C–C Cross-Coupling Reactions: Versatility and Practicality. *Angew. Chem., Int. Ed.* **2009**, *48*, 5094. (c) McGlacken, G. P.; Bateman, L. M. Recent Advances in Aryl–Aryl Bond Formation by Direct Arylation. *Chem. Soc. Rev.* **2009**, *38*, 2447. (d) Muñiz, K. High-Oxidation-State Palladium Catalysis: New Reactivity for Organic Synthesis. *Angew. Chem., Int. Ed.* **2009**, *48*, 9412. (e) Canty, A. J. Organopalladium and Platinum Chemistry in Oxidizing Milieu as Models for Organic Synthesis Involving the Higher Oxidation States of Palladium. *Dalton. Trans.* **2009**, *47*, 10409. (f) Lyons, T. W.; Sanford, M. S. Palladium-Catalyzed Ligand-Directed C–H Functionalization Reactions. *Chem. Rev.* **2010**, *110*, 1147. (g) Xu, L.-M.; Li, B.-J.; Yang, Z.; Shi, Z.-J. Organopalladium(IV) Chemistry. *Chem. Soc. Rev.* **2010**, *39*, 712. (h) Hickman, A. J.; Sanford, M. S. High-Valent Organometallic Copper and Palladium in Catalysis. *Nature* **2012**, *484*, 177.
5. Neufeldt, S. R.; Sanford, M. S. Controlling Site Selectivity in Palladium Catalyzed C–H Bond Functionalization. *Acc. Chem. Res.* **2012**, *45*, 936.
6. (a) Kalyani, D.; Deprez, N. R.; Desai, L. V.; Sanford, M. S. Oxidative C–H Activation/C–C Bond Forming Reactions: Synthetic Scope and Mechanistic Insights. *J. Am. Chem. Soc.* **2005**, *127*, 7330. (b) Deprez, N. R.; Sanford, M. S. Synthetic and Mechanistic Studies of Pd-Catalyzed C–H Arylation with Diaryliodonium Salts: Evidence for a Bimetallic High Oxidation State Pd Intermediate. *J. Am. Chem. Soc.* **2009**, *131*, 11234.
7. Previous examples from our group that merge transition metal catalysis with radical chemistry (a) Kalyani, D.; McMurtrey, K. B.; Neufeldt, S. R.; Sanford, M. S. Room-Temperature C–H Arylation: Merger of Pd-Catalyzed C–H Functionalization and Visible-Light Photocatalysis. *J. Am. Chem. Soc.* **2011**, *133*, 18566. (b) Ye, Y.; Sanford, M. S. Merging Visible-Light Photocatalysis and

Transition-Metal Catalysis in the Copper-Catalyzed Trifluoromethylation of Boronic Acids with CF<sub>3</sub>I. *J. Am. Chem. Soc.* **2012**, *134*, 9034.

8. Neufeldt, S. R.; Sanford, M. S. Combining Transition Metal Catalysis with Radical Chemistry: Dramatic Acceleration of Palladium-Catalyzed C–H Arylation with Diaryliodonium Salts. *Adv. Synth. Catal.*, **2012**, *in press*.
9. Neufeldt, S. R.; Sanford, M. S. Asymmetric Chiral Ligand-Directed Alkene Dioxygenation. *Org. Lett.* [Online early access]. DOI: 10.1021/ol303003g.
10. Neufeldt, S. R.; Sanford, M. S. *O*-Acetyl Oximes as Transformable Directing Groups for Pd-Catalyzed C–H Bond Functionalization. *Org. Lett.* **2010**, *12*, 532.

## CHAPTER 2

### Room-Temperature Photoredox Pd/Ir-Catalyzed C–H Arylation with $\text{Ph}_2\text{I}^+$

#### 2.1 Background and Significance

Substituted biphenyl scaffolds are prevalent in bioactive natural and synthetic products (Figure 2.1), including ~4.3% of known therapeutic drugs.<sup>1a</sup> Inclusion of this ‘privileged’ substructure in small molecules has been shown to impart binding affinity for a wide range of protein targets; furthermore, variation of the substituents on the scaffold can afford compounds with high levels of binding specificity.<sup>1</sup> Biaryl motifs are also common in numerous synthetic polymers, semiconductors, and other valuable materials. As such, vast amounts of research over the last century have been dedicated to developing methods to construct aryl–aryl bonds.<sup>2</sup>

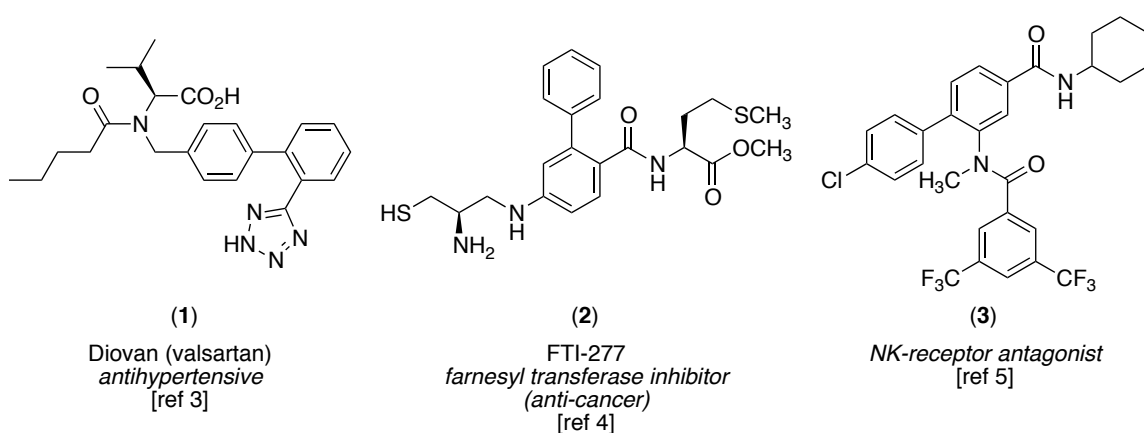
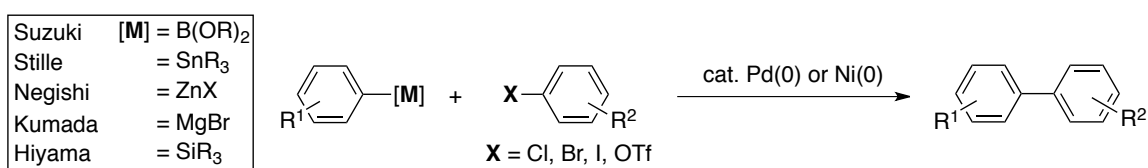


**Figure 2.1.** Examples of Biphenyl Motifs in Bioactive Molecules

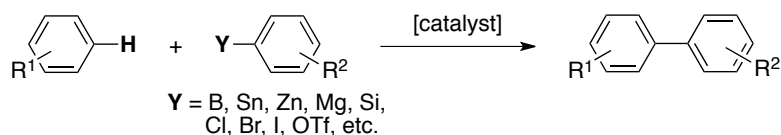
Without question, the most successful Ar–Ar bond-forming methodologies to date involve cross-coupling between an aryl organometallic reagent and an aryl halide (Scheme 2.1). Despite their well-deserved recognition with the 2010 Nobel Prize, such methodologies possess the disadvantage of requiring two prefunctionalized starting materials. Such precursors can be difficult or costly to access, particularly at a late stage of a lengthy synthesis, and they necessarily result in the formation of stoichiometric waste.

**Scheme 2.1.** Pd- and Ni-Catalyzed Aryl–Aryl Cross-Coupling Reactions



An attractive alternative to classic cross-coupling reactions would involve the direct arylation of a C–H bond, a transformation that would preclude the need for at least one prefunctionalized starting material (Scheme 2.2). A protocol for C–H arylation that is highly site-selective, utilizes mild reaction conditions, displays high functional group tolerance, and can successfully install diverse aryl groups could be extremely valuable for small molecule synthesis, particularly for late stage derivatization of complex molecules.

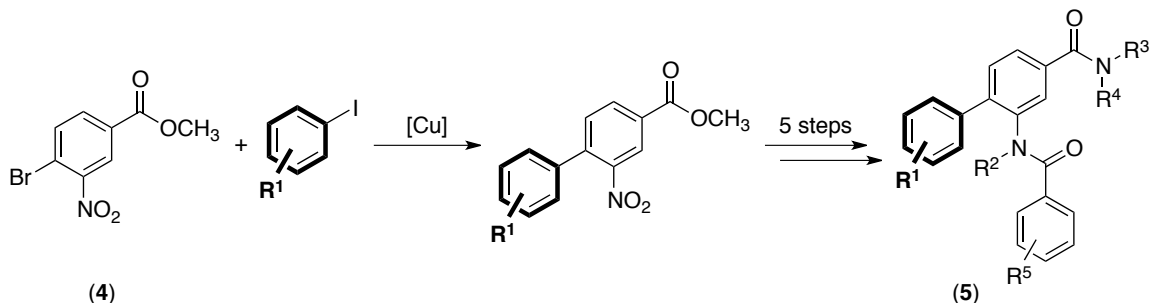
**Scheme 2.2.** Biaryl Formation by C–H Arylation



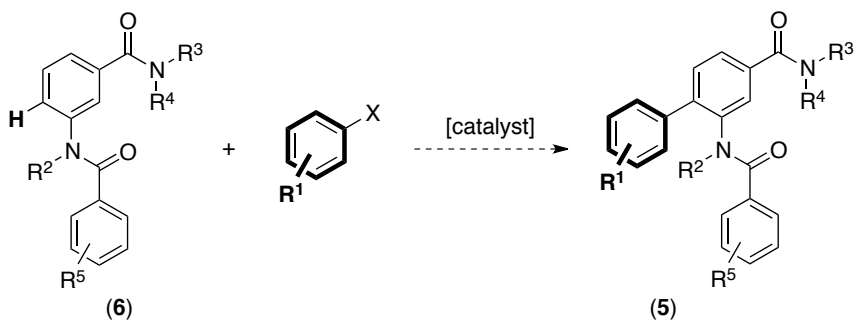
As an example, Scheme 2.3 presents a literature synthesis for a class of NK<sub>1</sub> receptor antagonists.<sup>5</sup> Structure-activity relationship studies were conducted by preparing a small library of derivatives of **5** (including **3** in Figure 2.1) via a synthetic route that utilizes a Cu-catalyzed cross-coupling reaction. Because the aryl–Br moiety in coupling partner **4** may be difficult to install at a later stage or to carry through over multiple steps, the aryl–aryl coupling reaction is conducted first. Consequently, the assorted final

products **5** do not share a common late-stage intermediate and their preparation is laborious. Instead, the synthesis of a library of compounds with diverse aryl- $R^1$  groups could be streamlined by the route presented in Scheme 2.4.

**Scheme 2.3.** Biaryl Formation at an Early Stage in the Synthesis of **5**

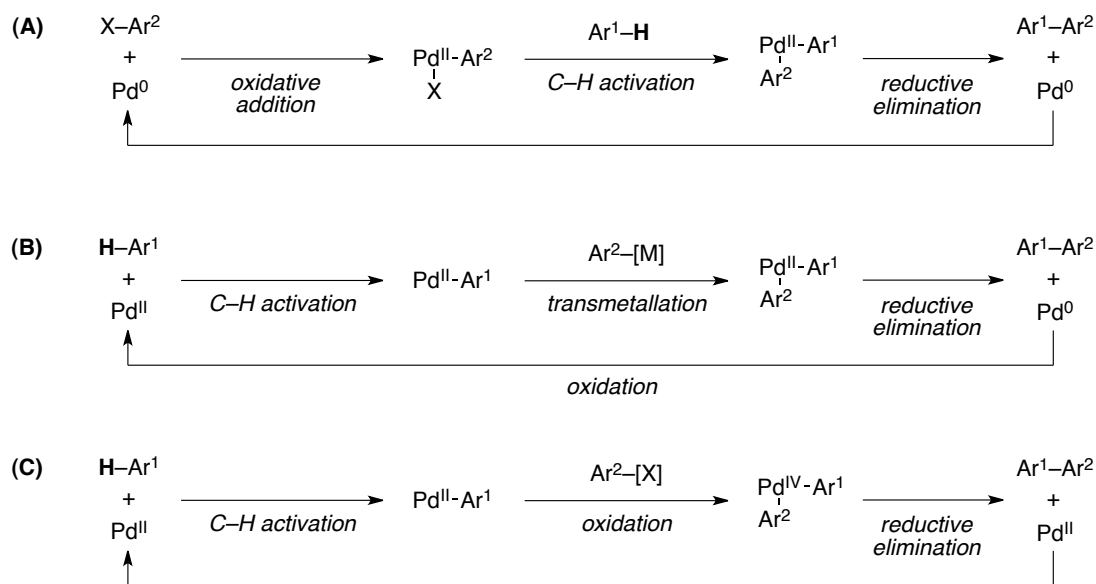


**Scheme 2.4.** Biaryl Formation at a Late Stage in the Synthesis of **5** via C–H Arylation



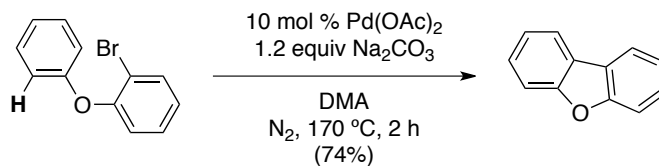
The past quarter of a century has seen an escalation of research efforts directed toward transition metal-mediated C–H arylation.<sup>6</sup> Palladium salts in particular have proven to be versatile catalysts for such transformations, and a large number of Pd-catalyzed C–H arylation reactions have been reported representing an eclectic assortment of aryl–H substrates and aryl coupling partners.<sup>6,7</sup> The mechanisms of these transformations are typically described by one of the manifolds depicted in Scheme 2.5 involving a  $Pd^{0/II}$ ,  $Pd^{II/0}$ , or  $Pd^{II/IV}$  catalytic cycle (for clarity, additional ligands on the metal centers are not shown).

**Scheme 2.5.** Common Mechanistic Manifolds for Pd-Catalyzed C–H Arylation Reactions



A key challenge associated with developing any practical C–H functionalization reaction is the issue of site selectivity (see Chapter 1), and C–H arylation methodology has been no exception. One approach to achieving selectivity is to couple two arenes that are within the same molecule. Seminal work by Ames and coworkers in the early 1980s demonstrated Pd-catalyzed intramolecular coupling of aryl–H with an aryl halide to afford dibenzofurans (Scheme 2.6), carbazoles, and fluorenones.<sup>8</sup> Many similar examples have since been reported; however, this intramolecular approach to controlling site selectivity is inherently limited to a small subset of target molecules and is only useful for forming cyclic products.

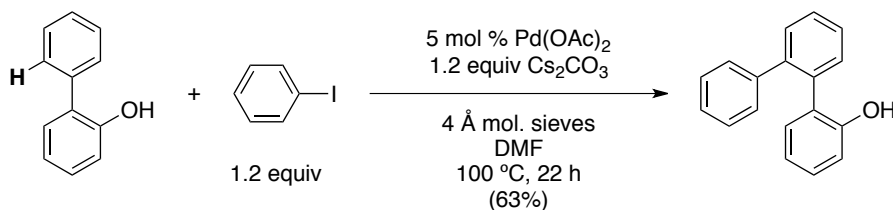
**Scheme 2.6.** Intramolecular C–H Arylation to Form Dibenzofurans<sup>8</sup>



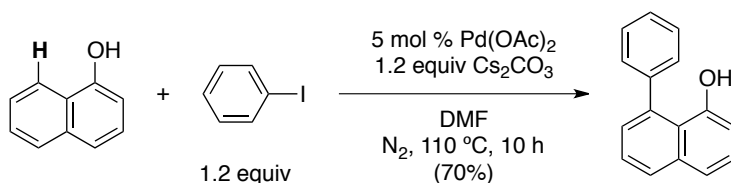
A more broadly applicable approach to controlling the site selectivity of C–H arylation is to use a directing group. Miura and coworkers demonstrated one of the first examples of Pd-catalyzed intermolecular direct arylation using a phenol as a directing

group.<sup>9</sup> Arylation occurs selectively at the 2'-position of 2-phenylphenols (Scheme 2.7) or the 8-position of 1-naphthol (Scheme 2.8).

**Scheme 2.7.** Directed C–H Arylation of 2-Phenylphenol<sup>9</sup>

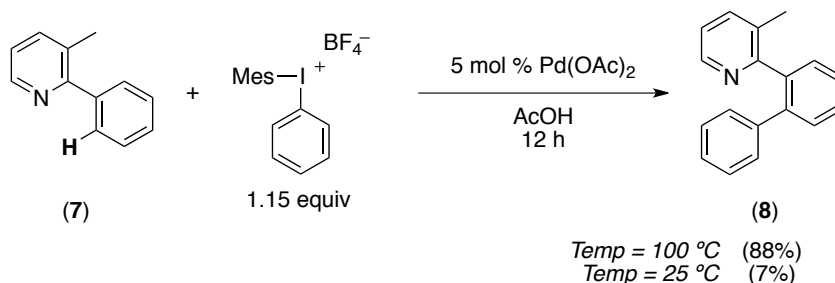


**Scheme 2.8.** Directed C–H Arylation of 1-Naphthol<sup>9</sup>



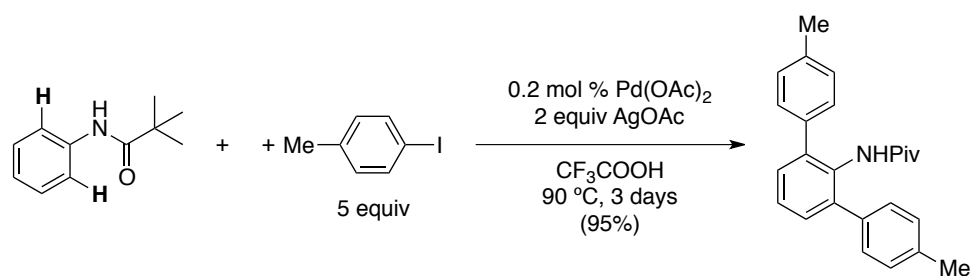
In 2005, our group reported a ligand-directed C–H arylation reaction that utilizes diaryliodonium reagents as the aryl source (Scheme 2.9).<sup>10–12</sup> This transformation is effective for a variety of directing groups (*e.g.*, pyridines, pyrrolidinones, oxizolidinones, and quinolines) and substituted arenes. However, like the majority of Pd-catalyzed methodologies for arylation of unactivated C–H bonds, arylation with Ar<sub>2</sub>I<sup>+</sup> oxidants has the drawback of requiring high reaction temperatures (>80 °C). For example, as depicted in Scheme 2.9, the phenylation of **7** is extremely sluggish at room temperature.

**Scheme 2.9.** Directed C–H Phenylation of **7** with Ar<sub>2</sub>I<sup>+</sup> Salts under Thermal/Ionic Conditions<sup>10</sup>

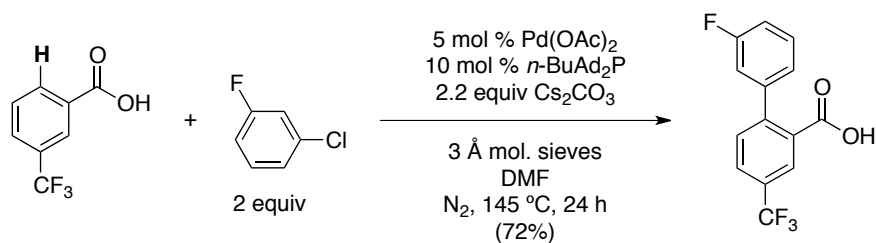


Similarly, most examples of Pd-catalyzed ligand-directed C–H arylation with aryl iodides<sup>13</sup> (Scheme 2.10), aryl chlorides<sup>13c</sup> (Scheme 2.11), aryl boronic acids<sup>14,15</sup> (Scheme 2.12), and trialkoxyarylsilanes<sup>13d</sup> (Scheme 2.13) all require elevated temperatures to proceed in high yield.

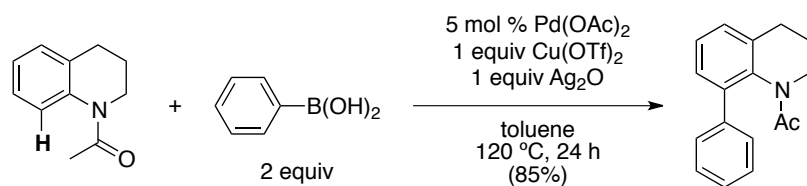
**Scheme 2.10.** Directed C–H Arylation with Aryl Iodides<sup>13a</sup>



**Scheme 2.11.** Directed C–H Arylation with Aryl Chlorides<sup>13c</sup>

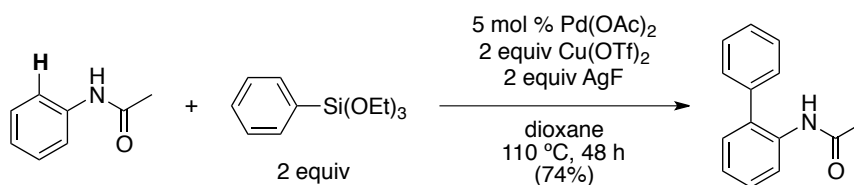


**Scheme 2.12.** Directed C–H Arylation with Arylboronic Acids<sup>14a</sup>



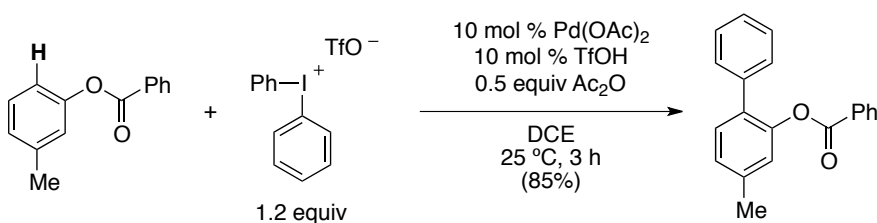


**Scheme 2.13.** Directed C–H Arylation with Trialkoxyarylsilanes<sup>13d</sup>



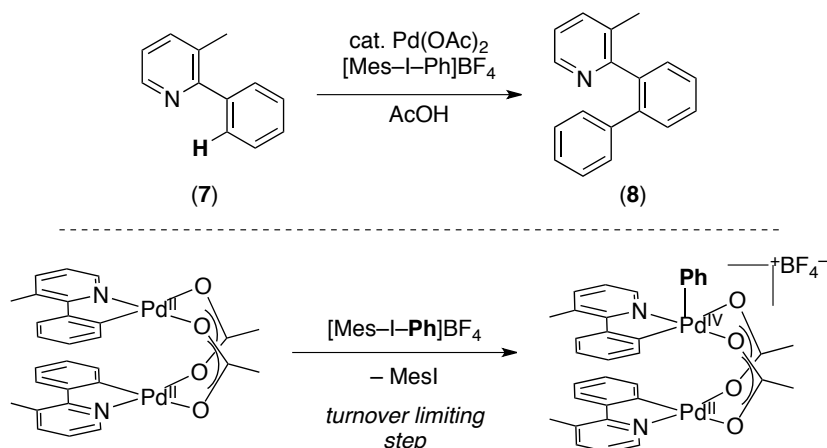
In one unusual example, room temperature C–H arylation of phenol esters with diaryliodonium salts was reported (Scheme 2.14).<sup>16</sup> However, this reaction requires TfOH as an additive and has not been demonstrated with any other directing groups. It is likely that these acid-catalyzed reaction conditions would be incompatible with more common nitrogen-containing directing groups that feature a basic site (*e.g.*, pyridines).

**Scheme 2.14.** Room-Temperature C–H Arylation of Phenol Esters with Diaryliodonium Oxidants<sup>11d</sup>



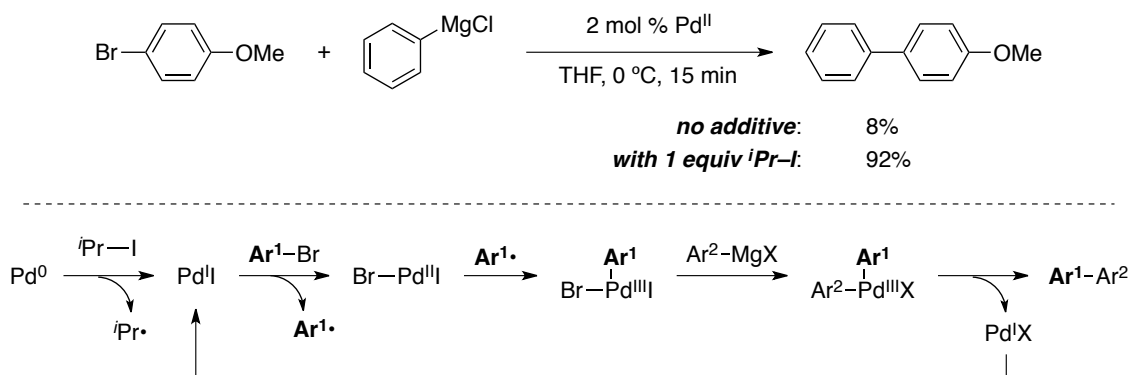
Some insight into the thermal requirements for C–H arylation with Ar<sub>2</sub>I<sup>+</sup> has been provided by recent mechanistic work from our group.<sup>17</sup> Kinetic studies of the arylation of **7** with diaryliodonium reagents revealed that the rate-limiting step of the transformation is oxidation of an intermediate palladacycle by Ar<sub>2</sub>I<sup>+</sup> (Scheme 2.15).

**Scheme 2.15.** Thermal C–H Arylation with  $\text{Ar}_2\text{I}^+$  is Limited by the Oxidation Step<sup>17</sup>



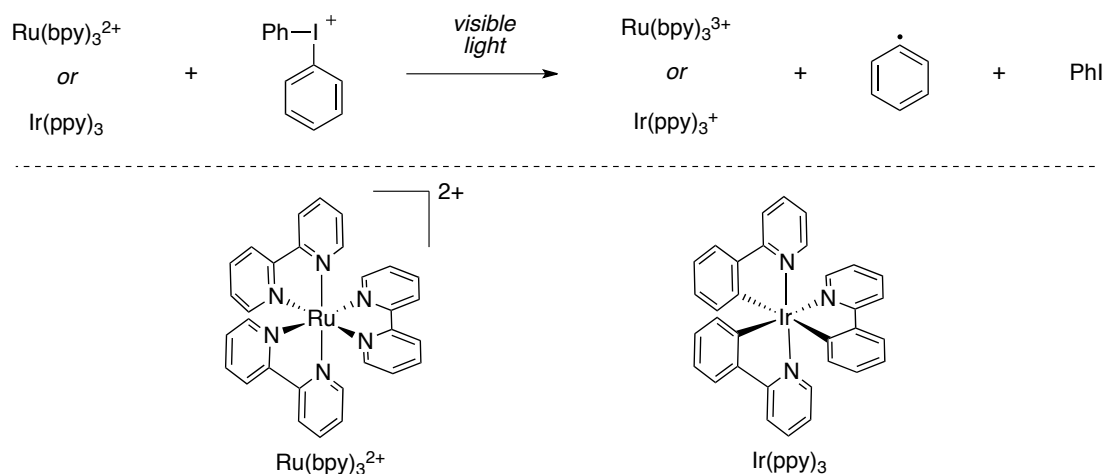
In light of these studies, we reasoned that the rate of C–H arylation could be accelerated by the use of kinetically more reactive oxidants for  $\text{Pd}^{\text{II}}$ . Recently, the combination of transition metal catalysis with radical chemistry has emerged as a powerful strategy for achieving fast, high-yielding transformations under mild conditions.<sup>18</sup> A striking example of this strategy’s potential in Pd catalysis was reported in 2009 by Knochel and coworkers.<sup>19</sup> In this example, an alkyl radical-mediated Kumada coupling displayed remarkable rate acceleration and functional group tolerance at room temperature (Scheme 2.16). This reaction utilizes textbook Kumada coupling reagents (an aryl Grignard, an aryl bromide, and a Pd catalyst), but is believed to proceed through a mechanistic manifold that is fundamentally different from ‘traditional’  $\text{Pd}^0/\text{Pd}^{\text{II}}$  catalysis. Intermediate alkyl radicals, putatively generated by the reaction of an added alkyl iodide with  $\text{Pd}^0$ , are proposed to initiate a  $\text{Pd}^{\text{I}}/\text{Pd}^{\text{III}}$  catalytic cycle that allows for more rapid product formation (*i.e.*, 92% vs 8% yield of the biaryl product after 15 min at 0 °C). Consequently, this transformation could be extended to the cross-coupling of diverse functionalized arenes, including aryl Grignards with poor stability at room temperature.

**Scheme 2.16.** Radical-Accelerated Kumada Cross-Coupling<sup>19</sup>



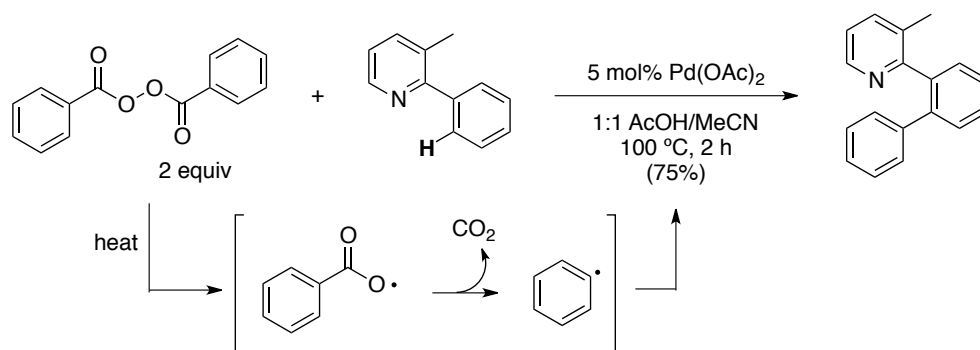
Although the thermal Pd-catalyzed arylation with  $\text{Ar}_2\text{I}^+$  is believed to proceed via an ionic mechanism involving  $2e^-$  oxidation of Pd by  $\text{Ar}_2\text{I}^+$  (Scheme 2.5 C), we reasoned that the rate of this reaction could potentially be enhanced by rerouting it through a radical pathway in which  $\text{Ar}_2\text{I}^+$  is converted into  $\text{Ar}\cdot$  *in situ*. Because  $\text{Ar}\cdot$  would be a more kinetically reactive oxidant than  $\text{Ar}_2\text{I}^+$ , the slow oxidation step should be accelerated relative to the thermal/ionic reaction. Intriguingly, sporadic reports from the polymer literature have shown that diaryliodonium salts can serve as precursors to  $\text{Ar}\cdot$  in the presence of visible light and a photoredox catalyst (Scheme 2.17).<sup>20</sup> Thus we envisioned that the combination of Pd- and photoredox catalysis could provide a means for achieving room temperature C–H arylation with diaryliodonium salts.

**Scheme 2.17.** Generation of  $\text{Ph}\cdot$  from  $\text{Ph}_2\text{I}^+$  by Photoredox Catalysis<sup>20</sup>

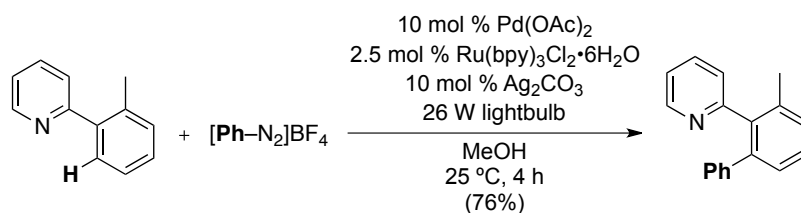


Precedent for Ar•-mediated Pd-catalyzed C–H arylation was provided by literature reports that used aryl acylperoxides or aryldiazonium salts as Ar• precursors. In the former case, a high reaction temperature (100 °C) is needed to generate Ar• from the aryl acylperoxide precursor (Scheme 2.18).<sup>21</sup> The latter case, a transformation published by our group, demonstrated the feasibility of room-temperature Pd-catalyzed C–H arylation with Ar• generated from ArN<sub>2</sub><sup>+</sup> using photoredox catalysis (Scheme 2.19).<sup>22</sup>

**Scheme 2.18.** Ar•-Mediated Pd-Catalyzed C–H Arylation using Aryl Acylperoxides<sup>21</sup>

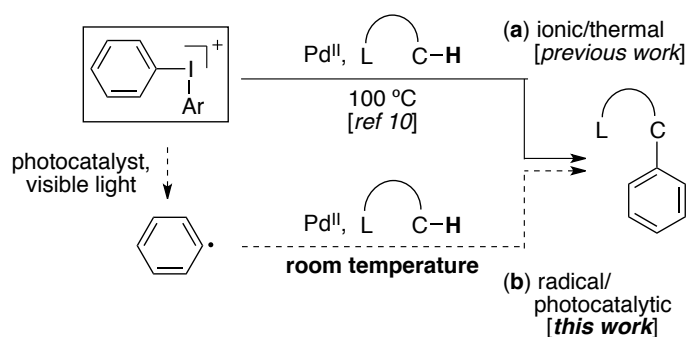


**Scheme 2.19.** Pd-Catalyzed C–H Arylation with ArN<sub>2</sub><sup>+</sup> Using Visible-Light Photoredox Catalysis<sup>22</sup>



Encouraged by this precedent, we began our studies with the goal of rerouting the mechanism of Pd-catalyzed C–H arylation with Ar<sub>2</sub>I<sup>+</sup> from an ionic pathway (Scheme 2.20, path a) to an alternative radical-mediated pathway (path b) that would enable the use of milder reaction temperatures.

**Scheme 2.20.** Two Different Pathways for Pd-Catalyzed C–H Arylation Using  $\text{Ph}_2\text{I}^+$



## 2.2 Reaction Optimization

We initiated our investigations of Pd-catalyzed C–H phenylation of substrate **9** with  $[\text{Ph}_2\text{I}]\text{BF}_4$  in combination with either  $\text{Ru}(\text{bpy})_3\text{Cl}_2$  or  $\text{Ir}(\text{ppy})_3$ , the photocatalysts precedented<sup>20</sup> for use with diaryliodonium salts (Scheme 2.17). Substrate **9** was selected for study because (1) its arylation with  $\text{Ar}_2\text{I}^+$  reagents under thermal conditions has been previously demonstrated,<sup>10,22</sup> (2) unlike aryl pyridines, it has not been shown to be undergo competing oxidative homodimerization,<sup>23</sup> and (3) it is a convenient commercially available crystalline solid. Visible light irradiation was provided by a 26 W household fluorescent light bulb, and the reactions were set up on the bench top with no precautions to exclude moisture or air. Remarkably, the use of  $\text{Ru}(\text{bpy})_3\text{Cl}_2$  resulted in a modest yield (18%) of the desired arylated product **10** after 15 h in MeOH at room temperature (Table 2.1, entry 1). Evaluation of a number of different  $\text{Pd}^{\text{II}}$  salts showed that  $\text{Pd}(\text{NO}_3)_2$  provided better results, affording **10** in 23% yield. Although  $\text{Ru}(\text{bpy})_3\text{Cl}_2$  and  $\text{Ir}(\text{ppy})_3$  afforded comparable results, the cationic photocatalyst  $\text{Ir}(\text{ppy})_2(\text{dtbbpy})\text{PF}_6$  ( $\text{dtbbpy}$  = 4,4'-di-*tert*-butyl-2,2'-bipyridine)<sup>24</sup> provided a significant improvement (57% yield). Replacing  $[\text{Ph}_2\text{I}]\text{BF}_4$  with the corresponding triflate salt led to a further enhancement in yield (66%). Finally, briefly sparging the mixture with  $\text{N}_2$  prior to the start of the reaction resulted in 94% yield of **10**. Notably,  $[\text{Ph}_2\text{I}]\text{BF}_4$  performed comparably to  $[\text{Ph}_2\text{I}]\text{OTf}$  when  $\text{O}_2$  was excluded (entry 7) for substrate **9**.

**Table 2.1.** Optimization of the Room-Temperature C–H Phenylation of **9** with  $\text{Ph}_2\text{I}^+$  <sup>a</sup>

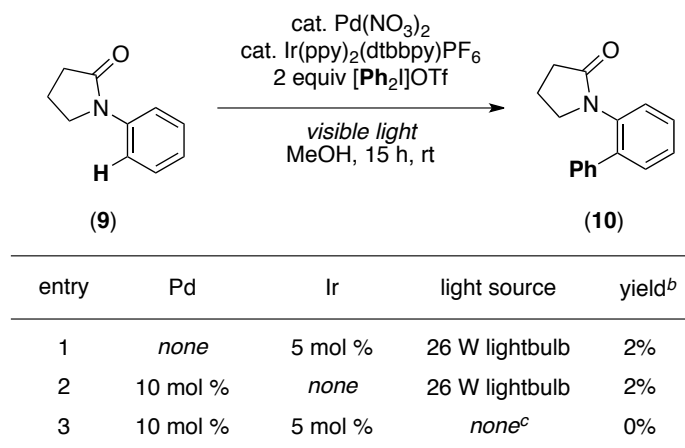
10 mol % Pd<sup>II</sup>  
5 mol % photocatalyst  
2 equiv [Ph<sub>2</sub>I]X

26 W lightbulb  
MeOH, 15 h, rt

entry	Pd <sup>II</sup>	photocatalyst	X	yield <sup>b</sup>
1	Pd(OAc) <sub>2</sub>	Ru(bpy) <sub>3</sub> Cl <sub>2</sub>	BF <sub>4</sub> <sup>-</sup>	18%
2	Pd(NO <sub>3</sub> ) <sub>2</sub>	Ru(bpy) <sub>3</sub> Cl <sub>2</sub>	BF <sub>4</sub> <sup>-</sup>	23%
3	Pd(NO <sub>3</sub> ) <sub>2</sub>	Ir(ppy) <sub>3</sub>	BF <sub>4</sub> <sup>-</sup>	17%
4	Pd(NO <sub>3</sub> ) <sub>2</sub>	Ir(ppy) <sub>2</sub> (dtbbpy)PF <sub>6</sub>	BF <sub>4</sub> <sup>-</sup>	57%
5	Pd(NO <sub>3</sub> ) <sub>2</sub>	Ir(ppy) <sub>2</sub> (dtbbpy)PF <sub>6</sub>	OTf <sup>-</sup>	66%
6 <sup>c</sup>	Pd(NO <sub>3</sub> ) <sub>2</sub>	Ir(ppy) <sub>2</sub> (dtbbpy)PF <sub>6</sub>	OTf <sup>-</sup>	94%
7 <sup>c</sup>	Pd(NO <sub>3</sub> ) <sub>2</sub>	Ir(ppy) <sub>2</sub> (dtbbpy)PF <sub>6</sub>	BF <sub>4</sub> <sup>-</sup>	94%

<sup>a</sup>General conditions: **9** (1 equiv), Pd<sup>II</sup> (0.10 equiv), photocatalyst (0.05 equiv), [Ph<sub>2</sub>I]X (2 equiv), MeOH (0.2 M in **9**), 26 W lightbulb, 15 h, rt. <sup>b</sup>Yields determined by GC. <sup>c</sup>Reaction was degassed by sparging with N<sub>2</sub> for 1 min.

Importantly, both of the metal catalysts, as well as visible light, are critical for efficient room temperature C–H phenylation. Without any one of these three components, only traces of product **10** were formed (0–2% yield, Table 2.2).

**Table 2.2.** Control Reactions for the Pd/Ir-Catalyzed C–H Phenylation of **9** with Ph<sub>2</sub>I<sup>+</sup> <sup>a</sup>

<sup>a</sup>General conditions: **9** (1 equiv), [Ph<sub>2</sub>I]OTf (2 equiv), MeOH (0.2 M in **9**), 15 h, rt, degassed by sparging with N<sub>2</sub> for 1 min. <sup>b</sup>Yields determined by GC. <sup>c</sup>Reaction vial was covered with aluminum foil.

The yield enhancement observed upon sparging with N<sub>2</sub> (Table 2.1, entries 5 vs 6) suggests that O<sub>2</sub> is detrimental to the desired transformation. This effect could be attributed to (i) radical termination by a reaction between Ar• and O<sub>2</sub> or (ii) quenching of photoexcited Ir<sup>3+\*</sup> by O<sub>2</sub>. Although we cannot conclusively rule out the first explanation, the expected byproduct of a reaction between Ar• and O<sub>2</sub>, phenol, has not been observed by gas chromatography. Instead, rationale (ii) appears to be more likely based on literature precedent<sup>25</sup> and a subsequent observation that O<sub>2</sub> is not detrimental to a related C–H arylation reaction that uses Ar• generated through a non-photoredox pathway (Chapter 3, section 3.10).

In contrast to the effect of oxygen, the presence of trace water does not appear to influence the course of the reaction. As illustrated in Figure 2.2, reactions set up with wet MeOH can be degassed by brief sparging with N<sub>2</sub> to afford results that are equally satisfactory to those obtained by setting up the reactions in a glovebox using rigorously dried and degassed MeOH.

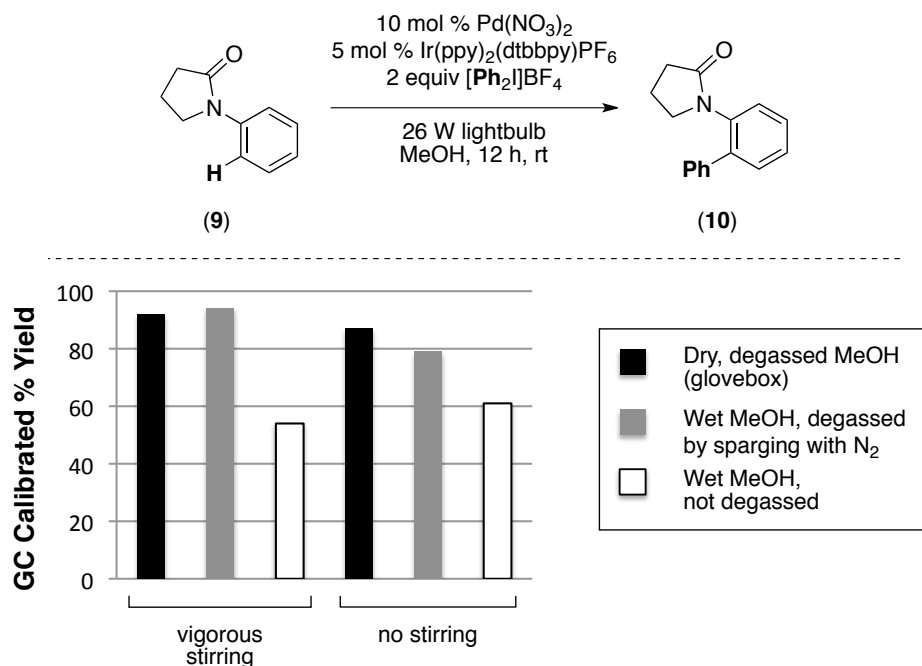


**Figure 2.2.** Comparison of Dry/Degassed, Wet/Degassed, and Wet/Non-Degassed MeOH for the Pd/Ir-Catalyzed C–H Arylation of **9**

The benchtop sparging method is arguably more convenient than the use of a glovebox. Furthermore, for liquid substrates such as arylpyridine **7**, we found the sparging method to provide *better* results with improved reproducibility (average yield = 61 ± 2% over 5 runs) than the glovebox method (average yield = 53 ± 10% over 7 runs) (Figure 2.3). This observation can likely be explained by the presence of small amounts of O<sub>2</sub> dissolved in the liquid substrate brought into the glovebox. In contrast, sparging of the entire reaction mixture displaces even this small quantity of O<sub>2</sub> from the solution. This discrepancy between sparging and glovebox conditions could presumably be eliminated by more careful degassing of liquid substrates prior to their use in the glovebox. Clearly, however, the simple sparging protocol is sufficient and is likely to be more convenient in many cases.



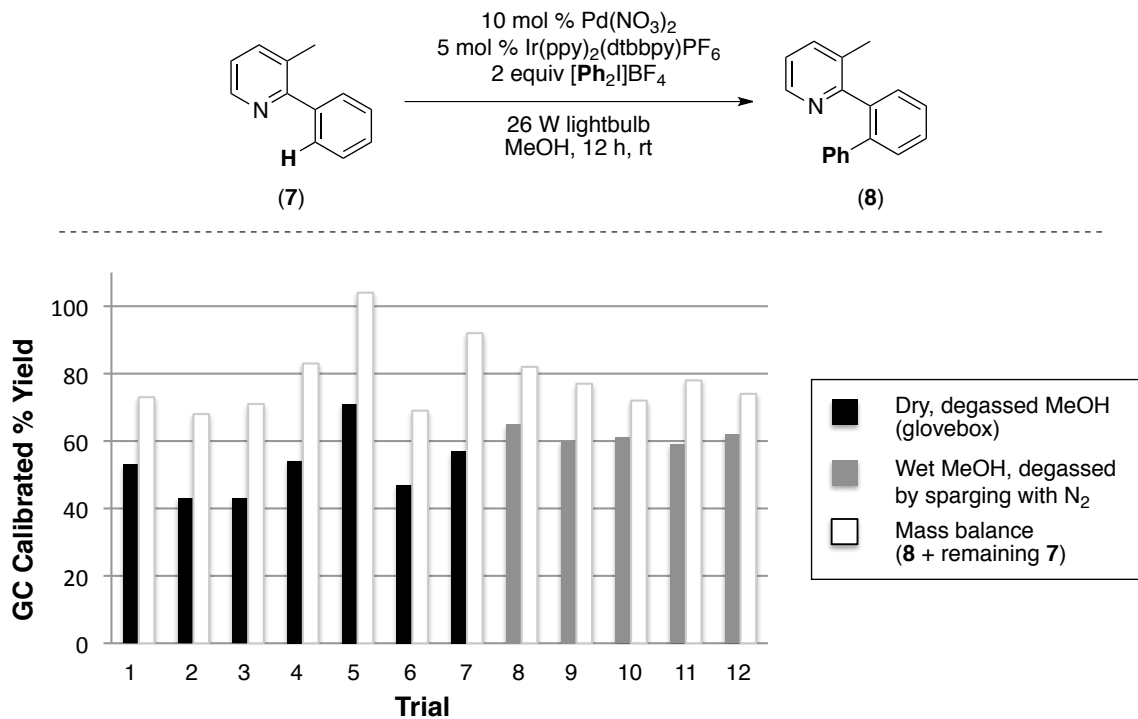


**Figure 2.3.** Comparison of Dry/Degassed and Wet/Degassed MeOH for the Pd/Ir-Catalyzed C–H Arylation of **7**

As described above, exclusion of O<sub>2</sub> was found to improve the yield of the arylation reaction of both **9** and **7**. Nevertheless, for arylpyridine **7**, only about 80% of the total mass balance could be accounted for by summing the product and remaining starting material (Figure 2.3, entries 8–12, white bars). Analysis by GCMS and comparison to authentic materials suggests that the remainder of the mass balance can be attributed to several undesired side products. Figure 2.4 shows an annotated copy of a typical gas chromatogram for the Pd/Ir-catalyzed arylation reaction of **7** with [Ph<sub>2</sub>I]BF<sub>4</sub>. As indicated, side products resulting from arylation of the pyridine ring (**A**),<sup>26</sup> diarylation (**B**), and homocoupling of **7** (**C**)<sup>23</sup> are observed.

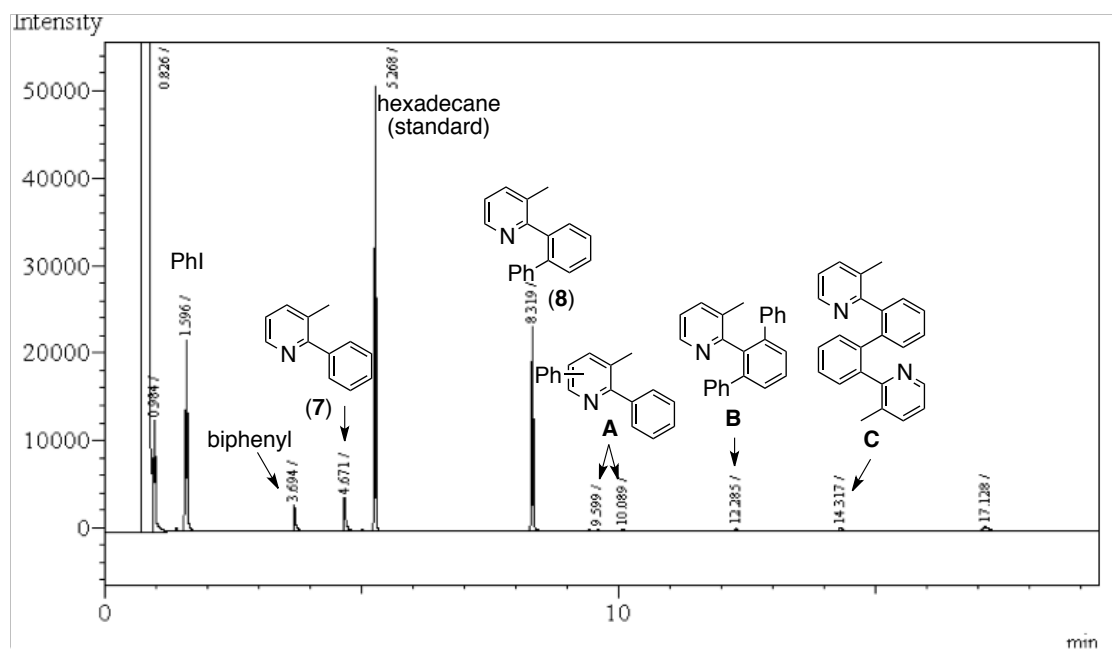


**Figure 2.4.** Typical Gas Chromatogram of the Pd/Ir-Catalyzed Arylation of **7**

As shown in Table 2.1, the use of  $[\text{Ph}_2\text{I}]\text{OTf}$  or  $[\text{Ph}_2\text{I}]\text{BF}_4$  provided similar yields of pyrrolidinone product **10** under  $\text{N}_2$ -sparging conditions. However, for other substrates such as arylpyridine **7**,  $[\text{Ph}_2\text{I}]\text{OTf}$  proved superior to  $[\text{Ph}_2\text{I}]\text{BF}_4$  (Figure 2.5, 76% vs 56% GC yield for  $\text{OTf}^-$  and  $\text{BF}_4^-$ , respectively). A more comprehensive screen of diphenyliodonium salts with substrate **7** confirmed that the yield of the transformation can be influenced by the oxidant counterion, although none of the other counterions screened were found to be superior to  $\text{OTf}^-$  (Figure 2.5). Consequently,  $[\text{Ph}_2\text{I}]\text{OTf}$  was used as the oxidant for the majority of subsequent experiments with other substrates (Section 2.3).

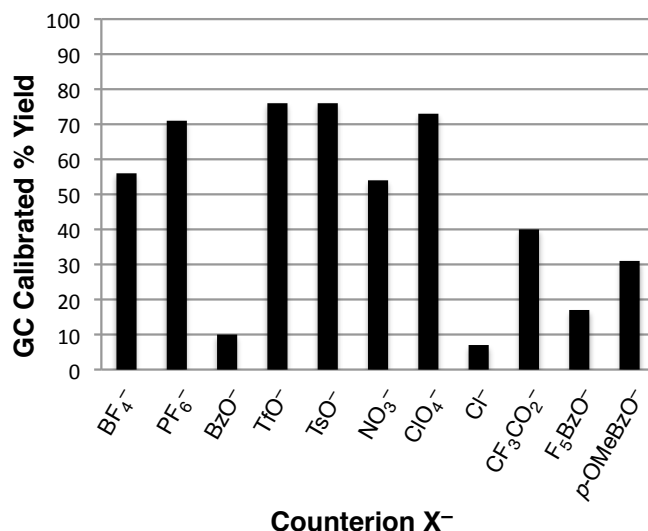
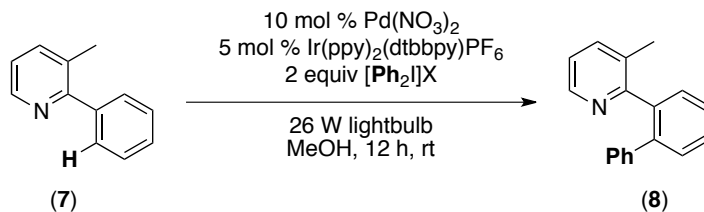


**Figure 2.5.** Oxidant Counterion Screen for the Pd/Ir-Catalyzed C–H Arylation of **7**

### 2.3 Substrate Scope

With optimized reaction conditions in hand (Table 2.1), we next investigated the substrate scope of the reaction. Gratifyingly, a variety of aromatic substrates underwent room temperature C–H phenylation under the Pd/Ir-catalyzed conditions (Table 2.3). In addition to pyrrolidinones **9** and **11**, other *N*-aryl amides were effective directing groups (entries 3 and 4). *C*-Aryl amides, such as benzamides **17** and **19**, also underwent room temperature C–H phenylation, albeit in moderate yields (40% and 54%). The *N,N*-disubstituted analog **21** provided phenylated product **22** in poor yield (9%), suggesting that C–H arylation is facilitated by the presence of at least one N–H bond in this substrate class. 2-Arylpyridines **23** and **25** as well as ketoxime and aldoxime ethers **27** and **29** were also good substrates. The ability to use oxime ethers as directing groups is particularly notable, as these do not undergo C–H arylation with diaryliodonium reagents under the previously reported thermal reaction conditions (Scheme 2.21).<sup>10,17</sup>

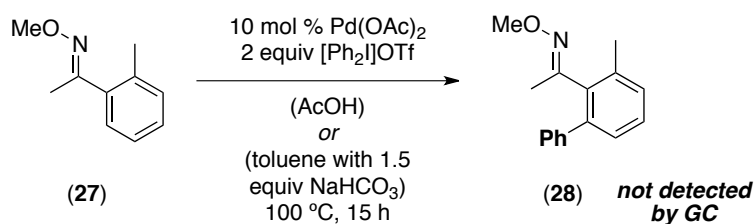
**Table 2.3.** Substrate Scope for the Pd/Ir-Catalyzed C–H Phenylation with  $\text{Ph}_2\text{I}^+$  <sup>a</sup>

10 mol %  $\text{Pd}(\text{NO}_3)_2$   
5 mol %  $\text{Ir}(\text{ppy})_2(\text{dtbbpy})\text{PF}_6$   
2 equiv  $[\text{Ph}_2\text{I}]\text{OTf}$   
26 W lightbulb  
MeOH, 15 h, rt

entry	substrate	product	isolated yield	entry	substrate	product	isolated yield
1			81%	7			9%
2			94%	8			62%
3 <sup>b</sup>			72%	9			67%
4 <sup>b,c,d</sup>			44%	10			60%
5			40%	11			57%
6			54%				

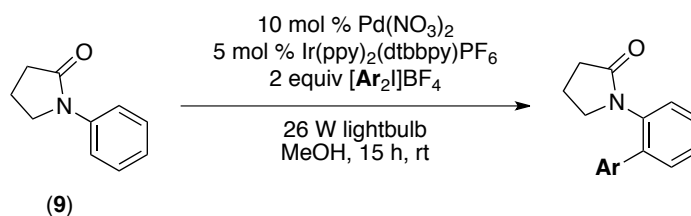
<sup>a</sup>General conditions: substrate (1 equiv),  $[\text{Ph}_2\text{I}]\text{OTf}$  (2 equiv),  $\text{Pd}(\text{NO}_3)_2$  (0.10 equiv),  $\text{Ir}(\text{ppy})_2(\text{dtbbpy})\text{PF}_6$  (0.05 equiv), MeOH, 26 W lightbulb, 15 h, rt, degassed by sparging with  $\text{N}_2$ . <sup>b</sup> $[\text{Ph}_2\text{I}]\text{BF}_4$  was used as the oxidant. <sup>c</sup>with 1 equiv MgO. <sup>d</sup>0.20 equiv  $\text{Pd}(\text{NO}_3)_2$

**Scheme 2.21.** Unsuccessful C–H Arylation of Oxime Ether **27** with  $\text{Ph}_2\text{I}^+$  Under Thermal Conditions



## 2.4 Scope of Diaryliodonium Oxidants

Diaryliodonium salts containing diverse aryl substituents were evaluated in this photocatalytic C–H arylation. As shown in Table 2.4, the highest yields were obtained with those bearing relatively electron neutral substituents (*e.g.*, *p*-Cl, *p*-Br, *p*-CH<sub>3</sub>, *o*-CH<sub>3</sub>, entries 4–7). Nonetheless, oxidants possessing more strongly electron-donating and electron-withdrawing substituents were also effective. For example, C–H arylation with *p*-methoxyphenyl (entry 9) as well as *p*-, *m*-, and *o*-trifluoromethylphenyl (entries 1–3) reagents proceeded in moderate to good yields. Remarkably, even the highly sterically hindered mesityl group could be transferred, albeit in low yield (11%, entry 8). Notably, the analogous thermal reaction of  $[\text{Mes}_2\text{I}]\text{OTf}$  with **9** did not provide detectable quantities of **38** (as determined by GC).

**Table 2.4.** Scope of Ar<sub>2</sub>I<sup>+</sup> Salts for the Pd/Ir-Catalyzed C–H Arylation of **9**<sup>a</sup>

entry	Ar	product	isolated yield	entry	Ar	product	isolated yield
1		(31)	69%	6		(36)	87%
2		(32)	56%	7		(37)	85%
3		(33)	46%	8 <sup>b</sup>		(38)	11%
4		(34)	77%	9		(39)	41%
5		(35)	79%				

<sup>a</sup>General conditions: **9** (1 equiv), [Ar<sub>2</sub>]BF<sub>4</sub> (2 equiv), Pd(NO<sub>3</sub>)<sub>2</sub> (0.10 equiv), Ir(ppy)<sub>2</sub>(dtbbpy)PF<sub>6</sub> (0.05 equiv), MeOH, 26 W lightbulb, 15 h, rt, degassed by sparging with N<sub>2</sub>. <sup>b</sup>OTf salt of oxidant was used.

## 2.5 Inhibition by Radical Scavengers and Chemoselectivity Studies

We propose that the Ir/Pd-catalyzed photocatalytic C–H arylation proceeds *via* a fundamentally different mechanism than the analogous thermal reaction, despite the fact that the reactants and products are the same in both processes. A first piece of evidence to support this proposal is the reaction outcome in the presence of free radical scavengers (2,2,6,6-tetramethylpiperidin-1-yl)oxyl (TEMPO) and galvinoxyl (Figure 2.6). As shown in Table 2.5, the thermal C–H arylation reaction is not inhibited by the addition of 25 mol % galvinoxyl or 100 mol % of TEMPO. With both radical scavengers, the reactions proceed to complete conversion and afford comparable yields (entries 1–3). In contrast, the % conversion and the % yield of the photocatalytic reaction are suppressed in a dose-

dependent manner by galvinoxyl and TEMPO (entries 4–8). These results are consistent with the intermediacy of radicals in the latter but not the former reaction.

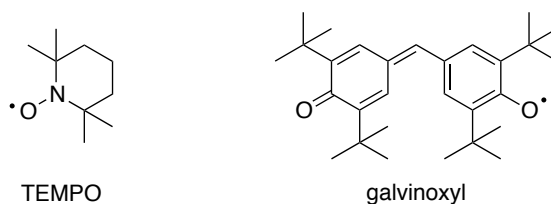
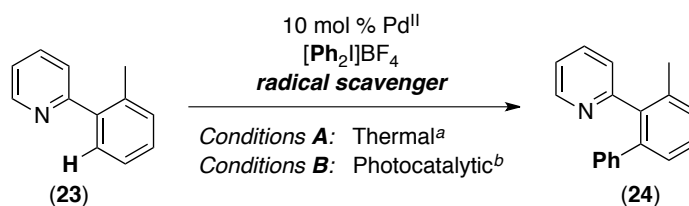


**Figure 2.6.** Structures of Radical Scavengers TEMPO and Galvinoxyl

**Table 2.5.** Effect of Radical Scavengers on the Pd/Ir-Catalyzed C–H Arylation of **23**



entry	scavenger	mol %	conditions	yield (%) <sup>c</sup>
1	none	--	<b>A</b>	79 ± 7
2	galvinoxyl	25%	<b>A</b>	81 ± 1
3	TEMPO	100%	<b>A</b>	74 ± 8
4	none	--	<b>B</b>	52 ± 4
5	galvinoxyl	10%	<b>B</b>	42 ± 2
6	galvinoxyl	25%	<b>B</b>	20 ± 9
7	TEMPO	50%	<b>B</b>	34 ± 14
8	TEMPO	100%	<b>B</b>	6 ± 2

<sup>a</sup>Thermal conditions **A**: **23** (1 equiv), [Ph<sub>2</sub>]BF<sub>4</sub> (1.1 equiv), Pd(OAc)<sub>2</sub> (0.10 equiv), AcOH (0.12 M in **23**), 15 h, 100 °C. <sup>b</sup>Photocatalytic conditions **B**: **23** (1 equiv), [Ph<sub>2</sub>]BF<sub>4</sub> (2 equiv), Pd(NO<sub>3</sub>)<sub>2</sub> (0.1 equiv), Ir(ppy)<sub>2</sub>(dtbbpy)PF<sub>6</sub> (0.05 equiv), MeOH (0.2 M in **23**), 26 W lightbulb, 15 h, rt, degassed by sparging with N<sub>2</sub>. <sup>c</sup>GC calibrated yield reported as % yield ± standard deviation.

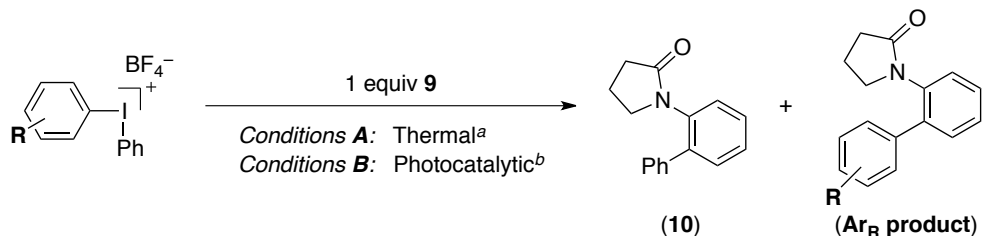
The chemoselectivity for arene transfer from unsymmetrical diaryliodonium salts of the type [Ar<sup>1</sup>–I–Ar<sup>2</sup>]<sup>+</sup> was next explored. These reagents are known to display different chemoselectivity trends in different classes of reactions.<sup>27</sup> For example, in metal-free arylations of nucleophiles, preferential transfer of the more electrophilic<sup>28</sup> or more

sterically hindered<sup>28c,29</sup> aryl group is commonly observed. On the other hand, transfer of sterically bulky aryl groups tends to be disfavored in metal-catalyzed arylations, and there is variation among electronic trends between different metal-catalyzed transformations.<sup>27a</sup>

A number of mixed [Ph-I-Ar]BF<sub>4</sub> reagents were prepared and the ratios of products resulting from phenyl versus aryl transfer were compared under the photocatalytic and thermal reaction conditions (Table 2.6). Under both sets of conditions, a modest preference was observed for transfer of the more electrophilic aryl group. Thus, *p*- and *m*-trifluoromethylphenyl are favored for transfer over phenyl under both sets of conditions (entries 1–4), while *p*-OMe is disfavored (entries 15 and 16). Additionally, a bulky *ortho*-disubstituted arene (mesityl) is disfavored for transfer under both the thermal and photocatalytic reaction conditions (entries 13 and 14).



**Table 2.6.** Comparison of Chemoselectivity for Pd-Catalyzed C–H Arylation with Mixed Diaryliodonium Oxidants for Thermal and Photocatalytic Reaction Conditions



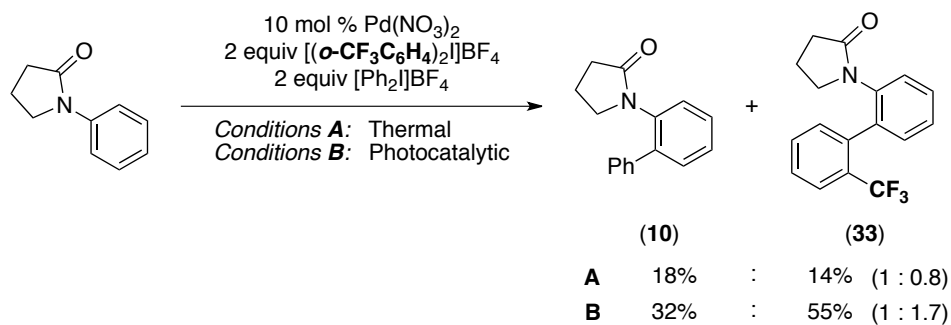
entry	R	Ar <sub>R</sub> Product	conditions	yield	(10) : (Ar <sub>R</sub> Prod.)
1	<i>p</i> -CF <sub>3</sub>	(31)	<b>A</b>	40%	1 : 2.5
2			<b>B</b>	70%	1 : 1.5
3	<i>m</i> -CF <sub>3</sub>	(32)	<b>A</b>	49%	1 : 1.7
4			<b>B</b>	46%	1 : 1.5
5	<i>o</i> -CF <sub>3</sub>	(33)	<b>A</b>	18%	1 : 0.2
6			<b>B</b>	46%	1 : 3.6
7	<i>p</i> -Cl	(34)	<b>A</b>	37%	1 : 1.1
8			<b>B</b>	63%	1 : 1.1
9	<i>p</i> -CH <sub>3</sub>	(36)	<b>A</b>	28%	1 : 1.2
10			<b>B</b>	78%	1 : 0.6
11	<i>o</i> -CH <sub>3</sub>	(37)	<b>A</b>	12%	1 : 0.9
12			<b>B</b>	81%	1 : 1.1
13	Mes	(38)	<b>A</b>	7%	1 : 0.0
14			<b>B</b>	65%	1 : 0.1
15	<i>p</i> -OMe	(39)	<b>A</b>	22%	1 : 0.5
16			<b>B</b>	61%	1 : 0.3

<sup>a</sup>Thermal conditions **A**: **9** (1 equiv), [Ar<sub>R</sub>-I-Ph]BF<sub>4</sub> (2 equiv), Pd(NO<sub>3</sub>)<sub>2</sub> (0.10 equiv), NaHCO<sub>3</sub> (1.5 equiv), toluene, 12 h, 100 °C. <sup>b</sup>Photocatalytic conditions **B**: **9** (1 equiv), [Ar<sub>R</sub>-I-Ph]BF<sub>4</sub> (2 equiv), Pd(NO<sub>3</sub>)<sub>2</sub> (0.10 equiv), Ir(ppy)<sub>2</sub>(dtbbpy)PF<sub>6</sub> (0.05 equiv) MeOH, 26 W lightbulb, 12 h, rt, degassed by sparging with N<sub>2</sub>.

Despite these similarities, differences in chemoselectivity for the two sets of reaction conditions arise in the case of aryl groups containing a single *ortho* substituent. Under thermal conditions, a less hindered Ph group is transferred preferentially over *ortho*-mono-substituted arenes, even when the latter aryl group is more electrophilic (e.g., Table 2.6, entry 5). In contrast, under photocatalytic reaction conditions, aryl groups with a single *ortho*-substituent are transferred *more* readily than phenyl (entries 6 and 12),

even when transfer of the analogous *para*-substituted aryl group is disfavored relative to phenyl (*e.g.*, entry 12 compared to entry 10). This trend is particularly pronounced with *o*-CF<sub>3</sub> (entry 6). Whereas phenyl is transferred selectively under the thermal reaction conditions (**10** : **33** = 1 : 0.2), selective transfer of the *o*-CF<sub>3</sub>C<sub>6</sub>H<sub>4</sub> group occurs under the photocatalytic conditions to afford a 1 : 3.6 ratio of **10** : **33**. Interestingly, the chemoselectivities observed for both the thermal and photocatalytic conditions are attenuated in an intermolecular competition experiment using two symmetrical diaryliodonium oxidants in one pot (Scheme 2.22).

**Scheme 2.22.** Attenuation of Chemoselectivity Differences Between Thermal and Photocatalytic Reaction Conditions for Intermolecular Competition



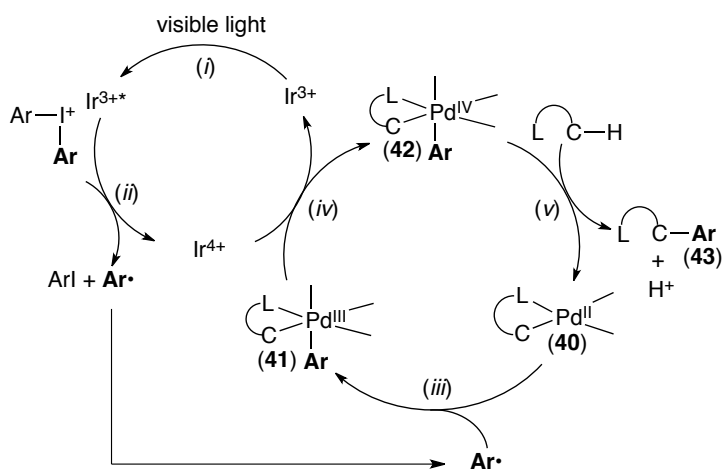
Thus, while chemoselectivities are generally modest under both sets of conditions, the selectivities under photocatalytic conditions do not always mirror those under the thermal reaction conditions, particularly when *ortho* substituents are present. These differences in chemoselectivity provide further support for divergent mechanistic pathways between the thermal and the photocatalytic reaction conditions.

## 2.6 Proposed Reaction Mechanism

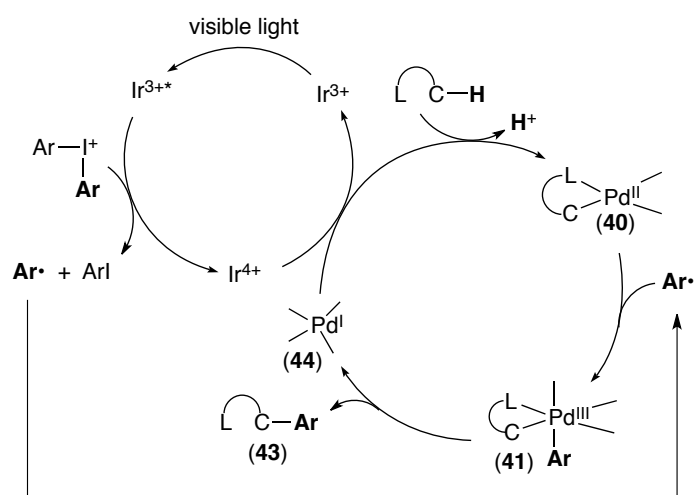
For the described photocatalytic arylation, we preliminarily propose a reaction pathway that merges Pd<sup>II/IV</sup> and Ir<sup>III/IV</sup> catalytic cycles. As shown in Scheme 2.23, ground state Ir<sup>3+</sup> undergoes photoexcitation by visible light (step *i*), and the resultant Ir<sup>3+\*</sup> complex can reduce Ar<sub>2</sub>I<sup>+</sup> to generate Ar•, ArI, and Ir<sup>4+</sup> (step *ii*).<sup>20,30</sup> Ar• could then enter the Pd catalytic cycle by oxidizing cyclopalladated complex **40** (step *iii*). Complex **41** could then be further oxidized to **42** by Ir<sup>4+</sup> (step *iv*), regenerating Ir<sup>3+</sup>. Finally, C–C

bond-forming reductive elimination from **42** would afford product **43** and regenerate Pd<sup>2+</sup> (step v). Importantly, a number of other pathways are also possible and cannot be distinguished based on the current data. For example a Pd<sup>I/III</sup> pathway could also be envisioned (Scheme 2.24).

**Scheme 2.23.** Possible Pd<sup>II/IV</sup> Mechanism for the Pd/Ir-Catalyzed C–H Arylation with Ar<sub>2</sub>I<sup>+</sup>



**Scheme 2.24.** Alternative Pd<sup>I/III</sup> Mechanism for the Pd/Ir-Catalyzed C–H Arylation with Ar<sub>2</sub>I<sup>+</sup>

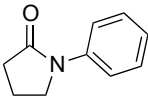
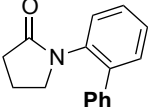
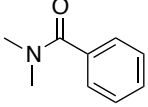
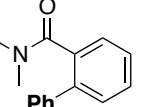
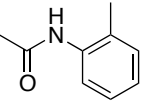
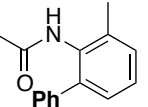
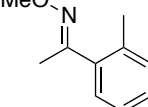
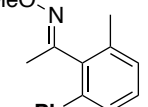
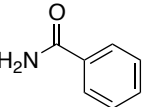
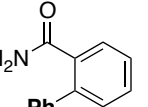
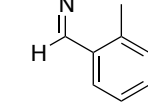
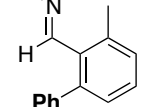
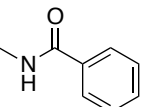
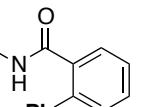
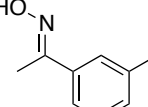
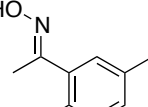


## 2.7 Comparison of $\text{Ph}_2\text{I}^+$ vs $\text{PhN}_2^+$ Reagents

A related room temperature Pd/Ru catalyzed C–H arylation reaction previously reported from our lab was proposed to proceed via a mechanism similar to that shown in Scheme 2.21. However, this transformation used a different  $\text{Ar}^\bullet$  precursor (aryl diazonium salts), photocatalyst ( $\text{Ru}(\text{bpy})_3\text{Cl}_2$ ), Pd catalyst ( $\text{Pd}(\text{OAc})_2$ ) and slightly different optimized reaction conditions. Thus, a final set of studies was conducted to compare these two processes.

As illustrated in Table 2.7, the performance of the two systems is often comparable (*e.g.*, for substrates **9** and **29**). However, for benzamide substrates **17** and **19** and ketoxime ether **27**, the Pd/Ir/ $\text{Ph}_2\text{I}^+$  protocol provided better yields of C–H phenylation. Conversely, the Pd/Ru/ $\text{PhN}_2^+$  system performed better for acetanilide **13**, and it is effective for hydroxyl oxime **45**, a substrate class that undergoes decomposition under the Pd/Ir/ $\text{Ph}_2\text{I}^+$  conditions. Overall, the room-temperature Pd/photocatalyzed C–H arylation methods using  $\text{Ar}_2\text{I}^+$  and  $\text{ArN}_2^+$  reagents are often complementary in terms of substrate scope.<sup>31</sup>

**Table 2.7.** Comparison of Pd/Ir-Catalyzed C–H Phenylation with Ph<sub>2</sub>I<sup>+</sup> vs Pd/Ru-Catalyzed C–H Phenylation with PhN<sub>2</sub><sup>+</sup>

entry	substrate	product	yield <sup>a,b</sup> (Ph <sub>2</sub> I <sup>+</sup> )	yield <sup>a,c</sup> (PhN <sub>2</sub> <sup>+</sup> )	entry	substrate	product	yield <sup>a,b</sup> (Ph <sub>2</sub> I <sup>+</sup> )	yield <sup>a,c</sup> (PhN <sub>2</sub> <sup>+</sup> )
1			89%	91%	5			11%	8%
	(9)	(10)				(21)	(22)		
2			69% <sup>d</sup>	89%	6			52%	23%
	(13)	(14)				(27)	(28)		
3			54%	25%	7			63%	68%
	(17)	(18)				(29)	(30)		
4			52%	38%	8			<1% <sup>e</sup>	66%
	(19)	(20)				(45)	(46)		

<sup>a</sup>GC calibrated yield. <sup>b</sup>General conditions: substrate (1 equiv), [Ph<sub>2</sub>I]OTf (2 equiv), Pd(NO<sub>3</sub>)<sub>2</sub> (0.10 equiv), Ir(ppy)<sub>2</sub>(dtbbpy)PF<sub>6</sub> (0.05 equiv), MeOH (0.2 M in substrate), 26 W lightbulb, 15 h, rt, degassed by sparging with N<sub>2</sub>. <sup>c</sup>General conditions: substrate (1 equiv), [PhN<sub>2</sub>]BF<sub>4</sub> (4 equiv), Pd(OAc)<sub>2</sub> (0.10 equiv), Ru(bpy)<sub>3</sub>Cl<sub>2</sub>·6H<sub>2</sub>O (0.025 equiv), MeOH (0.1 M in substrate), 26 W lightbulb, rt, 15 h, degassed by sparging with N<sub>2</sub>. <sup>d</sup>[Ph<sub>2</sub>I]BF<sub>4</sub> was the oxidant. <sup>e</sup>Product **46** was not detected by GC, and only traces of **45** and 3-methylacetophenone were observed.

## 2.8 Conclusions

In summary, a new photoredox Pd/Ir-catalyzed C–H arylation with diaryliodonium reagents has been described. The unusually low reaction temperature, the requirement for light and a photocatalyst, the inhibitory effect of radical scavengers, and the observed chemoselectivity trends are all consistent with a radical mechanism for this transformation. The characteristics of this transformation stand in contrast to the

analogous thermal reaction that requires a dramatically higher temperature (100 °C) and is believed to proceed *via* an ‘ionic’  $2e^-$  pathway.

This example adds to a growing body of work suggesting that re-routing traditional metal-catalyzed transformations *via* radical pathways can offer major advantages in terms of reaction rates, substrate scope, and functional group tolerance.<sup>18,32</sup>

## 2.9 Experimental Procedures and Characterization Data

### *General Procedures*

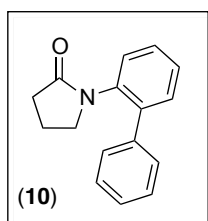
NMR spectra were obtained on a Varian vnmrs 700 (699.76 MHz for  $^1\text{H}$ ; 175.95 MHz for  $^{13}\text{C}$ ; 658.43 for  $^{19}\text{F}$ ), Varian vnmrs 500 (500.10 MHz for  $^1\text{H}$ ; 125.75 MHz for  $^{13}\text{C}$ , 470.56 MHz for  $^{19}\text{F}$ ), Varian Inova 500 (499.90 MHz for  $^1\text{H}$ ; 125.70 MHz for  $^{13}\text{C}$ ), or a Varian MR400 (400.52 MHz for  $^1\text{H}$ ; 100.71 for  $^{13}\text{C}$ , 376.87 MHz for  $^{19}\text{F}$ ) spectrometer.  $^1\text{H}$  NMR chemical shifts are reported in parts per million (ppm) relative to TMS, with the residual solvent peak used as an internal reference. Multiplicities are reported as follows: singlet (s), doublet (d), doublet of doublets (dd), doublet of doublets of doublets (ddd), doublet of triplets (dt), triplet (t), triplet of doublets (td), triplet of triplets (tt), quartet (q), quintet (quin), multiplet (m), and broad resonance (br). IR spectra were obtained on a Perkin-Elmer Spectrum BX FT-IR spectrometer. Melting points were determined with a Mel-Temp 3.0, a Laboratory Devices Inc, USA instrument, and are uncorrected. HRMS data were obtained on a Micromass AutoSpec Ultima Magnetic Sector mass spectrometer. Gas chromatography was carried out on a Shimadzu 17A using a Restek Rtx®-5 (Crossbond 5% diphenyl – 95% dimethyl polysiloxane; 15 m, 0.25 mm ID, 0.25  $\mu\text{m}$  df) column. GC calibrated yields are reported relative to hexadecane as an internal standard.

**Materials and Methods.** Substrates **11**<sup>33</sup> and **23**<sup>34</sup> were prepared according to literature procedures. Substrate **25** was prepared by a palladium-catalyzed Suzuki coupling between 2-methoxyboronic acid and 2-bromopyridine. Oxime ethers **27** and **29** were prepared by the reaction of the corresponding ketones with  $\text{MeONH}_2\cdot\text{HCl}$  in pyridine.<sup>35</sup> The remaining substrates were obtained from Aldrich (**9**, **17**, and **21**), Alfa Aesar (**13** and **15**), or Acros (**19**) and were used as received.  $[\text{Ph}_2\text{I}]\text{BF}_4$  and  $[\text{Mes-I-Ph}]\text{BF}_4$  were

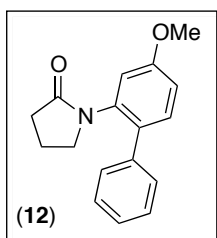
prepared by the reaction of  $\text{PhI}(\text{OAc})_2$  or  $\text{MesI}(\text{OAc})_2$  with  $\text{PhB}(\text{OH})_2$  in the presence of  $\text{BF}_3 \cdot \text{Et}_2\text{O}$ .<sup>36</sup>  $[\text{Ph}_2\text{I}]\text{OTf}$  and  $[\text{Mes}_2\text{I}]\text{OTf}$  were prepared by the reaction of iodobenzene or iodomesitylene with *m*CPBA and benzene or mesitylene in the presence of  $\text{TfOH}$ .<sup>37</sup> Unsymmetrical  $[\text{Ar-I-Ph}]\text{BF}_4$  salts were prepared by the reaction of an aryl iodide with *m*-CPBA and  $\text{PhB}(\text{OH})_2$  in the presence of  $\text{BF}_3 \cdot \text{Et}_2\text{O}$ .<sup>38</sup> Symmetrical  $[\text{Ar}_2\text{I}]\text{BF}_4$  salts were prepared by the reaction of an aryl iodide with *m*-CPBA and the corresponding arylboronic acid in the presence of  $\text{BF}_3 \cdot \text{Et}_2\text{O}$ .<sup>38</sup>  $\text{Pd}(\text{OAc})_2$ , obtained from Pressure Chemical, and  $\text{Pd}(\text{NO}_3)_2$  and  $\text{Ru}(\text{bpy})_3\text{Cl}_2 \cdot 6\text{H}_2\text{O}$ , obtained from Strem, were used as received.  $\text{Ir}(\text{ppy})_3$ <sup>39</sup> and  $\text{Ir}(\text{ppy})_2(\text{dtbbpy})\text{PF}_6$ <sup>40</sup> were prepared according to literature procedures. Solvents were obtained from Fisher Chemical and used without further purification. Flash chromatography was performed on EM Science silica gel 60 (0.040–0.063 mm particle size, 230–400 mesh) and thin layer chromatography was performed on Merck TLC plates pre-coated with silica gel 60 F<sub>254</sub>.

### *Synthesis and Characterization of Products in Table 2.3*

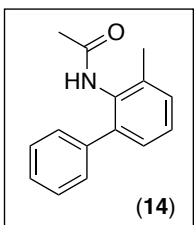
**General Procedure.** Substrate (1 equiv),  $[\text{Ph}_2\text{I}]\text{BF}_4$  or  $[\text{Ph}_2\text{I}]\text{OTf}$  (2 equiv),  $\text{Ir}(\text{ppy})_2(\text{dtbbpy})\text{PF}_6$  (0.05 equiv), and  $\text{Pd}(\text{NO}_3)_2 \cdot 2\text{H}_2\text{O}$  (0.10 equiv) were combined in MeOH in a 4 mL scintillation vial. For substrates containing *N*-acetyl moieties (noted below), MgO (1 equiv) was also included and appeared to help prevent substrate and/or product degradation. The reaction mixture was cooled in an ice bath (to prevent evaporation) and sparged with  $\text{N}_2$  using a submerged needle for 10 min, and the vial was then immediately sealed with a Teflon-lined cap. The vial was placed on a stir plate with two 26 W compact fluorescent light bulbs (one on either side of the vial about 5–8 cm away), and the reaction mixture was allowed to stir at room temperature for 15 h. The reaction mixture was diluted with EtOAc (50 mL) and washed with 10% aqueous  $\text{Na}_2\text{SO}_3$  (2 x 25 mL) and brine (1 x 25 mL). The combined aqueous layers were extracted with EtOAc (3 x 10 mL), and the organic layers were then combined, dried over  $\text{MgSO}_4$ , filtered, concentrated, and purified by column chromatography on silica gel.



**Pyrrolidinone 10.** The general procedure was followed utilizing substrate **9** (80.6 mg, 0.50 mmol, 1.0 equiv),  $[\text{Ph}_2\text{I}]\text{OTf}$  (430 mg, 1.00 mmol, 2 equiv),  $\text{Ir}(\text{ppy})_2(\text{dtbbpy})\text{PF}_6$  (22.8 mg, 0.025 mmol, 0.05 equiv),  $\text{Pd}(\text{NO}_3)_2 \cdot 2\text{H}_2\text{O}$  (13.3 mg, 0.05 mmol, 0.10 equiv), and MeOH (2.5 mL). Product **10** was obtained as a pale yellow oil (96.3 mg, 81% yield,  $R_f = 0.17$  in 20% hexanes/80% Et<sub>2</sub>O). <sup>1</sup>H and <sup>13</sup>C NMR data matched those reported in the literature.<sup>22</sup>

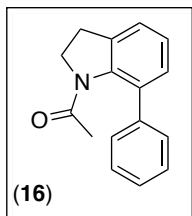


**Pyrrolidinone 12.** The general procedure was followed utilizing substrate **11** (47.8 mg, 0.25 mmol, 1.0 equiv),  $[\text{Ph}_2\text{I}]\text{OTf}$  (215 mg, 0.50 mmol, 2 equiv),  $\text{Ir}(\text{ppy})_2(\text{dtbbpy})\text{PF}_6$  (11.4 mg, 0.0125 mmol, 0.05 equiv),  $\text{Pd}(\text{NO}_3)_2 \cdot 2\text{H}_2\text{O}$  (6.7 mg, 0.025 mmol, 0.10 equiv), and MeOH (1.8 mL). Product **12** was obtained as a pale yellow solid [62.5 mg, 94% yield,  $R_f = 0.10$  in 20% hexanes/80% Et<sub>2</sub>O, mp = 72.9-74.7 °C (lit.<sup>11</sup> 61–64 °C)]. <sup>1</sup>H and <sup>13</sup>C NMR data matched those reported in the literature.<sup>22</sup>

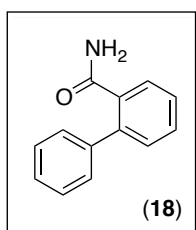


**Acetanilide 14.** The general procedure was followed utilizing substrate **13** (37.3 mg, 0.25 mmol, 1.0 equiv),  $[\text{Ph}_2\text{I}]\text{BF}_4$  (184 mg, 0.50 mmol, 2 equiv),  $\text{Ir}(\text{ppy})_2(\text{dtbbpy})\text{PF}_6$  (11.4 mg, 0.0125 mmol, 0.05 equiv),  $\text{Pd}(\text{NO}_3)_2 \cdot 2\text{H}_2\text{O}$  (6.7 mg, 0.025 mmol, 0.10 equiv), and MeOH (1.25 mL), with the addition of MgO (10.1 mg, 0.25 mmol, 1.0 equiv). Product **14** was obtained as a pale yellow solid [40.6 mg, 72% yield,  $R_f = 0.17$  in 30% hexanes/70% Et<sub>2</sub>O, mp = 134.5-136.0 °C (lit. 139-140 °C)].<sup>13a</sup> <sup>1</sup>H NMR (700 MHz, CD<sub>3</sub>CN): δ 7.64 (br s, 1H); 7.42–7.39 (multiple peaks, 2H); 7.35 (t,  $J = 7.4$  Hz, 1H); 7.32–7.31 (multiple peaks, 2H); 7.27 (d,  $J = 4.9$  Hz, 2H); 7.17 (t,  $J = 4.9$  Hz, 1H); 2.23 (s, 3H); 1.85 (s, 3H). <sup>13</sup>C {<sup>1</sup>H} NMR (176 MHz, CD<sub>3</sub>CN): δ 170.04; 141.30; 140.97; 138.16; 134.58; 130.52; 129.67; 129.03; 128.72; 128.14; 128.05; 22.76; 18.54. IR (thin film, CH<sub>2</sub>Cl<sub>2</sub>) 3246, 3026, 2922, 1652, 1522 cm<sup>-1</sup>. HRMS  $[\text{M}+\text{H}]^+$  Calcd for C<sub>15</sub>H<sub>16</sub>NO: 226.1226; Found: 226.1234.

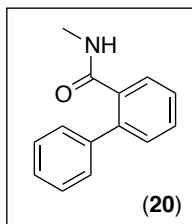




**Acetylidoline 16.** The general procedure was followed utilizing substrate **15** (80.5 mg, 0.50 mmol, 1.0 equiv),  $[\text{Ph}_2\text{I}]\text{BF}_4$  (368 mg, 1.00 mmol, 2 equiv),  $\text{Ir}(\text{ppy})_2(\text{dtbbpy})\text{PF}_6$  (22.8 mg, 0.025 mmol, 0.05 equiv),  $\text{Pd}(\text{NO}_3)_2 \cdot 2\text{H}_2\text{O}$  (26.6 mg, 0.100 mmol, 0.20 equiv), and MeOH (2.5 mL), with the addition of MgO (20.2 mg, 0.50 mmol, 1.0 equiv). Product **16** was obtained as a pale yellow solid [51.7 mg, 44% yield,  $R_f = 0.30$  in 20% hexanes/80% Et<sub>2</sub>O, mp = 116.3-117.8 °C (lit. 117-119 °C)].<sup>10</sup> <sup>1</sup>H and <sup>13</sup>C NMR data matched those reported in the literature.<sup>10</sup>

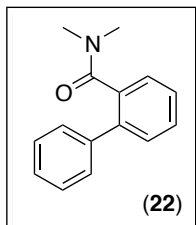


**Benzamide 18.** The general procedure was followed utilizing substrate **17** (33.8 mg, 0.50 mmol, 1.0 equiv),  $[\text{Ph}_2\text{I}]\text{BF}_4$  (368 mg, 1.00 mmol, 2 equiv),  $\text{Ir}(\text{ppy})_2(\text{dtbbpy})\text{PF}_6$  (22.8 mg, 0.025 mmol, 0.05 equiv),  $\text{Pd}(\text{NO}_3)_2 \cdot 2\text{H}_2\text{O}$  (13.3 mg, 0.050 mmol, 0.10 equiv), and MeOH (2.5 mL). Product **18** was obtained as a white solid (39 mg, 40% yield,  $R_f = 0.26$  in 1:1:1 benzene:CH<sub>2</sub>Cl<sub>2</sub>:Et<sub>2</sub>O, mp = 169.0-173.0 °C). <sup>1</sup>H NMR (700 MHz, CDCl<sub>3</sub>): δ 7.79 (d,  $J = 7.7$  Hz, 1H), 7.50 (td,  $J = 7.7, 0.7$  Hz, 1H), 7.46-7.42 (multiple peaks, 5H), 7.39 (m, 1H), 7.37 (dd,  $J = 7.7, 0.7$  Hz, 1H), 5.62 (br s, 1H), 5.25 (br s, 1H). <sup>13</sup>C{<sup>1</sup>H} NMR (176 MHz, CDCl<sub>3</sub>): δ 171.21, 140.15, 139.80, 134.30, 130.54, 130.38, 129.08, 128.77, 128.69, 127.93, 127.62. IR (thin film, CDCl<sub>3</sub>) 3383, 3178, 1653, 1643 cm<sup>-1</sup>. HRMS  $[\text{M}+\text{H}]^+$  Calcd for C<sub>13</sub>H<sub>12</sub>NO: 198.0913; Found: 198.0920.

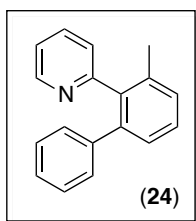


**Benzamide 20.** The general procedure was followed utilizing substrate **19** (67.6 mg, 0.50 mmol, 1.0 equiv),  $[\text{Ph}_2\text{I}]\text{OTf}$  (430 mg, 1.00 mmol, 2 equiv),  $\text{Ir}(\text{ppy})_2(\text{dtbbpy})\text{PF}_6$  (22.8 mg, 0.025 mmol, 0.05 equiv),  $\text{Pd}(\text{NO}_3)_2 \cdot 2\text{H}_2\text{O}$  (13.3 mg, 0.05 mmol, 0.10 equiv), and MeOH (2.5 mL). Product **20** was obtained as a pale yellow solid (56.7 mg, 54% yield,  $R_f = 0.27$  in 20% hexanes/80% Et<sub>2</sub>O, mp = 164.5-166.8 °C). <sup>1</sup>H NMR (400 MHz, CDCl<sub>3</sub>): δ 7.69 (dd,  $J = 7.6, 1.6$  Hz, 1H), 7.47 (td,  $J = 7.6, 1.2$  Hz, 1H), 7.42-7.35 (multiple peaks, 7H), 5.19 (br s, 1H), 2.67 (d,  $J = 4.8$  Hz, 3H). <sup>13</sup>C{<sup>1</sup>H} NMR (100 MHz, CDCl<sub>3</sub>): δ 170.24, 140.12, 139.29, 135.68, 130.11, 130.10, 128.82, 128.60, 128.58,

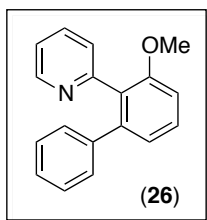
127.75, 127.59, 26.64. IR (thin film, CDCl<sub>3</sub>) 3286, 3060, 2936, 1636, 1540, 1313 cm<sup>-1</sup>. HRMS [M+H]<sup>+</sup> Calcd for C<sub>14</sub>H<sub>14</sub>NO: 212.1070; Found: 212.1074.



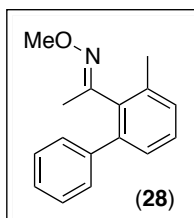
**Benzamide 22.** The general procedure was followed utilizing substrate **21** (74.6 mg, 0.50 mmol, 1.0 equiv), [Ph<sub>2</sub>I]OTf (430 mg, 1.00 mmol, 2 equiv), Ir(ppy)<sub>2</sub>(dtbbpy)PF<sub>6</sub> (22.8 mg, 0.025 mmol, 0.05 equiv), Pd(NO<sub>3</sub>)<sub>2</sub>•2H<sub>2</sub>O (13.3 mg, 0.05 mmol, 0.10 equiv), and MeOH (2.5 mL). Product **22** was obtained as a yellow oil (9.8 mg, 9% yield, R<sub>f</sub> = 0.27 in 20% hexanes/80% Et<sub>2</sub>O). <sup>1</sup>H NMR (400 MHz, CDCl<sub>3</sub>): δ 7.48-7.44 (multiple peaks, 3H), 7.42-7.32 (multiple peaks, 6H), 2.85 (s, 3H), 2.39 (s, 3H). <sup>13</sup>C{<sup>1</sup>H} NMR (100 MHz, CDCl<sub>3</sub>): δ 171.33, 139.93, 138.67, 135.74, 129.30, 128.47, 128.36, 127.70, 127.58, 127.41, 37.94, 24.53. Two aromatic <sup>13</sup>C resonances are coincidentally overlapping. IR (thin film, CDCl<sub>3</sub>) 3057, 2924, 1624, 1394 cm<sup>-1</sup>. HRMS [M+H]<sup>+</sup> Calcd for C<sub>15</sub>H<sub>16</sub>NO: 226.1226; Found: 226.1232.



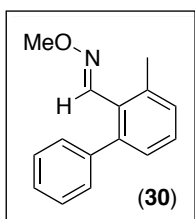
**Pyridine 24.** The general procedure was followed utilizing substrate **23** (84.6 mg, 0.50 mmol, 1.0 equiv), [Ph<sub>2</sub>I]OTf (430 mg, 1.00 mmol, 2 equiv), Ir(ppy)<sub>2</sub>(dtbbpy)PF<sub>6</sub> (22.8 mg, 0.025 mmol, 0.05 equiv), Pd(NO<sub>3</sub>)<sub>2</sub>•2H<sub>2</sub>O (13.3 mg, 0.050 mmol, 0.10 equiv), and MeOH (2.5 mL). Product **24** was obtained as a clear viscous oil (76.0 mg, 62% yield, R<sub>f</sub> = 0.09 in 90% hexanes/10% Et<sub>2</sub>O). <sup>1</sup>H and <sup>13</sup>C NMR data matched those reported in the literature.<sup>22</sup>



**Pyridine 26.** The general procedure was followed utilizing substrate **25** (92.6 mg, 0.50 mmol, 1.0 equiv), [Ph<sub>2</sub>I]OTf (430 mg, 1.00 mmol, 2 equiv), Ir(ppy)<sub>2</sub>(dtbbpy)PF<sub>6</sub> (22.8 mg, 0.025 mmol, 0.05 equiv), Pd(NO<sub>3</sub>)<sub>2</sub>•2H<sub>2</sub>O (13.3 mg, 0.050 mmol, 0.10 equiv), and MeOH (2.5 mL). Product **26** was obtained as a pale yellow solid [88.0 mg, 67% yield, R<sub>f</sub> = 0.11 in 60% hexanes/40% Et<sub>2</sub>O, mp = 83.5-86.4 °C (lit. 77.7-85.4 °C)].<sup>22</sup> <sup>1</sup>H and <sup>13</sup>C NMR data matched those reported in the literature.<sup>22</sup>



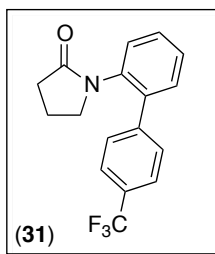
**Oxime ether 28.** The general procedure was followed utilizing substrate **27** (81.6 mg, 0.50 mmol, 1.0 equiv), [Ph<sub>2</sub>I]OTf (430 mg, 1.00 mmol, 2 equiv), Ir(ppy)<sub>2</sub>(dtbbpy)PF<sub>6</sub> (22.8 mg, 0.025 mmol, 0.05 equiv), Pd(NO<sub>3</sub>)<sub>2</sub>•2H<sub>2</sub>O (13.3 mg, 0.050 mmol, 0.10 equiv), and MeOH (2.5 mL). Product **28** was obtained as a colorless oil (71.4 mg, 60% yield, R<sub>f</sub> = 0.14 in 98% hexanes/2% Et<sub>2</sub>O). <sup>1</sup>H NMR (700 MHz, CDCl<sub>3</sub>): δ 7.39–7.36 (multiple peaks, 4H), 7.32 (m, 1H), 7.29 (d, *J* = 7.7 Hz, 1H), 7.23 (dd, *J* = 7.0, 0.7 Hz, 1H), 7.20 (dd, *J* = 7.7, 0.7 Hz, 1H), 3.92 (s, 3H), 2.37 (s, 3H), 1.69 (s, 3H). <sup>13</sup>C{<sup>1</sup>H} NMR (176 MHz, CDCl<sub>3</sub>): δ 156.52, 141.21, 140.97, 136.19, 136.07, 129.38, 129.34, 128.13, 127.94, 127.63, 126.92, 61.62, 20.08, 16.56. IR (thin film, neat) 3060, 2936, 1459, 1041 cm<sup>-1</sup>. HRMS [M+H]<sup>+</sup> Calcd for C<sub>16</sub>H<sub>18</sub>NO: 240.1383; Found: 240.1387.



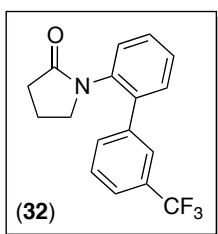
**Oxime ether 30.** The general procedure was followed utilizing substrate **29** (74.6 mg, 0.50 mmol, 1.0 equiv), [Ph<sub>2</sub>I]OTf (430 mg, 1.00 mmol, 2 equiv), Ir(ppy)<sub>2</sub>(dtbbpy)PF<sub>6</sub> (22.8 mg, 0.025 mmol, 0.05 equiv), Pd(NO<sub>3</sub>)<sub>2</sub>•2H<sub>2</sub>O (13.3 mg, 0.050 mmol, 0.10 equiv), and MeOH (2.5 mL). Product **30** was obtained as a colorless oil consisting of a ~1.5:1 mixture of oxime stereoisomers (64.7 mg, 57% yield, R<sub>f</sub> = 0.28 (major) and 0.14 (minor) in 6:1:0.2 hexanes/benzene/methylene chloride). Major Isomer: <sup>1</sup>H NMR (700 MHz, C<sub>6</sub>D<sub>6</sub>): δ 8.26 (s, 1H); 7.22 (m, 2H), 7.09 (tt, *J* = 7.4, 1.4 Hz, 2H); 7.06-7.05 (multiple peaks, 2H); 7.04-7.02 (multiple peaks, 2H); 3.76 (s, 3H), 2.62 (s, 3H). <sup>13</sup>C{<sup>1</sup>H} NMR (100 MHz, CDCl<sub>3</sub>): δ 149.09, 143.18, 140.66, 137.83, 130.33, 129.83, 128.48, 128.12, 127.84, 127.21, 61.85, 22.46. Two aromatic <sup>13</sup>C resonances are coincidentally overlapping. IR (thin film, neat) 3059, 2935, 1460, 1048 cm<sup>-1</sup>. HRMS [M+H]<sup>+</sup> Calcd for C<sub>15</sub>H<sub>16</sub>NO: 226.1226; Found: 226.1227. Minor Isomer: <sup>1</sup>H NMR (700 MHz, C<sub>6</sub>D<sub>6</sub>): δ 7.40 (d, *J* = 7.7 Hz, 2H); 7.24 (s, 1H); 7.19 (t, *J* = 7.7 Hz, 2H); 7.13-7.10 (multiple peaks, 2H); 7.08 (t, *J* = 7.7 Hz, 1H); 6.98 (d, *J* = 7.7 Hz, 1H); 3.66 (s, 3H); 2.22 (s, 3H). <sup>13</sup>C{<sup>1</sup>H} NMR (100 MHz, CDCl<sub>3</sub>): δ 147.58, 140.70, 140.66, 136.43, 130.19, 128.87, 128.84, 128.74, 128.05, 127.36, 126.99, 61.79, 20.13. IR (thin film, CDCl<sub>3</sub>) 3059, 2935, 1460, 1057 cm<sup>-1</sup>. HRMS [M+H]<sup>+</sup> Calcd for C<sub>15</sub>H<sub>16</sub>NO: 226.1226; Found: 226.1228.

### Synthesis and Characterization of Products in Table 2.4

**General Procedure.** Substrate (1 equiv), [Ar<sub>2</sub>I]BF<sub>4</sub> (2 equiv), Ir(ppy)<sub>2</sub>(dtbbpy)PF<sub>6</sub> (0.05 equiv), and Pd(NO<sub>3</sub>)<sub>2</sub>•2H<sub>2</sub>O (0.10 equiv) were combined in MeOH in a 4 mL scintillation vial. The reaction mixture was cooled in an ice bath (to prevent evaporation) and sparged with N<sub>2</sub> using a submerged needle for 10 min, and the vial was then immediately sealed with a Teflon-lined cap. The vial was placed on a stir plate with two 26 W compact fluorescent light bulbs (one on either side of the vial about 5–8 cm away), and the reaction mixture was allowed to stir at room temperature for 15 h. The reaction mixture was diluted with EtOAc (50 mL) and washed with 10% aqueous Na<sub>2</sub>SO<sub>3</sub> (2 x 25 mL) and brine (1 x 25 mL). The combined aqueous layers were extracted with EtOAc (3 x 10 mL), and the organic layers were then combined, dried over MgSO<sub>4</sub>, filtered, concentrated, and purified by column chromatography on silica gel.

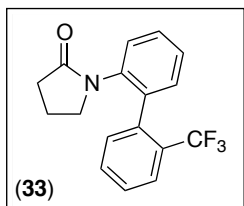


**Pyrrolidinone 31.** The general procedure was followed utilizing substrate **9** (80.6 mg, 0.50 mmol, 1.0 equiv), [(*p*-CF<sub>3</sub>C<sub>6</sub>H<sub>4</sub>)<sub>2</sub>I]BF<sub>4</sub> (504 mg, 1.00 mmol, 2 equiv), Ir(ppy)<sub>2</sub>(dtbbpy)PF<sub>6</sub> (22.8 mg, 0.025 mmol, 0.05 equiv), Pd(NO<sub>3</sub>)<sub>2</sub>•2H<sub>2</sub>O (13.3 mg, 0.050 mmol, 0.10 equiv), and MeOH (2.5 mL). Product **31** was obtained as a tan solid [106 mg, 69% yield, R<sub>f</sub> = 0.17 in 20% hexanes/80% Et<sub>2</sub>O, mp = 87.6-89.2 °C (lit. 86.1–88.0 °C)].<sup>22</sup> <sup>1</sup>H and <sup>13</sup>C NMR data matched those reported in the literature.<sup>22</sup>

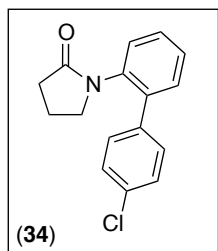


**Pyrrolidinone 32.** The general procedure was followed utilizing substrate **9** (80.6 mg, 0.50 mmol, 1.0 equiv), [(*m*-CF<sub>3</sub>C<sub>6</sub>H<sub>4</sub>)<sub>2</sub>I]BF<sub>4</sub> (504 mg, 1.00 mmol, 2 equiv), Ir(ppy)<sub>2</sub>(dtbbpy)PF<sub>6</sub> (22.8 mg, 0.025 mmol, 0.05 equiv), Pd(NO<sub>3</sub>)<sub>2</sub>•2H<sub>2</sub>O (13.3 mg, 0.050 mmol, 0.10 equiv), and MeOH (2.5 mL). Product **32** was obtained as a tan solid [86.1 mg, 56% yield, R<sub>f</sub> = 0.23 in 20% hexanes/80% Et<sub>2</sub>O, mp = 79.2-83.5 °C]. <sup>1</sup>H NMR (700 MHz, CDCl<sub>3</sub>): δ 7.64 (br s, 1H), 7.62 (d, *J* = 8.4 Hz, 1H), 7.60 (d, *J* = 7.7 Hz, 1H), 7.53 (t, *J* = 7.7 Hz, 1H), 7.45 (m, 1H), 7.41–7.40 (multiple peaks, 2H), 7.33 (d, *J* = 7.7 Hz, 1H), 3.28 (t, *J* = 7.0 Hz, 2H), 2.40 (t, *J* = 8.1 Hz, 2H), 1.91 (tt, *J* = 8.1, 7.0 Hz, 2H). <sup>13</sup>C{<sup>1</sup>H} NMR (176 MHz, CDCl<sub>3</sub>): δ 175.42, 139.84, 138.11, 136.29, 131.80, 130.71 (q,

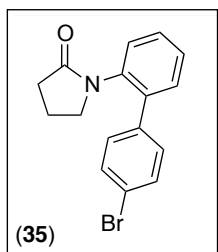
$J_{C-F} = 32$  Hz), 130.60, 129.25, 128.96, 128.30, 128.25, 124.99 (q,  $J_{C-F} = 3.6$  Hz), 124.21 (q,  $J_{C-F} = 3.8$  Hz), 123.97 (q,  $J_{C-F} = 272$  Hz), 50.30, 30.93, 18.83.  $^{19}\text{F}$  NMR (376 MHz,  $\text{CDCl}_3$ ):  $\delta$  -62.65 (s). IR (thin film,  $\text{CDCl}_3$ ) 2918, 1692, 1333, 1117  $\text{cm}^{-1}$ . HRMS  $[\text{M}+\text{H}]^+$  Calcd for  $\text{C}_{17}\text{H}_{15}\text{F}_3\text{NO}$ : 306.1100; Found: 306.1110.



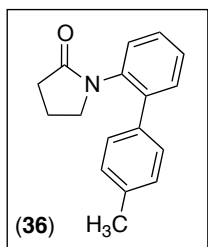
**Pyrrolidinone 33.** The general procedure was followed utilizing substrate **9** (40.3 mg, 0.25 mmol, 1.0 equiv),  $[(o\text{-CF}_3\text{C}_6\text{H}_4)_2\text{I}]\text{BF}_4$  (252 mg, 0.50 mmol, 2 equiv),  $\text{Ir}(\text{ppy})_2(\text{dtbbpy})\text{PF}_6$  (11.4 mg, 0.0125 mmol, 0.05 equiv),  $\text{Pd}(\text{NO}_3)_2 \cdot 2\text{H}_2\text{O}$  (6.7 mg, 0.025 mmol, 0.10 equiv), and MeOH (1.25 mL). Product **33** was obtained as a white solid (35.0 mg, 46% yield,  $R_f = 0.13$  in 20% hexanes/80%  $\text{Et}_2\text{O}$ , mp = 61.8-63.9  $^\circ\text{C}$ ).  $^1\text{H}$  NMR (700 MHz,  $\text{CDCl}_3$ ):  $\delta$  7.76 (d,  $J = 7.7$  Hz, 1H), 7.54 (t,  $J = 7.7$  Hz, 1H), 7.49 (t,  $J = 7.7$  Hz, 1H), 7.46 (td,  $J = 7.7, 1.4$  Hz, 1H), 7.41 (d,  $J = 7.7$  Hz, 1H), 7.36 (td,  $J = 7.4, 1.4$  Hz, 1H), 7.33–7.32 (multiple peaks, 2H), 3.36 (ddd,  $J = 14.0, 7.7, 5.6$  Hz, 1H), 3.03 (ddd,  $J = 14.0, 8.4, 5.6$  Hz, 1H), 2.40 (ddd,  $J = 16.4, 9.1, 6.3$  Hz, 1H), 2.22 (ddd,  $J = 16.4, 9.1, 6.3$  Hz, 1H), 1.94 (m, 1H), 1.67 (m, 1H).  $^{13}\text{C}\{^1\text{H}\}$  NMR (176 MHz,  $\text{CDCl}_3$ ):  $\delta$  175.57, 137.43, 136.99, 136.76, 132.08, 131.25, 131.05 (q,  $J_{C-F} = 2.1$  Hz), 129.25, 128.28 (q,  $J_{C-F} = 30$  Hz), 128.08, 127.96, 127.17, 126.21 (q,  $J_{C-F} = 5.3$  Hz), 124.06 (q,  $J_{C-F} = 274$  Hz), 49.90, 30.98, 19.05.  $^{19}\text{F}$  NMR (376 MHz,  $\text{CDCl}_3$ ):  $\delta$  -57.09 (s). IR (thin film,  $\text{CDCl}_3$ ) 2920, 1697, 1313, 1111  $\text{cm}^{-1}$ . HRMS  $[\text{M}+\text{H}]^+$  Calcd for  $\text{C}_{17}\text{H}_{15}\text{F}_3\text{NO}$ : 306.1100; Found: 306.1112.



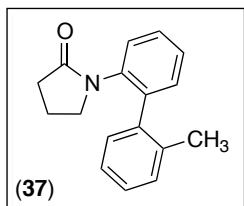
**Pyrrolidinone 34.** The general procedure was followed utilizing substrate **9** (80.6 mg, 0.50 mmol, 1.0 equiv),  $[(p\text{-ClC}_6\text{H}_4)_2\text{I}]\text{BF}_4$  (437 mg, 1.00 mmol, 2 equiv),  $\text{Ir}(\text{ppy})_2(\text{dtbbpy})\text{PF}_6$  (22.8 mg, 0.025 mmol, 0.05 equiv),  $\text{Pd}(\text{NO}_3)_2 \cdot 2\text{H}_2\text{O}$  (13.3 mg, 0.050 mmol, 0.10 equiv), and MeOH (2.5 mL). Product **34** was obtained as a tan solid [104 mg, 77% yield,  $R_f = 0.13$  in 20% hexanes/80%  $\text{Et}_2\text{O}$ , mp = 95.6-97.4  $^\circ\text{C}$  (lit. 93.9-96.0  $^\circ\text{C}$ )].<sup>22</sup>  $^1\text{H}$  and  $^{13}\text{C}$  NMR data matched those reported in the literature.<sup>22</sup>



**Pyrrolidinone 35.** The general procedure was followed utilizing substrate **9** (80.6 mg, 0.50 mmol, 1.0 equiv), [*p*-BrC<sub>6</sub>H<sub>4</sub>)<sub>2</sub>I]BF<sub>4</sub> (526 mg, 1.00 mmol, 2 equiv), Ir(ppy)<sub>2</sub>(dtbbpy)PF<sub>6</sub> (22.8 mg, 0.025 mmol, 0.05 equiv), Pd(NO<sub>3</sub>)<sub>2</sub>•2H<sub>2</sub>O (13.3 mg, 0.050 mmol, 0.10 equiv), and MeOH (2.5 mL). Product **35** was obtained as a pale yellow oil (125 mg, 79% yield, R<sub>f</sub> = 0.13 in 20% hexanes/80% Et<sub>2</sub>O). <sup>1</sup>H NMR (500 MHz, CDCl<sub>3</sub>): δ 7.54 (d, *J* = 8.5 Hz, 2H), 7.44–7.35 (multiple peaks, 3H) 7.33 (d, *J* = 7.5 Hz, 1H), 7.27 (d, *J* = 8.5 Hz, 2H), 3.27 (t, *J* = 7.0 Hz, 2H), 2.44 (t, *J* = 8.0 Hz, 2H), 1.93 (tt, *J* = 8.0, 7.0 Hz, 2H). <sup>13</sup>C{<sup>1</sup>H} NMR (126 MHz, CDCl<sub>3</sub>): δ 175.61, 138.48, 138.01, 136.18, 131.56, 130.61, 130.00, 128.95, 128.40, 128.18, 121.87, 50.26, 31.09, 18.94. IR (thin film, neat) 2879, 1680, 1402 cm<sup>-1</sup>. HRMS [M+H]<sup>+</sup> Calcd for C<sub>16</sub>H<sub>15</sub>BrNO: 316.0332; Found: 316.0340.

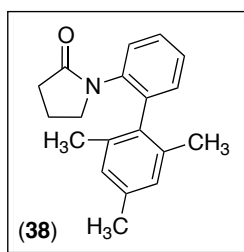


**Pyrrolidinone 36.** The general procedure was followed utilizing substrate **9** (80.6 mg, 0.50 mmol, 1.0 equiv), [*p*-MeC<sub>6</sub>H<sub>4</sub>)<sub>2</sub>I]BF<sub>4</sub> (396 mg, 1.00 mmol, 2 equiv), Ir(ppy)<sub>2</sub>(dtbbpy)PF<sub>6</sub> (22.8 mg, 0.025 mmol, 0.05 equiv), Pd(NO<sub>3</sub>)<sub>2</sub>•2H<sub>2</sub>O (13.3 mg, 0.050 mmol, 0.10 equiv), and MeOH (2.5 mL). Product **36** was obtained as a tan solid (109.8 mg, 87% yield, R<sub>f</sub> = 0.17 in 20% hexanes/80% Et<sub>2</sub>O, mp = 78.6-80.4 °C). <sup>1</sup>H NMR (700 MHz, CDCl<sub>3</sub>): δ 7.40-7.35 (multiple peaks, 3H), 7.31 (d, *J* = 7.3 Hz, 1H), 7.27 (d, *J* = 8.0 Hz, 2H), 7.20 (d, *J* = 8.0 Hz, 2H), 3.22 (t, *J* = 6.9 Hz, 2H), 2.43 (t, *J* = 8.0 Hz, 2H), 2.39 (s, 3H), 1.88 (tt, *J* = 8.0, 6.9 Hz, 2H). <sup>13</sup>C{<sup>1</sup>H} NMR (176 MHz, CDCl<sub>3</sub>): δ 175.61, 139.52, 137.28, 136.27, 136.16, 130.86, 129.12, 128.34, 128.30, 128.18, 127.98, 50.06, 31.20, 21.18, 18.97. IR (thin film, CDCl<sub>3</sub>) 3026, 2920, 1694, 1487, 1407, 1301 cm<sup>-1</sup>. HRMS [M+H]<sup>+</sup> Calcd for C<sub>17</sub>H<sub>18</sub>NO: 252.1383; Found: 252.1391.

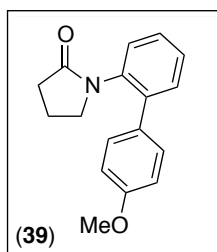


**Pyrrolidinone 37.** The general procedure was followed utilizing substrate **9** (80.6 mg, 0.50 mmol, 1.0 equiv), [*o*-MeC<sub>6</sub>H<sub>4</sub>)<sub>2</sub>I]BF<sub>4</sub> (396 mg, 1.00 mmol, 2 equiv), Ir(ppy)<sub>2</sub>(dtbbpy)PF<sub>6</sub> (22.8 mg, 0.025 mmol, 0.05 equiv), Pd(NO<sub>3</sub>)<sub>2</sub>•2H<sub>2</sub>O (13.3 mg, 0.050 mmol, 0.10

equiv), and MeOH (2.5 mL). Product **37** was obtained as a pale yellow oil (107 mg, 85% yield,  $R_f = 0.20$  in 20% hexanes/80% Et<sub>2</sub>O). NMR (500 MHz, CDCl<sub>3</sub>):  $\delta$  7.40 (ddd,  $J = 7.7, 7.0, 1.4$  Hz, 1H), 7.36 (dd,  $J = 8.4, 1.4$  Hz, 1H), 7.34 (td,  $J = 7.7, 1.4$  Hz, 1H), 7.27–7.24 (multiple peaks, 3H), 7.19 (m, 1H), 7.16 (d, 7.0 Hz, 1H), 3.23 (ddd,  $J = 9.1, 8.4, 5.6$  Hz, 1H), 3.09 (ddd,  $J = 9.1, 7.7, 5.6$  Hz, 1H) 2.32 (m, 2H), 2.15 (s, 3H), 1.82 (m, 1H), 1.75 (m, 1H). <sup>13</sup>C{<sup>1</sup>H} NMR (126 MHz, CDCl<sub>3</sub>):  $\delta$  175.10, 138.89, 138.60, 136.96, 135.88, 131.11, 130.13, 129.39, 128.3, 128.1, 127.72, 127.29, 125.47, 49.94, 31.15, 19.93, 19.02. IR (thin film, neat) 2952, 1696, 1398 cm<sup>-1</sup>. HRMS [M+H]<sup>+</sup> Calcd for C<sub>17</sub>H<sub>18</sub>NO: 252.1383; Found: 252.1392.



**Pyrrolidinone 38.** The general procedure was followed utilizing substrate **9** (40.3 mg, 0.25 mmol, 1.0 equiv), [Mes<sub>2</sub>I]OTf (257 mg, 0.50 mmol, 2 equiv), Ir(ppy)<sub>2</sub>(dtbbpy)PF<sub>6</sub> (11.3 mg, 0.0125 mmol, 0.05 equiv), Pd(NO<sub>3</sub>)<sub>2</sub>•2H<sub>2</sub>O (6.7 mg, 0.025 mmol, 0.10 equiv), and MeOH (1.25 mL). Product **38** was obtained as a white solid (8 mg, 11% yield,  $R_f = 0.17$  in 96% CH<sub>2</sub>Cl<sub>2</sub>/4% Et<sub>2</sub>O, mp = 121.2–123.8 °C). <sup>1</sup>H NMR (700 MHz, CDCl<sub>3</sub>):  $\delta$  7.44–7.39 (multiple peaks, 2H), 7.34 (td,  $J = 7.5, 1.5$  Hz, 1H), 7.13 (dd,  $J = 7.5, 1.2$  Hz, 1H), 6.92 (s, 2H), 3.12 (t,  $J = 6.9$  Hz, 2H), 2.36 (t,  $J = 8.0$  Hz, 2H), 2.34 (s, 3H), 1.98 (s, 6H), 1.80 (tt,  $J = 8.0, 6.9$  Hz, 2H). <sup>13</sup>C{<sup>1</sup>H} NMR (176 MHz, CDCl<sub>3</sub>):  $\delta$  174.82, 137.32, 137.16, 137.01, 136.23, 135.62, 131.27, 128.25, 128.06, 127.97, 127.33, 49.16, 31.35, 21.06, 20.41, 19.07. IR (thin film, CH<sub>2</sub>Cl<sub>2</sub>) 2918, 1699, 1398, 1301 cm<sup>-1</sup>. HRMS [M+H]<sup>+</sup> Calcd for C<sub>19</sub>H<sub>22</sub>NO: 280.1699; Found: 280.1705.



**Pyrrolidinone 39.** The general procedure was followed utilizing substrate **9** (80.6 mg, 0.50 mmol, 1.0 equiv), [(*p*-OMeC<sub>6</sub>H<sub>4</sub>)<sub>2</sub>I]BF<sub>4</sub> (428 mg, 1.00 mmol, 2 equiv), Ir(ppy)<sub>2</sub>(dtbbpy)PF<sub>6</sub> (22.8 mg, 0.025 mmol, 0.05 equiv), Pd(NO<sub>3</sub>)<sub>2</sub>•2H<sub>2</sub>O (13.3 mg, 0.050 mmol, 0.10 equiv), and MeOH (2.5 mL). Product **39** was obtained as a tan viscous oil (54.3 mg, 41% yield,  $R_f = 0.07$  in 20% hexanes/80% Et<sub>2</sub>O). <sup>1</sup>H and <sup>13</sup>C NMR data matched those reported in the literature.<sup>22</sup>

*Experimental Details for Table 2.5*

**Ionic/Thermal Procedure for Reactions in Table 2.5 (entries 1–3).** Substrate **23** (8.5 mg, 0.050 mmol, 1 equiv), [Ph<sub>2</sub>I]BF<sub>4</sub> (20.2 mg, 0.055 mmol, 1.1 equiv), Pd(OAc)<sub>2</sub> (1.1 mg, 0.005 mmol, 0.10 equiv), and galvinoxyl (0 or 5.3 mg; 0 or 0.0125 mmol; 0 or 0.25 equiv) or TEMPO (0 or 7.8 mg; 0 or 0.050 mmol; 0 or 1.0 equiv) were combined in AcOH (0.42 mL) in a 4 mL scintillation vial. The reaction was heated to 100 °C for 15 h, then quenched with 10% aqueous Na<sub>2</sub>SO<sub>3</sub> (0.25 mL), diluted with EtOAc (3.5 mL), and analyzed by GC-FID. GC calibrated yields are reported relative to hexadecane as an internal standard. The yields reported in Table 2.5 are the averages of three separate trials. These conditions are similar to those reported previously for 2-arylpyridine substrates,<sup>10</sup> however, the catalyst loading was increased to 10% (instead of 5%) to more closely resemble the conditions of the photocatalytic/radical trials.

**Radical/Photocatalytic Procedure for Reactions in Table 2.5 (entries 4–8).** Substrate **23** (8.5 mg, 0.050 mmol, 1 equiv), [Ph<sub>2</sub>I]BF<sub>4</sub> (36.8 mg, 0.100 mmol, 2 equiv), Ir(ppy)<sub>2</sub>(dtbbpy)PF<sub>6</sub> (2.3 mg, 0.0025 mmol, 0.05 equiv), Pd(NO<sub>3</sub>)<sub>2</sub>•2H<sub>2</sub>O (1.3 mg, 0.005 mmol, 0.10 equiv), and galvinoxyl (0, 2.1, or 5.3 mg; 0, 0.005, or 0.0125 mmol; 0, 0.10, or 0.25 equiv) or TEMPO (0, 3.9, or 7.8 mg; 0, 0.025, or 0.050 mmol; 0, 0.50, or 1.0 equiv) were combined in MeOH (0.25 mL) in a 4 mL scintillation vial. The reaction mixture was cooled in an ice bath (to prevent evaporation) and sparged with N<sub>2</sub> using a submerged needle for 1 min, and the vial was then immediately sealed with a Teflon-lined cap. The vial was placed on a stir plate with two 26 W compact fluorescent light bulbs (one on either side of the vial about 5–8 cm away), and the reaction mixture was allowed to stir at room temperature for 15 h. Reactions were then quenched with 10% aqueous Na<sub>2</sub>SO<sub>3</sub> (0.25 mL), diluted with EtOAc (3.5 mL), and analyzed by GC-FID. GC calibrated yields are reported relative to hexadecane as an internal standard. The yields reported in Table 2.5 are the averages of three separate trials.

*Experimental Details for Table 2.6 and Scheme 2.22*

**Radical/Photocatalytic Procedure for Reactions in Table 2.6 (even-numbered entries).** Substrate **9** (8.1 mg, 0.050 mmol, 1 equiv), [Ar–I–Ph]BF<sub>4</sub> (0.100 mmol, 2



equiv), Ir(ppy)<sub>2</sub>(dtbbpy)PF<sub>6</sub> (2.3 mg, 0.0025 mmol, 0.05 equiv), and Pd(NO<sub>3</sub>)<sub>2</sub>•2H<sub>2</sub>O (1.3 mg, 0.005 mmol, 0.10 equiv) were combined in MeOH (0.25 mL) in a 4 mL scintillation vial. The reaction mixture was cooled in an ice bath (to prevent evaporation) and sparged with N<sub>2</sub> using a submerged needle for 1 min, and the vial was then immediately sealed with a Teflon-lined cap. The vial was placed on a stir plate with two 26 W compact fluorescent light bulbs (one on either side of the vial about 5–8 cm away), and the reaction mixture was allowed to stir at room temperature for 15 h. Reactions were then quenched with 10% aq. Na<sub>2</sub>SO<sub>3</sub> (0.25 mL), diluted with EtOAc (3.5 mL), and analyzed by GC-FID. GC calibrated yields are reported relative to hexadecane as an internal standard.

**Ionic/Thermal Procedure for Reactions in Table 2.6 (odd-numbered entries).**

Substrate **9** (8.1 mg, 0.050 mmol, 1 equiv), [ArI–Ph]BF<sub>4</sub> (0.100 mmol, 2 equiv), Pd(OAc)<sub>2</sub> (1.1 mg, 0.005 mmol, 0.10 equiv), and NaHCO<sub>3</sub> (6.3 mg, 0.075 mmol, 1.5 equiv) were combined in toluene (0.42 mL). The reaction was heated to 100 °C for 15 h, then quenched with 10% aq. Na<sub>2</sub>SO<sub>3</sub> (0.25 mL), diluted with EtOAc (3.5 mL), and analyzed by GC-FID. GC calibrated yields are reported relative to hexadecane as an internal standard. These conditions are similar to the thermal conditions reported previously for substrate **1**;<sup>10</sup> however, the equivalents of oxidant were increased to 2 (instead of 1.5) and the catalyst loading was increased to 10% (instead of 5%) to more closely resemble the conditions of the photocatalytic/radical trials.

*Experimental Details for Table 2.7*

**PhN<sub>2</sub><sup>+</sup> procedure.**<sup>22</sup> Substrate (0.050 mmol, 1 equiv), Pd(OAc)<sub>2</sub> (1.1 mg, 0.005 mmol, 0.10 equiv), Ru(bpy)<sub>3</sub>Cl<sub>2</sub>•6H<sub>2</sub>O (0.94 mg, 0.00125 mmol, 0.025 equiv), and [PhN<sub>2</sub>]BF<sub>4</sub> (38.4 mg, 0.200 mmol, 4 equiv) were combined in MeOH (500 μL) in a 4 mL scintillation vial. The reaction mixture was cooled in an ice bath (to prevent evaporation) and sparged with N<sub>2</sub> using a submerged needle for 1 min, and the vial was then immediately sealed with a Teflon-lined cap. The vial was placed on a stir plate with two 26 W compact fluorescent light bulbs (one on either side of the vial about 5–8 cm away), and the reaction mixture was allowed to stir at room temperature for 15 h. Reactions were

then quenched with 10% aq.  $\text{Na}_2\text{SO}_3$  (0.25 mL), diluted with EtOAc (3.5 mL), and analyzed by GC-FID. GC calibrated yields are reported relative to hexadecane as an internal standard.

**$\text{Ph}_2\text{I}^+$  procedure.** GC calibrated yields were obtained from the reactions described above for Table 2.3 and are reported relative to hexadecane as an internal standard.

## 2.10 References

1. (a) Hajduk, P. J.; Bures, M.; Praestgaard, J.; Fesik, S. W. Privileged Molecules for Protein Binding Identified from NMR-Based Screening. *J. Med. Chem.* **2000**, *43*, 3443. (b) Horton, D. A.; Bourne, G. T.; Smythe, M. L. The Combinatorial Synthesis of Bicyclic Privileged Structures or Privileged Substructures. *Chem. Rev.* **2003**, *103*, 893. (c) Costantino, L.; Barlocco, D. Privileged Structures as Leads in Medicinal Chemistry. *Curr. Med. Chem.* **2006**, *13*, 65. (d) Welsch, M. E.; Snyder, S. A.; Stockwell, B. R. Privileged Scaffolds for Library Design and Drug Discovery. *Curr. Opin. Chem. Biol.* **2010**, *14*, 347.
2. Hassan, J.; Sévignon, M.; Gozzi, C.; Schulz, E.; Lemaire, M. Aryl–Aryl Bond Formation One Century after the Discovery of the Ullmann Reaction. *Chem. Rev.* **2002**, *102*, 1359.
3. Ciba-Geigy Corp., US-5399578.
4. (a) Mazzocca, A.; Giusti, S.; Hamilton, A. D.; Sebti, S. M.; Pantaleo, P.; Carloni, V. Growth Inhibition by the Farnesyltransferase Inhibitor FTI-277 Involves Bcl-2 Expression and Defective Association with Raf-1 in Liver Cancer Cell Lines. *Mol. Pharmacol.* **2003**, *63*, 159. (b) Bolick, S. C. E.; Landowski, T. H.; Boulware, D.; Oshiro, M. M.; Ohkanda, J.; Hamilton, A. D.; Sebti, S. M.; Dalton, W. S. The Farnesyl Transferase Inhibitor, FTI-227, Inhibits Growth and Induces Apoptosis in Drug-Resistant Myeloma Tumor Cells. *Leukemia* **2003**, *17*, 451.
5. Mah, R.; Gerspacher, M.; von Sprecher, A.; Stutz, S.; Tschinke, V.; Anderson, G. P.; Bertrand, C.; Subramanian, N.; Ball, H. A. Biphenyl Derivatives as Novel Dual NK1/NK2-Receptor Antagonists. *Bioorg. Med. Chem. Lett.* **2002**, *12*, 2065.
6. (a) Alberico, D.; Scott, M. E.; Lautens, M. Aryl–Aryl Bond Formation by Transition-Metal-Catalyzed Direct Arylation. *Chem. Rev.* **2007**, *107*, 174. (b) McGlacken, G. P.; Bateman, L. M. Recent Advances in Aryl–Aryl Bond Formation by Direct Arylation. *Chem. Soc. Rev.* **2009**, *38*, 2447.
7. (a) Chen, X.; Engle, K. M.; Wang, D.-H.; Yu, J.-Q. Palladium(II)-Catalyzed C–H Activation/C–C Cross-Coupling Reactions: Versatility and Practicality. *Angew. Chem., Int. Ed.* **2009**, *48*, 5094. (b) Lyons, T. W.; Sanford, M. S. Palladium-Catalyzed Ligand-Directed C–H Functionalization Reactions. *Chem. Rev.* **2010**, *110*, 1147.
8. (a) Ames, D. E.; Opalko, A. Synthesis of Dibenzofurans by Palladium-Catalyzed Intramolecular Dehydrobromination of 2-Bromophenyl Phenyl Ethers. *Synthesis*, **1983**, 234. (b) Ames, D. E.; Opalko, A. Palladium-Catalyzed Cyclization of 2-Substituted Halogenoarenes by Dehydrohalogenation. *Tetrahedron* **1984**, *40*, 1919.
9. Satoh, T.; Kawamura, Y.; Miura, M.; Nomura, M. Palladium-Catalyzed Regioselective Mono- and Diarylation Reactions of 2-Phenylphenols and Naphthols with Aryl Halides. *Angew. Chem., Int. Ed.* **1997**, *36*, 1740.

10. Kalyani, D.; Deprez, N. R.; Desai, L. V.; Sanford, M. S. Oxidative C–H Activation/C–C Bond Forming Reactions: Synthetic Scope and Mechanistic Insights. *J. Am. Chem. Soc.* **2005**, *127*, 7330.
11. Other Pd-catalyzed C–H arylations using Ar<sub>2</sub>I<sup>+</sup>: (a) Daugulis, O.; Zaitsev, V. Anilide *ortho*-Arylation by Using C–H Activation Methodology. *Angew. Chem., Int. Ed.* **2005**, *44*, 4046. (b) Deprez, N. R.; Kalyani, D.; Krause, A.; Sanford, M. S. Room Temperature Palladium-Catalyzed 2-Arylation of Indoles. *J. Am. Chem. Soc.* **2006**, *128*, 4972. (c) Spencer, J.; Chowdhry, B. Z.; Mallet, A. I.; Rathnam, R. P.; Adatia, T.; Bashall, A.; Rominger, F. C–H Activations on 1*H*-1,4-Benzodiazepin-2(3*H*)-one Template. *Tetrahedron* **2008**, *64*, 6082. (d) Xiao, B.; Fu, Y.; Xu, J.; Gong, T.-J.; Dai, J.-J.; Yi, J.; Liu, L. Pd(II)-Catalyzed C–H Activation/Aryl–Aryl Coupling of Phenol Esters. *J. Am. Chem. Soc.* **2009**, *132*, 468. (e) Wagner, A.; Sanford, M. S. Palladium-Catalyzed C–H Arylation of 2,5-Substituted Pyrroles. *Org. Lett.* **2011**, *13*, 288. (f) Hickman, A. J.; Sanford, M. S. Catalyst Control of Site Selectivity in the Pd<sup>II/IV</sup>-Catalyzed Direct Arylation of Naphthalene. *ACS Catal.* **2011**, *1*, 170.
12. For Cu-catalyzed C–H arylation reactions with Ar<sub>2</sub>I<sup>+</sup> see: (a) Phipps, R. J.; Grimster, N. P.; Gaunt, M. J. Cu(II)-Catalyzed Direct and Site-Selective Arylation of Indoles Under Mild Conditions. *J. Am. Chem. Soc.* **2008**, *130*, 8172. (b) Phipps, R. J.; Gaunt, M. J. A Meta-Selective Copper-Catalyzed C–H Bond Arylation. *Science* **2009**, *323*, 1593 (c) Ciana, C.-L.; Phipps, R. J.; Brandt, J. R.; Meyer, F.-M.; Gaunt, M. J. A Highly *Para*-Selective Copper(II)-Catalyzed Direct Arylation of Aniline and Phenol Derivatives. *Angew. Chem., Int. Ed.* **2011**, *50*, 458 (d) Duong, H. A.; Gilligan, R. E.; Cooke, M. L.; Phipps, R. J.; Gaunt, M. J. Copper(II)-Catalyzed *meta*-Selective Direct Arylation of  $\alpha$ -Aryl Carbonyl Compounds. *Angew. Chem., Int. Ed.* **2011**, *50*, 463.
13. (a) Daugulis, O.; Zaitsev, V. G. Anilide *ortho*-Arylation by Using C–H Activation Methodology. *Angew. Chem., Int. Ed.* **2005**, *44*, 4046. (b) Shabashov, D.; Daugulis, O. Catalytic Coupling of C–H and C–I Bonds Using Pyridine As a Directing Group. *Org. Lett.* **2005**, *7*, 3657. (c) Chiong, H. A.; Pham, Q.-N.; Daugulis, O. Two Methods for Direct *ortho*-Arylation of Benzoic Acids. *J. Am. Chem. Soc.* **2007**, *129*, 9879. (d) Yang, S.; Li, B.; Wan, X.; Shi, Z. Ortho Arylation of Acetanilides via Pd(II)-Catalyzed C–H Functionalization. *J. Am. Chem. Soc.* **2007**, *129*, 6066. (e) Shabashov, D.; Maldonado, J. R. M.; Daugulis, O. Carbon–Hydrogen Bond Functionalization Approach for the Synthesis of Fluorenones and *ortho*-Arylated Benzonitriles. *J. Org. Chem.* **2008**, *73*, 7818. (f) Daugulis, O.; Do, H.-Q.; Shabashov, D. Palladium- and Copper-Catalyzed Arylation of Carbon–Hydrogen Bonds. *Acc. Chem. Res.* **2009**, *42*, 1074.
14. (a) Shi, Z.; Li, B.; Wan, X.; Cheng, J.; Fang, Z.; Cao, B.; Qin, C.; Wang, Y. Suzuki-Miyaura Coupling Reaction by PdII-Catalyzed Aromatic C–H Bond Activation Directed by an *N*-Alkyl Acetamino Group. *Angew. Chem., Int. Ed.* **2007**, *46*, 5554. (b) Giri, R.; Maugel, N.; Li, J.-J.; Wang, D. H.; Breazzano, S. P.; Saunders, L. B.; Yu, J.-Q. Palladium-Catalyzed Methylation and Arylation of sp<sup>2</sup>

- and  $sp^3$  C–H Bonds in Simple Carboxylic Acids. *J. Am. Chem. Soc.* **2007**, *129*, 3510. (c) Kirchberg, S.; Vogler, T.; Studer, A. Directed Palladium-Catalyzed Oxidative C–H Arylation of (Hetero)arenes with Arylboronic Acids by Using TEMPO. *Synlett* **2008**, 2841. (d) Wang, D.-H.; Mei, T.-S.; Yu, J.-Q. Versatile Pd(II)-Catalyzed C–H Activation/Aryl–Aryl Coupling of Benzoic and Phenyl Acetic Acids. *J. Am. Chem. Soc.* **2008**, *130*, 17676. (e) Wang, D.-H.; Wasa, M.; Giri, R.; Yu, J.-Q. Pd(II)-Catalyzed Cross-Coupling of  $sp^3$  C–H Bonds with  $sp^2$  and  $sp^3$  Boronic Acids Using Air as the Oxidant. *J. Am. Chem. Soc.* **2008**, *130*, 7190. (f) Sun, C.-L.; Liu, N.; Li, B.-J.; Yu, D.-G.; Wang, Y.; Shi, Z.-J. Pd-Catalyzed C–H Functionalizations of *O*-Methyl Oximes with Arylboronic Acids. *Org. Lett.* **2010**, *12*, 184. (g) Chu, J.-H.; Lin, P.-S.; Wu, M.-J. Palladium(II)-Catalyzed *Ortho* Arylation of 2-Phenoxy pyridines with Potassium Aryltrifluoroborates via C–H Functionalization. *Organometallics* **2010**, *29*, 4058. (h) Engle, K. M.; Thuy-Boun, P. S.; Dang, M.; Yu, J.-Q. Ligand-Accelerated Cross-Coupling of  $C(sp^2)$ –H Bonds with Arylboron Reagents. *J. Am. Chem. Soc.* **2011**, *133*, 18183. (i) Dai, H.-X.; Stepan, A. F.; Plummer, M. S.; Zhang, Y.-H.; Yu, J.-Q. Divergent C–H Functionalizations Directed by Sulfonamide Pharmacophores: Late-Stage Diversification as a Tool for Drug Discovery. *J. Am. Chem. Soc.* **2011**, *133*, 7222. (j) Romero-Revilla, J. A.; García-Rubia, A.; Arrayás, R.; Fernández-Ibáñez, M. Á.; Carretero, J. C. Palladium-Catalyzed Coupling of Arene C–H Bonds with Methyl- and Arylboron Reagents Assisted by the Removable 2-Pyridylsulfinyl Group. *J. Org. Chem.* **2011**, *76*, 9525. (k) Wasa, M.; Chan, K. S. L.; Yu, J.-Q. Pd(II)-catalyzed Cross-coupling of  $C(sp^2)$ –H Bonds and Alkyl-, Aryl-, and Vinyl–Boron Reagents via Pd(II)/Pd(0) Catalysis. *Chem. Lett.* **2011**, *40*, 1004. (l) Koley, M.; Dastbaravardeh, N.; Schnürch, M.; Mihovilovic, M. D. Palladium(II)-Catalyzed Regioselective *Ortho* Arylation of  $sp^2$  C–H Bonds of *N*-Aryl-2-amino Pyridine Derivatives. *ChemCatChem* **2012**, *4*, 1345. (m) Zhang, X.; Yu, M.; Yao, J.; Zhang, Y. Palladium-Catalyzed Regioselective Arylation of Arene C–H Bond Assisted by the Removable 2-Pyridylsulfinyl Group. *Synlett* **2012**, *23*, 463.
15. For examples of Pd-catalyzed C–H arylation with arylboronic acids at mild temperatures ( $\leq 40$  °C) see (a) Nishikata, T.; Abela, A. R.; Huang, S.; Lipshutz, B. H. Cationic Palladium(II) Catalysis: C–H Activation/Suzuki–Miyaura Couplings at Room Temperature. *J. Am. Chem. Soc.* **2010**, *132*, 4978. (b) Tredwell, M. J.; Gulias, M.; Bremeyer, N. G.; Johansson, C. C. C.; Collins, B. S. L.; Gaunt, M. J. Palladium(II)-Catalyzed C–H Bond Arylation of Electron-Deficient Arenes at Room Temperature. *Angew. Chem., Int. Ed.* **2011**, *50*, 1076.
  16. Xiao, B.; Fu, Y.; Xu, J.; Gong, T.-J.; Dai, J.-J.; Yi, J.; Liu, L. Pd(II)-Catalyzed C–H Activation/Aryl–Aryl Coupling of Phenol Esters. *J. Am. Chem. Soc.* **2009**, *132*, 468.
  17. Deprez, N. R.; Sanford, M. S. Synthetic and Mechanistic Studies of Pd-Catalyzed C–H Arylation with Diaryliodonium Salts: Evidence for a Bimetallic High Oxidation State Pd Intermediate. *J. Am. Chem. Soc.* **2009**, *131*, 11234.

18. For recent reviews, see (a) Ford, L.; Jahn, U. Radicals and Transition-Metal Catalysis: An Alliance Par Excellence to Increase Reactivity and Selectivity in Organic Chemistry. *Angew. Chem., Int. Ed.* **2009**, *48*, 6386 (b) Jahn, U. Radicals in Transition Metal Catalyzed Reactions? Transition Metal Catalyzed Radical Reactions? A Fruitful Interplay Anyway. Part 1: Radical Catalysis by Group 4 to Group 7 Elements. *Top. Curr. Chem.* **2012**, *320*, 121. (c) Jahn, U. Radicals in Transition Metal Catalyzed Reactions? Transition Metal Catalyzed Radical Reactions? A Fruitful Interplay Anyway. Part 2: Radical Catalysis by Group 8 and 9 Elements. *Top. Curr. Chem.* **2012**, *320*, 191. (d) Jahn, U. Radicals in Transition Metal Catalyzed Reactions? Transition Metal Catalyzed Radical Reactions? A Fruitful Interplay Anyway. Part 3: Catalysis by Group 10 and 11 Elements and Bimetallic Catalysis. *Top. Curr. Chem.* **2012**, *320*, 323.
19. (a) Manolikakes, G.; Knochel, P. Radical Catalysis of Kumada Cross-Coupling Reactions Using Functionalized Grignard Reagents. *Angew. Chem., Int. Ed.* **2009**, *48*, 205. (b) For a related radical-accelerated Negishi cross-coupling see: Kienle, M.; Knochel, P. *i*-PrI Acceleration of Negishi Cross-Coupling Reactions. *Org. Lett.* **2010**, *12*, 2702.
20. (a) Lalevée, J.; Blanchard, N.; Tehfe, M.-A.; Morlet-Savary, F.; Fouassier, J. P. Green Bulb Light Source Induced Epoxy Cationic Polymerization under Air Using Tris(2,2'-bipyridine)ruthenium(II) and Silyl Radicals. *Macromolecules* **2010**, *43*, 10191. (b) Lalevée, J.; Blanchard, N.; Tehfe, M.-A.; Peter, M.; Morlet-Savary, F.; Fouassier, J. P. A Novel Photopolymerization Initiating System Based on an Iridium Complex Photocatalyst. *Macromol. Rapid Commun.* **2011**, *32*, 917.
21. Yu, W.-Y.; Sit, W. N.; Zhou, Z.; Chan, A. S.-C. Palladium-Catalyzed Decarboxylative Arylation of C–H Bonds by Aryl Acylperoxides. *Org. Lett.* **2009**, *11*, 3174.
22. Kalyani, D.; McMurtrey, K. B.; Neufeldt, S. R.; Sanford, M. S. Room-Temperature C–H Arylation: Merger of Pd-Catalyzed C–H Functionalization and Visible-Light Photocatalysis. *J. Am. Chem. Soc.* **2011**, *133*, 18566.
23. Hull, K. L.; Lanni, E. L.; Sanford, M. S. Highly Regioselective Catalytic Oxidative Coupling Reactions: Synthetic and Mechanistic Investigations. *J. Am. Chem. Soc.* **2006**, *128*, 14047.
24. (a) Nagib, D. A.; Scott, M. E.; MacMillan, D. W. C. Enantioselective  $\alpha$ -Trifluoromethylation of Aldehydes via Photoredox Organocatalysis. *J. Am. Chem. Soc.* **2009**, *131*, 10875. (b) Condie, A. G.; González-Gómez, J. C.; Stephenson, C. R. J. Visible-Light Photoredox Catalysis: Aza-Henry Reactions via C–H Functionalization. *J. Am. Chem. Soc.* **2010**, *132*, 1464.
25. Demas, J. N.; Harris, E. W.; McBride, R. P. Energy Transfer from Luminescent Transition Metal Complexes to Oxygen. *J. Am. Chem. Soc.* **1977**, *99*, 3547.
26. Minisci-type direct C–H arylation of pyridines by Ar• has been demonstrated using Ar–B(OH)<sub>2</sub> or Ar–N<sub>2</sub><sup>+</sup>: (a) Seiple, I. B.; Su, S.; Rodriguez, R. A.;

- Gianatassio, R.; Fujiwara, Y.; Sobel, A. L.; Baran, P. S. Direct C–H Arylation of Electron-Deficient Heterocycles with Arylboronic Acids. *J. Am. Chem. Soc.* **2010**, *132*, 13194. (b) Hari, D. P.; Schroll, P.; König, B. Metal-Free, Visible-Light-Mediated Direct C–H Arylation of Heteroarenes with Aryl Diazonium Salts. *J. Am. Chem. Soc.* **2012**, *134*, 2958.
27. For reviews on the chemistry of diaryliodonium salts see: (a) Deprez, N. R.; Sanford, M. S. Reactions of Hypervalent Iodine Reagents with Palladium: Mechanisms and Applications in Organic Synthesis. *Inorg. Chem.* **2006**, *46*, 1924. (b) Merritt, E. A.; Olofsson, B. Diaryliodonium Salts: A Journey from Obscurity to Fame. *Angew. Chem., Int. Ed.* **2009**, *48*, 9052.
  28. For examples see: (a) Yamada, Y.; Kashima, K.; Okawara, M. *Bull. Chem. Soc. Jpn.* **1974**, *47*, 3179. (b) Oh, C. H.; Kim, J. S.; Jung, H. H. *J. Org. Chem.* **1999**, *64*, 1338. (c) Petersen, T. B.; Khan, R.; Olofsson, B. *Org. Lett.* **2011**, *13*, 3462.
  29. For examples see: (a) Yamada, Y.; Okawara, M. Substituent Effect in the Nucleophilic Attack by the Bromide Ion on the *p*-Tolyl-Substituted Phenyliodonium Ions. *Bull. Chem. Soc. Jpn.* **1972**, *45*, 1860. (b) Carroll, M. A.; Wood, R. A. Arylation of Anilines: Formation of Diarylamines Using Diaryliodonium Salts. *Tetrahedron* **2007**, *63*, 11349.
  30. Photolysis of Ar<sub>2</sub>I<sup>+</sup> under ultraviolet irradiation (248–300 nm) in the presence or absence of organic triplet sensitizers is also known; see: Dektar, J. L.; Hacker, N. P. Photochemistry of Diaryliodonium Salts. *J. Org. Chem.* **1990**, *55*, 639.
  31. The comparative advantages/drawbacks of diaryliodonium salts versus aryldiazonium salts is somewhat subjective and has been the topic of a recent review: Bonin, H.; Fouquet, E.; Felpin, F.-X. Aryl Diazonium *versus* Iodonium Salts: Preparation, Applications and Mechanisms for the Suzuki-Miyaura Cross-Coupling Reaction. *Adv. Synth. Catal.* **2011**, *353*, 3063.
  32. For another recent example from our group, see: Ye, Y.; Sanford, M. S. Merging Visible-Light Photocatalysis and Transition-Metal Catalysis in the Copper-Catalyzed Trifluoromethylation of Boronic Acids with CF<sub>3</sub>I. *J. Am. Chem. Soc.* **2012**, *134*, 9034.
  33. Shakespeare, W. C. Palladium-Catalyzed Coupling of Lactams with Bromobenzenes. *Tetrahedron Lett.* **1999**, *40*, 2035.
  34. Stowers K. J.; Sanford, M. S. Mechanistic Comparison between Pd-Catalyzed Ligand-Directed C–H Chlorination and C–H Acetoxylation. *Org. Lett.* **2009**, *11*, 4584.
  35. Neufeldt, S. R.; Sanford, M. S. *O*-Acetyl Oximes as Transformable Directing Groups for Pd-Catalyzed C–H Bond Functionalization. *Org. Lett.* **2010**, *12*, 532.
  36. Chen, D. W.; Ochiai, M. Chromium(II)-Mediated Reactions of Iodonium Tetrafluoroborates with Aldehydes: Umpolung of Reactivity of Diaryl-

- Alkenyl(aryl)-, and Alkynyl(aryl)iodonium Tetrafluoroborates. *J. Org. Chem.* **1999**, *64*, 6804.
37. Bielawski, M.; Olofsson, B. High-Yielding One-Pot Synthesis of Diaryliodonium Triflates from Arenes and Iodine or Aryl Iodides. *Chem. Commun.* **2007**, 2521.
  38. Bielawski, M.; Aili, D.; Olofsson, B. Regiospecific One-Pot Synthesis of Diaryliodonium Tetrafluoroborates from Arylboronic Acids and Aryl Iodides. *J. Org. Chem.* **2008**, *73*, 4602.
  39. Stoessel, P.; Fortte, R.; Parham, A.; Breuning, E.; Heil, H.; Vestweber, H. U.S. Patent 20080312396A1, December 18, 2008.
  40. Slinker, J. D.; Gorodetsky, A. A.; Lowry, M. S.; Wang, J.; Parker, S.; Rohl, R.; Bernhard, S.; Malliaras, G. G. Efficient Yellow Electroluminescence from a Single Layer of a Cyclometalated Iridium Complex. *J. Am. Chem. Soc.* **2004**, *126*, 2763.



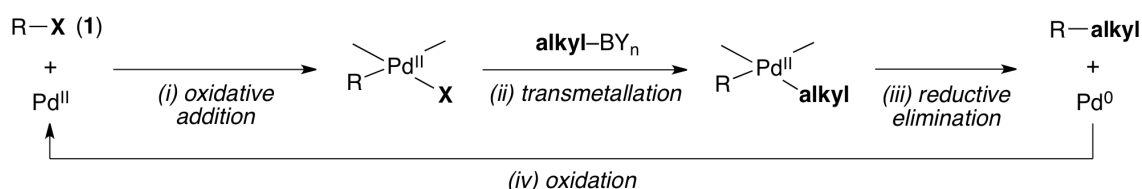
## CHAPTER 3

### Pd-Catalyzed Radical-Mediated C–H Alkylation Using Potassium Alkyltrifluoroborates

#### 3.1 Background and Significance

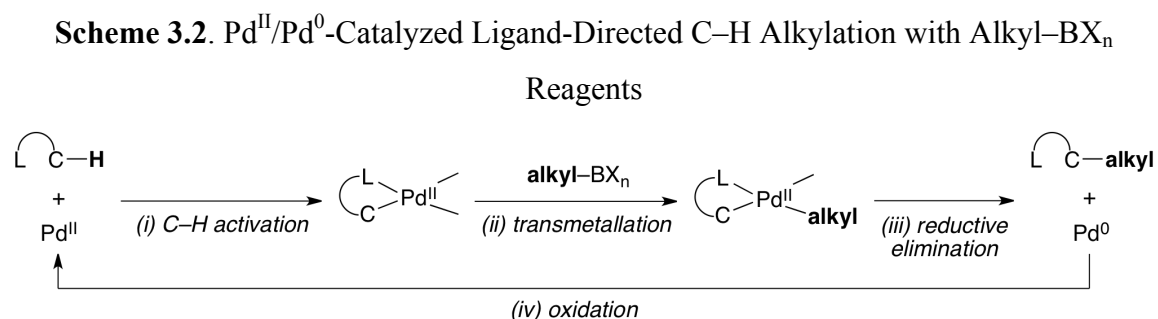
Carbon–alkyl bonds are indispensable structural elements in organic compounds. Nevertheless, mild and general strategies for incorporating alkyl groups into complex molecules remain elusive. Diverse C–alkyl coupling reactions can be effected with nucleophilic organometallic alkylating agents (*e.g.*, alkyl Grignards and alkyllithiums);<sup>1</sup> however, many of these reagents are too reactive for late stage applications. The use of strongly basic nucleophiles is avoided in Suzuki-Miyaura cross-coupling reactions that employ alkylboron reagents in conjunction with a palladium catalyst (Scheme 3.1).<sup>2</sup> This strategy is powerful, yet it carries a number of limitations that include the following: (1) the substrate (**1**) must be prefunctionalized with a halide or pseudohalide, (2) each substrate/alkyl combination typically requires extensive optimization with respect to additives and ancillary ligands, (3) reagents are usually air-sensitive and often moisture-sensitive, and (4) stoichiometric base is required.

**Scheme 3.1.** Suzuki-Miyaura Cross-Coupling with Alkylboron Reagents



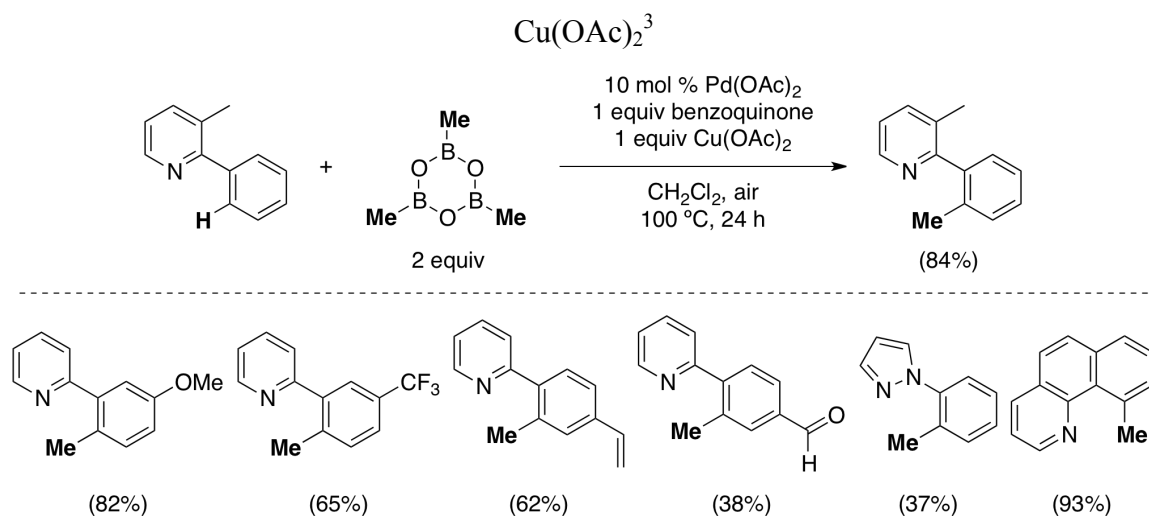
An alternative Pd-catalyzed C–H activation/alkylation sequence addresses the first of these limitations by precluding the requirement for halogenated substrates. This

strategy could be particularly appealing for late stage derivatization of complex molecules; in such situations it may not be feasible (or desirable) to carry a halogen substituent through several steps or to regioselectively introduce a halide into the substrate at a late stage. Over the past few years, a limited number of examples of ligand-directed Pd<sup>II</sup>-catalyzed C–H alkylations have been reported using alkylboron reagents.<sup>3–14</sup> These transformations are believed to proceed through Pd<sup>II</sup>/Pd<sup>0</sup> catalytic cycles (Scheme 3.2) involving (i) C–H activation at Pd<sup>II</sup>, (ii) transmetalation of the alkyl group from boron to palladium, (iii) C–C bond-forming reductive elimination, and (iv) reoxidation of Pd<sup>0</sup> to Pd<sup>II</sup>.

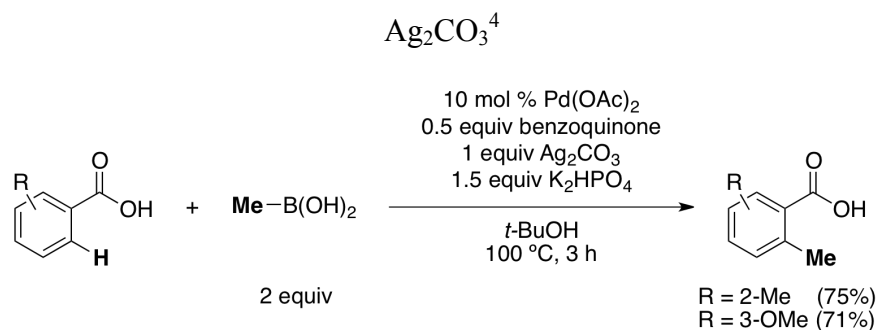


Within this mechanistic manifold, ligand-directed C–H methylation using methylboronic acid or trimethylboroxine has been demonstrated with pyridines and pyrazoles (Scheme 3.3),<sup>3</sup> carboxylic acids (Scheme 3.4),<sup>4</sup> 2-pyridylsulfonyls (Scheme 3.5),<sup>7</sup> and *N*-(perfluoroaryl)sulfonamides<sup>5</sup> serving as directing groups.

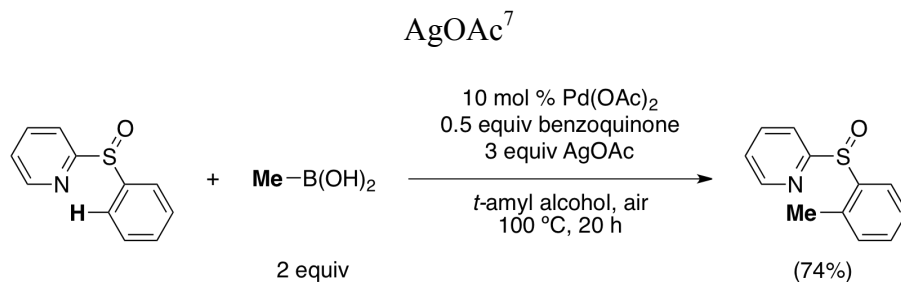
**Scheme 3.3.** Pyridine- and Pyrazole-Directed C–H Methylation with Methylboroxine and



**Scheme 3.4.** Carboxylic Acid-Directed C–H Methylation with Methylboronic Acid and

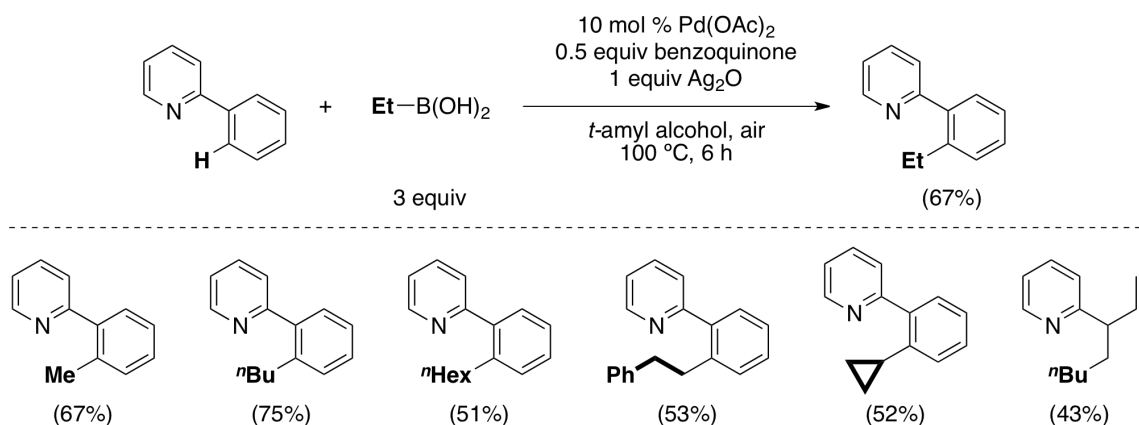


**Scheme 3.5.** 2-Pyridylsulfonyl-Directed C–H Methylation with Methylboronic Acid and

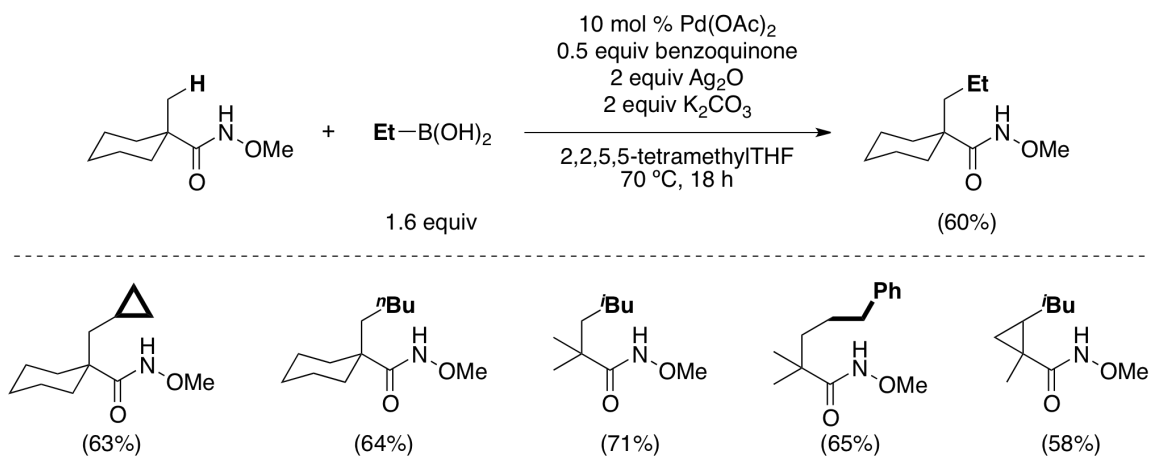


Although the installation of longer-chain alkyls has proven more challenging, pyridine- (Scheme 3.6),<sup>3</sup> methyl hydroxamic acid- (Scheme 3.7),<sup>5</sup> and *N*-(perfluoroaryl)amide-containing substrates<sup>7,9</sup> (Scheme 3.8) have been functionalized with ethyl-, *n*-butyl-, *i*-butyl-, *n*-hexyl-, phenethyl-, cyclohexylmethyl-, and cyclopropyl boronic acid or trifluoroborate reagents.

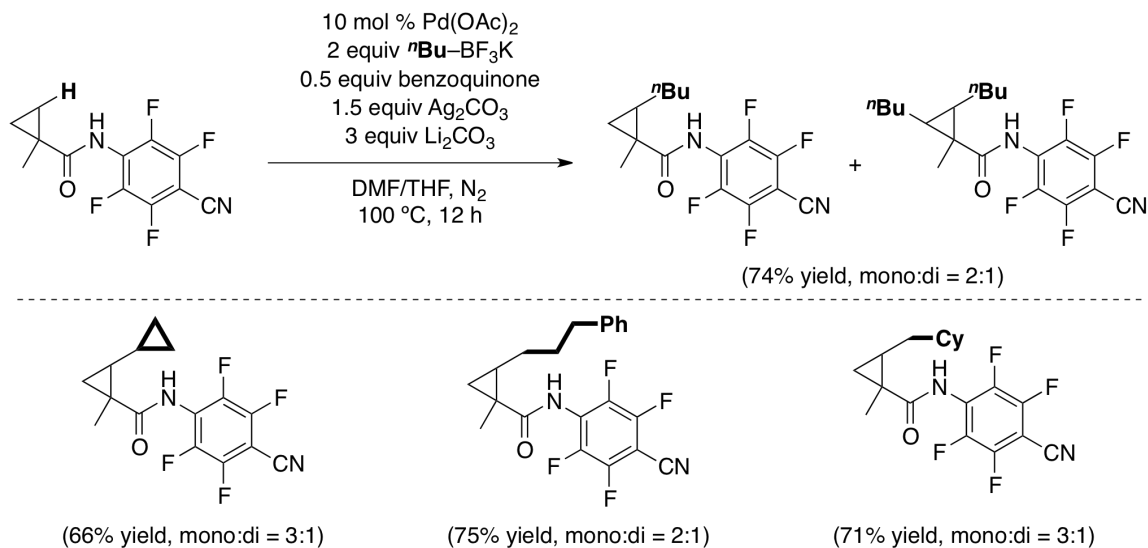
**Scheme 3.6.** Pyridine-Directed C–H Alkylation with Alkylboronic Acids and Ag<sub>2</sub>O<sup>3</sup>



**Scheme 3.7.** Methyl Hydroxamic Acid-Directed sp<sup>3</sup> C–H Alkylation with Alkylboronic Acids and Ag<sub>2</sub>O<sup>5</sup>

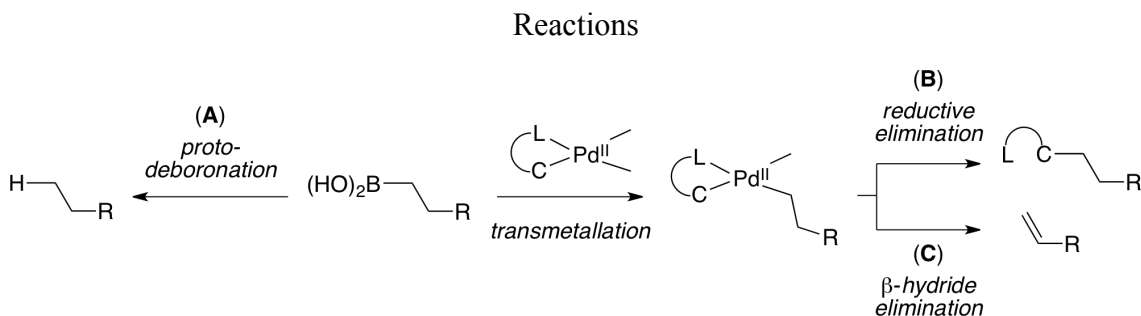


**Scheme 3.8.** *N*-(Perfluoroaryl)benzamide -Directed C–H Alkylation of Cyclopropanes  
with Alkyltrifluoroborates and Ag<sub>2</sub>CO<sub>3</sub><sup>7</sup>



A key challenge associated with Pd-catalyzed C–alkyl bond formation is the propensity for undesired reaction pathways (Scheme 3.9), such as proto-deboronation (path A) or Pd-catalyzed  $\beta$ -hydride elimination (path C), which compete with the desired cross-coupling (path B).<sup>2,3</sup> To date, the efforts to develop and improve C–H alkylation reactions have focused on identifying promoters for each sequential step of the Pd<sup>II</sup>/Pd<sup>0</sup> catalytic cycle shown in Scheme 3.2. This strategy, largely advanced by Yu and coworkers,<sup>3–6,8,9</sup> aims to increase the rate of the desired transformation relative to the rates of undesired mechanistic pathways.

**Scheme 3.9.** Competing Unproductive Processes in Pd-Catalyzed C–H Alkylation



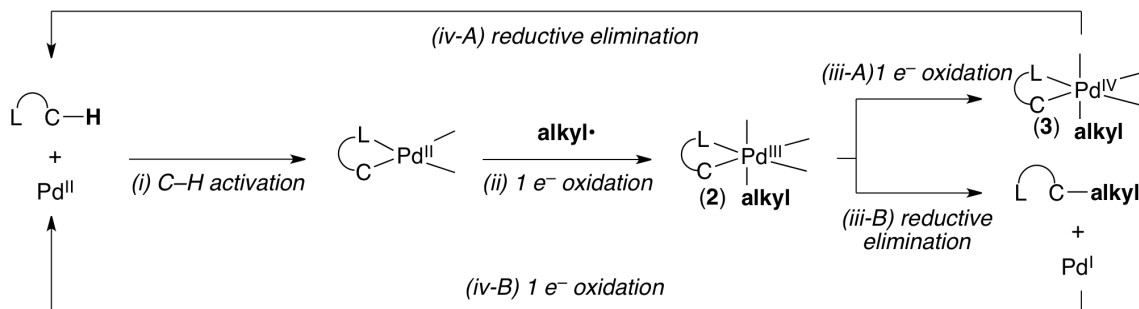
For example, benzoquinone is included in all reported protocols for Pd-catalyzed C–H alkylation with alkylboron reagents. This additive is believed to promote reductive elimination,<sup>3,13,15</sup> and it may also act as a cooxidant.<sup>3</sup> Silver salts are usually employed, serving as oxidants and purportedly promoting transmetallation.<sup>3</sup> Careful optimization has led to the identification of ligands that promote the alkylation of certain substrates. For instance, 2,2,5,5-tetramethyltetrahydrofuran was used as the reaction solvent for the sp<sup>3</sup>-C–H alkylation of *O*-methyl hydroxamic acids (Scheme 3.4). It was hypothesized that this highly substituted ether serves as a bulky ligand for Pd to slow the rate of undesired homocoupling and β-hydride elimination.<sup>5</sup>

As exemplified in Schemes 3.3–3.8, efforts to identify promoters have resulted in several elegant examples of Pd<sup>II</sup>/Pd<sup>0</sup>-catalyzed C–H alkylation with alkylboron reagents. Nevertheless, current methodologies are characterized by a number of key limitations similar to those of traditional Suzuki-Miyaura cross-coupling reactions. Importantly, no set of reaction conditions is general for more than one type of directing group (the low-yielding pyrazole example in Scheme 3.3 is the sole exception shown to proceed under the same conditions as another substrate class). Instead, extensive optimization of base, oxidants, and solvents has been necessary for each transformation. Furthermore, a minimum reaction temperature of 70 °C has been reported,<sup>5,8</sup> and higher temperatures (100–120 °C) are more common. The requirement for elevated temperatures, in addition to the need for superstoichiometric base, renders the current methodology impractical for substrates with sensitive functional groups. In light of all these limitations, the identification of more general and efficient promoters would be necessary to develop improved protocols for C–H alkylation *via* a Pd<sup>II</sup>/Pd<sup>0</sup> mechanistic manifold.

We envisioned a new strategy that would effect the desired transformation through an alternative alkyl radical-mediated pathway (Scheme 3.10). In contrast to Pd<sup>II</sup>/Pd<sup>0</sup>-catalysis, the proposed strategy would replace the traditional transmetallation step with a 1 *e*<sup>−</sup> oxidation of Pd<sup>II</sup> by alkyl• (step *ii*). Although transmetallation from boron can be slow in Pd<sup>II</sup>/Pd<sup>0</sup>-catalyzed C–C bond-forming reactions, literature precedent suggests that the reaction between carbon-centered radicals and palladacycles can be extremely fast.<sup>16–18</sup> Furthermore, reductive elimination is expected to be more facile from a high valent Pd–alkyl intermediate (**2** or **3**, step *iv-A* or *iii-B*) than from a Pd<sup>II</sup>–alkyl

species. Finally,  $\beta$ -hydride elimination (an unproductive reaction pathway in this case) is much less facile from octahedral high valent Pd–alkyl complexes than from Pd<sup>II</sup>–alkyl species.<sup>19</sup>

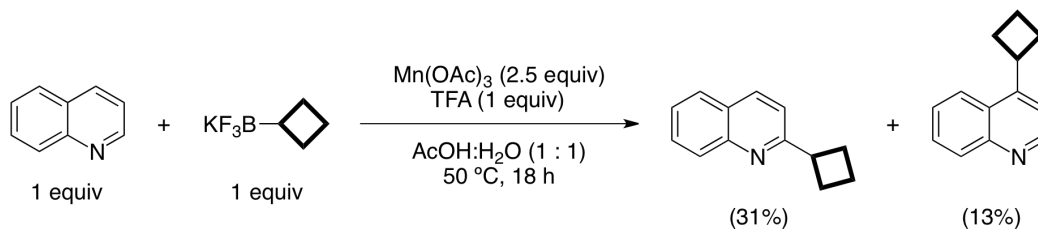
**Scheme 3.10.** Envisioned Alkyl Radical-Mediated Pd-Catalyzed C–H Alkylation



To develop the proposed transformation, we sought to identify a suitable system for generating alkyl radicals that would be compatible with cyclopalladation. A number of radical-mediated Pd-catalyzed C–H arylation<sup>16</sup> and acylation<sup>17</sup> reactions have been reported by our group and others using benzoic acids,<sup>16a</sup> aryldiazonium salts,<sup>16b</sup> diaryliodonium salts,<sup>16c</sup> diethylazodicarboxylates,<sup>17a</sup> and aldehydes<sup>17b–d</sup> as radical precursors. However, none of these reagent classes are practical sources of analogous alkyl radicals. For instance, although aryldiazonium and diaryliodonium salts are commonplace, the corresponding alkyl reagents are typically too unstable to isolate.<sup>20</sup>

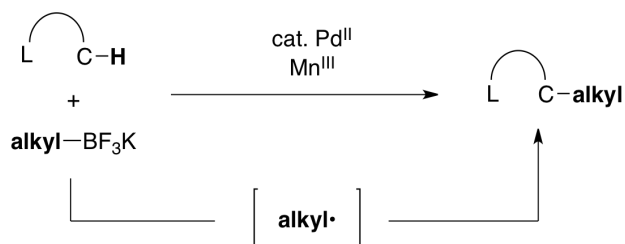
Molander and coworkers recently reported the use of potassium alkyltrifluoroborates as precursors to alkyl radicals for the alkylation of electron-deficient heteroarenes (Scheme 3.11).<sup>21,22</sup> This transformation is believed to involve oxidation of alkyl–BF<sub>3</sub>K to alkyl• by a Mn<sup>III</sup> reagent. The intermediacy of alkyl radicals is supported by the observed regioselectivity, which is consistent with a radical aromatic substitution mechanism in which alkylation occurs at the more electron-deficient 2- and 4-positions of the pyridine ring (trifluoroacetic acid is used as an additive to generate a more electrophilic pyridinium species).<sup>23</sup> This selectivity stands in contrast to that of electrophilic aromatic substitution (*e.g.*, Friedel-Crafts alkylation), in which functionalization occurs at the most nucleophilic positions of an aromatic ring.

**Scheme 3.11.** Alkylation of Electron-Deficient Heteroarenes with Alkyl Radicals  
Generated from Alkyltrifluoroborates and  $\text{Mn}(\text{OAc})_3$ <sup>21</sup>



Inspired by this precedent, we hypothesized that Pd-catalyzed C–H activation could be coupled with  $\text{Mn}^{\text{III}}$ -mediated alkyl– $\text{BF}_3\text{K}$  1  $e^-$  oxidation to provide a net C–H alkylation (Scheme 3.12). Encouragingly, numerous C–H functionalization reactions have been documented in acetic acid,<sup>24</sup> the same solvent used by Molander and coworkers in conjunction with  $\text{Mn}(\text{OAc})_3$ . This precedent suggests compatibility between the conditions required for C–H activation and alkyl– $\text{BF}_3\text{K}$  oxidation. Furthermore, alkyltrifluoroborates are attractive reagents for C–H alkylation because (1) they are readily prepared from inexpensive commercial starting materials, and (2) they are typically air- and moisture-stable crystalline solids that are convenient to handle.<sup>25</sup>

**Scheme 3.12.** Ligand-Directed Pd-Catalyzed C–H Alkylation with Alkyltrifluoroborates and  $\text{Mn}^{\text{III}}$



Although an attractive strategy, several possible undesired processes could impede the development of the proposed Pd-catalyzed ligand-directed C–H alkylation reaction. In particular, two potential side reactions are unique to this approach. First, although pyridines are highly effective directing groups for diverse C–H functionalizations, heterocycles such as these might undergo uncatalyzed Minisci-type alkylation (*vide supra*) in the presence of alkyl radicals. Second, C–OAc bond-forming

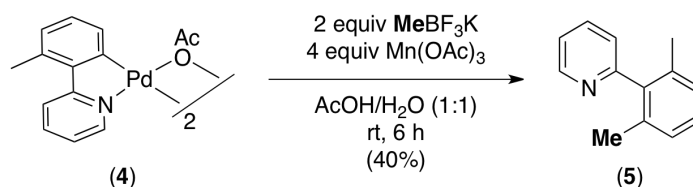


reductive elimination could occur from high-valent Pd intermediates in competition with the desired C–alkyl bond formation. Analogous ligand-directed Pd-catalyzed formation of C–H acetoxyated products has been described numerous times under conditions involving strong oxidants, especially in the presence of acetic acid.<sup>26</sup> As such, reaction conditions must be developed under which the rate of C–H alkylation outcompetes the rates of these undesired processes.

### 3.2 Reaction Optimization

Our initial experiments were directed toward assessing the feasibility of the unprecedented steps of the envisioned catalytic cycle, namely, those that occur after cyclopalladation (Scheme 3.10). We thus began by examining the stoichiometric reaction of cyclopalladated complex **4** with MeBF<sub>3</sub>K in the presence of Mn(OAc)<sub>3</sub>. Excitingly, after 6 h at room temperature in AcOH/H<sub>2</sub>O (1:1), 40% yield of methylated product **5** was obtained (GC calibrated yield, Scheme 3.13). This result indicates that methyl radicals, putatively generated by 1 e<sup>-</sup> oxidation of MeBF<sub>3</sub>K, react with palladacycle **4** under these conditions to effect C–C bond formation.

**Scheme 3.13.** Reaction of Cyclopalladated Complex **4** With MeBF<sub>3</sub>K and Mn(OAc)<sub>3</sub>



With this promising stoichiometric result in hand, we next turned to the catalytic reaction. We were pleased to find that methylation of substrate **6** occurred under analogous conditions in the presence of 10 mol % Pd(OAc)<sub>2</sub>, albeit in low yield (Table 3.1, entry 1, 9%). Not surprisingly, the addition of 1 equiv TFA did not substantially improve the yield of the transformation (entry 2), as protonation of the pyridine directing group is not a productive step in the envisioned catalytic cycle. However, changing the oxidant from Mn(OAc)<sub>3</sub> to MnF<sub>3</sub> doubled the yield of the catalytic reaction to 22% (entry 3). A further increase in yield was observed when the reaction temperature was raised

slightly to 40 °C (entry 4). Finally, after screening a number of solvents, we found that the use of a solvent mixture of trifluoroethanol (TFE)/acetic acid/water (8:1:1) resulted in a high yield of **5** (entry 5).

**Table 3.1.** Optimization of the Pd-Catalyzed C–H Methylation with MeBF<sub>3</sub>K and Mn<sup>III</sup> <sup>a</sup>

entry	oxidant	solvent	temp	% conversion <sup>b</sup>	% yield <sup>b</sup>
1	Mn(OAc) <sub>3</sub>	AcOH/H <sub>2</sub> O (1:1)	25 °C	26	9
2 <sup>c</sup>	Mn(OAc) <sub>3</sub>	AcOH/H <sub>2</sub> O (1:1)	25 °C	30	13
3	MnF <sub>3</sub>	AcOH/H <sub>2</sub> O (1:1)	25 °C	40	22
4	MnF <sub>3</sub>	AcOH/H <sub>2</sub> O (1:1)	40 °C	65	36
<b>5</b>	<b>MnF<sub>3</sub></b>	<b>TFE/H<sub>2</sub>O/AcOH (8:1:1)</b>	<b>40 °C</b>	<b>100</b>	<b>89</b>
6	MnF <sub>3</sub>	TFE	40 °C	8	0
7	MnF <sub>3</sub>	TFE/H <sub>2</sub> O (9:1)	40 °C	29	26
8	MnF <sub>3</sub>	TFE/AcOH (9:1)	40 °C	96	79
9	MnF <sub>3</sub>	TFE/H <sub>2</sub> O/AcOH (8:1:1)	rt	84	80
10	MnF <sub>3</sub>	TFE/H <sub>2</sub> O/AcOH (8:1:1)	50 °C	100	89
11 <sup>d</sup>	MnF <sub>3</sub>	TFE/H <sub>2</sub> O/AcOH (8:1:1)	40 °C	90	80
12 <sup>e</sup>	MnF <sub>3</sub>	TFE/H <sub>2</sub> O/AcOH (8:1:1)	40 °C	92	83
13 <sup>f</sup>	MnF <sub>3</sub>	TFE/H <sub>2</sub> O/AcOH (8:1:1)	40 °C	92	86

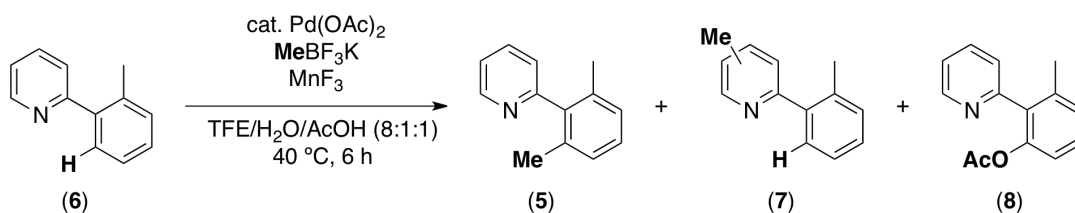
<sup>a</sup>Conditions: **6** (8.5 mg, 0.050 mmol, 1 equiv), Pd(OAc)<sub>2</sub> (1.1 mg, 0.005 mmol, 0.10 equiv), MeBF<sub>3</sub>K (12.2 mg, 0.100 mmol, 2 equiv), oxidant (4 equiv), solvent (0.067 M in **6**), 6 h. <sup>b</sup>Based on calibrated GC yield relative to hexadecane as standard. <sup>c</sup>With TFA (5.7 mg, 0.050 mmol, 1 equiv). <sup>d</sup>2 equiv MeB(OH)<sub>2</sub> were used instead of MeBF<sub>3</sub>K. <sup>e</sup>0.67 equiv trimethylboroxine were used instead of MeBF<sub>3</sub>K. <sup>f</sup>2 equiv trimethylboroxine were used instead of MeBF<sub>3</sub>K.

Interestingly, the methylation reaction does not proceed in trifluoroethanol alone (entry 6). Small quantities of both water and AcOH were necessary to achieve optimum yields (compare entries 6–8 with entry 5; see section 3.9 for further details). Although the best results were obtained at 40 °C, running the reaction at room temperature was only slightly detrimental to the reaction yield (entry 9), and increasing the reaction temperature to 50 °C offered no further advantage (entry 10). Finally, both methylboronic acid (entry 11) and trimethylboroxine (entries 12 and 13) performed nearly as well as the

corresponding trifluoroborate, although these classes of reagents are not as convenient to prepare and handle as trifluoroborate salts.<sup>25</sup>

Importantly, no methylation occurs in the absence of Pd, providing support for a Pd-catalyzed process (Table 3.2, entry 2). When Mn<sup>III</sup> is excluded from the reaction, no methylated product (**5**) is detected (entry 3). Finally, in the absence of MeBF<sub>3</sub>K, significant quantities of acetoxyated product **8** are observed (entry 4).

**Table 3.2.** Control Reactions for the Pd-Catalyzed Radical-Mediated C–H Methylation of Substrate **6**<sup>a,b</sup>



entry	Pd(OAc) <sub>2</sub> (equiv)	MeBF <sub>3</sub> K (equiv)	MnF <sub>3</sub> (equiv)	% conversion <sup>c</sup>	<b>5</b> (% yield) <sup>c</sup>	<b>7</b> (% yield)	<b>8</b> (% yield)
1	0.10	2	4	100	89	0	0
2	0	2	4	3	0	0	0
3	0.10	2	0	3	0	0	0
4	0.10	0	4	59	0	0	35 <sup>d</sup>

<sup>a</sup>Conditions unless otherwise indicated: **6** (8.5 mg, 0.050 mmol, 1 equiv), Pd(OAc)<sub>2</sub> (1.1 mg, 0.005 mmol, 0.10 equiv), MeBF<sub>3</sub>K (12.2 mg, 0.100 mmol, 2 equiv), MnF<sub>3</sub> (22.4 mg, 0.200 mmol, 4 equiv), TFE/H<sub>2</sub>O/AcOH (8:1:1, 0.067 M in **6**), 40 °C, 6 h. <sup>b</sup>A yield of 0 means that the indicated product was not detected by GC analysis. <sup>c</sup>Based on calibrated GC yield relative to hexadecane as standard. <sup>d</sup>Uncalibrated GC yield.

It is noteworthy that Minisci-type methylation of the pyridine ring (**7**) was not detected under any conditions, even when Pd was excluded from the reaction. This observation was encouraging; however, pyridine alkylation with alkyl–BF<sub>3</sub>K has only been demonstrated with alkyl–BF<sub>3</sub>K reagents that produce 2°, longer-chain 1°, and heteroatom-stabilized 1° radicals.<sup>21</sup> As such, the absence of pyridine-methylation products in this control reaction did not rule out the possibility of competing pyridine alkylation with other alkyltrifluoroborates.

### 3.3 Methylation Scope

The optimal conditions were applied to the C–H methylation of other arylpyridine derivatives as well as diverse anilide substrates (Table 3.3). Products derived from the C–H methylation of acetanilide (**12**, **14**, **16**, and **18**), pyrrolidinone (**20**), acetylidoline (**22**), and tetrahydroacetylquinoline (**24**) derivatives were all obtained in good to excellent isolated yields at 25–40 °C. Furthermore, the presence of an aryl iodide functional group was well tolerated under these mild reaction conditions (**18**).

**Table 3.3.** Substrate Scope for the Pd-Catalyzed Radical Mediated Methylation<sup>a</sup>

entry	substrate	product	% yield <sup>b</sup>	entry	substrate	product	% yield <sup>b</sup>
1 <sup>c</sup>			81	6			83
2 <sup>c</sup>			70	7			73
3 <sup>d</sup>			96	8			83
4			72	9			74
5			53				

<sup>a</sup>Conditions: substrate (1 equiv), Pd(OAc)<sub>2</sub> (0.10 equiv), MeBF<sub>3</sub>K (2 equiv), MnF<sub>3</sub> (4 equiv), AcOH (2 equiv), TFE/H<sub>2</sub>O (9:1, 0.067 M in substrate), 40 °C, 3 h. <sup>b</sup>Isolated yield. <sup>c</sup>Reaction solvent was TFE/H<sub>2</sub>O/AcOH (8:1:1); this corresponds to approximately 26 equiv AcOH. <sup>d</sup>Reaction was run at room temperature.

A limitation to the current methodology is that electron-deficient substrates display low reactivity under the optimized conditions. Table 3.4 depicts a number of additional substrates that were evaluated for the methylation reaction under conditions similar to those optimized for **6**. Methylated products were identified by GCMS, and the GC yields presented are uncalibrated. Particularly poor reactivity was observed with substrates containing electron-withdrawing substituents (entries 6–9). Further studies will be needed to explain the poor efficiency of this substrate class; however, electron withdrawing substituents are expected to slow the rate of cyclopalladation by making the directing group less basic and/or by making the C–H bond less nucleophilic (step *i*, Scheme 3.10).<sup>27</sup> Additionally, the Pd<sup>II</sup> center formed by cyclopalladation of more electron deficient substrates would have a less negative redox potential, and thus likely undergo less facile oxidation by alkyl• (step *ii*, Scheme 3.10).

**Table 3.4.** Reactivity of Substituted Arylpyridine Substrates Under the Radical-Mediated

Methylation Conditions

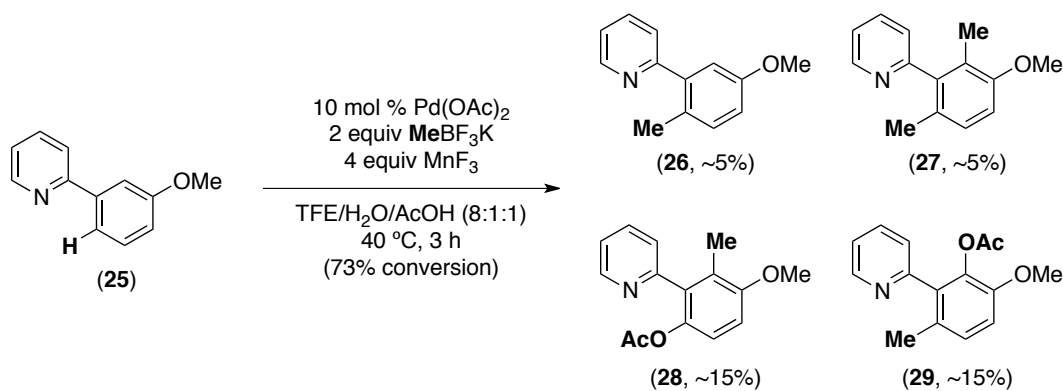
entry	R <sup>1</sup>	R <sup>2</sup>	% conversion <sup>a</sup>	% yield <sup>b</sup>
1	H	2'-Me	100	93
2	4-Me	2'-Me	100	99
3	5-Me	2'-Me	100	97
4	3-Me	4'-F	86	74
5	6-OMe	H	81	62 <sup>c</sup>
6	H	3'-CF <sub>3</sub>	68	28
7	5-Cl	2'-Me	32	26
8	3-CN	H	37	12
9	4-CN	2'-Me	57	28

<sup>a</sup>Based on remaining starting material by GC, calculated using the calibration curve of substrate **6** relative to hexadecane standard. <sup>b</sup>GC yield calculated using the calibration curve of product **5** relative to hexadecane standard. <sup>c</sup>Sum of mono- and di-methylated products.

Interestingly, 3'-methoxy substituted arylpyridine **25** displayed very different reactivity than the analogous 2'-substituted substrate **9** (Scheme 3.14). When **25** was

subjected to the reaction conditions, only ~5% of methylated product **26** was observed. Instead, the major products were consistent with the structures of **28** and **29** by GCMS analysis.

**Scheme 3.14.** Reactivity of 3'-Methoxyphenylpyridine **25** Under the Radical-Mediated Methylation Conditions



Additional substrates containing diverse directing groups were screened for the methylation reaction, but they yielded less than 10% of the corresponding methylated products as detected by GC. These substrates are summarized in Figure 3.1.

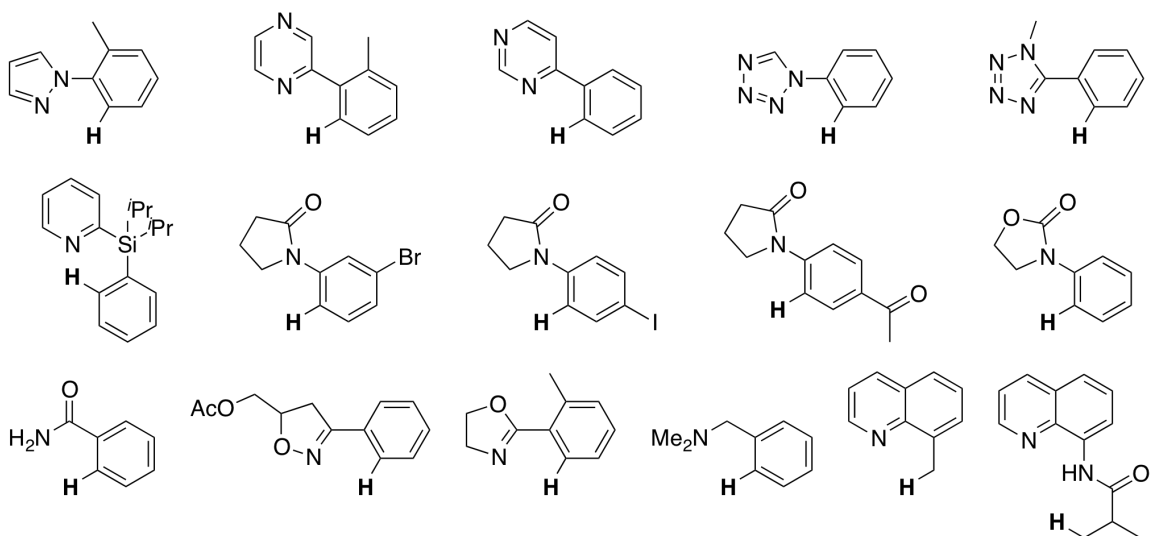


**Figure 3.1.** Substrates Screened That Provided <10% Yield of Methylated Product by GC Under the C–H Methylation Conditions

### 3.4 Alkyl Scope

A wide variety of other 1° alkyl groups were installed using the corresponding alkyltrifluoroborate salts (Table 3.5). Alkylation of both arylpyridine **6** and acetanilide **11** with ethyl, *n*-butyl, and *n*-hexyl groups proceeded efficiently to afford **30**, **31**, **32**, and **40**. The sterically hindered neopentyl group was introduced in 40% yield (**34**), and alkyl chains bearing phenyl, ester, ketone, and trifluoromethyl substituents were compatible with the reaction conditions (**33**, **35**, **36**, **37**, **39**, and **40**).

**Table 3.5.** Alkyl Scope of the Radical-Mediated Pd-Catalyzed C–H Alkylation<sup>a</sup>

10 mol % Pd(OAc)<sub>2</sub>  
2 equiv RBF<sub>3</sub>K  
4 equiv MnF<sub>3</sub>  
TFE/H<sub>2</sub>O/AcOH  
25–40 °C

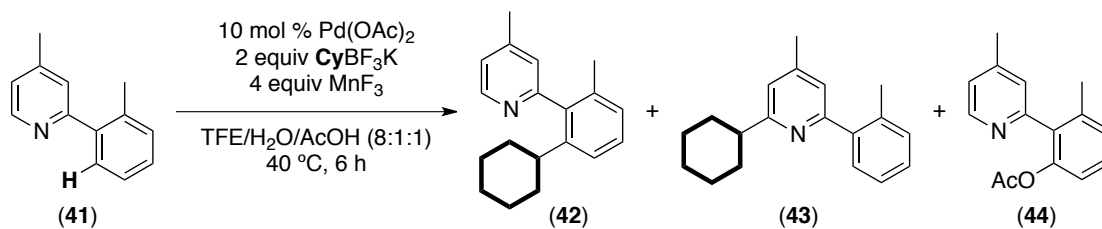
entry	RBF <sub>3</sub> K	product	yield <sup>b</sup>	entry	RBF <sub>3</sub> K	product	yield <sup>b</sup>
1	EtBF <sub>3</sub> K		75%	7 <sup>f</sup>			25%
2 <sup>c</sup>	<i>n</i> BuBF <sub>3</sub> K		77%	8 <sup>e</sup>			30%
3 <sup>c</sup>	<i>n</i> HexBF <sub>3</sub> K		62%	9 <sup>e,g</sup>	<i>n</i> HexBF <sub>3</sub> K		72%
4	Ph-CH <sub>2</sub> -CH <sub>2</sub> -BF <sub>3</sub> K		49%	10 <sup>e,g</sup>	EtO <sub>2</sub> C-CH <sub>2</sub> -CH <sub>2</sub> -BF <sub>3</sub> K		60%
5 <sup>c,d</sup>	<i>t</i> Bu-CH <sub>2</sub> -BF <sub>3</sub> K		40%	11 <sup>e,g</sup>	Ph-CH <sub>2</sub> -CH <sub>2</sub> -BF <sub>3</sub> K		54%
6 <sup>e</sup>	EtO-C(=O)-CH <sub>2</sub> -CH <sub>2</sub> -BF <sub>3</sub> K		46%				

<sup>a</sup>Conditions: substrate (1 equiv), Pd(OAc)<sub>2</sub> (0.10 equiv), alkyl-BF<sub>3</sub>K (2 equiv), MnF<sub>3</sub> (4 equiv), TFE/H<sub>2</sub>O/AcOH (8:1:1, 0.067 M in substrate), 40 °C, 3–6 h. <sup>b</sup>Isolated yield. <sup>c</sup>4 equiv alkyl-BF<sub>3</sub>K and 3 equiv MnF<sub>3</sub> were used. <sup>d</sup>Solvent was TFE/AcOH/H<sub>2</sub>O (4.5:4.5:1). <sup>e</sup>solvent was TFE/H<sub>2</sub>O (9:1) with 2 equiv AcOH. <sup>f</sup>Solvent was TFE/H<sub>2</sub>O (9:1, 0.13 M in substrate) with 1 equiv AcOH. <sup>g</sup>Substrate was **11** and reaction was run at 25 °C.



In contrast to the 1° alkyltrifluoroborates shown in Table 3.5, 2° alkyl-BF<sub>3</sub>K reagents did not perform well under the reaction conditions. The use of cyclopropyl-BF<sub>3</sub>K yielded no detectable products, and the reaction between arylpyridine **41** and cyclohexyltrifluoroborate afforded a mixture of the desired product **42** and the Molander-type undirected alkylation product **43** (Table 3.6, entry 1). Unlike **43**, product **42** was not detected in the control reaction without Pd (entry 2), suggesting that **42** is formed by a Pd-catalyzed process. A second competing side product is acetoxyated product **44**, which requires both Pd and Mn, but not CyBF<sub>3</sub>K, for formation. The observed side products provide insight into the mechanism of the current transformation (see section 3.6), and the results shown in Table 3.6 demonstrate the feasibility of Pd-catalyzed C-H alkylation with 2° alkylboron reagents. However, further optimization of the reaction conditions will be necessary to achieve high-yielding transformations using 2° alkyltrifluoroborates.

**Table 3.6.** Reaction of Cyclohexyltrifluoroborate with **41** Under the Pd-Catalyzed C-H Alkylation Conditions



entry	Pd(OAc) <sub>2</sub> (equiv)	MnF <sub>3</sub> (equiv)	CyBF <sub>3</sub> K (equiv)	% conversion	<b>42</b> % yield	<b>43</b> % yield	<b>44</b> % yield
1	0.10	4	2	42	9	5	3
2	0	4	2	35	0	6	0
3	0.10	0	2	18	0	0	0
4	0.10	4	0	53	0	0	41

<sup>a</sup>Determined by gas chromatographic analysis of the crude reaction mixture using hexadecane as an internal standard.

The use of a primary alkyltrifluoroborate containing an  $\alpha$ -heteroatom (**45**) resulted in the formation of only Molander-type products (Scheme 3.15). Additionally, several alkyltrifluoroborates were screened that did not afford any detectable quantities of the desired alkylated product (Figure 3.2).

**Scheme 3.15.** Reaction of BnOCH<sub>2</sub>BF<sub>3</sub>K with **6** Under the Pd-Catalyzed C–H Alkylation

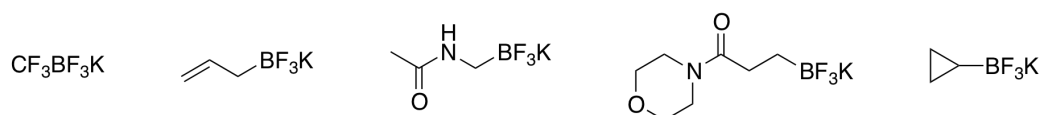
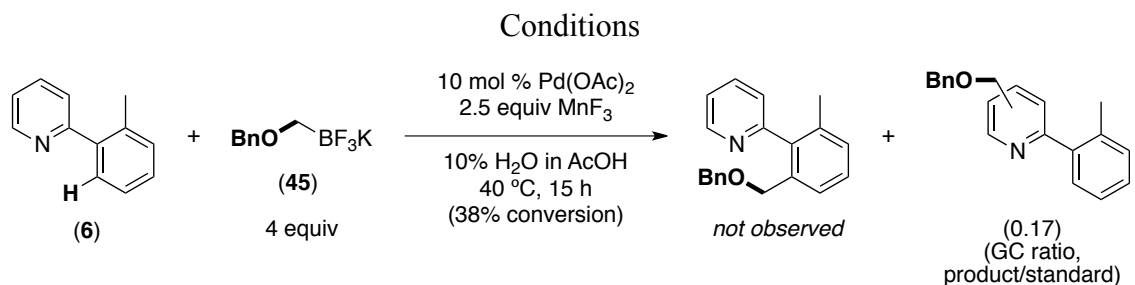


**Figure 3.2.** Alkyltrifluoroborate Reagents that Afforded no Detectable C–H Alkylation Products

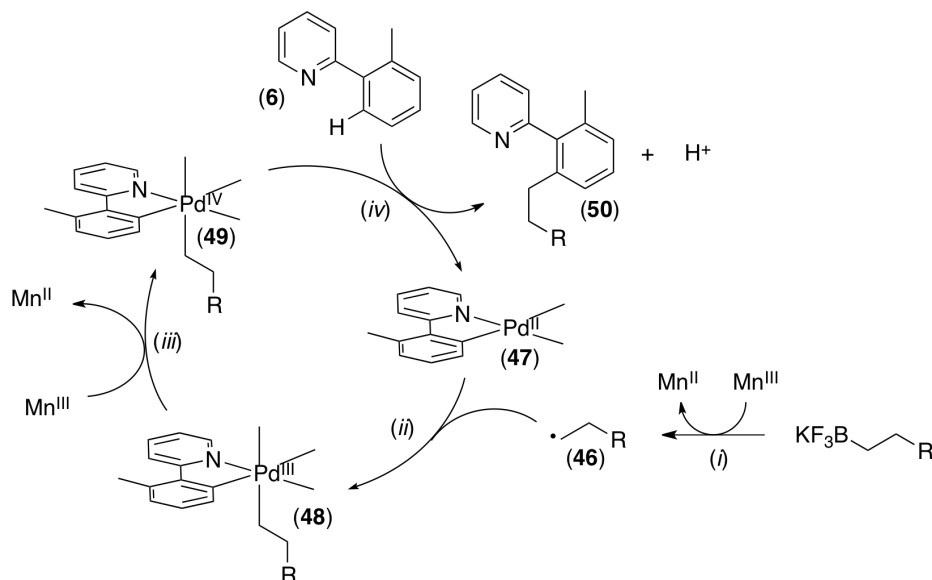
The observed trends in reactivity of different alkyltrifluoroborates can be summarized as follows. Alkylation with MeBF<sub>3</sub>K tends to afford high yields of methylated products (*e.g.*, 81% isolated yield of **5**). The use of 1° alkyltrifluoroborates results in modest to good yields of alkylated products, although the yields tend to be lower than methylation (25–77% isolated yield, Table 3.5). In contrast, use of alkyltrifluoroborates that generate 2° or resonance-stabilized alkyl radicals (*e.g.*, cyclohexyl, benzyl, benzyloxymethyl) leads to none or very little of the desired products (<10% yield).

### 3.5 Proposed Radical-Mediated Reaction Mechanism

In contrast to previous reports of Pd<sup>II</sup>/Pd<sup>0</sup>-catalyzed C–H alkylation with alkylboron reagents, the dramatically lower temperatures required for this Pd<sup>II</sup>/Mn<sup>III</sup>-mediated transformation are consistent with a fundamentally different operating mechanism for this reaction. One possible Pd<sup>II</sup>/Pd<sup>III</sup>/Pd<sup>IV</sup> mechanism (Scheme 3.16) could involve (i) 1 *e*<sup>−</sup> oxidation of alkyl–BF<sub>3</sub>K by Mn<sup>III</sup> to generate alkyl radical **46**, (ii) 1 *e*<sup>−</sup> oxidation of palladacycle **47** by **46** to afford Pd<sup>III</sup>–alkyl species **48**, (iii) 1 *e*<sup>−</sup> oxidation of **48** by a second equivalent of Mn<sup>III</sup> to provide Pd<sup>IV</sup>–alkyl species **49**, and finally (iv) C–C

bond-forming reductive elimination to generate the alkylated product **50** and a Pd<sup>II</sup> species that undergoes cyclometallation with **6** to regenerate **47**. A related Pd<sup>II</sup>/Pd<sup>III</sup>/Pd<sup>I</sup> catalytic cycle could also be envisioned.

**Scheme 3.16.** Proposed Pd<sup>II</sup>/Pd<sup>III</sup>/Pd<sup>IV</sup> Mechanism for the Alkylation Reaction



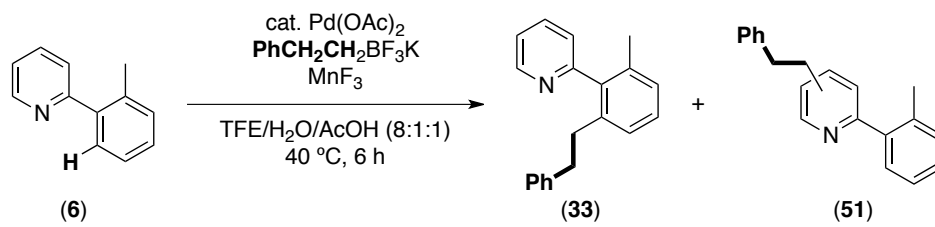
Several pieces of evidence support the intermediacy of alkyl radicals in this transformation. These points are discussed in sections 3.6–3.8 and include: (1) the observation of Molander-type alkylated side products in the reaction of arylpyridine substrate **6**, (2) the trends in reactivity of different alkyltrifluoroborates, and (3) the lack of reactivity seen with traditional 2 e<sup>-</sup> oxidants.

### 3.6 Evidence for an Alkyl Radical-Mediated Mechanism: Molander-Type Side Products

As illustrated by Table 3.6 and Scheme 3.15, Molander-type pyridine alkylation products are observed when CyBF<sub>3</sub>K or BnOCH<sub>2</sub>BF<sub>3</sub>K salts are employed. Notably, we have also observed these Molander-type side products in Pd-free control reactions using alkyltrifluoroborates that normally afford higher yields of the desired C–H alkylated products in the presence of Pd. For instance, pyridine-alkylated products **51** are observed in the Pd-free control reaction with PhCH<sub>2</sub>CH<sub>2</sub>BF<sub>3</sub>K (Table 3.7, entry 2). These results

suggest that alkyl radicals are present under reaction conditions that are relevant to our catalytic system.

**Table 3.7.** Observation of Undirected Pyridine-Alkylated Products with Phenethyl–BF<sub>3</sub>K

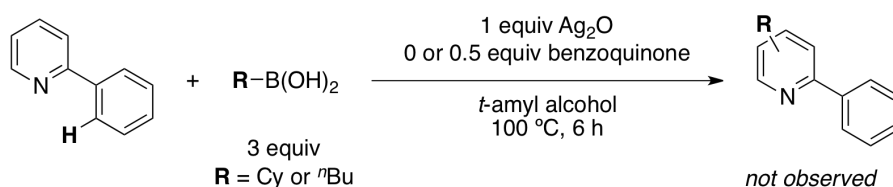


entry	Pd (equiv)	MnF <sub>3</sub> (equiv)	RBF <sub>3</sub> K (equiv)	% conversion <sup>a</sup>	<b>33</b> (% yield) <sup>b</sup>	<b>51</b> (% yield) <sup>c</sup>
1	0.10	4	2	61	41	0
2	0	4	2	12	0	11
3	0.10	0	2	4	0	0

<sup>a</sup>Based on calibrated GC yield relative to hexadecane as standard. <sup>b</sup>GC calibrated yield relative to hexadecane as standard. <sup>c</sup>GC yield using calibration for **33**, relative to hexadecane as standard.

In contrast, this type of non-directed alkylation is not reported as a side reaction under the conditions developed by Yu and coworkers for arylpyridine C–H alkylation.<sup>3</sup> Furthermore, in our hands, these products were not observed even in the absence of Pd (Scheme 3.17). The observation of undirected pyridine-alkylated products in our system, but not in Yu's, is consistent with a mechanism involving alkyl radicals in the former system, but not in the latter.

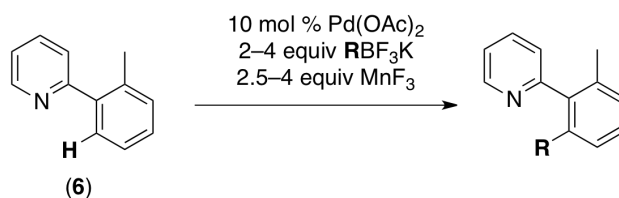
**Scheme 3.17.** Control Reactions for Yu's Pd<sup>II</sup>/Pd<sup>0</sup>-Catalyzed C–H Arylation



### 3.7 Evidence for an Alkyl Radical-Mediated Mechanism: Reactivity Trends of Alkyltrifluoroborates

A second piece of evidence supporting the proposed radical-mediated mechanism is provided by the observed trends in reactivity of different alkyltrifluoroborates. These trends are consistent with steps involving alkyl-BF<sub>3</sub>K acting as a reductant for Mn<sup>III</sup> (step *i*, Scheme 3.16) and an alkyl radical serving as an oxidant for Pd<sup>II</sup> (step *ii*, Scheme 3.16). Specifically, the yields of C–H alkylated products track with the redox potentials of the corresponding RBF<sub>3</sub>K reagents and R• intermediates (Table 3.8). The majority of the alkyltrifluoroborates that were used successfully are expected to provide alkyl radicals with redox potentials similar to ethyl• (entry 3).<sup>28</sup>

**Table 3.8.** Comparison of Alkylation Yields vs Redox Potentials of Alkyl•



entry	RBF <sub>3</sub> K	R•	<i>E</i> <sup>0</sup> vs NHE (V) <sup>a</sup>	Yield
1	CH <sub>3</sub> BF <sub>3</sub> K	H <sub>3</sub> C•	2.54	81 <sup>b</sup>
2			1.42	0 <sup>c</sup>
3			1.23	75 <sup>d</sup>
4			0.96	<10 <sup>e</sup>
5			0.63	<10 <sup>e</sup>
6			0.36	0 <sup>c</sup>
7	Ph-CH <sub>2</sub> -O-CH <sub>2</sub> -BF <sub>3</sub> K	Ph-CH <sub>2</sub> -O-CH <sub>2</sub> •	~0.35 <sup>f</sup>	0 <sup>c</sup>
8			0.05	0 <sup>c</sup>

<sup>a</sup>Values are obtained from reference 28 and represent quantum chemical predictions of standard redox potentials in acetonitrile relative to NHE.

<sup>b</sup>Isolated yield; see entry 1 of Table 3.3. <sup>c</sup>Alkylated product was not detected by gas chromatography. <sup>d</sup>Isolated yield; see entry 1 of Table 3.5.

<sup>e</sup>Uncalibrated GC yield suggested only trace (<10%) product was formed.

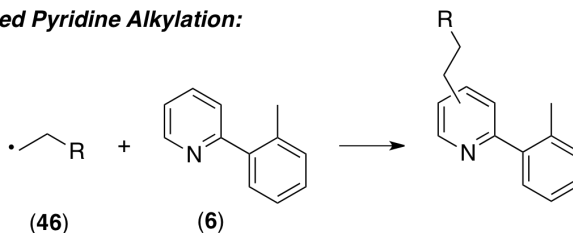
<sup>f</sup>Value is for the structurally similar radical MeOCH<sub>2</sub>•.

As shown in Table 3.8, substituted  $sp^3$  carbon-centered radicals are characterized by lower redox potentials than that of methyl• (*i.e.*, substituted alkyl• is less easily reduced than Me•).<sup>28</sup> Alkyl radicals substituted with resonance stabilizing moieties (*e.g.*, heteroatoms) have even lower redox potentials (*e.g.*, entries 4, 6, 7, and 9). By extension, the corresponding substituted alkyl–BF<sub>3</sub>K species should have lower redox potentials than MeBF<sub>3</sub>K (*i.e.*, substituted alkyl–BF<sub>3</sub>K are more easily oxidized than MeBF<sub>3</sub>K).

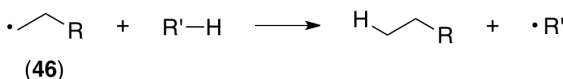
Taking these redox trends into consideration, it is expected that stabilizing substituents on the alkyl radical may have the following effects on the reaction pathway: (1) the rate of reaction between alkyl• and the intermediate palladacycle could be slowed (step *ii* in Scheme 3.16), allowing competing side reactions of alkyl• to occur; and (2) the rate of radical generation (step *i* in Scheme 3.16) may be accelerated, particularly when alkyl is substituted with a stabilizing heteroatom(s). The latter effect could be detrimental to the overall yield of the desired transformation because only 10 mol % of palladacycle **47** can be in solution at any given time to participate in step *ii* of the catalytic cycle. A large excess of alkyl• relative to **47** would likely be consumed by unproductive side processes (*e.g.*, those shown in Scheme 3.18).

**Scheme 3.18.** Examples of Side Reactions of Alkyl• that Could Compete with Step *ii* of the Proposed Catalytic Cycle

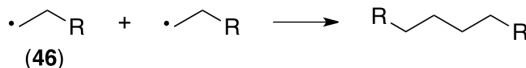
**Undirected Pyridine Alkylation:**



**H-Atom Abstraction**

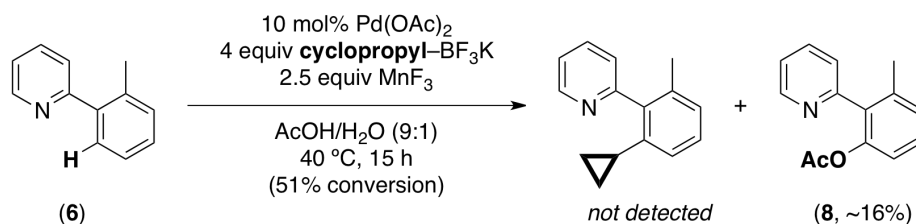


**Homocoupling**

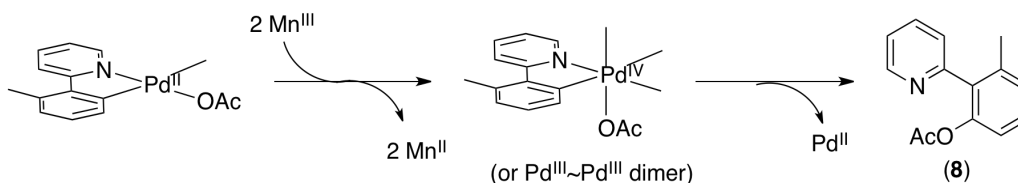


If alkyl-BF<sub>3</sub>K (and the resultant alkyl•) is consumed rapidly at the start of the reaction by unproductive processes, the observation of products similar to those detected in control reactions without alkyl-BF<sub>3</sub>K would be expected (assuming that an excess of Mn<sup>III</sup> is present). (Such products would also be expected in a converse scenario; namely, if alkyl-BF<sub>3</sub>K is stable toward oxidation by Mn<sup>III</sup>, allowing Mn<sup>III</sup> to instead participate in undesired side reactions). As shown in Section 3.2, acetoxyated arylpyridine **8** is the main product observed upon subjection of **6** to the reaction conditions in the absence of an alkyl-BF<sub>3</sub>K reagent (Table 3.2, entry 4 in Section 3.2). Indeed, this product (**8**) was also detected in significant quantities when cyclopropyl-BF<sub>3</sub>K was used as the alkylating reagent, and none of the desired C-H functionalized product was formed (Scheme 3.19). Based on redox potentials, cyclopropyl-BF<sub>3</sub>K is expected to produce a radical that is a poor oxidant ( $E^0 = 0.05$  V, Table 3.8), resulting in a slow step *ii*. As such, cyclopropyl-BF<sub>3</sub>K may be quickly consumed early into the reaction without generating any of the desired C-H functionalized product. A number of mechanisms for formation of side product **8** could be envisioned. Scheme 3.20 illustrates one possible reaction pathway involving oxidation of Pd<sup>II</sup> by Mn<sup>III</sup> (instead of by cyclopropyl•) followed by C-O bond-forming reductive elimination from a Pd<sup>IV</sup> complex.

**Scheme 3.19.** Reaction of Cyclopropyl-BF<sub>3</sub>K with **6** Under the Pd-Catalyzed C-H Alkylation Conditions



**Scheme 3.20.** Possible Mechanism for Formation of Acetoxyated Product **8**

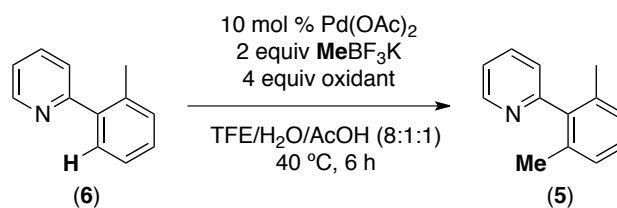


In summary, the observed trends in reactivity of the alkyltrifluoroborates are consistent with a hypothesis that, as redox potentials of alkyl-BF<sub>3</sub>K (or alkyl•) become less positive, the rate of step (ii) in the proposed reaction mechanism (Scheme 3.16) becomes less favorable relative to the rates of unproductive side reactions. Importantly, the observed correlation between alkyl radical redox potentials and reaction yields does not provide conclusive evidence to support or refute the proposed reaction mechanism. Detailed studies will be needed to elucidate the origin of the observed correlation, and to investigate the contribution of other factors to the observed trends in reactivity. For instance, many of the putative Pd-alkyl intermediates could undergo competing  $\beta$ -hydride elimination, a process that is not possible from Pd-methyl intermediates. The olefin moiety in allyltrifluoroborate may participate in divergent Pd-catalyzed reactions. Lastly, factors such as the nucleophilicity and the sterics of the alkyl radicals, as well as the rates of reductive elimination from a Pd-alkyl species, may contribute to the observed trends.

### 3.8 Evidence for an Alkyl Radical-Mediated Mechanism: Results of Screening Alternative Oxidants

A number of oxidants were screened for the methylation reaction of **6** in the optimized solvent system (Table 3.9). Other manganese salts besides MnF<sub>3</sub> were ineffective, including those in higher and lower oxidation states (entries 3, 5, and 6). Importantly, oxidants that have been used for C-H alkylation under a proposed Pd<sup>II</sup>/Pd<sup>0</sup> catalytic cycle<sup>3-9</sup> were also ineffective under our conditions (entries 8-11). However, potassium persulfate promoted the desired transformation, albeit in poor yield (entries 11 and 12). This peroxide oxidant has been used previously in conjunction with catalytic AgNO<sub>3</sub> or FeS to promote aryl• formation from arylboronic acids.<sup>29</sup> The ineffectiveness of all oxidants screened, except those previously shown to generate carbon-centered radicals from organoboron species, is consistent with the hypothesis of a radical-mediated reaction mechanism for this transformation.<sup>30</sup>



**Table 3.9.** Oxidant Screen for the Pd-Catalyzed C–H Alkylation Reaction

entry	oxidant	% conversion <sup>b,c</sup>	% yield <sup>b</sup>
1	MnF <sub>3</sub>	100	89
2	Mn(OAc) <sub>3</sub>	10	0
3	Mn(OAc) <sub>2</sub>	7	0
4	Mn <sub>2</sub> O <sub>3</sub>	0	0
5	MnO <sub>2</sub>	6	0
6	KMnO <sub>4</sub>	21	0
7	PhI(O <sub>2</sub> CCF <sub>3</sub> ) <sub>2</sub>	38	0
8	benzoquinone	11	0
9	Ag <sub>2</sub> CO <sub>3</sub>	7	0
10	Ag <sub>2</sub> O	11	0
11	Ag <sub>2</sub> O + 0.5 equiv benzoquinone	4	0
12	<sup>t</sup> BuOOH	22	0
13	K <sub>2</sub> S <sub>2</sub> O <sub>8</sub>	100	9
14	K <sub>2</sub> S <sub>2</sub> O <sub>8</sub> + 0.2 equiv AgNO <sub>3</sub>	100	10

<sup>a</sup>Conditions: **6** (8.5 mg, 0.050 mmol, 1 equiv), Pd(OAc)<sub>2</sub> (1.1 mg, 0.005 mmol, 0.10 equiv), MeBF<sub>3</sub>K (12.2 mg, 0.100 mmol, 2 equiv), oxidant (4 equiv), TFE/H<sub>2</sub>O/AcOH (8:1:1, 0.067 M in **6**), 6 h. <sup>b</sup>Based on calibrated GC yield relative to hexadecane as standard. <sup>c</sup>In cases with high conversion but low yield of methylated product **5**, **6** may undergo a high oxidation-state Pd-catalyzed homodimerization process, which has been previously published in reference 31. The product of homodimerization is difficult to observe and quantify by GC because it appears as a broad peak in the baseline.

### 3.9 Discussion of the Roles of Acetic Acid and Water

As shown in Section 3.2, both acetic acid and water were found to be necessary components of the reaction mixture. It is believed that water improves the solubility of the trifluoroborate salt in the reaction solvent. For instance, at least ~50 equiv H<sub>2</sub>O were necessary to achieve high yields of methylated product **20** from **19** after 2 h (Figure 3.3).

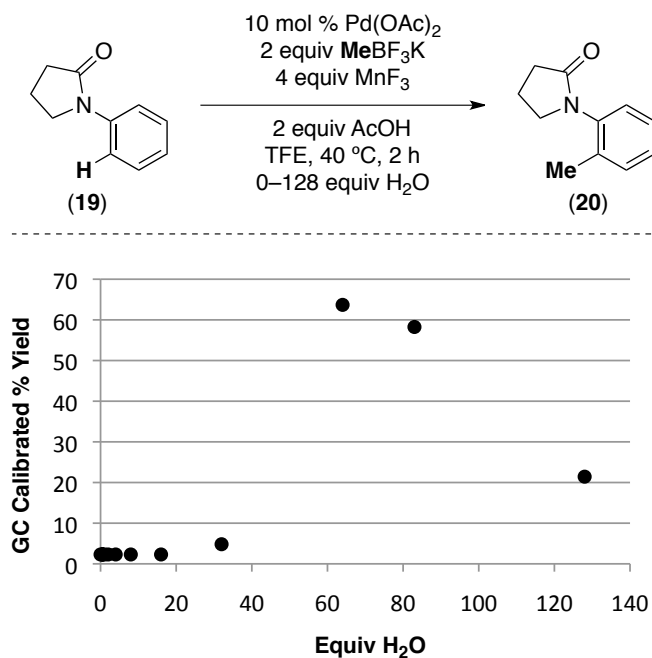


**Figure 3.3.** Yield of Methylated Product **20** in the Presence of Varying Equivalents of Water

Acetic acid (or other carboxylic acid additives) was also necessary for the alkylation reactions; however, the optimal equivalents of AcOH varied with different substrates. For arylpyridine **6**, the highest yields of **5** were obtained when 10–30 equiv AcOH were included in the reaction mixture (Figure 3.4). In contrast, the best yields of pyrrolidinone product **20** were obtained with just 2 equiv AcOH (Figure 3.5).

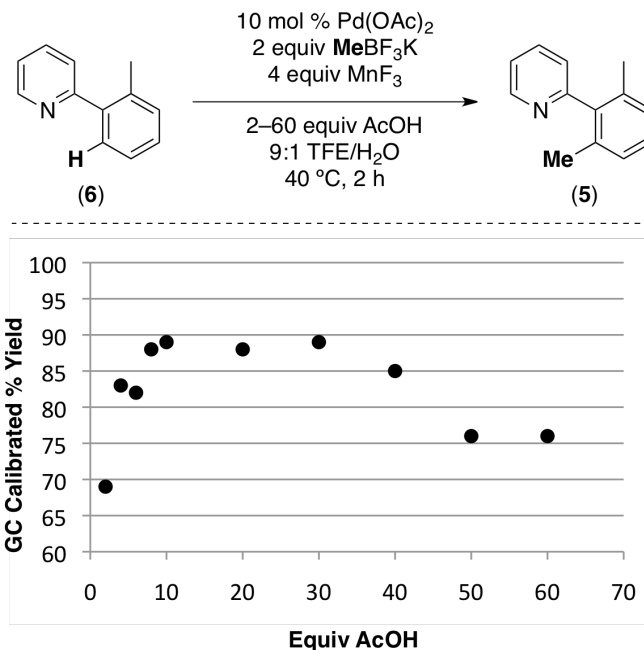


**Figure 3.4.** Yield of Methylated Product **5** in the Presence of Varying Equivalents of Acetic Acid

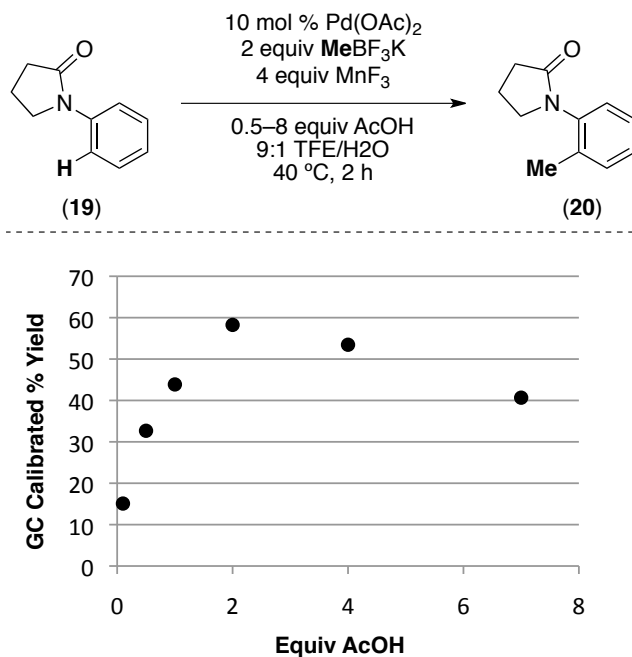


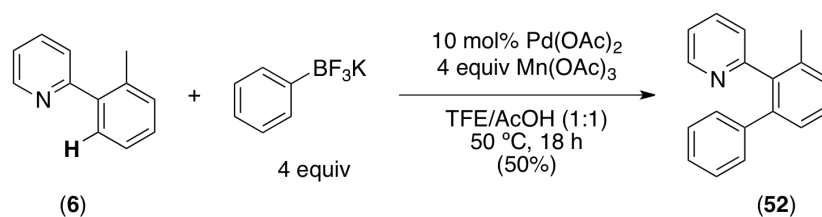
**Figure 3.5.** Yield of Methylated Product **20** in the Presence of Varying Equivalents of Acetic Acid

Further studies will be necessary to elucidate the role of acid in this reaction. We tentatively hypothesize that it may be involved in cyclopalladation or with modulating the activity of  $\text{MnF}_3$ .

### 3.10 C–H Arylation with Potassium Aryltrifluoroborates

In collaboration with my colleague Cydney Seigerman, we have found that the use of aryltrifluoroborates under conditions similar to the C–H alkylation conditions can provide C–H arylated products (Scheme 3.21). Pd-catalyzed C–H arylation reactions using arylboronic acid derivatives have been previously reported at both elevated (70–110 °C)<sup>4–7,9,32</sup> and mild ( $\leq 40$  °C)<sup>8,33</sup> reaction temperatures through putative  $\text{Pd}^{\text{II}}/\text{Pd}^0$  catalytic cycles. We believe that the C–H arylation in the presence of  $\text{Mn}^{\text{III}}$  proceeds through a high oxidation-state Pd-catalyzed mechanism; however, insufficient evidence is currently available to distinguish between a radical or an ionic reaction mechanism.

**Scheme 3.21.** Pd-Catalyzed C–H Arylation with Aryltrifluoroborates and  $\text{Mn}(\text{OAc})_3$



### 3.11 Conclusions and Outlook

This chapter describes a Pd-catalyzed ligand directed C–H alkylation using alkyltrifluoroborate reagents in conjunction with  $\text{MnF}_3$ . This new approach is highly complementary to previously reported methodologies for C–H alkylation. Unlike earlier examples, this reaction does not require the use of high temperatures or stoichiometric bases or silver salts. Alkylation proceeds under remarkably mild temperatures (25–40 °C) with short reaction times (2–6 h). Pyridine- and amide-containing aryl substrates can be alkylated with methyl and a variety of 1° alkyl groups in good to excellent yields. Furthermore, aryltrifluoroborates can be used under similar reaction conditions to provide C–H arylated products.

Several pieces of evidence support an alkyl radical-mediated reaction mechanism for the alkylation reaction. This evidence includes: (1) the observation of non-directed pyridine-alkylation side products in control reactions without Pd, (2) the trends in reactivity observed with different alkyltrifluoroborates, and (3) the ineffectiveness of traditional  $2 e^-$  oxidants for this transformation.

### 3.12 Experimental Procedures and Characterization Data

#### *General Procedures*

NMR spectra were obtained on a Varian vnmrs 700 (699.76 MHz for  $^1\text{H}$ ; 175.95 MHz for  $^{13}\text{C}$ ) or a Varian MR400 (400.52 MHz for  $^1\text{H}$ ; 100.71 for  $^{13}\text{C}$ , 376.87 MHz for  $^{19}\text{F}$ ) spectrometer.  $^1\text{H}$  and  $^{13}\text{C}$  NMR chemical shifts are reported in parts per million (ppm) relative to TMS, with the residual solvent peak used as an internal reference. Multiplicities are reported as follows: singlet (s), doublet (d), doublet of doublets (dd), doublet of doublets of doublets (ddd), doublet of triplets (dt), triplet (t), triplet of doublets (td), triplet of triplets (tt), quartet (q), quintet (quin), multiplet (m), and broad resonance (br). IR spectra were obtained on a Perkin-Elmer Spectrum BX FT-IR spectrometer. Melting points were determined with a Mel-Temp 3.0, a Laboratory Devices Inc, USA instrument, and are uncorrected. HRMS data were obtained on a Micromass AutoSpec Ultima Magnetic Sector mass spectrometer. Gas chromatography was carried out on a Shimadzu 17A using a Restek Rtx®-5 (Crossbond 5% diphenyl – 95% dimethyl polysiloxane; 15 m, 0.25 mm ID, 0.25  $\mu\text{m}$  df) column. GC calibrated yields are reported relative to hexadecane as an internal standard.

**Materials and Methods.** Substrate **6** was prepared by a literature procedure.<sup>34</sup> Substrate **9** was prepared by a palladium-catalyzed Suzuki coupling between 2-methoxyboronic acid and 2-bromopyridine. The remaining substrates were obtained from Aldrich (**15** and **19**), Acros (**11**), Alfa Aesar (**13**), Lancaster Synthesis (**21**), or TCI America (**23**). *n*-BuBF<sub>3</sub>K and EtBF<sub>3</sub>K were obtained from Aldrich, and all other potassium trifluoroborates were obtained from Frontier Chemical. MnF<sub>3</sub> and Pd(OAc)<sub>3</sub> were obtained Alfa Aesar and Pressure Chemical, respectively. Trifluoroethanol was obtained from TCI America, and all other solvents were from Fisher Chemical. All commercial

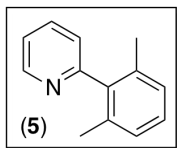
substrates, reagents, and solvents were used as received without further purification. Flash chromatography was performed on EM Science silica gel 60 (0.040–0.063 mm particle size, 230–400 mesh) and thin layer chromatography was performed on Merck TLC plates pre-coated with silica gel 60 F<sub>254</sub>.

### *Synthesis and Characterization of Methylated Products in Table 3.3*

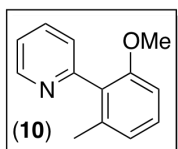
#### **General Procedures**

**Method A:** To a solution of substrate (1 equiv), Pd(OAc)<sub>2</sub> (0.10 equiv), and potassium methyltrifluoroborate (2 equiv) in TFE/H<sub>2</sub>O/AcOH (8:1:1, 0.067 M with respect to substrate) in a scintillation vial was added MnF<sub>3</sub> (4 equiv). The vial was sealed with a Teflon-lined cap, and the mixture was stirred at 40 °C for 2-6 h. The reaction was quenched with 10 wt % aqueous Na<sub>2</sub>SO<sub>3</sub> (0.5 times the volume of total solvent), and then the reaction mixture was poured into a saturated solution of aqueous NaHCO<sub>3</sub> and diluted by 10-fold with EtOAc or Et<sub>2</sub>O. The organic layer was washed twice with aqueous NaHCO<sub>3</sub>, and the combined aqueous layers were extracted three times with EtOAc or Et<sub>2</sub>O. The combined organic layers were washed with brine, dried over MgSO<sub>4</sub>, and concentrated to afford the crude product, which was then purified by column chromatography.

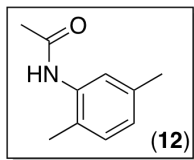
**Method B:** To a solution of substrate (1 equiv), Pd(OAc)<sub>2</sub> (0.10 equiv), potassium methyltrifluoroborate (2 equiv), and AcOH (2 equiv) in TFE/H<sub>2</sub>O (9:1, 0.067 M with respect to substrate) in a scintillation vial was added MnF<sub>3</sub> (4 equiv). The vial was sealed with a Teflon-lined cap, and the mixture was stirred at 25 or 40 °C for 2-6 h. The reaction was quenched with 10 wt % aqueous Na<sub>2</sub>SO<sub>3</sub> (0.5 times the volume of total solvent), and then the reaction mixture was poured into a saturated solution of aqueous NaHCO<sub>3</sub> and diluted by 10-fold with EtOAc or Et<sub>2</sub>O. The organic layer was washed twice with aqueous NaHCO<sub>3</sub>, and the combined aqueous layers were extracted three times with EtOAc or Et<sub>2</sub>O. The combined organic layers were washed with brine, dried over MgSO<sub>4</sub>, and concentrated to afford the crude product which was then purified by column chromatography.



**Aryl Pyridine 5.** Method A was followed using substrate **6** (84.6 mg, 0.50 mmol, 1.0 equiv), Pd(OAc)<sub>2</sub>, (11.2 mg, 0.050 mmol, 0.10 equiv), MeBF<sub>3</sub>K (122 mg, 1.00 mmol, 2 equiv), and MnF<sub>3</sub> (224 mg, 2.00 mmol, 4 equiv) in TFE/H<sub>2</sub>O/AcOH (8:1:1; 7.5 mL total) at 40 °C for 3 h. Product **5** was obtained as a pale yellow oil (74.1 mg, 81% yield, R<sub>f</sub> = 0.22 in 80% hexanes/20% Et<sub>2</sub>O). <sup>1</sup>H NMR (700 MHz, CDCl<sub>3</sub>): δ 8.72 (ddd, *J* = 4.9, 1.9, 1.2 Hz, 1H), 7.76 (td, *J* = 7.8, 1.9 Hz, 1H), 7.26 (ddd, *J* = 7.8, 4.9, 1.2 Hz, 1H), 7.23 (dt, *J* = 7.8, 1.2 Hz, 1H), 7.19 (t, *J* = 7.6 Hz, 1H), 7.10 (d, *J* = 7.6 Hz, 2H), 2.04 (s, 6H). <sup>13</sup>C{<sup>1</sup>H} NMR (176 MHz, CDCl<sub>3</sub>): δ 159.9, 149.7, 140.5, 136.2, 135.7, 127.8, 127.5, 124.4, 121.6, 20.2. HRMS [M+H]<sup>+</sup> Calcd for C<sub>13</sub>H<sub>14</sub>N: 184.1121; Found: 184.1121.

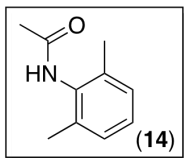


**Aryl Pyridine 10.** Method A was followed using substrate **9** (92.6 mg, 0.50 mmol, 1.0 equiv), Pd(OAc)<sub>2</sub>, (11.2 mg, 0.050 mmol, 0.10 equiv), MeBF<sub>3</sub>K (122 mg, 1.00 mmol, 2 equiv), and MnF<sub>3</sub> (224 mg, 2.00 mmol, 4 equiv) in TFE/H<sub>2</sub>O/AcOH (8:1:1; 7.5 mL total) at 40 °C for 3 h. Product **10** was obtained as a pale yellow oil (69.3 mg, 70% yield, R<sub>f</sub> = 0.20 in 60% hexanes/40% Et<sub>2</sub>O). <sup>1</sup>H NMR (700 MHz, CDCl<sub>3</sub>): δ 8.72 (ddd, *J* = 4.9, 1.9, 1.1 Hz, 1H), 7.73 (td, *J* = 7.6, 1.9 Hz, 1H), 7.29 (dt, *J* = 7.8, 1.1 Hz, 1H), 7.25 (dd, *J* = 8.2, 7.7 Hz, 1H), 7.24 (ddd, *J* = 7.5, 4.9, 1.1 Hz, 1H), 6.89 (d, *J* = 7.7 Hz, 1H), 6.83 (d, *J* = 8.2 Hz, 1H), 3.71 (s, 3H), 2.08 (s, 3H). <sup>13</sup>C{<sup>1</sup>H} NMR (176 MHz, CDCl<sub>3</sub>): δ 157.2, 157.0, 149.4, 137.9, 135.8, 129.9, 128.8, 125.5, 122.6, 121.6, 108.4, 55.7, 19.8. HRMS [M+H]<sup>+</sup> Calcd for C<sub>13</sub>H<sub>14</sub>NO: 200.1070; Found: 200.1070.

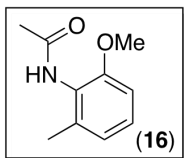


**Acetanilide 12.** Method B was followed using substrate **11** (74.6 mg, 0.50 mmol, 1.0 equiv), Pd(OAc)<sub>2</sub>, (11.2 mg, 0.050 mmol, 0.10 equiv), MeBF<sub>3</sub>K (122 mg, 1.00 mmol, 2 equiv), MnF<sub>3</sub> (224 mg, 2.00 mmol, 4 equiv), and AcOH (57 μL, 1.00 mmol, 2.0 equiv) in TFE/H<sub>2</sub>O (9:1; 7.5 mL total) at room temperature for 3 h. Product **12** was obtained as a white solid [78.2 mg, 96% yield, R<sub>f</sub> = 0.27 in 50% hexanes/50% EtOAc, mp = 137.0–138.3 °C (lit.<sup>35</sup> 138–141 °C)]. <sup>1</sup>H NMR (700 MHz, CD<sub>3</sub>CN, major rotamer): δ 7.77 (br s, 1H), 7.34 (s, 1H), 7.08 (d, *J* = 7.8 Hz, 1H), 6.90 (d, *J* = 7.8 Hz, 1H), 2.27 (s, 3H), 2.17 (s, 3H), 2.07 (s, 3H).

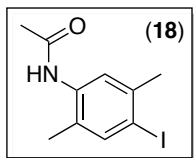
$^{13}\text{C}\{^1\text{H}\}$  NMR (176 MHz,  $\text{CD}_3\text{CN}$ , major rotamer):  $\delta$  169.5, 137.2, 126.7, 121.1, 129.1, 126.8, 126.0, 23.8, 21.0, 17.6. IR (thin film,  $\text{CH}_2\text{Cl}_2$ ) 3278, 2922, 1657  $\text{cm}^{-1}$ . HRMS  $[\text{M}+\text{H}]^+$  Calcd for  $\text{C}_{10}\text{H}_{14}\text{NO}$ : 164.1070; Found: 164.1070.



**Acetanilide 14.** Method B was followed using substrate **13** (74.6 mg, 0.50 mmol, 1.0 equiv),  $\text{Pd}(\text{OAc})_2$  (11.2 mg, 0.050 mmol, 0.10 equiv),  $\text{MeBF}_3\text{K}$  (122 mg, 1.00 mmol, 2 equiv),  $\text{MnF}_3$  (224 mg, 2.00 mmol, 4 equiv), and  $\text{AcOH}$  (57  $\mu\text{L}$ , 1.00 mmol, 2.0 equiv) in  $\text{TFE}/\text{H}_2\text{O}$  (9:1; 7.5 mL total) at 40  $^\circ\text{C}$  for 3 h. Product **14** was obtained as a white solid [58.7 mg, 72% yield,  $R_f = 0.19$  in 50% hexanes/50% EtOAc, mp = 166.6–170.2  $^\circ\text{C}$  (lit.<sup>36</sup> 176–177  $^\circ\text{C}$ )].  $^1\text{H}$  NMR (700 MHz,  $\text{CD}_3\text{CN}$ , major rotamer):  $\delta$  7.70 (br s, 1H), 7.08–7.06 (multiple peaks, 3H), 2.17 (s, 6H), 2.07 (s, 3H).  $^{13}\text{C}\{^1\text{H}\}$  NMR (176 MHz,  $\text{CD}_3\text{CN}$ , major rotamer):  $\delta$  169.4, 136.8, 136.1, 128.7, 127.7, 22.9, 18.4. IR (thin film,  $\text{CH}_2\text{Cl}_2$ ) 3233, 3044, 1648  $\text{cm}^{-1}$ . HRMS  $[\text{M}+\text{H}]^+$  Calcd for  $\text{C}_{10}\text{H}_{14}\text{NO}$ : 164.1070; Found: 164.1071.



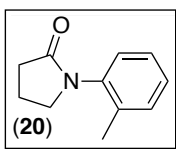
**Acetanilide 16.** Method B was followed using substrate **15** (82.6 mg, 0.50 mmol, 1.0 equiv),  $\text{Pd}(\text{OAc})_2$  (11.2 mg, 0.050 mmol, 0.10 equiv),  $\text{MeBF}_3\text{K}$  (122 mg, 1.00 mmol, 2 equiv),  $\text{MnF}_3$  (224 mg, 2.00 mmol, 4 equiv), and  $\text{AcOH}$  (57  $\mu\text{L}$ , 1.00 mmol, 2.0 equiv) in  $\text{TFE}/\text{H}_2\text{O}$  (9:1; 7.5 mL total) at 40  $^\circ\text{C}$  for 3 h. Product **16** was obtained as a white solid [43.6 mg, 53% yield,  $R_f = 0.16$  in 50% hexanes/50% EtOAc, mp = 124.1–124.4  $^\circ\text{C}$  (lit.<sup>37</sup> 123  $^\circ\text{C}$ )].  $^1\text{H}$  NMR (700 MHz,  $\text{CD}_3\text{CN}$ , major rotamer):  $\delta$  7.59 (br s, 1H), 7.14 (dd,  $J = 8.2, 7.5$  Hz, 1H), 6.83 (d,  $J = 8.2$  Hz, 1H), 6.82 (d,  $J = 7.5$  Hz, 1H), 3.77 (s, 3H), 2.15 (s, 3H), 2.05 (s, 3H).  $^{13}\text{C}\{^1\text{H}\}$  NMR (176 MHz,  $\text{CDCl}_3$ ):  $\delta$  169.5, 155.8, 138.1, 128.1, 126.0, 123.0, 109.7, 56.3, 23.1, 18.3. IR (thin film,  $\text{CH}_2\text{Cl}_2$ ) 3252, 3004, 2935, 2837, 1660  $\text{cm}^{-1}$ . HRMS  $[\text{M}+\text{H}]^+$  Calcd for  $\text{C}_{10}\text{H}_{14}\text{NO}_2$ : 180.1019; Found: 180.1020.



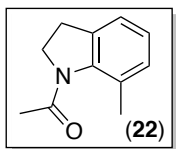
**Acetanilide 18.** Method B was followed using substrate **17** (137.5 mg, 0.50 mmol, 1.0 equiv),  $\text{Pd}(\text{OAc})_2$  (11.2 mg, 0.050 mmol, 0.10 equiv),  $\text{MeBF}_3\text{K}$  (122 mg, 1.00 mmol, 2 equiv),  $\text{MnF}_3$  (224 mg, 2.00 mmol, 4 equiv), and  $\text{AcOH}$  (57  $\mu\text{L}$ , 1.00 mmol, 2.0 equiv) in  $\text{TFE}/\text{H}_2\text{O}$  (9:1; 7.5 mL total) at 40  $^\circ\text{C}$  for 3 h. Product **18** was obtained as a white solid [119.8 mg, 83%



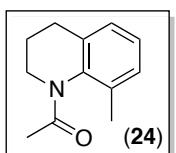
yield,  $R_f = 0.25$  in 50% hexanes/50% EtOAc, mp = 211.4–213.3 °C (lit.<sup>38</sup> 212–214 °C)].  $^1\text{H}$  NMR (700 MHz, DMSO- $d_6$ ):  $\delta$  9.26 (s, 1H), 7.64 (s, 1H), 7.39 (s, 1H), 2.29 (s, 3H), 2.12 (s, 3H), 2.04 (s, 3H).  $^{13}\text{C}\{^1\text{H}\}$  NMR (176 MHz, DMSO- $d_6$ ):  $\delta$  168.2, 139.6, 138.0, 136.8, 131.2, 126.1, 96.0, 27.0, 23.3, 16.8. IR (thin film,  $\text{CH}_2\text{Cl}_2$ ) 3286, 1654  $\text{cm}^{-1}$ . HRMS  $[\text{M}+\text{H}]^+$  Calcd for  $\text{C}_{10}\text{H}_{13}\text{INO}$ : 290.0036; Found: 290.0038.



**Pyrrolidinone 20.** Method B was followed using substrate **19** (80.6 mg, 0.50 mmol, 1.0 equiv),  $\text{Pd}(\text{OAc})_2$  (11.2 mg, 0.050 mmol, 0.10 equiv),  $\text{MeBF}_3\text{K}$  (122 mg, 1.00 mmol, 2 equiv),  $\text{MnF}_3$  (224 mg, 2.00 mmol, 4 equiv), and AcOH (57  $\mu\text{L}$ , 1.00 mmol, 2.0 equiv) in TFE/ $\text{H}_2\text{O}$  (9:1; 7.5 mL total) at 40 °C for 2 h. Product **20** was obtained as a pale yellow oil (63.8 mg, 73% yield,  $R_f = 0.16$  in 50% hexanes/50% EtOAc).  $^1\text{H}$  NMR (700 MHz,  $\text{CDCl}_3$ ):  $\delta$  7.27 (m, 1H), 7.23–7.22 (multiple peaks, 2H), 7.14 (m, 1H), 3.73 (t,  $J = 7.1$  Hz, 2H), 2.58 (t,  $J = 8.1$  Hz, 2H), 2.24 (s, 3H), 2.23 (m, 2H).  $^{13}\text{C}\{^1\text{H}\}$  NMR (176 MHz,  $\text{CDCl}_3$ ):  $\delta$  174.3, 137.4, 135.5, 131.2, 127.9, 126.8, 126.6, 50.7, 31.2, 19.1, 17.9. IR (thin film, neat) 2956, 1682  $\text{cm}^{-1}$ . HRMS  $[\text{M}+\text{H}]^+$  Calcd for  $\text{C}_{11}\text{H}_{14}\text{NO}$ : 176.1070; Found: 176.1069.



**Acetylidoline 22.** Method B was followed using substrate **21** (80.6 mg, 0.50 mmol, 1.0 equiv),  $\text{Pd}(\text{OAc})_2$  (11.2 mg, 0.050 mmol, 0.10 equiv),  $\text{MeBF}_3\text{K}$  (122 mg, 1.00 mmol, 2 equiv),  $\text{MnF}_3$  (224 mg, 2.00 mmol, 4 equiv), and AcOH (57  $\mu\text{L}$ , 1.00 mmol, 2.0 equiv) in TFE/ $\text{H}_2\text{O}$  (9:1; 7.5 mL total) at 40 °C for 2 h. Product **22** was obtained as a white solid [72.7 mg, 83% yield,  $R_f = 0.34$  in 50% hexanes/50% EtOAc, mp = 86.9–88.1 °C (lit.<sup>39</sup> 89–90 °C)].  $^1\text{H}$  NMR (700 MHz,  $\text{CD}_3\text{CN}$ ):  $\delta$  7.08 (t,  $J = 4.4$  Hz, 1H), 7.00–6.99 (multiple peaks, 2H), 4.04 (t,  $J = 7.6$  Hz, 2H), 3.00 (t,  $J = 7.6$  Hz, 2H), 2.20 (s, 3H), 2.19 (s, 3H).  $^{13}\text{C}\{^1\text{H}\}$  NMR (176 MHz,  $\text{CD}_3\text{CN}$ ):  $\delta$  169.5, 143.0, 136.1, 130.1, 129.5, 125.7, 122.7, 51.9, 30.5, 24.0, 20.8. IR (thin film,  $\text{CH}_2\text{Cl}_2$ ) 2920, 1666  $\text{cm}^{-1}$ . HRMS  $[\text{M}+\text{H}]^+$  Calcd for  $\text{C}_{11}\text{H}_{14}\text{NO}$ : 176.1070; Found: 176.1068.



**Tetrahydroquinoline 24.** Method B was followed using substrate **23** (87.6 mg, 0.50 mmol, 1.0 equiv),  $\text{Pd}(\text{OAc})_2$  (11.2 mg, 0.050 mmol, 0.10 equiv),  $\text{MeBF}_3\text{K}$  (122 mg, 1.00 mmol, 2 equiv),  $\text{MnF}_3$  (224 mg, 2.00

mmol, 4 equiv), and AcOH (57  $\mu$ L, 1.00 mmol, 2.0 equiv) in TFE/H<sub>2</sub>O (9:1; 7.5 mL total) at 40 °C for 2 h. Product **24** was obtained as a pale yellow oil (70.0 mg, 74% yield,  $R_f = 0.38$  in 50% hexanes/50% EtOAc). <sup>1</sup>H NMR (700 MHz, C<sub>6</sub>D<sub>6</sub>, major rotamer):  $\delta$  6.89 (t,  $J = 7.6$  Hz, 1H), 6.83 (d,  $J = 7.6$  Hz, 1H), 6.74 (d,  $J = 7.6$  Hz, 1H), 4.93 (ddd,  $J = 12.8, 9.2, 5.9$  Hz, 1H), 2.51 (ddd,  $J = 12.8, 8.4, 5.8$  Hz, 1H), 2.15 (ddd,  $J = 14.7, 6.2, 3.3$  Hz, 1H), 2.10 (ddd,  $J = 14.7, 10.9, 6.7$  Hz, 1H), 1.95 (s, 3H), 1.83 (m, 1H), 1.73 (s, 3H), 1.14 (m, 1H). <sup>13</sup>C {<sup>1</sup>H} NMR (176 MHz, CDCl<sub>3</sub>, major rotamer):  $\delta$  170.9, 139.8, 137.3, 133.1, 128.9, 126.5, 125.2, 41.4, 26.6, 24.0, 21.3, 17.6. IR (thin film, neat) 2946, 1650 cm<sup>-1</sup>. HRMS [M+H]<sup>+</sup> Calcd for C<sub>12</sub>H<sub>16</sub>NO: 190.1226; Found: 190.1229.

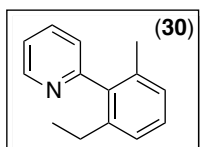
### *Synthesis and Characterization of Alkylated Products in Table 3.5*

#### **General Procedures**

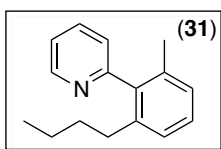
**Method A:** To a solution of substrate (1 equiv), Pd(OAc)<sub>2</sub> (0.10 equiv), and potassium alkyltrifluoroborate (2–4 equiv) in TFE/H<sub>2</sub>O/AcOH (8:1:1 or 4.5:1:4.5, 0.067 M with respect to substrate) in a scintillation vial was added MnF<sub>3</sub> (3–4 equiv). The vial was sealed with a Teflon-lined cap, and the mixture was stirred at 40 °C for 2-6 h. The reaction was quenched with 10 wt % aqueous Na<sub>2</sub>SO<sub>3</sub> (0.5 times the volume of total solvent), and then the reaction mixture was poured into a saturated solution of aqueous NaHCO<sub>3</sub> and diluted by 10-fold with EtOAc or Et<sub>2</sub>O. The organic layer was washed twice with aqueous NaHCO<sub>3</sub>, and the combined aqueous layers were extracted three times with EtOAc or Et<sub>2</sub>O. The combined organic layers were washed with brine, dried over MgSO<sub>4</sub>, and concentrated to afford the crude product, which was then purified by column chromatography.

**Method B:** To a solution of substrate (1 equiv), Pd(OAc)<sub>2</sub> (0.10 equiv), potassium alkyltrifluoroborate (2 equiv), and AcOH (1 or 2 equiv) in TFE/H<sub>2</sub>O (9:1, 0.067 or 0.133 M with respect to substrate) in a scintillation vial was added MnF<sub>3</sub> (4 equiv). The vial was sealed with a Teflon-lined cap, and the mixture was stirred at 25 or 40 °C for 2-6 h. The reaction was quenched with 10 wt % aqueous Na<sub>2</sub>SO<sub>3</sub> (0.5 times the volume of total solvent), and then the reaction mixture was poured into a saturated solution of aqueous

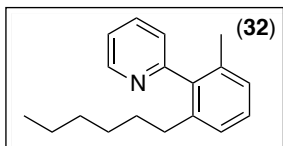
NaHCO<sub>3</sub> and diluted by 10-fold with EtOAc or Et<sub>2</sub>O. The organic layer was washed twice with aqueous NaHCO<sub>3</sub>, and the combined aqueous layers were extracted three times with EtOAc or Et<sub>2</sub>O. The combined organic layers were washed with brine, dried over MgSO<sub>4</sub>, and concentrated to afford the crude product, which was then purified by column chromatography.



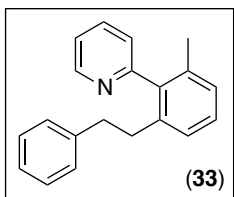
**Aryl Pyridine 30.** Method A was followed using substrate **6** (84.6 mg, 0.50 mmol, 1.0 equiv), Pd(OAc)<sub>2</sub> (11.2 mg, 0.050 mmol, 0.10 equiv), EtBF<sub>3</sub>K (136 mg, 1.00 mmol, 2 equiv), and MnF<sub>3</sub> (224 mg, 2.00 mmol, 4 equiv) in TFE/H<sub>2</sub>O/AcOH (8:1:1; 7.5 mL total) at 40 °C for 3 h. Product **30** was obtained as a pale yellow oil (73.8 mg, 75% yield, R<sub>f</sub> = 0.26 in 80% hexanes/20% Et<sub>2</sub>O). <sup>1</sup>H NMR (700 MHz, CDCl<sub>3</sub>): δ 8.72 (ddd, *J* = 5.0, 1.6, 1.0 Hz, 1H), 7.75 (td, *J* = 7.6, 1.7 Hz, 1H), 7.27–7.23 (multiple peaks, 3H), 7.14 (d, *J* = 7.3 Hz, 1H), 7.10 (d, *J* = 7.3 Hz, 1H), 2.35 (br m, 2H), 2.02 (s, 3H), 1.03 (t, *J* = 7.3 Hz, 3H). <sup>13</sup>C {<sup>1</sup>H} NMR (176 MHz, CDCl<sub>3</sub>): δ 159.8, 149.6, 141.9, 140.0, 136.1, 135.8, 128.0, 127.4, 125.8, 124.6, 121.6, 26.5, 20.2, 15.4. HRMS [M+H]<sup>+</sup> Calcd for C<sub>14</sub>H<sub>16</sub>N: 198.1277; Found: 198.1276.



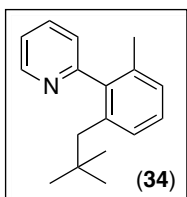
**Aryl Pyridine 31.** Method A was followed using substrate **6** (42.3 mg, 0.25 mmol, 1.0 equiv), Pd(OAc)<sub>2</sub> (5.6 mg, 0.025 mmol, 0.10 equiv), <sup>n</sup>BuBF<sub>3</sub>K (164 mg, 1.00 mmol, 4 equiv), and MnF<sub>3</sub> (84 mg, 0.75 mmol, 3 equiv) in TFE/H<sub>2</sub>O/AcOH (8:1:1; 3.75 mL total) at 40 °C for 6 h. Product **31** was obtained as a pale yellow oil (43.2 mg, 77% yield, R<sub>f</sub> = 0.30 in 80% hexanes/20% Et<sub>2</sub>O). <sup>1</sup>H NMR (700 MHz, CDCl<sub>3</sub>): δ 8.71 (ddd, *J* = 4.8, 1.8, 1.2 Hz, 1H), 7.75 (td, *J* = 7.7, 1.8 Hz, 1H), 7.26 (ddd, *J* = 7.7, 4.8, 1.2 Hz, 1H), 7.24 (dt, *J* = 7.7, 1.2 Hz, 1H), 7.22 (t, *J* = 7.6 Hz, 1H), 7.12 (d, *J* = 7.6 Hz, 1H), 7.09 (d, *J* = 7.6 Hz, 1H), 2.32 (t, *J* = 7.9 Hz, 2H), 2.02 (s, 3H), 1.38 (br m, 2H), 1.16 (sext, *J* = 7.4 Hz, 2H), 0.74 (t, *J* = 7.4 Hz, 3H). <sup>13</sup>C {<sup>1</sup>H} NMR (176 MHz, CDCl<sub>3</sub>): δ 159.8, 149.5, 140.6, 140.2, 136.0, 135.8, 127.9, 127.4, 126.6, 124.7, 121.6, 33.3, 33.1, 22.5, 20.3, 13.7. HRMS [M+H]<sup>+</sup> Calcd for C<sub>16</sub>H<sub>20</sub>N: 226.1590; Found: 226.1594.



**Aryl Pyridine 32.** Method A was followed using substrate **6** (42.3 mg, 0.25 mmol, 1.0 equiv), Pd(OAc)<sub>2</sub> (5.6 mg, 0.025 mmol, 0.10 equiv), *n*-hexylBF<sub>3</sub>K (192 mg, 1.00 mmol, 4 equiv), and MnF<sub>3</sub> (84 mg, 0.75 mmol, 3 equiv) in TFE/H<sub>2</sub>O/AcOH (8:1:1; 3.75 mL total) at 40 °C for 6 h. Product **32** was obtained as a pale yellow oil (39.0 mg, 62% yield, R<sub>f</sub> = 0.35 in 80% hexanes/20% Et<sub>2</sub>O). <sup>1</sup>H NMR (700 MHz, CDCl<sub>3</sub>): δ 8.71 (ddd, *J* = 4.7, 1.9, 1.2 Hz, 1H), 7.75 (td, *J* = 7.7, 1.9 Hz, 1H), 7.27–7.24 (multiple peaks, 3H), 7.13 (d, *J* = 7.6 Hz, 1H), 7.09 (d, *J* = 7.6 Hz, 1H), 2.31 (t, *J* = 8.1 Hz, 2H), 2.02 (s, 3H), 1.39 (br m, 2H), 1.18 (sext, *J* = 7.3 Hz, 2H), 1.15–1.09 (multiple peaks, 4H), 0.81 (t, *J* = 7.2 Hz, 3H) <sup>13</sup>C{<sup>1</sup>H} NMR (176 MHz, CDCl<sub>3</sub>): δ 159.8, 149.5, 140.7, 140.2, 136.0, 135.8, 127.9, 127.4, 126.6, 124.6, 121.6, 33.4, 31.4, 31.0, 29.1, 22.4, 20.3, 14.0. HRMS [M+H]<sup>+</sup> Calcd for C<sub>18</sub>H<sub>24</sub>N: 254.1903; Found: 254.1906.

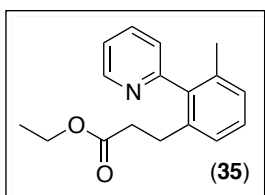


**Aryl Pyridine 33.** Method A was followed using substrate **6** (84.6 mg, 0.50 mmol, 1.0 equiv), Pd(OAc)<sub>2</sub> (11.2 mg, 0.050 mmol, 0.10 equiv), potassium phenethyltrifluoroborate (212 mg, 1.00 mmol, 2 equiv), and MnF<sub>3</sub> (224 mg, 2.00 mmol, 4 equiv) in TFE/H<sub>2</sub>O/AcOH (8:1:1; 7.5 mL total) at 40 °C for 6 h. Product **33** was obtained as a pale yellow oil (67.0 mg, 49% yield, R<sub>f</sub> = 0.23 in 80% hexanes/20% Et<sub>2</sub>O). <sup>1</sup>H NMR (700 MHz, CDCl<sub>3</sub>): δ 8.75 (ddd, *J* = 5.00, 1.6, 1.0 Hz, 1H), 7.75 (td, *J* = 7.7, 1.6 Hz, 1H), 7.29 (ddd, *J* = 7.5, 5.0, 1.0 Hz, 1H), 7.25 (t, *J* = 7.6 Hz, 1H), 7.20–7.18 (multiple peaks, 3H), 7.16–7.12 (multiple peaks, 3H), 6.92 (d, *J* = 7.7 Hz, 2H), 2.71 (br m, 2H), 2.63 (t, *J* = 8.5 Hz, 2H), 2.05 (s, 3H). <sup>13</sup>C{<sup>1</sup>H} NMR (176 MHz, CDCl<sub>3</sub>): δ 159.6, 149.6, 142.1, 140.3, 139.6, 136.2, 136.0, 128.24, 128.20, 128.0, 127.8, 126.7, 125.7, 124.7, 121.8, 37.8, 36.0, 20.3. HRMS [M+H]<sup>+</sup> Calcd for C<sub>20</sub>H<sub>20</sub>N: 274.1590; Found: 274.1596.

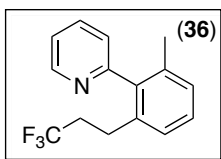


**Aryl Pyridine 34.** Method A was followed using substrate **6** (42.3 mg, 0.25 mmol, 1.0 equiv), Pd(OAc)<sub>2</sub> (5.6 mg, 0.025 mmol, 0.10 equiv), potassium neopentyltrifluoroborate (178 mg, 1.00 mmol, 4 equiv), and MnF<sub>3</sub> (84 mg, 0.75 mmol, 3 equiv) in TFE/H<sub>2</sub>O/AcOH (4.5:1:4.5; 3.75 mL total) at 40 °C for 6 h. Product **34** was obtained as a pale yellow oil (23.7 mg, 40%

yield,  $R_f = 0.32$  in 80% hexanes/20% Et<sub>2</sub>O). <sup>1</sup>H NMR (700 MHz, CDCl<sub>3</sub>): δ 8.71 (ddd,  $J = 4.7, 1.7, 1.2$  Hz, 1H), 7.72 (td,  $J = 7.6, 1.8$  Hz, 1H), 7.24-7.23 (multiple peaks, 2H), 7.20 (t,  $J = 7.5$  Hz, 1H), 7.14 (d,  $J = 7.5$  Hz, 1H), 7.12 (d,  $J = 7.5$  Hz, 1H), 2.46 (s, 2H), 2.04 (s, 3H), 0.71 (s, 9H). <sup>13</sup>C{<sup>1</sup>H} NMR (176 MHz, CDCl<sub>3</sub>): δ 160.1, 149.2, 141.2, 137.5, 136.0, 135.6, 129.2, 127.9, 127.0, 125.9, 121.4, 45.6, 32.4, 29.9, 20.8. HRMS [M+H]<sup>+</sup> Calcd for C<sub>17</sub>H<sub>22</sub>N: 240.1747; Found: 240.1748.

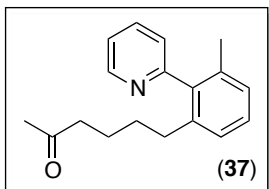


**Aryl Pyridine 35.** Method B was followed using substrate **6** (84.6 mg, 0.50 mmol, 1.0 equiv), Pd(OAc)<sub>2</sub> (11.2 mg, 0.050 mmol, 0.10 equiv), potassium 3-trifluoroboropropionate ethyl ester (208 mg, 1.00 mmol, 2 equiv), MnF<sub>3</sub> (224 mg, 2.00 mmol, 4 equiv), and AcOH (57 μL, 1.00 mmol, 2 equiv) in TFE/H<sub>2</sub>O (9:1; 7.5 mL total) at 40 °C for 6 h. Product **35** was obtained as a pale yellow oil (62.4 mg, 46% yield,  $R_f = 0.23$  in 80% hexanes/20% Et<sub>2</sub>O). <sup>1</sup>H NMR (700 MHz, CDCl<sub>3</sub>): δ 8.72 (ddd,  $J = 4.9, 1.8, 0.9$  Hz, 1H), 7.77 (td,  $J = 7.8, 1.8$  Hz, 1H), 7.28-7.26 (multiple peaks, 2H), 7.23 (t,  $J = 7.5$  Hz, 1H), 7.134 (d,  $J = 7.5$  Hz, 1H), 7.131 (d,  $J = 7.5$  Hz, 1H), 4.04 (q,  $J = 7.2$  Hz, 2H), 2.67 (br m, 2H), 2.42 (br m, 2H), 2.02 (s, 3H), 1.18 (t,  $J = 7.2$  Hz, 3H). <sup>13</sup>C{<sup>1</sup>H} NMR (176 MHz, CDCl<sub>3</sub>): δ 173.0, 159.3, 149.7, 140.3, 138.4, 136.3, 136.1, 128.1, 126.5, 124.6, 121.9, 60.2, 35.5, 28.7, 20.3, 14.1. Two aromatic <sup>13</sup>C resonances are coincidentally overlapping. IR (thin film, neat) 2980, 1728 cm<sup>-1</sup>. HRMS [M+H]<sup>+</sup> Calcd for C<sub>17</sub>H<sub>20</sub>NO<sub>2</sub>: 270.1489; Found: 270.1493.

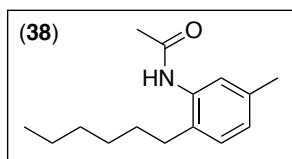


**Aryl Pyridine 36.** Method B was followed using substrate **6** (84.6 mg, 0.50 mmol, 1.0 equiv), Pd(OAc)<sub>2</sub> (11.2 mg, 0.050 mmol, 0.10 equiv), potassium 3,3,3-trifluoropropane-1-trifluoroborate (204 mg, 1.00 mmol, 2 equiv), MnF<sub>3</sub> (224 mg, 2.00 mmol, 4 equiv), and AcOH (29 μL, 0.50 mmol, 1 equiv) in TFE/H<sub>2</sub>O (9:1; 3.75 mL total) at 40 °C for 6 h. Product **36** was obtained as a pale yellow oil (33.8 mg, 25% yield,  $R_f = 0.30$  in 80% hexanes/20% Et<sub>2</sub>O). <sup>1</sup>H NMR (700 MHz, CDCl<sub>3</sub>): δ 8.73 (ddd,  $J = 5.0, 1.8, 0.9$  Hz, 1H), 7.79 (td,  $J = 7.7, 1.8$  Hz, 1H), 7.30 (ddd,  $J = 7.7, 5.0, 1.1$  Hz, 1H), 7.27-7.25 (multiple peaks, 2H), 7.17 (d,  $J = 7.7$  Hz, 1H), 7.12 (d,  $J = 7.7$  Hz, 1H), 2.58 (br m, 2H), 2.22 (br

m, 2H), 2.05 (s, 3H).  $^{13}\text{C}\{^1\text{H}\}$  NMR (176 MHz,  $\text{CDCl}_3$ ):  $\delta$  158.9, 149.8, 140.4, 137.0, 136.4, 126.3, 128.6, 128.4, 126.6, 126.5 (q,  $^1J_{\text{C-F}} = 277$  Hz) 124.5, 122.1, 35.3 (q,  $^2J_{\text{C-F}} = 28$  Hz), 26.2 (q,  $^3J_{\text{C-F}} = 3$  Hz), 20.3.  $^{19}\text{F}$  NMR (376 MHz,  $\text{CDCl}_3$ ):  $\delta$  -67.20 (t,  $J = 11.0$  Hz). HRMS  $[\text{M}+\text{H}]^+$  Calcd for  $\text{C}_{15}\text{H}_{15}\text{F}_3\text{N}$ : 266.1151; Found: 266.1157.

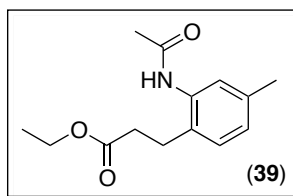


**Aryl Pyridine 37.** Method A was followed using substrate **6** (84.6 mg, 0.50 mmol, 1.0 equiv),  $\text{Pd}(\text{OAc})_2$  (11.2 mg, 0.050 mmol, 0.10 equiv), potassium 5-oxohexyltrifluoroborate (206 mg, 1.00 mmol, 2 equiv), and  $\text{MnF}_3$  (224 mg, 2.00 mmol, 4 equiv) in TFE/ $\text{H}_2\text{O}$ / $\text{AcOH}$  (8:1:1; 7.5 mL total) at 40 °C for 6 h. Product **37** was obtained as a pale yellow oil (40.2 mg, 30%,  $R_f = 0.19$  in 60% benzene/20%  $\text{CH}_2\text{Cl}_2$ /20%  $\text{Et}_2\text{O}$ ).  $^1\text{H}$  NMR (700 MHz,  $\text{CDCl}_3$ ):  $\delta$  8.71 (ddd,  $J = 4.9, 1.7, 1.1$  Hz, 1H), 7.76 (td,  $J = 7.6, 1.7$  Hz, 1H), 7.27 (ddd,  $J = 7.6, 4.9, 1.1$  Hz, 1H), 7.23 (dt,  $J = 7.6, 1.1$  Hz, 1H), 7.22 (t,  $J = 6.9$  Hz, 1H), 7.11-7.09 (multiple peaks, 2H), 2.33 (br t,  $J = 7.4$  Hz, 2H), 2.26 (br m, 2H), 2.05 (s, 3H), 2.01 (s, 3H), 1.42-1.41 (multiple peaks, 4H)  $^{13}\text{C}\{^1\text{H}\}$  NMR (176 MHz,  $\text{CDCl}_3$ ):  $\delta$  209.0, 159.7, 149.5, 140.1, 139.9, 136.1, 135.9, 128.0, 127.6, 126.5, 124.7, 121.7, 43.4, 33.2, 30.5, 29.8, 23.6, 20.3. IR (thin film, neat) 2934, 1711  $\text{cm}^{-1}$ . HRMS  $[\text{M}+\text{H}]^+$  Calcd for  $\text{C}_{18}\text{H}_{22}\text{NO}$ : 268.1696; Found: 268.1701.

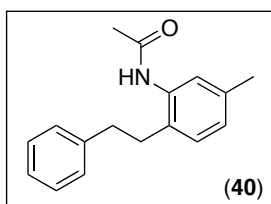


**Acetanilide 38.** Method B was followed using substrate **11** (37.3 mg, 0.25 mmol, 1.0 equiv),  $\text{Pd}(\text{OAc})_2$ , (5.6 mg, 0.025 mmol, 0.10 equiv), *n*-hexyl $\text{BF}_3\text{K}$  (96 mg, 0.50 mmol, 2 equiv),  $\text{MnF}_3$  (112 mg, 1.00 mmol, 4 equiv), and  $\text{AcOH}$  (29  $\mu\text{L}$ , 0.50 mmol, 2.0 equiv) in TFE/ $\text{H}_2\text{O}$  (9:1; 3.75 mL total) at 40 °C for 3 h. Product **38** was obtained as a white solid (42.1 mg, 72% yield,  $R_f = 0.50$  in 50% hexanes/50%  $\text{EtOAc}$ , mp = 113.4–114.7 °C).  $^1\text{H}$  NMR (700 MHz,  $\text{CD}_3\text{CN}$ , major rotamer):  $\delta$  7.73 (br s, 1H), 7.27 (s, 1H), 7.09 (d,  $J = 7.6$  Hz, 1H), 6.94 (d,  $J = 7.6$  Hz, 1H), 2.52 (t,  $J = 7.7$  Hz, 2H), 2.27 (s, 3H), 2.06 (s, 3H), 1.50 (quin,  $J = 7.7$  Hz, 2H), 1.35-1.29 (multiple peaks, 6H), 0.89 (t,  $J = 7.0$  Hz, 3H).  $^{13}\text{C}\{^1\text{H}\}$  NMR (176 MHz,  $\text{CD}_3\text{CN}$ , major rotamer):  $\delta$  169.8, 136.7, 126.6, 134.4, 130.3, 127.2, 127.1, 32.4, 31.5, 30.9, 29.8, 23.8, 23.3, 20.9, 14.3 IR

(thin film, CH<sub>2</sub>Cl<sub>2</sub>) 3273, 2925, 1654 cm<sup>-1</sup>. HRMS [M+H]<sup>+</sup> Calcd for C<sub>15</sub>H<sub>24</sub>NO: 234.1852; Found: 234.1857.



**Acetanilide 39.** Method B was followed using substrate **11** (37.3 mg, 0.25 mmol, 1.0 equiv), Pd(OAc)<sub>2</sub> (5.6 mg, 0.025 mmol, 0.10 equiv), potassium 3-trifluoroboropropionate ethyl ester (104 mg, 0.50 mmol, 2 equiv), MnF<sub>3</sub> (112 mg, 1.00 mmol, 4 equiv), and AcOH (29 μL, 0.50 mmol, 2.0 equiv) in TFE/H<sub>2</sub>O (9:1; 3.75 mL total) at 40 °C for 3 h. Product **39** was obtained as a white solid (37.2 mg, 60% yield, R<sub>f</sub> = 0.25 in 50% hexanes/50% EtOAc, mp = 109.5–110.1 °C). <sup>1</sup>H NMR (700 MHz, CD<sub>3</sub>CN, major rotamer): δ 8.10 (br s, 1H), 7.30 (s, 3H), 7.11 (d, *J* = 7.8 Hz, 1H), 6.95 (d, *J* = 7.8 Hz, 1H), 4.07 (q, *J* = 7.1 Hz, 2H), 2.81 (t, *J* = 7.7 Hz, 2H), 2.56 (t, *J* = 7.7 Hz, 2H), 2.27 (s, 3H), 2.08 (s, 3H), 1.18 (t, *J* = 7.1 Hz, 3H). <sup>13</sup>C{<sup>1</sup>H} NMR (176 MHz, CD<sub>3</sub>CN, major rotamer): δ 173.3, 168.8, 136.4, 135.8, 131.5, 129.4, 126.4, 126.2, 60.3, 34.5, 25.4, 22.9, 20.0, 13.5. IR (thin film, CH<sub>2</sub>Cl<sub>2</sub>) 3277, 1716, 1654 cm<sup>-1</sup>. HRMS [M+H]<sup>+</sup> Calcd for C<sub>14</sub>H<sub>20</sub>NO<sub>3</sub>: 250.1438; Found: 250.1440.



**Acetanilide 40.** Method B was followed using substrate **11** (74.6 mg, 0.50 mmol, 1.0 equiv), Pd(OAc)<sub>2</sub> (11.2 mg, 0.050 mmol, 0.10 equiv), potassium phenethyltrifluoroborate (212 mg, 1.00 mmol, 2 equiv), MnF<sub>3</sub> (224 mg, 2.00 mmol, 4 equiv), and AcOH (57 μL, 0.50 mmol, 2.0 equiv) in TFE/H<sub>2</sub>O (9:1; 7.5 mL total) at room temperature for 3 h. Product **40** was obtained as a white solid (68.4 mg, 54% yield, R<sub>f</sub> = 0.41 in 50% hexanes/50% EtOAc, mp = 144.4–145.9 °C). <sup>1</sup>H NMR (700 MHz, CD<sub>3</sub>CN, major rotamer): δ 7.66 (s, 1H), 7.28 (t, *J* = 7.4 Hz, 2H), 7.24 (s, 1H), 7.21 (d, *J* = 7.4 Hz, 2H), 7.19 (t, *J* = 7.4 Hz, 1H), 7.11 (d, *J* = 7.7 Hz, 1H), 6.95 (d, *J* = 7.7 Hz, 1H), 2.83–2.82 (multiple peaks, 4H), 2.28 (s, 3H), 2.05 (s, 3H). <sup>13</sup>C{<sup>1</sup>H} NMR (176 MHz, CD<sub>3</sub>CN, major rotamer): δ 169.8, 143.0, 137.0, 136.7, 125.6, 133.6, 130.4, 129.9, 129.4, 129.3, 129.2, 127.4, 126.8, 37.0, 33.7, 23.8, 20.9. IR (thin film, CH<sub>2</sub>Cl<sub>2</sub>) 3273, 3024, 2926, 1655 cm<sup>-1</sup>. HRMS [M+H]<sup>+</sup> Calcd for C<sub>17</sub>H<sub>20</sub>NO: 254.1539; Found: 254.1545.

### 3.13 References

1. Trost, B. M.; Fleming, I., editors. *Comprehensive Organic Synthesis*. Vol. 3. Pergamon Press; Oxford: 1991. Tamao K. Coupling Reactions; p. 435.
2. (a) Miyaura, N.; Suzuki, A. Palladium-Catalyzed Cross-Coupling Reactions of Organoboron Compounds. *Chem. Rev.* **1995**, *95*, 2457. (b) Chemler, S. R.; Trauner, D.; Danishefsky, S. J. The *B*-Alkyl Suzuki–Miyaura Cross-Coupling Reaction: Development, Mechanistic Study, and Applications in Natural Product Synthesis. *Angew. Chem., Int. Ed.* **2001**, *40*, 4544. (c) Jana, R.; Pathak, T. P.; Sigman, M. S. Advances in Transition Metal (Pd, Ni, Fe)-Catalyzed Cross-Coupling Reactions Using Alkyl-organometallics as Reaction Partners. *Chem. Rev.* **2011**, *111*, 1417.
3. Chen, X.; Goodhue, C. E.; Yu, J.-Q. Palladium-Catalyzed Alkylation of  $sp^2$  and  $sp^3$  C–H Bonds with Methylboroxine and Alkylboronic Acids: Two Distinct C–H Activation Pathways. *J. Am. Chem. Soc.* **2006**, *128*, 12634.
4. Giri, R.; Mangel, N.; Li, J.-J.; Wang, D. H.; Breazzano, S. P.; Saunders, L. B.; Yu, J.-Q. Palladium-Catalyzed Methylation and Arylation of  $sp^2$  and  $sp^3$  C–H Bonds in Simple Carboxylic Acids. *J. Am. Chem. Soc.* **2007**, *129*, 3510.
5. Wang, D.-H.; Wasa, M.; Giri, R.; Yu, J.-Q. Pd(II)-Catalyzed Cross-Coupling of  $sp^3$  C–H Bonds with  $sp^2$  and  $sp^3$  Boronic Acids Using Air as the Oxidant. *J. Am. Chem. Soc.* **2008**, *130*, 7190.
6. Dai, H.-X.; Stepan, A. F.; Plummer, M. S.; Zhang, Y.-H.; Yu, J.-Q. Divergent C–H Functionalizations Directed by Sulfonamide Pharmacophores: Late-Stage Diversification as a Tool for Drug Discovery. *J. Am. Chem. Soc.* **2011**, *133*, 7222.
7. Romero-Revilla, J. A.; García-Rubia, A.; Arrayás, R.; Fernández-Ibañez, M. Á.; Carretero, J. C. Palladium-Catalyzed Coupling of Arene C–H Bonds with Methyl- and Arylboron Reagents Assisted by the Removable 2-Pyridylsulfinyl Group. *J. Org. Chem.* **2011**, *76*, 9525.
8. Wasa, M.; Engle, K. M.; Lin, D. W.; Yoo, E. J.; Yu, J.-Q. Pd(II)-Catalyzed Enantioselective C–H Activation of Cyclopropanes. *J. Am. Chem. Soc.* **2011**, *133*, 19598.
9. Wasa, M.; Chan, K. S. L.; Yu, J.-Q. Pd(II)-catalyzed Cross-coupling of  $C(sp^2)$ –H Bonds and Alkyl-, Aryl-, and Vinyl–Boron Reagents via Pd(II)/Pd(0) Catalysis. *Chem. Lett.* **2011**, *40*, 1004.
10. For examples of Pd-catalyzed C–H alkylation using alkyl halides see (a) Hennessy, E. J.; Buchwald, S. L. Synthesis of Substituted Oxindoles from  $\alpha$ -Chloroacetanilidies via Palladium-Catalyzed C–H Functionalization. *J. Am. Chem. Soc.* **2003**, *125*, 12084. (b) Rudolph, A.; Rackelmann, N.; Lautens, M. Stereochemical and Mechanistic Investigations of a Palladium-Catalyzed Annulation of Secondary Alkyl Iodides. *Angew. Chem., Int. Ed.* **2007**, *46*, 1485. (c) Hwang, S. J.; Cho, S. H.; Chang, S. Synthesis of Condensed Pyrroloindoles



- via Pd-Catalyzed Intramolecular C–H Bond Functionalization of Pyrroles. *J. Am. Chem. Soc.* **2008**, *130*, 16158. (d) Zhang, Y.-H.; Shi, B.-F.; Yu, J.-Q. Palladium(II)-Catalyzed *ortho* Alkylation of Benzoic Acids with Alkyl Halides. *Angew. Chem., Int. Ed.* **2009**, *48*, 6097. (e) Lapointe, D.; Fagnou, K. Palladium-Catalyzed Benzoylation of Heterocyclic Aromatic Compounds. *Org. Lett.* **2009**, *11*, 4160. (f) Shabashov, D.; Daugulis, O., Auxiliary-Assisted Palladium-Catalyzed Arylation and Alkylation of  $sp^2$  and  $sp^3$  Carbon–Hydrogen Bonds. *J. Am. Chem. Soc.* **2010**, *132*, 3965. (g) Zhao, Y.; Chen, G. Palladium-Catalyzed Alkylation of *ortho*-C( $sp^2$ )–H Bonds of Benzylamide Substrates with Alkyl Halides. *Org. Lett.* **2011**, *13* 4850. (h) Tran, L. D.; Daugulis, O. Nonnatural Amino Acid Synthesis by Using Carbon–Hydrogen Bond Functionalization Methodology. *Angew. Chem., Int. Ed.* **2012**, *51*, 5188.
11. Stoichiometric C–H alkylation with alkyl iodides: Tremont, S. J.; Rahman, H. U. *Ortho*-Alkylation of Acetanilides Using Alkyl Halides and Palladium Acetate. *J. Am. Chem. Soc.* **1984**, *106*, 5759.
  12. C–H benzoylation using benzyl carbonates: Mukai, T.; Hirano, K.; Satoh, T.; Miura, M. Palladium-Catalyzed Direct Benzoylation of Azoles with Benzyl Carbonates. *Org. Lett.* **2010**, *12*, 1360.
  13. C–H alkylation with alkyltin reagents: Chen, X.; Li, J.-J.; Hao, X.-S.; Goodhue, C. E.; Yu, J.-Q. Palladium-Catalyzed Alkylation of Aryl C–H Bonds with  $sp^3$  Organotin Reagents Using Benzoquinone as a Crucial Promoter. *J. Am. Chem. Soc.* **2006**, *128*, 78.
  14. For a single example of room-temperature C–H methylation with methyl iodide, see Jang, M. J.; Youn, S. W. Pd-Catalyzed *ortho*-Methylation of Acetanilides via Directed C–H Activation. *Bull. Korean Chem. Soc.* **2011**, *32*, 2865.
  15. Hull, K. L.; Sanford, M. S. Mechanism of Benzoquinone-Promoted Palladium-Catalyzed Oxidative Cross-Coupling Reactions. *J. Am. Chem. Soc.* **2009**, *131*, 9651.
  16. (a) Yu, W.-Y.; Sit, W. N.; Zhou, Z.; Chan, A. S.-C. Palladium-Catalyzed Decarboxylative Arylation of C–H Bonds by Aryl Acylperoxides. *Org. Lett.* **2009**, *11*, 3174. (b) Kalyani, D.; McMurtrey, K. B.; Neufeldt, S. R.; Sanford, M. S. Room-Temperature C–H Arylation: Merger of Pd-Catalyzed C–H Functionalization and Visible-Light Photocatalysis. *J. Am. Chem. Soc.* **2011**, *133*, 18566. (c) Neufeldt, S. R.; Sanford, M. S. Combining Transition Metal Catalysis with Radical Chemistry: Dramatic Acceleration of Palladium-Catalyzed C–H Arylation with Diaryliodonium Salts. *Adv. Synth. Catal.*, **2012**, *in press*.
  17. (a) Yu, W.-Y.; Sit, W. N.; Lai, K.-M.; Zhou, Z.; Chan, A. S. C. Palladium-Catalyzed Oxidative Ethoxycarbonylation of Aromatic C–H Bond with Diethyl Azodicarboxylate. *J. Am. Chem. Soc.* **2008**, *130*, 3304. (b) Chan, C.-W.; Zhou, Z.; Chan, A. S. C.; Yu, W.-Y. Pd-Catalyzed *Ortho* C–H Acylation/Cross Coupling of Aryl Ketone *O*-Methyl Oximes with Aldehydes Using *tert*-Butyl Hydroperoxide

- as Oxidant. *Org. Lett.* **2010**, *12*, 3926. (c) Baslé, O.; Bidange, J.; Shuai, Q.; Li, C.-J. Palladium-Catalyzed Oxidative  $sp^2$  C–H Bond Acylation with Aldehydes. *Adv. Synth. Catal.* **2010**, *352*, 1145. (d) Chan, C.-W.; Zhou, Z.; Yu, W.-Y. Palladium(II)-Catalyzed Direct *ortho*-C–H Acylation of Anilides by Oxidative Cross-Coupling with Aldehydes using *tert*-Butyl Hydroperoxide as Oxidant. *Adv. Synth. Catal.* **2011**, *353*, 2999.
18. The existence of examples of aryl and acyl radical-mediated Pd-catalyzed C–H functionalizations (see references above) suggests that the reaction between R• and Pd is fast enough to outcompete the rate of H-atom abstraction from solvent molecules, which are present in large excess. Notably, the rates of H-atom abstraction from many solvent molecules (*e.g.*, MeOH) by Ph• is expected to be extremely fast (diffusion-controlled): (a) Kryger, R. G.; Lorand, J. P.; Stevens, N. R.; Herron, N. R. Radicals and Scavengers. 7. Diffusion Controlled Scavenging of Phenyl Radicals and Absolute Rate Constants of Several Phenyl Radical Reactions. *J. Am. Chem. Soc.* **1977**, *99*, 7589. (b) Minisci, F.; Vismara, E.; Fontana, F.; Morini, G.; Serravalle, M. Polar Effects in Free-Radical Reactions. Rate Constants in Phenylation and New Methods of Selective Alkylation of Heteroaromatic Bases. *J. Org. Chem.* **1986**, *51*, 4411.
  19. For a review see: Muñiz, K. High-Oxidation-State Palladium Catalysis: New Reactivity for Organic Synthesis. *Angew. Chem., Int. Ed.* **2009**, *48*, 9412.
  20. (a) King, R. B. Thirty Years of Organometallic Aryldiazenido Arylazo Derivatives. *J. Organomet. Chem.* **1995**, *500*, 187. (b) Zhdankin, V. V.; Stang, P. J. Chemistry of Polyvalent Iodine. *Chem. Rev.* **2008**, *108*, 5299.
  21. Molander, G. A.; Colombel, V.; Braz, V. A. Direct Alkylation of Heteroaryls Using Potassium Alkyl- and Alkoxyethyltrifluoroborates. *Org. Lett.* **2011**, *13*, 1852.
  22. Generation of aryl radicals from  $ArB(OH)_2$  with  $Mn(OAc)_3$  has also been reported: (a) Demir, A. S.; Reis, Ö.; Emrullahoglu, M. Generation of Aryl Radicals from Arylboronic Acids by Manganese(III) Acetate: Synthesis of Biaryls and Heterobiaryls. *J. Org. Chem.* **2003**, *68*, 578 (b) Guchhait, S. K.; Kashyap, M.; Saraf, S. Direct C–H Bond Arylation of (Hetero)arenes with Aryl and Heteroarylboronic Acids. *Synthesis* **2010**, 1166. (c) Dickschat, A.; Studer, A. Radical Addition of Arylboronic Acids to Various Olefins Under Oxidative Conditions. *Org. Lett.* **2010**, *12*, 3972
  23. (a) Minisci, F.; Bernardi, R.; Bertini, F.; Galli, R.; Perchinnunno, M. Nucleophilic Character of Alkyl Radicals–VI. A New Convenient Selective Alkylation of Heteroaromatic Bases. *Tetrahedron* **1971**, *27*, 3575. (b) Bowman, W. R.; Storey, J. M. D. Synthesis Using Aromatic Homolytic Substitution – Recent Advances. *Chem. Soc. Rev.* **2007**, *36*, 1803.
  24. Lyons, T. W.; Sanford, M. S. Palladium-Catalyzed Ligand-Directed C–H Functionalization Reactions. *Chem. Rev.* **2010**, *110*, 1147.

25. (a) Molander, G. A.; Ellis, N. Organotrifluoroborates: Protected Boronic Acids that Expand the Versatility of the Suzuki Coupling Reaction. *Acc. Chem. Res.* **2007**, *40*, 275. (b) Darses, S.; Genet, J.-P. Potassium Organotrifluoroborates: New Perspectives in Organic Synthesis. *Chem. Rev.* **2008**, *108*, 288. (c) Molander, G. A.; Sandrock, D. L. Potassium Trifluoroborate Salts as Convenient, Stable Reagents for Difficult Alkyl Transfers. *Curr. Opin. Drug Discov. Devel.* **2009**, *12*, 811.
26. For seminal examples see: (a) Dick, A. R.; Hull, K. L.; Sanford, M. S. A Highly Selective Catalytic Method for the Oxidative Functionalization of C–H Bonds. *J. Am. Chem. Soc.* **2004**, *126*, 2300. (b) Desai, L. V.; Malik, H. A.; Sanford, M. S. Oxone as an Inexpensive, Safe, and Environmentally Benign Oxidant for C–H Bond Oxygenation. *Org. Lett.* **2006**, *8*, 1141.
27. Desai, L. V.; Stowers, K. J.; Sanford, M. S. Insights into Directing Group Ability in Palladium-Catalyzed C–H Bond Functionalization. *J. Am. Chem. Soc.* **2008**, *130*, 13285.
28. Fu, Y.; Liu, L.; Yu, H.-Z.; Wang, Y.-M.; Guo, Q.-X. Quantum-Chemical Predictions of Absolute Standard Redox Potentials of Diverse Organic Molecules and Free Radicals in Acetonitrile. *J. Am. Chem. Soc.* **2005**, *127*, 7227.
29. (a) Seiple, I. B.; Rodriguez, R. A.; Gianatassio, R.; Fujiwara, Y.; Sobel, A. L.; Baran, P. S. Direct C–H Arylation of Electron-Deficient Heterocycles with Arylboronic Acids. *J. Am. Chem. Soc.* **2010**, *132*, 13194. (b) Lockner, J. W.; Dixon, D. D.; Risgaard, R.; Baran, P. S. Practical Radical Cyclizations with Arylboronic Acids and Trifluoroborates. *Org. Lett.* **2011**, *13*, 5628. (c) Wang, J.; Wang, S.; Wang, G.; Zhang, J.; Yu, X.-Q. Iron-Mediated Direct Arylation with Arylboronic Acids Through an Aryl Radical Transfer Pathway. *Chem. Commun.* **2012**, *48*, 11769.
30. In contrast to the catalytic results in Table 3.9, formation of product **5** is observed under stoichiometric reaction conditions in AcOH/H<sub>2</sub>O (9:1) at 25 °C using any of the following oxidants: MnF<sub>3</sub>, Mn(OAc)<sub>3</sub>, PhI(O<sub>2</sub>CCF<sub>3</sub>)<sub>2</sub>, benzoquinone, *t*-BuOOH, and K<sub>2</sub>S<sub>2</sub>O<sub>8</sub>. Formation of **5** is not observed in the stoichiometric reaction using Ag<sub>2</sub>O or Cu(OAc)<sub>2</sub>. We tentatively propose that transmetallation is a viable mechanistic step under stoichiometric conditions, and strong oxidants can facilitate oxidatively-induced C–C bond-forming reductive elimination from high-valent Pd. Benzoquinone may promote C–C bond-forming reductive elimination from Pd<sup>II</sup>.
31. Hull, K. L.; Lanni, E. L.; Sanford, M. S. Highly Regioselective Catalytic Oxidative Coupling Reactions: Synthetic and Mechanistic Investigations. *J. Am. Chem. Soc.* **2006**, *128*, 14047.
32. (a) Shi, Z.; Li, B.; Wan, X.; Cheng, J.; Fang, Z.; Cao, B.; Qin, C.; Wang, Y. Suzuki-Miyaura Coupling Reaction by Pd(II)-Catalyzed Aromatic C–H Bond Activation Directed by an N-Alkyl Acetamino Group. *Angew. Chem., Int. Ed.*

- 2007, 46, 5554. (b) Kirchberg, S.; Vogler, T.; Studer, A. Directed Palladium-Catalyzed Oxidative C–H Arylation of (Hetero)arenes with Arylboronic Acids by Using TEMPO. *Synlett* **2008**, 2841. (c) Wang, D.-H.; Mei, T.-S.; Yu, J.-Q. Versatile Pd(II)-Catalyzed C–H Activation/Aryl–Aryl Coupling of Benzoic and Phenyl Acetic Acids. *J. Am. Chem. Soc.* **2008**, 130, 17676. (d) Sun, C.-L.; Liu, N.; Li, B.-J.; Yu, D.-G.; Wang, Y.; Shi, Z.-J. Pd-Catalyzed C–H Functionalizations of *O*-Methyl Oximes with Arylboronic Acids. *Org. Lett.* **2010**, 12, 184. (e) Chu, J.-H.; Lin, P.-S.; Wu, M.-J. Palladium(II)-Catalyzed *Ortho* Arylation of 2-Phenoxy pyridines with Potassium Aryltrifluoroborates via C–H Functionalization. *Organometallics* **2010**, 29, 4058. (f) Engle, K. M.; Thuy-Boun, P. S.; Dang, M.; Yu, J.-Q. Ligand-Accelerated Cross-Coupling of C(sp<sup>2</sup>)-H Bonds with Arylboron Reagents. *J. Am. Chem. Soc.* **2011**, 133, 18183. (g) Koley, M.; Dastbaravardeh, N.; Schnürch, M.; Mihovilovic, M. D. Palladium(II)-Catalyzed Regioselective *Ortho* Arylation of sp<sup>2</sup> C–H Bonds of *N*-Aryl-2-amino Pyridine Derivatives. *ChemCatChem* **2012**, 4, 1345. (h) Zhang, X.; Yu, M.; Yao, J.; Zhang, Y. Palladium-Catalyzed Regioselective Arylation of Arene C–H Bond Assisted by the Removable 2-Pyridylsulfinyl Group. *Synlett* **2012**, 23, 463.
33. (a) Nishikata, T.; Abela, A. R.; Huang, S.; Lipshutz, B. H. Cationic Palladium(II) Catalysis: C–H Activation/Suzuki–Miyaura Couplings at Room Temperature. *J. Am. Chem. Soc.* **2010**, 132, 4978. (b) Tredwell, M. J.; Gulias, M.; Bremeyer, N. G.; Johansson, C. C. C.; Collins, B. S. L.; Gaunt, M. J. Palladium(II)-Catalyzed C–H Bond Arylation of Electron-Deficient Arenes at Room Temperature. *Angew. Chem., Int. Ed.* **2011**, 50, 1076.
34. Stowers K. J.; Sanford, M. S. Mechanistic Comparison between Pd-Catalyzed Ligand-Directed C–H Chlorination and C–H Acetoxylation. *Org. Lett.* **2009**, 11, 4584.
35. Wang, X.-J.; Yang, Q.; Liu, F.; You, Q.-D. Microwave-Assisted Synthesis of Amide under Solvent-free Conditions. *Synth. Commun.* **2008**, 38, 1028.
36. Tashiro, M.; Fukuda, Y.; Yamato, T. Selective Preparation. 38. A Convenient Preparation of 2-(Acylamino)biphenyls and *N*-Acetylaniline Derivatives Using the *tert*-Butyl Group as a Positional Protective Function. *J. Org. Chem.* **1983**, 48, 1927.
37. Kovach, E. G.; Barnes, D. E. Preparation and Properties of Some New Chelating Agents. *J. Am. Chem. Soc.* **1954**, 76, 1176.
38. Kajigaeshi, S.; Kakinami, T.; Watanabe, F.; Okamoto, T. Halogenation Using Quaternary Ammonium Polyhalides. XVII. Iodination of Acetanilide Derivatives with Benzyltrimethylammonium Dichloroiodate and Zinc Chloride. *Bull. Chem. Soc. Jpn.* **1989**, 62, 1349.
39. Somei, M.; Kawasaki, T.; Ohta, T. A Simple Synthesis of 7-Substituted 1-Acetyl-2,3-dihydroindoles. *Heterocycles* **1988**, 27, 2363.

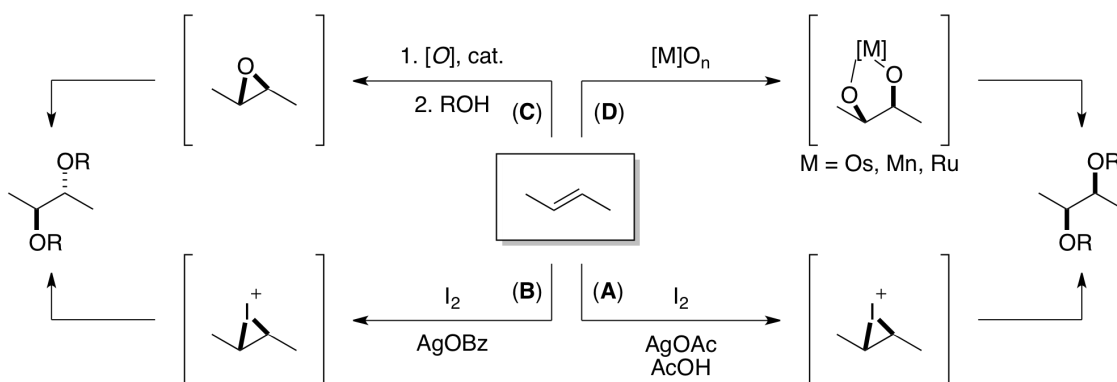
## CHAPTER 4

### Asymmetric Pd-Catalyzed Chiral Ligand-Directed Alkene Dioxygenation

#### 4.1 Background and Significance

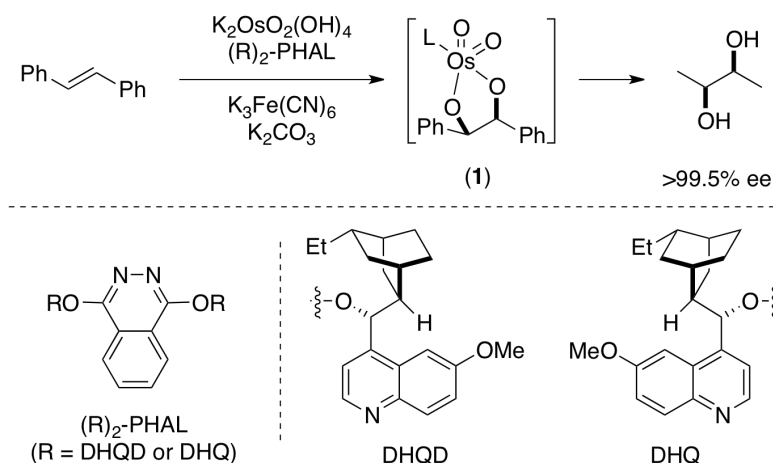
Alkene difunctionalization reactions are synthetically valuable transformations that introduce two functional groups and up to two new stereocenters into a substrate. Dioxygenation is particularly widely studied, and several catalytic and non-catalytic strategies for alkene dihydroxylation have emerged including the Woodward dihydroxylation (Scheme 4.1, path A),<sup>1</sup> the Prévost reaction (path B),<sup>2</sup> epoxidation/ring-opening (path C),<sup>3</sup> and metal mediated *syn*-dihydroxylation reactions (path D).<sup>4,5</sup>

Scheme 4.1. Strategies for Alkene Dioxygenation

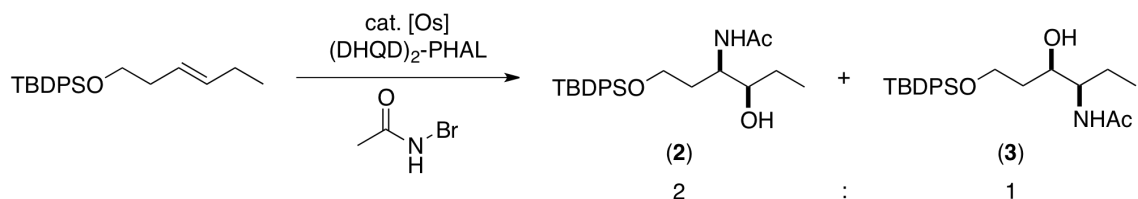


Of these strategies, Sharpless' osmium-catalyzed asymmetric dihydroxylation has proven particularly valuable, and has a reputation for being a reliable route to *syn* vicinal diols (Scheme 4.2).<sup>4</sup> A related Os-catalyzed aminohydroxylation reaction provides access to chiral 1,2-amino alcohols in an analogous fashion (Scheme 4.3).<sup>4c,6</sup>

### Scheme 4.2. Sharpless Asymmetric Dihydroxylation<sup>4</sup>



### Scheme 4.3. Sharpless Osmium-Catalyzed Aminohydroxylation<sup>6a</sup>

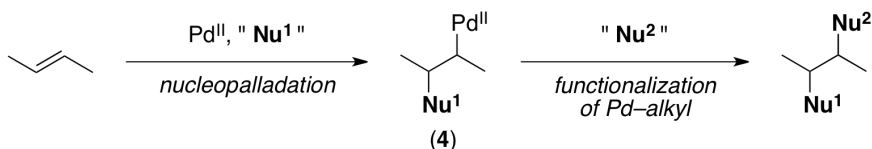


Despite the significance of these methodologies, osmium catalysis remains limited. Most importantly, the ability to extend this approach toward the installation of diverse nucleophiles beyond hydroxyl/hydroxyl and hydroxyl/amine has not been demonstrated. Furthermore, control over the regioselectivity of aminohydroxylation (*e.g.*, **2** vs **3**, Scheme 4.3) is challenging and highlights the need for an alternative strategy for installing two non-identical nucleophiles across an alkene. Lastly, the toxicity of osmium is often cited as a drawback to these transformations.

A vast amount of literature on palladium catalysis, and particularly the recent surge of work involving high-oxidation-state Pd,<sup>7</sup> has opened the door to considering this versatile metal as a powerful alternative catalyst for alkene difunctionalization transformations.<sup>8</sup> Whereas Os<sup>VIII</sup> catalysis involves concerted *syn* addition of two heteroatoms across an alkene (intermediate **1**, Scheme 4.2), Pd reacts with olefins by a fundamentally different mechanism that forms each new carbon–X bond in a discrete step

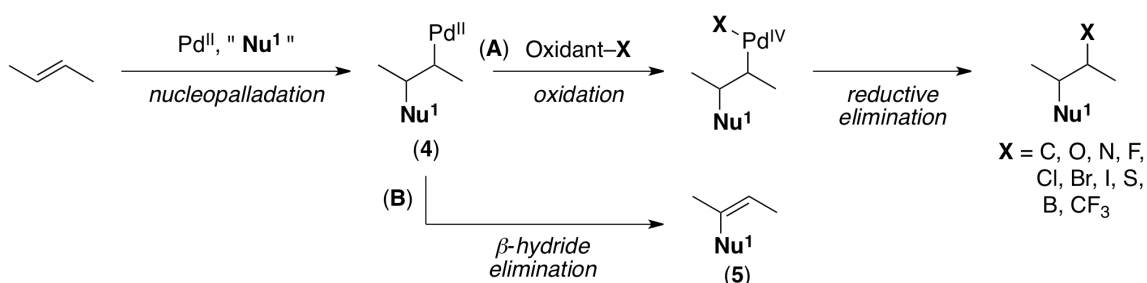
(Scheme 4.4).<sup>8</sup> This feature of palladium catalysis provides an opportunity to control the regioselectivity of alkene difunctionalization with non-identical nucleophiles.

**Scheme 4.4.** General Mechanism of Pd-Catalyzed Alkene Difunctionalization



The use of high-oxidation state Pd catalysis for alkene difunctionalization (instead of Pd<sup>II</sup>/Pd<sup>0</sup> catalysis) is particularly attractive. Although Pd<sup>II</sup>–alkyl species like **4** tend to undergo facile  $\beta$ -hydride elimination, analogous Pd<sup>IV</sup> intermediates are often resistant to this decomposition pathway. As such, oxidative interception of the Pd<sup>II</sup>–alkyl intermediate **4** generated by nucleopalladation (Scheme 4.5, path A) could suppress formation of undesired Wacker-type side products (**5**, path B). Additionally, there is significant precedent for a large variety of bond constructions at Pd<sup>IV</sup>, including the formation of C–O, C–N, C–C, and C–halogen linkages. For these reasons, a high-oxidation state Pd-catalyzed mechanistic manifold could provide a powerful approach to achieving a diverse scope of alkene difunctionalizations.

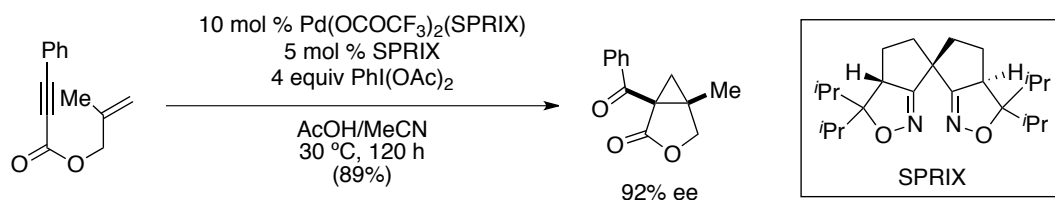
**Scheme 4.5.** Alkene Difunctionalization by High-Oxidation-State Palladium Catalysis



Indeed, numerous Pd-catalyzed oxidative alkene difunctionalization reactions have been developed in recent years, including dioxygenations,<sup>9</sup> aminoxygenations,<sup>10</sup> aminoarylations,<sup>11</sup> diaminations,<sup>12</sup> aminofluorinations,<sup>13</sup> chloroaminations,<sup>14</sup> arylhalogenations,<sup>15</sup> and cyclopropanations.<sup>16</sup> These transformations often proceed with good selectivity for either *syn* or *anti* addition of the vicinal groups. However, the

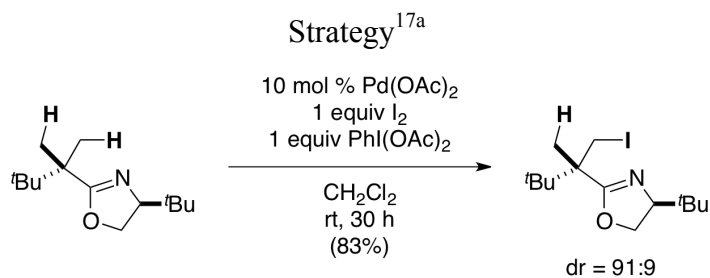
stereoselective formation of *non-racemic* difunctionalized products by high-oxidation-state Pd-catalysis has remained largely elusive. A single example of asymmetric alkene difunctionalization via Pd<sup>II</sup>/Pd<sup>IV</sup> catalysis utilizes chiral SPRIX ligands and produces chiral nonracemic cyclopropanes (Scheme 4.6).<sup>16d</sup>

**Scheme 4.6.** Asymmetric Pd<sup>II</sup>/Pd<sup>IV</sup>-Catalyzed Oxidative Cyclization of Enynes



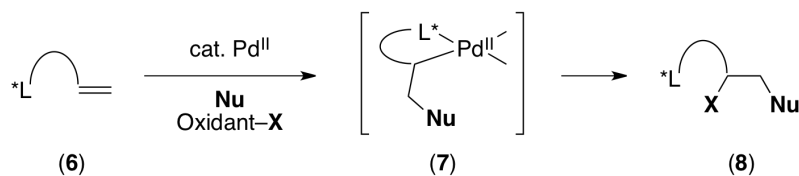
One attractive approach for achieving asymmetric Pd-catalyzed alkene difunctionalization would involve the use of a chiral directing group. Analogous chiral directing group-based strategies have been successfully employed by Yu and coworkers to achieve asymmetric C–H bond oxidation via high-oxidation-state Pd catalysis (Scheme 4.7).<sup>17,18</sup> In a similar fashion, we envisioned that a chiral directing ligand (L\* in substrate **6**, Scheme 4.8) could potentially relay stereochemical information to the stereocenter(s) formed upon alkene difunctionalization (product **8**) via a chiral palladacycle intermediate **7**.

**Scheme 4.7.** Pd-Catalyzed Asymmetric C–H Iodination using a Chiral Directing Group



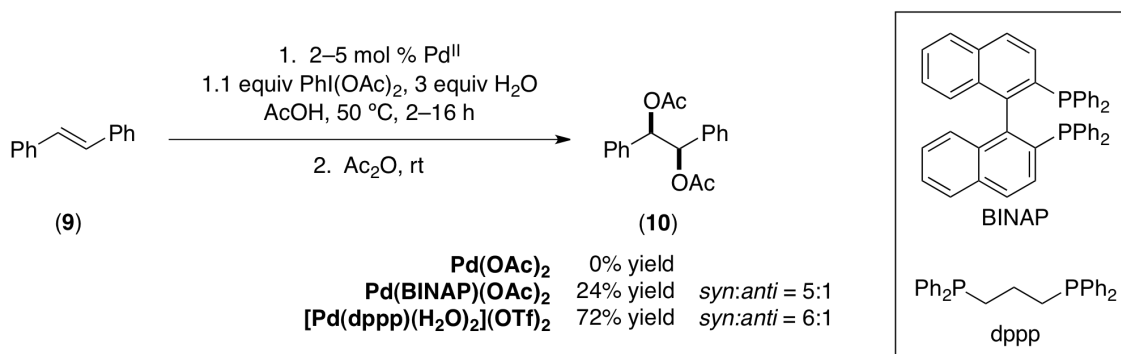


**Scheme 4.8.** Chiral Directing Group Strategy for Pd-Catalyzed Asymmetric Alkene Difunctionalization

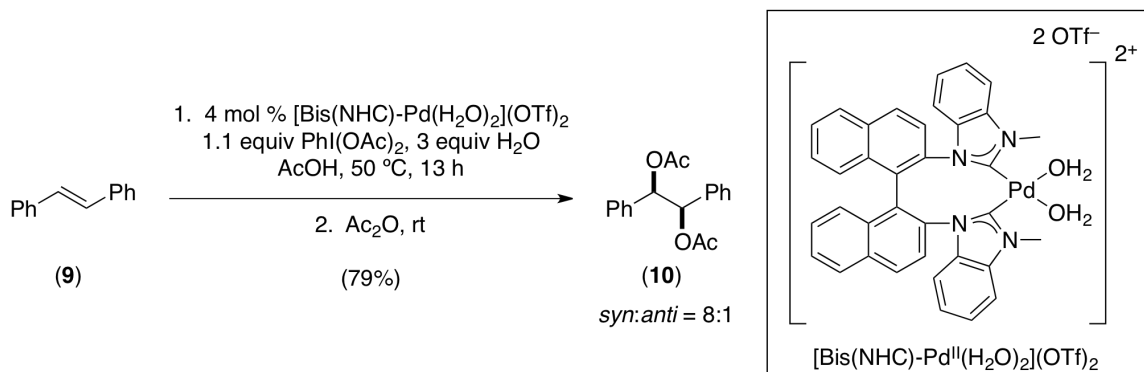


In addition to providing stereocontrol, the use of this ligand-directed strategy could accelerate the rate of Pd-catalyzed alkene difunctionalization by bringing the Pd center proximal to the target olefin. Dong and coworkers have shown that simple palladium salts like  $\text{Pd}(\text{OAc})_2$  and  $\text{PdCl}_2(\text{MeCN})_2$  do not effect any detectable dioxygenation of alkene **9** with  $\text{PhI}(\text{OAc})_2$  at 50 °C after 16 h (Scheme 4.9).<sup>9a</sup> Instead, both Dong (Scheme 4.9) and Shi<sup>9c</sup> found that the use of ancillary BINAP or NHC ligands was necessary to achieve any reactivity with  $\text{Pd}(\text{OAc})_2$ , and good yields of dioxygenated product **10** were only obtained with cationic Pd triflate salts. In contrast, we expected that the increased reactivity of a directing-group-containing substrate (**6**, Scheme 4.8) might enable the use of simple Pd salts for alkene diacetoxylation with  $\text{PhI}(\text{OAc})_2$ . As such, we chose to focus our initial studies on alkene dioxygenation with  $\text{PhI}(\text{O}_2\text{CR})_2$  oxidants, using the work by Dong and Shi as a benchmark for testing the effectiveness of the envisioned directing group strategy.

**Scheme 4.9.** Diacetoxylation of an Undirected Substrate with  $\text{PhI}(\text{OAc})_2$  using a Cationic Pd Triflate Salt vs  $\text{Pd}(\text{OAc})_2$ <sup>9a</sup>

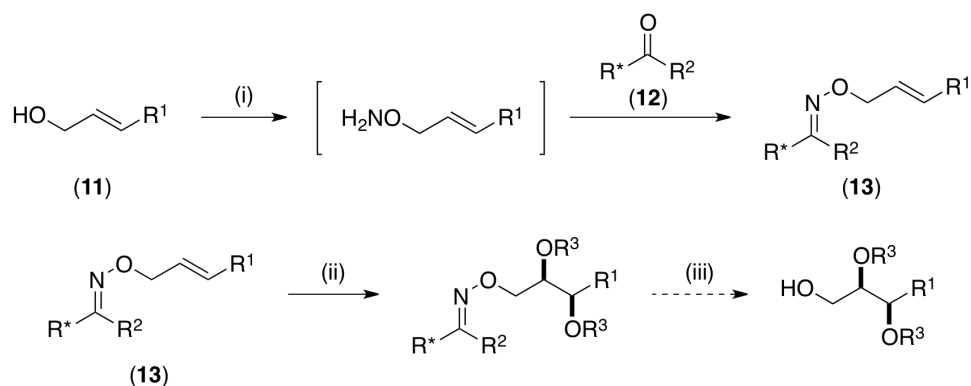


**Scheme 4.10.** Diacetoxylation of an Undirected Substrate with  $\text{PhI}(\text{OAc})_2$  Using a Cationic  $\text{Pd}(\text{NHC})$  Triflate Salt<sup>9c</sup>



For the work described in this chapter, we focused on the use of chiral oxime ethers as directing groups for asymmetric alkene dioxygenation (**13**, Scheme 4.11). These directing groups were selected based on several key criteria: (1) oxime ethers are known to be effective directing ligands for other Pd-catalyzed reactions,<sup>19</sup> (2) the substrates can easily be prepared from an allyl alcohol **11** and a chiral ketone **12** (Scheme 4.11, step i), (3) the chiral auxiliary could potentially be cleaved off at a later stage (step iii) and (4) diverse chiral non-racemic ketones are readily available.

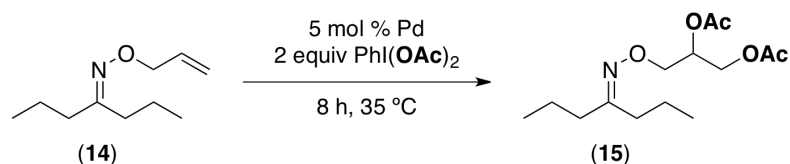
**Scheme 4.11.** Chiral Oxime Ethers as Directing Groups for Asymmetric Alkene Dioxygenation



## 4.2 Reaction Optimization

Diacetoxylation of substrate **14** using a Pd<sup>II</sup> catalyst and PhI(OAc)<sub>2</sub> was found to proceed in a variety of solvents at relatively mild temperatures (25–50 °C), and numerous Pd<sup>II</sup> salts were effective catalysts for this transformation (Table 4.1). These observations stand in contrast to the work by Dong and Shi, in which cationic Pd complexes and acidic solvents were necessary to obtain good yields of the diacetoxyated products (*vide supra*). As such, these results provide evidence in support of the hypothesis that a directing group can facilitate Pd-catalyzed alkene difunctionalization.

**Table 4.1.** Solvent and Catalyst Optimization for Pd-Catalyzed Ligand Directed Diacetoxylation of **14**



entry	solvent	Pd	% yield <sup>a</sup>
1	AcOH/Ac <sub>2</sub> O (1:1)	PdCl <sub>2</sub> (PhCN) <sub>2</sub>	37
2	ClCH <sub>2</sub> CH <sub>2</sub> Cl	PdCl <sub>2</sub> (PhCN) <sub>2</sub>	51
3	ClCHCCl <sub>2</sub>	PdCl <sub>2</sub> (PhCN) <sub>2</sub>	49
4	acetone	PdCl <sub>2</sub> (PhCN) <sub>2</sub>	43
5	MeCN	PdCl <sub>2</sub> (PhCN) <sub>2</sub>	23
6	NO <sub>2</sub> Me	PdCl <sub>2</sub> (PhCN) <sub>2</sub>	10
7	benzene	PdCl <sub>2</sub> (PhCN) <sub>2</sub>	60
8	toluene	PdCl <sub>2</sub> (PhCN) <sub>2</sub>	58
9	PhNO <sub>2</sub>	PdCl <sub>2</sub> (PhCN) <sub>2</sub>	41
10	PhCl	PdCl <sub>2</sub> (PhCN) <sub>2</sub>	55
11	PhCl	Pd(OAc) <sub>2</sub>	58
12	PhCl	Pd(O <sub>2</sub> CCF <sub>3</sub> ) <sub>2</sub>	49
13	PhCl	PdCl <sub>2</sub> (COD)	36
14	PhCl	Pd(acac) <sub>2</sub>	35
15	PhCl	Pd(NO <sub>3</sub> ) <sub>2</sub>	43
16	PhCl	PdCl <sub>2</sub> (PPh <sub>3</sub> ) <sub>2</sub>	44
17	PhCl	Pd(MeCN) <sub>4</sub> [BF <sub>4</sub> ] <sub>2</sub>	28
18	PhCl	Na <sub>2</sub> PdCl <sub>4</sub>	47
19	PhCl	Pd <sub>2</sub> (dba) <sub>3</sub>	54

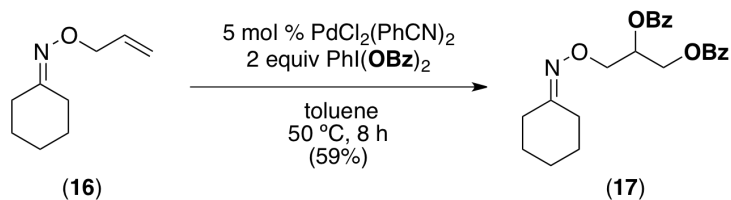
<sup>a</sup>GC calibrated yield relative to dinitrobenzene as an internal standard

In our system, the highest yields of product **15** were obtained in dry aromatic solvents like benzene, toluene, and chlorobenzene (Table 4.1, entries 7, 8, and 10). Although PdCl<sub>2</sub>(PhCN)<sub>2</sub> and Pd(OAc)<sub>2</sub> afforded comparable results with **15** (entries 10

and 11) subsequent studies on chiral substrates revealed that the use of  $\text{PdCl}_2(\text{PhCN})_2$  provided better stereocontrol (see section 4.13 for details).

Furthermore, we found that  $\text{PhI}(\text{OBz})_2$  could essentially be used interchangeably with  $\text{PhI}(\text{OAc})_2$  to afford the analogous dibenzoylated products. The dibenzoylated products offer the advantage of facile visualization on TLC plates. Additionally, we later found that diastereomeric dibenzoylated products are easier to differentiate by NMR spectroscopy than their diacetoxyated counterparts. For these reasons, much of the work presented in this chapter utilizes  $\text{PhI}(\text{OBz})_2$  instead of  $\text{PhI}(\text{OAc})_2$ . For instance, we examined the Pd-catalyzed dioxygenation of achiral oxime ether substrate **16** with  $\text{PhI}(\text{OBz})_2$ . Using  $\text{PdCl}_2(\text{MeCN})_2$  as catalyst, this transformation proceeded in 59% isolated yield under mild conditions (8 h at 50 °C in toluene, Scheme 4.12).

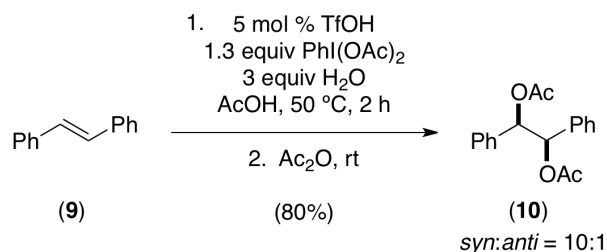
**Scheme 4.12.** Dibenzoylation of **16** with  $\text{PhI}(\text{OBz})_2$  and  $\text{PdCl}_2(\text{PhCN})_2$



### 4.3 Control Reactions

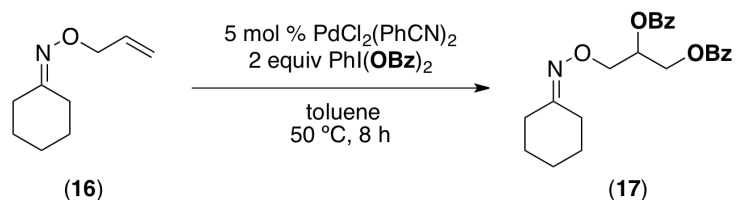
We next sought confirmation that the dioxygenation reaction was proceeding through a Pd-catalyzed pathway. Notably, Gade and coworkers have recently demonstrated metal-free TfOH-catalyzed alkene diacetoxylation with  $\text{PhI}(\text{OAc})_2$  (Scheme 4.13).<sup>20,21</sup> Their work provided evidence that the reactions in Schemes 4.9<sup>a</sup> and 4.10<sup>c</sup> using cationic Pd triflate salts, as well as related diacetoxylation reactions using  $\text{Cu}(\text{OTf})_2$ ,<sup>22</sup> may be catalyzed by triflic acid generated *in situ* rather than by Pd.

**Scheme 4.13.** Metal-Free TfOH-Catalyzed Alkene Diacetoxylation with  $\text{PhI}(\text{OAc})_2$ <sup>20</sup>



We hypothesized that an analogous acid-catalyzed pathway was not feasible in our system because of the presence of a basic nitrogen in the oxime ether substrate. However, because the envisioned chiral ligand-directed alkene difunctionalization relies on the involvement of a palladium catalyst to achieve absolute stereocontrol, it was important to rule out the possibility of a competing acid-catalyzed reaction pathway. Evidence for the role of Pd, rather than  $\text{H}^+$ , as the active catalyst is presented in Table 4.2. Importantly, no dioxygenation was observed in the absence of Pd under our reaction conditions, even upon the addition of 5–10 mol % TfOH or  $\text{BF}_3\cdot\text{OEt}_2$  (see section 4.13 for further details).

**Table 4.2.** Control Reactions for the Dibenzoylation of **16**<sup>a,b</sup>



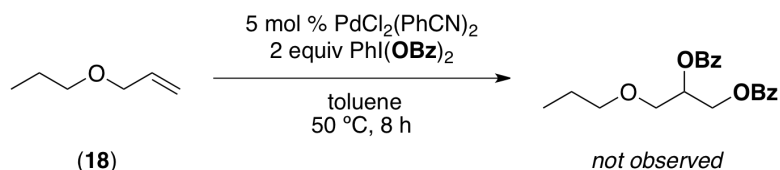
entry	Pd (mol %)	additive	% yield
1	5	none	59 <sup>b</sup>
2	0	none	<1 <sup>c</sup>
3	0	5 mol % TfOH	<1 <sup>c</sup>
4	0	10 mol % $\text{BF}_3\cdot\text{OEt}_2$	<1 <sup>c</sup>

<sup>a</sup>Conditions: **16** (1 equiv),  $\text{PdCl}_2(\text{PhCN})_2$  (0.05 equiv),  $\text{PhI}(\text{OBz})_2$  (2 equiv), dry toluene (0.12 M in substrate),  $50\text{ }^\circ\text{C}$ , 8 h. <sup>b</sup>Isolated yield. <sup>c</sup>Product was not detected by NMR spectroscopic analysis of the crude reaction mixture.

Finally, support for the role of the oxime ether directing ligand is provided in Scheme 4.14. Like **16**, substrate **18** contains an olefin that is allylic to an oxygen atom.

Unlike **16**, however, **18** does not include a good ligand for palladium. As expected, substrate **18** was completely unreactive under the optimized conditions. This observation indicates that the oxime ether moiety in **16** is necessary to enable alkene difunctionalization under our reaction conditions.

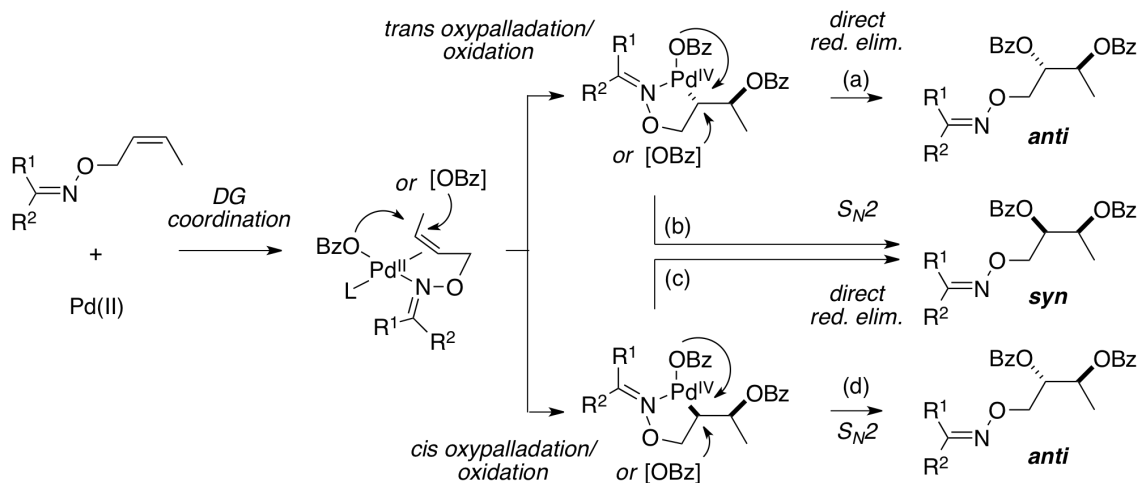
**Scheme 4.14.** No Observed Reactivity in a Substrate Lacking a Directing Group



#### 4.4 *Syn* Diastereoselectivity and Reaction Mechanism

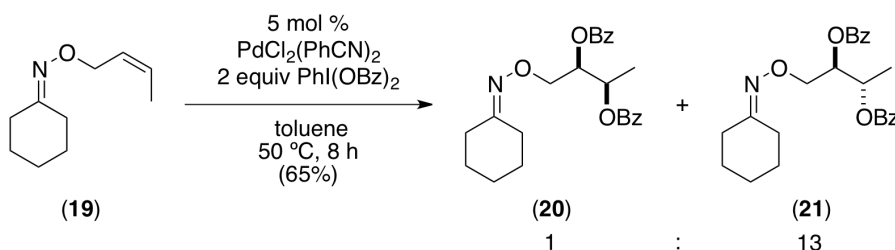
Several mechanistic pathways for the described dioxygenation reaction can be imagined (Scheme 4.15) involving either *trans* (paths A and B) or *cis* oxypalladation (paths C and D), and direct (paths A and C) or  $\text{S}_{\text{N}}2$ -type reductive elimination (paths B and D). In an achiral system, these four pathways would lead to two possible products resulting from overall *syn* or *anti* addition.

**Scheme 4.15.** Possible Mechanistic Pathways for the Oxime-Directed Dibenzoylation

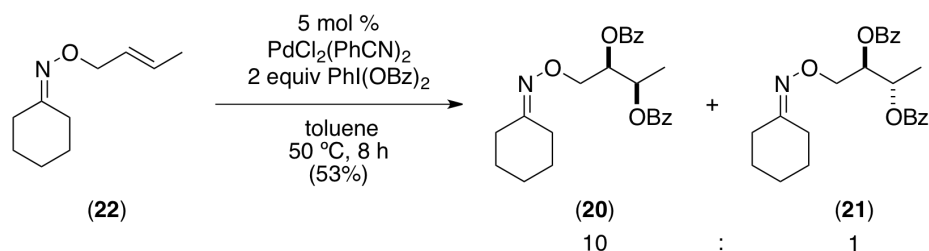


Previous reports have indicated that each of these pathways is possible in the context of Pd-catalyzed alkene difunctionalization reactions.<sup>8</sup> However, to achieve an asymmetric difunctionalization with high stereochemical fidelity, it is important that a single reaction pathway is dominant. If two pathways are competing, asymmetric induction is likely to be eroded. Thus, in order to assess the feasibility of developing an asymmetric transformation, we examined the stereospecificity of dioxygenation of achiral *cis* and *trans* alkene substrates **19** and **22**. In this system, only two dibenzoylated products are possible (*threo* product **20** and *erythro* product **21**). Poor selectivity between **20** and **21** could suggest the existence of competing reaction pathways. Gratifyingly, under the optimal conditions, dioxygenation of both alkenes proceeded with high (~10:1) selectivity for the *syn* addition product (Schemes 4.16 and 4.17).

**Scheme 4.16.** *Syn* Selective Dibenzoylation of *cis* Alkene Substrate **19**

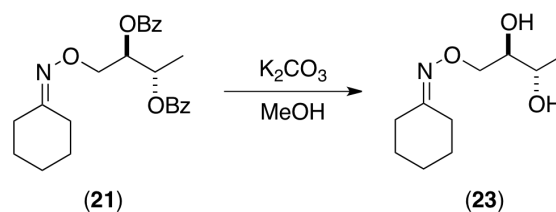


**Scheme 4.17.** *Syn* Selective Dibenzoylation of *trans* Alkene Substrate **22**

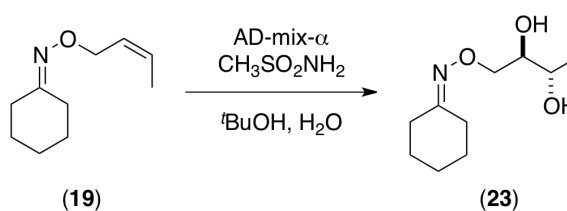


The relative stereochemistry of the two products was determined by deprotection of **20** and **21** to the corresponding diols (Scheme 4.18) and spectroscopic comparison to an authentic sample of **23** prepared by Os-catalyzed *syn* dihydroxylation<sup>23</sup> of **19** (Scheme 4.19).

**Scheme 4.18.** Preparation of *Erythro* Diol **23** By Deprotection of **21**



**Scheme 4.19.** Preparation of Authentic *Erythro* Diol **23** by Os-Catalyzed *Syn* Dihydroxylation of **19**



#### 4.5 Use of Chiral Auxiliaries Derived from Commercial Ketones

With these results in hand, we next examined chiral oxime auxiliaries. A series of terminal (allyl) oxime ethers **24–30** were prepared from commercially available chiral ketones containing diverse patterns of  $\alpha$ -substitution (Table 4.3). The *E* and *Z* oxime isomers of the same parent ketone provide significantly different steric environments for a coordinated Pd center. Therefore, the *E* and *Z* diastereomers were separated and studied individually when possible (substrates **24**, **25**, **27**, and **28**). Importantly, a new stereocenter is created upon dioxygenation of these chiral substrates, and the resulting products are diastereomers. Thus, control over absolute stereochemistry is reported as a diastereomeric ratio (dr, not to be confused with *syn/anti* relative stereochemistry).



**Table 4.3.** Dibenzoylation with Chiral Auxiliaries Derived from Commercial Ketones<sup>a</sup>

entry	substrate	product	yield <sup>b</sup>	dr <sup>c</sup>
1			63%	52:48
2			64%	63:37
3			68%	59:41
4			25%	75:25
5			67%	66:34
6			<1% <sup>d</sup>	--
7			75%	74:26

<sup>a</sup>Conditions: substrate (1 equiv), PdCl<sub>2</sub>(PhCN)<sub>2</sub> (0.05 equiv), PhI(OBz)<sub>2</sub> (2 equiv), dry toluene (0.12 M in substrate), 50 °C, 8 h. <sup>b</sup>Isolated yield. <sup>c</sup>Determined by relative integrations of at least 2 pairs of peaks in the <sup>13</sup>C and/or <sup>1</sup>H NMR spectra; see section 4.13 for details. <sup>d</sup>Product was not detected by NMR spectroscopic analysis of the crude reaction mixture.

Oxime stereoisomers **24** and **25** reacted under our standard Pd-catalyzed dioxygenation conditions to afford two spectroscopically different sets of products. These results indicate that the oxime ether is configurationally stable under the reaction conditions. The stereocenter at the  $\alpha$  position of the auxiliary is expected to be in closer proximity to the coordinated Pd center in **25** relative to **24**. Consistent with this proposal, **25** reacts to form **32** in modest 63:37 dr, while **24** yields **31** with essentially no selectivity (dr = 52:48). These results demonstrate that the steric environment created by the chiral oxime auxiliary significantly impacts the stereochemical outcome of the dibenzoylation.

In keeping with the trend observed with **24** and **25**, the dr's obtained with substrates derived from other commercial chiral ketones showed a significant correlation with the steric environment at the  $\alpha$ -position of the oxime. For example, the diastereoselectivity of the reaction of **26** was lower than seen with **25**. This may be rationalized based on the fact that the 3°- $\alpha$  stereocenter of **26** is tied back into a bicyclic scaffold. Improved diastereoselectivity (75:25) was observed in **27**, which contains a 4°- $\alpha$  stereocenter. However, the overall yield was low, likely due to the highly congested steric environment proximal to the oxime. Consistent with this proposal, the other oxime isomer (**28**) afforded dioxygenated product in lower dr (66:34) but with higher yield. An even bulkier 4°- $\alpha$  group (**29**) resulted in dramatically decreased reactivity, and no dioxygenated product was observed. Among the substrates in Table 4.3, the best balance between reactivity and selectivity appeared to be found with **30**, which features  $\beta$ -branching adjacent to the 3°- $\alpha$  substituent.

#### 4.6 Use of Auxiliaries Derived from 8-Substituted Menthone

We next sought to improve on the selectivity seen with **30** by preparing a number of 8-substituted menthone derivatives to use as auxiliaries. Excitingly, the addition of a third methyl group to the  $\beta$ -position of the ketone (**38**) provided a substantial improvement in stereoselectivity (dr = 86:14 for **43**, compared to 74:26 for **37**). The selectivity remained unchanged with additional mono-substitution at the  $\gamma$  position (**39** and **40**). As seen in Table 4.4, however, reaction yields began to decline as the steric bulk of the auxiliary increased (compare **45** and **47** to **44**). The highest selectivity was seen

with **42**, which has a 3° carbon at the  $\gamma$  position, albeit with only moderate yield of dibenzoylated product **47**.

**Table 4.4.** Dibenzoylation with Chiral Auxiliaries Derived from 8-Substituted Menthone<sup>a</sup>

entry	substrate	product	yield <sup>b</sup>	dr <sup>c</sup>
1			69%	86:14
2			70%	86:14
3			54%	86:14
4			44%	85:15
5			37%	90:10

<sup>a</sup>Conditions: substrate (1 equiv), PdCl<sub>2</sub>(PhCN)<sub>2</sub> (0.05 equiv), PhI(OBz)<sub>2</sub> (2 equiv), dry toluene (0.12 M in substrate), 50 °C, 8 h. <sup>b</sup>Isolated yield. <sup>c</sup>Determined by relative integrations of at least 2 pairs of peaks in the <sup>13</sup>C and/or <sup>1</sup>H NMR spectra; see section 4.13 for details. <sup>d</sup>2 equiv PhI(OBz)<sub>2</sub> were used.

#### 4.7 E/Z Stereochemical Assignment of Oxime Ether Substrates

Most of the oxime ether substrates in Tables 3 and 4 were isolated as single isomers, presumably with an *E* configuration. This geometry should be thermodynamically favored, as it places the bulkier  $\alpha$  group *trans* to the oxime ether N–O bond. However, the oxime ethers prepared from  $\alpha$ -thujone (**24** and **25**) and camphor (**27** and **28**) were isolated as two distinct isomers. In each case, the major isomer was expected to be the *E* stereoisomer. This assignment was confirmed spectroscopically by comparing the chemical shifts of the  $\alpha$  carbons (from  $^{13}\text{C}$  NMR spectra) and the  $\alpha$  methylene or methine protons (from  $^1\text{H}$  NMR) of the two isomers. Literature precedent indicates that the chemical shifts of the  $\alpha$  carbons should be further *upfield* when *cis* to the N–O bond than when *trans* (resulting from steric compression).<sup>24</sup> Conversely, the chemical shifts of the  $\alpha$  methylene or methine protons should be further *downfield* when *cis* to the N–O bond than when *trans* (resulting from shielding by the lone pair on nitrogen, Figure 4.1).<sup>25</sup>

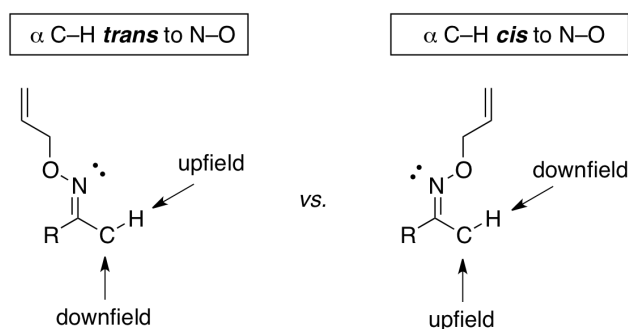


**Figure 4.1.** Relative Chemical Shifts of  $\alpha$  Protons and Carbons of *E* and *Z* Oximes<sup>24,25</sup>

Proton and carbon assignments for substrates **24**, **25**, **27**, and **28** were made using standard 2D NMR techniques (COSY, HSQC, and HMBC). The relative chemical shifts of the  $\alpha$  carbons were consistent with the assigned *E* or *Z* configurations of these substrates (Figure 4.2). Additionally, for both sets of substrates, at least one of the  $\alpha$  protons followed the expected trend. It is believed that the deviation from the literature trend seen with  $\text{H}^{2a}$  in **24** and **25** is a result of the rigid cyclic conformation of the

substrate. It is likely that the geometry of **24** permits only one of H<sup>2a</sup> or H<sup>2b</sup> to experience a shielding effect by the lone pair on the oxime nitrogen.

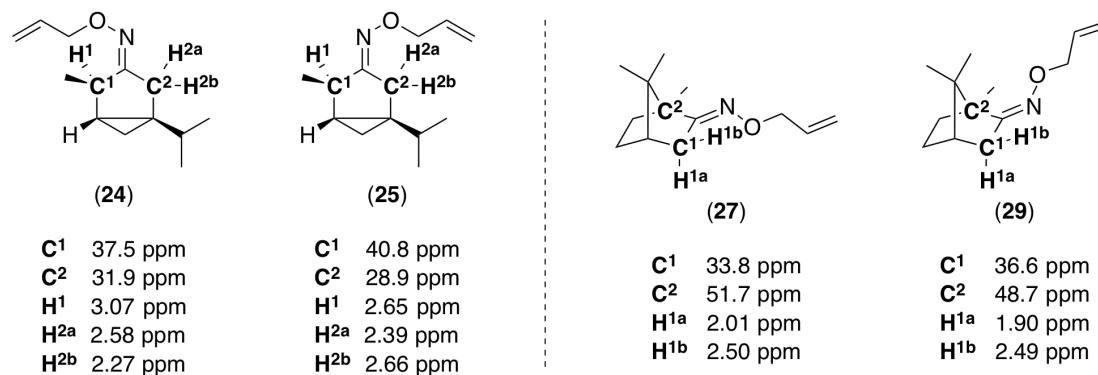


**Figure 4.2.** Chemical Shifts of  $\alpha$  Carbons and Protons of **24**, **25**, **27**, and **28**

#### 4.8 Quantification of Diastereomeric Ratios

For the products in Tables 4.3 and 4.4, diastereomeric ratios were obtained from <sup>13</sup>C NMR spectra. This method of analysis was chosen because, for the majority of the products isolated, <sup>1</sup>H NMR peaks corresponding to the minor product were fully or partially overlapping with peaks corresponding to the major product, making isomer ratio determination by <sup>1</sup>H NMR integration impossible in most cases. In contrast, for all of the products isolated, a large number of the peaks in the <sup>13</sup>C NMR spectra corresponding to the minor product were distinguishable from the peaks corresponding to the major product. Each minor product peak, when distinguishable, appeared as a smaller peak immediately to the left or right of the major product peak, representing the analogous carbon in the opposite diastereomer. Thus, diastereomeric ratios were obtained from the relative integrations of major product peaks and minor product peaks representing *analogous carbons*.

Although <sup>13</sup>C NMR is not generally used to obtain quantitative integrations, we hypothesized that analogous carbon nuclei on two diastereomers would have identical or nearly identical relaxation times. If so, <sup>13</sup>C NMR integrations could be used quantitatively. To test this hypothesis, we acquired <sup>13</sup>C NMR spectra of **43** using relaxation delays of 10 s and 0.10 s (default). As expected, the ratio of integrations of major and minor peaks for analogous carbons did *not* change with relaxation delay (ratio

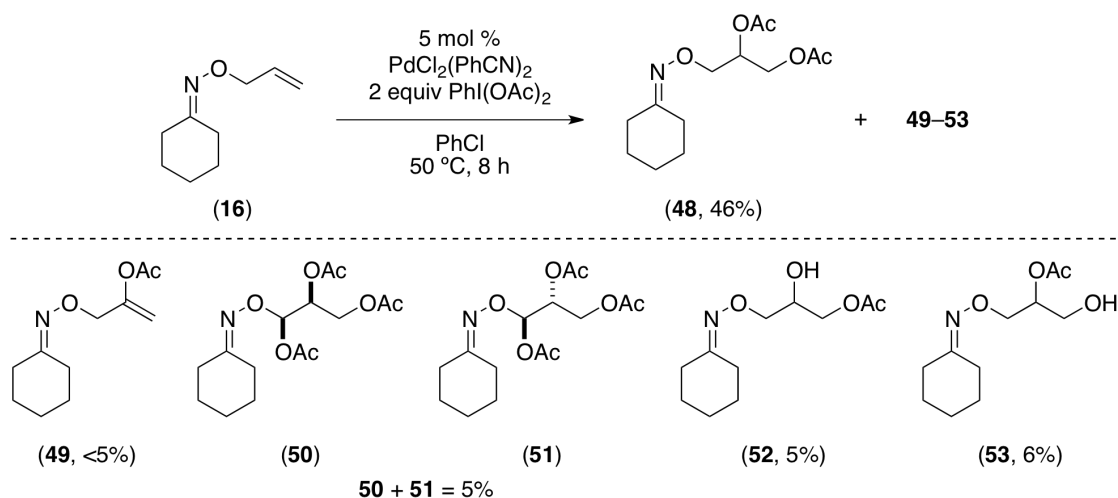
= 85.5 : 13.5 for both experiments). (The ratio of integrations between peaks representing *different* carbons did change, as is typical.) Thus the  $^{13}\text{C}$  NMR spectra used to obtain quantitative integrations were acquired with the default relaxation delay (0.10 s), allowing satisfactory spectra to be obtained within a reasonable length of time. A minimum of *two* sets of peaks in the  $^{13}\text{C}$  NMR spectra (chosen for having the best separation) were integrated to confirm that the ratio was consistent. In the few instances where it was possible, integrations from  $^1\text{H}$  NMR spectra were also used to confirm the results of  $^{13}\text{C}$  integrations.

Notably, chiral GC and HPLC were initially explored to obtain dr values (the diastereomeric products typically did not separate using achiral columns). While these methods often allowed observation of two distinct products, reliable integration by GC was not possible as a result of broad peak shapes and poor separation. This may be due in part to the high molecular weight of the products; typically very long run times (*e.g.*, 90 min) were necessary to obtain separation. Although chiral HPLC provided better separation in some cases, it did not prove general for the majority of the products.

#### 4.9 Identification of Side Products

In many cases, the yield of the dioxygenation reaction was relatively poor. This can be accounted for, in part, by the formation of several side products analogous to those isolated from the diacetoxylation reaction of substrate **16** with  $\text{PhI}(\text{OAc})_2$  (Scheme 4.20). Although these side products have not all been fully characterized,  $^1\text{H}$  NMR analysis suggests that they include monoacetoxyalkene **49**, diastereomeric triacetoxyalkene products **50** and **51**, and hydroxy/acetoxy products **52** and **53**.

#### Scheme 4.20. Side Products Isolated from the Diacetoxylation Reaction of **16**



Resubjection of **48** to the reaction conditions did not result in the formation of any of these side products. This result suggests that side products **49–53** are not derived from **48**.

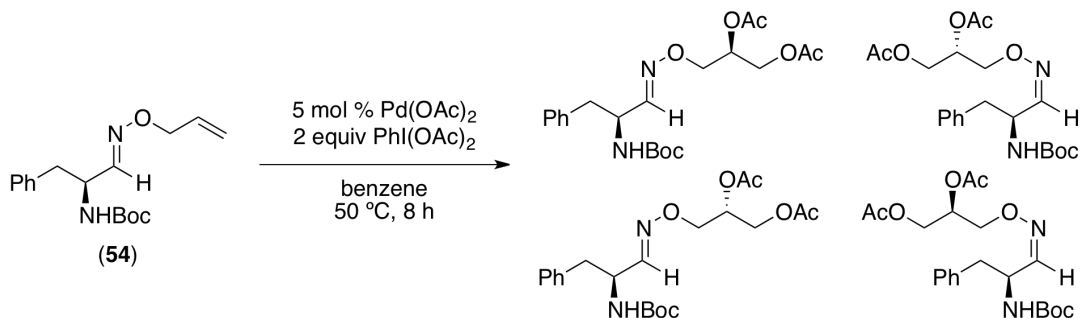
#### 4.10 Preliminary Results with Additional Directing Groups

In addition to the chiral ketone auxiliaries presented in Tables 4.3 and 4.4, a number of auxiliaries derived from other non-commercial chiral ketones and aldehydes were prepared and are described in this section. These auxiliaries did not provide as high levels of selectivity as the substrates in Table 4.4, and so full characterization of the substrates and products was not pursued. However, studies of these auxiliaries provide two important pieces of information about these reactions. First, unlike ketoxime ethers, aldoxime ethers appear to be prone to *E/Z* isomerization under the optimized reaction conditions. Second, branching at positions that are remote to the C=N ( $\delta$  and farther) does not appear to have a substantial influence on the stereoselectivity of the dioxygenation reaction.

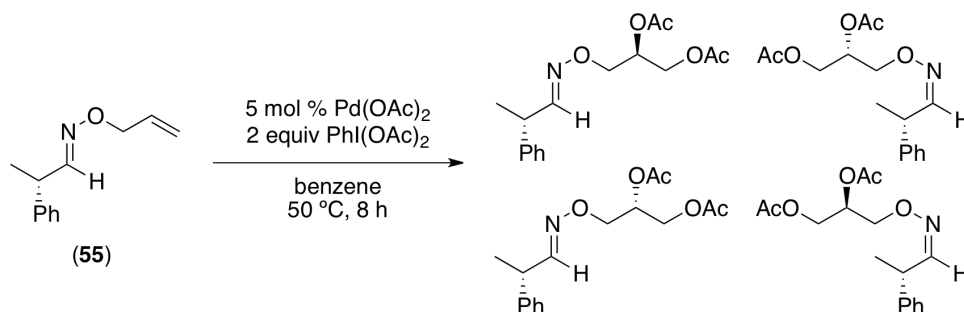
Subjection of aldoximes **54** and **55** to the reaction conditions with PhI(OAc)<sub>2</sub> resulted in the formation of four distinct diacetoxyated products (analyzed by chiral HPLC). This stands in contrast to the typical set of 2 products seen with the ketoxime ether substrates in Tables 4.3 and 4.4. The products resulting from diacetoxylation of **54**

and **55** are expected to be the four diastereomers shown in Schemes 4.21 and 4.22. These results suggest that aldoxime substrates are not configurationally stable under the dioxygenation conditions.

**Scheme 4.21.** Diacetoxylation of Aldoxime **54** to Afford Four Diastereomeric Products



**Scheme 4.22.** Diacetoxylation of Aldoxime **55** to Afford Four Diastereomeric Products



In an effort to systematically vary the sterics of an oxime ether auxiliary, we prepared several derivatives of ketoxime ether **56** substituted at the  $\beta$ -oxygen. Table 4.5 lists the yields and approximate dr's for the diacetoxylation of these substrates with PhI(OAc)<sub>2</sub>. Based on the consistently low selectivities with these auxiliaries, it appears that the sterics at remote positions do not substantially influence the stereoselectivity of the transformation.



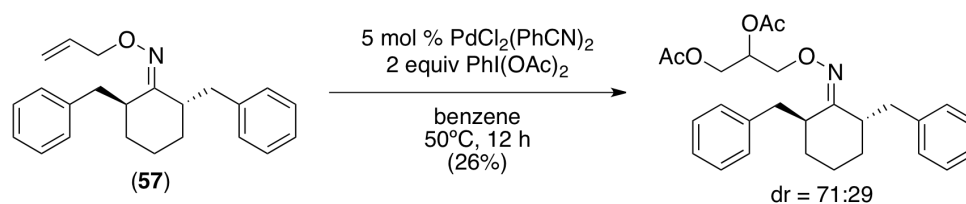
**Table 4.5.** Diacetoxylation of Derivatives of Oxime Ether **56**

entry	substrate	product	yield <sup>b</sup>	dr <sup>c</sup>
1			62%	61:39
2			75%	64:36
3			72%	55:45
4			65%	60:40

<sup>a</sup>Conditions: substrate (1 equiv), PdCl<sub>2</sub>(PhCN)<sub>2</sub> (0.05 equiv), PhI(OAc)<sub>2</sub> (2 equiv), dry benzene (0.12 M in substrate), 50 °C, 12 h. <sup>b</sup>Crude NMR yield relative to dinitrobenzene <sup>c</sup>Determined by chiral GC

Early on in our studies, before determining that ketoxime ethers are configurationally stable under the dioxygenation conditions, we were interested in exploring substrates derived from C2 symmetric ketones. Such substrates would consist of a single isomer regardless of any dynamic isomerization. Substrate **57** was prepared by Ir-catalyzed asymmetric hydrogenation of dibenzylidenecyclohexanone<sup>26</sup> followed by conversion to the allyl oxime ether. Diacetoxylation of **57** proceeded in relatively poor yield with 71:29 dr, and further optimization of this transformation was not pursued (Scheme 4.23).

### Scheme 4.23. Diacetoxylation of C2-Symmetric Substrate **57**



#### 4.11 Substituted Alkene Substrates

The previous sections described dioxygenation of terminal (allyl) or simple internal (crotyl) alkenes. In addition to these substrates, more highly substituted alkenes were also tested under the dioxygenation conditions. As detailed below, these substrates presented significant challenges in terms of reactivity, site-selectivity, and/or chemoselectivity; therefore, further exploration of the use of such substrates has not yet been pursued, and the products of the attempted dioxygenation reactions have not been fully characterized. Table 4.6 summarizes this work.

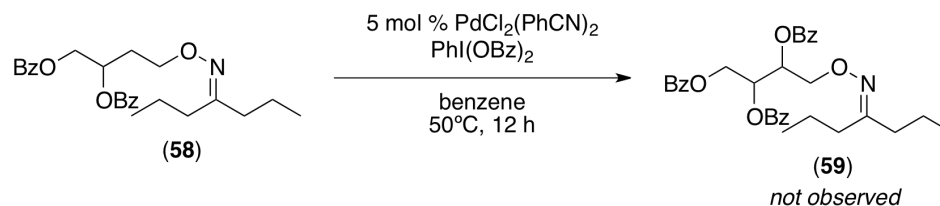
**Table 4.6.** Efforts Toward Dioxygenation of Substituted Alkene Substrates

entry	substrate	isolated products (% yield)	
1			
		(16%)	(8%)
2			
		(61%)	(11%)
3			
		(58, 26%)	
		(59, 13%)	trace
4		complex mixture of products	

<sup>a</sup>Conditions: substrate (1 equiv), PdCl<sub>2</sub>(PhCN)<sub>2</sub> (0.05 equiv), PhI(OBz)<sub>2</sub> (2 equiv), dry benzene (0.12 M in substrate), 50 °C, 12 h.

In the case of entry 3, we observed a significant amount of a triacetoxylated product. To test whether dibenzoylated product **58** was undergoing a third oxygenation, we resubjected **58** to the reaction conditions. However, conversion to **59** was not observed from **58**, suggesting that **58** is not an intermediate in the reaction pathway that forms **59** (Scheme 4.24).

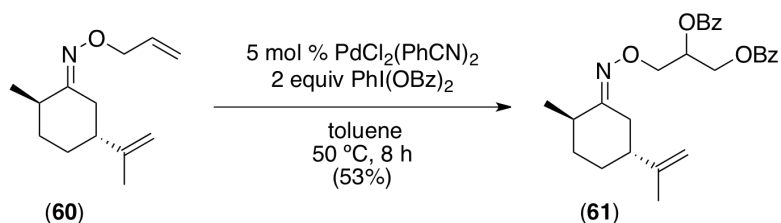
**Scheme 4.24.** Resubjection of **58** to the Dibenzoylation Conditions



## 4.12 Conclusions and Outlook

In summary, the results presented in this chapter demonstrate that a chiral directing group can facilitate Pd-catalyzed alkene difunctionalization with control over the absolute stereoselectivity of the transformation. Preliminary results indicate that this directing group strategy also allows for site selective functionalization of proximal olefins in the presence of remote alkenes (Scheme 4.25).

**Scheme 4.25.** Site Selective Functionalization of Diene **60**



Conceptually, this approach could prove quite powerful if it can be extended to the use of diverse nucleophiles. Efforts thus far to apply the developed reaction conditions toward the asymmetric dioxygenation of disubstituted alkenes (crotyl oxime ethers of achiral ketones) have resulted in erosion of control over relative stereochemistry (*syn* vs *anti* difunctionalization). Consequently, further optimization will be necessary to broaden the scope of this work.

## 4.13 Experimental Procedures and Characterization Data

### *General Procedures and Materials and Methods*

NMR spectra were obtained on a Varian vnmrs 700 (699.76 MHz for <sup>1</sup>H; 175.95 MHz for <sup>13</sup>C), Varian vnmrs 500 (500.10 MHz for <sup>1</sup>H; 125.75 MHz for <sup>13</sup>C), Varian Inova 500 (499.90 MHz for <sup>1</sup>H; 125.70 MHz for <sup>13</sup>C), or a Varian MR400 (400.52 MHz for <sup>1</sup>H; 100.71 for <sup>13</sup>C) spectrometer. <sup>1</sup>H and <sup>13</sup>C NMR chemical shifts are reported in parts per million (ppm) relative to TMS, with the residual solvent peak used as an internal reference. Multiplicities are reported as follows: singlet (s), doublet (d), doublet of doublets (dd), doublet of doublet of doublets (ddd), doublet of doublet of doublet of doublets (dddd), triplet (t), quartet (q), quintet (quin), sextet (sext), septet (sept), doublet

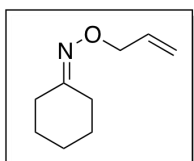
of triplets (dt), doublet of doublet of triplets (ddt), doublet of triplet of doublets (dtd), doublet of quartets (dq), triplet of triplets (tt), quartet of doublets (qd), multiplet (m), and broad resonance (br). IR spectra were obtained on a Perkin-Elmer Spectrum BX FT-IR spectrometer. HRMS data were obtained on a Micromass AutoSpec Ultima Magnetic Sector mass spectrometer. Gas chromatography was carried out on a Shimadzu 17A using a Restek Rtx®-5 (Crossbond 5% diphenyl – 95% dimethyl polysiloxane; 15 m, 0.25 mm ID, 0.25  $\mu$ m df) column. Chiral gas chromatography was carried out on a Shimadzu 17A using an Agilent Cyclosil-B [30% heptakis (2,3-di-O-methyl-6-O-t-butyl dimethylsilyl)- $\beta$ -cyclodextrin in DB-1701; 30 m, 0.25 mm ID, 0.25 $\mu$ m df) column. Chiral HPLC was performed on a Varian Prostar 210 HPLC using a Daicel Chiralcel 20  $\mu$ m silica (46 x 500 mm) column.

**Materials and Methods.** Commercial ketones were obtained from Aldrich [4-heptanone, (-)-( $\alpha$ )-thujone, (1*R*)-(+)-nopinone, (-)-menthone, and (*1R*)-(+)-camphor], Acros [(*R*)-(+)-2-(2'-carbomethoxyethyl)-2-methylcyclohexanone], or Mallinckrodt (cyclohexanone) and used as received. (+)-Dihydrocarvone was obtained from Acros as a mixture of (2*R*,5*R*) and (2*R*,5*S*) diastereomers, and the major isomer (2*R*,5*R*) was isolated by column chromatography ( $R_f$  = 0.14 and 0.10 in 96% hexanes/4% diethyl ether for the major and minor isomers, respectively) prior to use. (*R*)-(+)-Pulegone was obtained from Acros and was used as received to prepare ketones **62–66**. PdCl<sub>2</sub>(PhCN)<sub>2</sub><sup>27</sup> and PhI(OBz)<sub>2</sub><sup>28</sup> were prepared according to literature procedures. Toluene was purified using an Innovative Technology (IT) solvent purification system composed of activated alumina, copper catalyst, and molecular sieves. Flash chromatography was performed on EM Science silica gel 60 (0.040-0.063 mm particle size, 230-400 mesh) and thin layer chromatography was performed on Merck TLC plates pre-coated with silica gel 60 F254.

*Synthesis and Characterization of Allyl Oxime Ether Substrates in Schemes 4.12 and 4.25 and Table 4.3*

**General Procedure.** Ketone and *O*-allyl hydroxylamine hydrochloride were combined in pyridine in a scintillation vial. The vial was sealed with a Teflon-lined cap, and the mixture was heated to 80 °C for 30 min and then stirred at room temperature overnight.

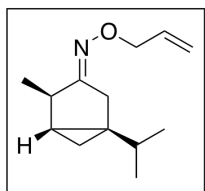
The reaction mixture was diluted by 5-fold with EtOAc or Et<sub>2</sub>O and washed with 20% aqueous AcOH (5 x equal volume to the organic layer) to remove pyridine. The organic layer was then neutralized with aqueous NaHCO<sub>3</sub>, washed with brine, dried over MgSO<sub>4</sub>, and concentrated to yield the oxime ether. Where noted, some oxime ethers were obtained as mixtures of *E* and *Z* stereoisomers. In these cases, the major (*E*) stereoisomer and the minor (*Z*) stereoisomer were obtained in isomerically pure form following column chromatography.



**Oxime Ether 16.** The general procedure was followed using cyclohexanone (1.00 g, 10.2 mmol, 1.0 equiv), *O*-allyl hydroxylamine hydrochloride (1.34 g, 12.2 mmol, 1.2 equiv), and pyridine (4.4 mL).

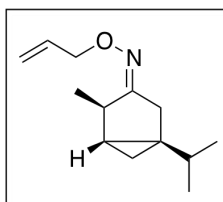
Oxime ether **16** was obtained as a colorless oil (1.37 g, 88% yield). <sup>1</sup>H NMR (700 MHz, CDCl<sub>3</sub>): δ 5.99 (ddt, *J* = 17.5, 10.5, 5.6 Hz, 1H), 5.29 (dd, *J* = 17.5, 1.4 Hz, 1H), 5.19 (dd, *J* = 10.5, 1.4 Hz, 1H), 4.52 (d, *J* = 5.6 Hz, 2H), 2.48 (t, *J* = 6.0 Hz, 2H), 2.20 (t, *J* = 6.3 Hz, 2H), 1.67 (quin, *J* = 6.0 Hz, 2H), 1.62–1.57 (multiple peaks, 4H). <sup>13</sup>C{<sup>1</sup>H} NMR (176 MHz, CDCl<sub>3</sub>): δ 160.6, 134.6, 116.9, 74.0, 32.2, 27.0, 25.8, 25.7, 25.3. IR (thin film, neat) 2932, 2860, 1449 cm<sup>-1</sup>. HRMS [M+H]<sup>+</sup> Calcd for C<sub>9</sub>H<sub>15</sub>NO: 154.1226; Found: 154.1221.

**Oxime Ethers 24 and 25.** The general procedure was followed using (–)-(α)-thujone (428 mg, 2.81 mmol, 1 equiv), *O*-allyl hydroxylamine hydrochloride (370 mg, 3.37 mmol, 1.2 equiv), and pyridine (1.2 mL) affording the products as a colorless oil consisting of an ~2 : 1 mixture of *E/Z* stereoisomers (545 mg, 94% yield). *E* and *Z* isomers were obtained in isomerically pure form following column chromatography (*R*<sub>f</sub> = 0.22 and 0.21 for *Z* and *E* isomers, respectively, in 2:1:0.1 hexanes/benzene/CH<sub>2</sub>Cl<sub>2</sub>). HRMS electrospray (*m/z*): [M+H]<sup>+</sup> calcd for C<sub>13</sub>H<sub>22</sub>NO (mixture of oxime isomers), 208.1696; found, 208.1698.

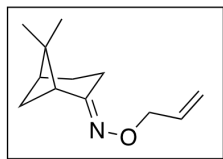


Major (*E*) Isomer (25): <sup>1</sup>H NMR (700 MHz, CDCl<sub>3</sub>): δ 5.97 (ddt, *J* = 17.3, 10.6, 5.5 Hz, 1H), 5.26 (ddt, *J* = 17.3, 1.7, 1.7 Hz, 1H), 5.18 (ddt, *J* = 10.6, 1.7, 1.3 Hz, 1H), 4.50 (m, 2H), 2.66 (d, *J* = 17.9 Hz, 1H), 2.65 (m, 1H), 2.39 (app dt, *J* = 17.9, 1.9 Hz, 1H), 1.33 (sept, *J* = 6.8

Hz, 1H), 1.16 (d,  $J = 7.2$  Hz, 3H), 0.98 (d,  $J = 6.8$  Hz, 3H), 0.93 (d,  $J = 6.8$  Hz, 3H), 0.91 (dd,  $J = 8.0, 3.9$  Hz, 1H), 0.53 (ddd,  $J = 8.0, 5.3, 2.2$  Hz, 1H), 0.04 (dd,  $J = 5.3, 3.9$  Hz, 1H).  $^{13}\text{C}\{^1\text{H}\}$  NMR (176 MHz,  $\text{CDCl}_3$ ):  $\delta$  168.3, 134.4, 117.1, 74.4, 40.8, 32.3, 31.5, 28.9, 26.8, 21.5, 20.0, 19.7, 16.8. IR (thin film, neat): 2958, 1454  $\text{cm}^{-1}$ .



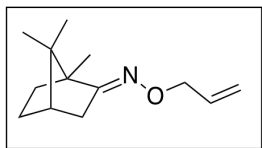
**Minor (*Z*) Isomer (24):**  $^1\text{H}$  NMR (700 MHz,  $\text{CDCl}_3$ ):  $\delta$  5.94 (ddt,  $J = 17.3, 10.6, 5.4$  Hz, 1H), 5.24 (ddt,  $J = 17.3, 1.6, 0.6$  Hz, 1H), 5.16 (ddt,  $J = 10.6, 1.6, 0.6$  Hz, 1H), 4.48 (m, 2H), 3.07 (qd,  $J = 7.0, 1.7$  Hz, 1H), 2.58 (d,  $J = 16.5$  Hz, 1H), 2.27 (d,  $J = 16.5$  Hz, 1H), 1.36 (sept,  $J = 6.8$  Hz, 1H), 1.11 (d,  $J = 7.2$  Hz, 3H), 0.97 (d,  $J = 6.8$  Hz, 3H), 0.91 (d,  $J = 6.8$  Hz, 3H), 0.906 (dd,  $J = 8.0, 3.9$  Hz, 1H), 0.50 (ddd,  $J = 8.0, 5.1, 1.7$  Hz, 1H), 0.03 (dd,  $J = 4.6, 4.1$  Hz, 1H).  $^{13}\text{C}\{^1\text{H}\}$  NMR (176 MHz,  $\text{CDCl}_3$ ):  $\delta$  167.7, 134.7, 116.7, 74.2, 37.5, 32.2, 31.9, 30.2, 26.9, 20.0, 19.8, 17.4, 15.8. IR (thin film, neat): 2957, 1457  $\text{cm}^{-1}$ .



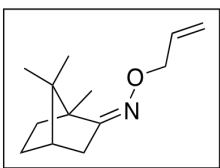
**Oxime Ether 26.** The general procedure was followed using (1*R*)-(+)-nopinone (829 mg, 6.00 mmol, 1 equiv), *O*-allyl hydroxylamine hydrochloride (986 mg, 9.00 mmol, 1.5 equiv), and pyridine (2.6 mL) affording the product as a colorless oil consisting of an ~8 : 1 mixture of *E/Z* stereoisomers (1.09 g, 94% yield). The *E* isomer (**26**) was obtained in isomerically pure form following column chromatography ( $R_f = 0.26$  in 3:3:0.2 hexanes/benzene/ $\text{CH}_2\text{Cl}_2$ ).  $^1\text{H}$  NMR (700 MHz,  $\text{CDCl}_3$ ):  $\delta$  5.98 (ddt,  $J = 17.3, 10.6, 5.5$  Hz, 1H), 5.28 (ddt,  $J = 17.3, 2.7, 1.4$  Hz, 1H), 5.18 (ddt,  $J = 10.5, 2.7, 1.4$  Hz, 1H), 4.52 (ddd,  $J = 5.5, 1.4, 1.4$  Hz, 2H), 2.77 (ddd,  $J = 19.8, 9.8, 2.6$  Hz, 1H), 2.59, (dd,  $J = 5.6, 5.6$  Hz, 1H), 2.48–2.42 (multiple peaks, 2H), 2.06 (m, 1H), 1.93 (m, 1H), 1.87 (m, 1H), 1.37 (d,  $J = 10.6$  Hz, 1H), 1.27 (s, 3H), 0.81 (s, 3H).  $^{13}\text{C}\{^1\text{H}\}$  NMR (176 MHz,  $\text{CDCl}_3$ ):  $\delta$  164.8, 134.8, 116.7, 74.1, 48.1, 40.6, 40.5, 27.3, 25.6, 22.2, 22.1, 18.7. IR (thin film, neat): 2918, 1458  $\text{cm}^{-1}$ . HRMS electrospray ( $m/z$ ):  $[\text{M}+\text{H}]^+$  calcd for  $\text{C}_{12}\text{H}_{20}\text{NO}$ , 194.1539; found, 194.1543.

**Oxime Ethers 27 and 28.** The general procedure was followed using (1*R*)-(+)-camphor (761 mg, 5.00 mmol, 1 equiv), *O*-allyl hydroxylamine hydrochloride (822 mg, 7.50 mmol, 1.5 equiv), and pyridine (2.2 mL) affording the products as a colorless oil

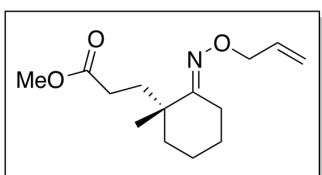
consisting of an ~1.7 : 1 mixture of *E/Z* stereoisomers (888 mg, 86% yield). *E* and *Z* isomers were obtained in isomerically pure form following column chromatography ( $R_f = 0.18$  and  $0.08$  for *E* and *Z* isomers, respectively, in 98% hexanes/2% Et<sub>2</sub>O).



**Major (*E*) Isomer (27):** <sup>1</sup>H NMR (700 MHz, CDCl<sub>3</sub>): δ 5.98 (ddt,  $J = 17.3, 10.6, 5.4$  Hz, 1H), 5.26 (ddt,  $J = 17.3, 1.5, 1.5$  Hz, 1H), 5.16 (ddt,  $J = 10.6, 1.5, 1.5$  Hz, 1H), 4.53 (ddd,  $J = 5.4, 1.5, 1.5$  Hz, 2H), 2.50 (ddd,  $J = 17.9, 4.4, 3.3$  Hz, 1H), 2.01 (d,  $J = 17.9$  Hz, 1H), 1.87 (dd,  $J = 4.4, 4.4$  Hz, 1H), 1.82 (m, 1H), 1.69 (m, 1H), 1.44 (m, 1H), 1.22 (m, 1H), 1.00 (s, 3H), 0.90 (s, 3H), 0.78 (s, 3H). <sup>13</sup>C{<sup>1</sup>H} NMR (176 MHz, CDCl<sub>3</sub>): δ 169.6, 134.8, 116.7, 74.1, 51.7, 48.1, 43.7, 33.8, 32.8, 27.3, 19.5, 18.5, 11.2. IR (thin film, neat): 2956, 1456 cm<sup>-1</sup>. HRMS electrospray ( $m/z$ ): [M+H]<sup>+</sup> calcd for C<sub>13</sub>H<sub>22</sub>NO, 208.1696; found, 208.1697.



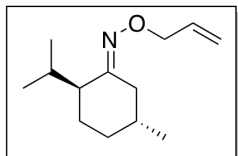
**Minor (*Z*) Isomer (28):** <sup>1</sup>H NMR (700 MHz, CDCl<sub>3</sub>): δ 5.96 (ddt,  $J = 17.3, 10.6, 5.3$  Hz, 1H), 5.27 (d,  $J = 17.3$  Hz, 1H), 5.16 (d,  $J = 10.6$  Hz, 1H), 4.44 (d, 5.3 Hz, 2H), 2.49 (ddd,  $J = 16.3, 3.7, 3.7$  Hz, 1H), 1.90 (d,  $J = 16.3$  Hz, 1H), 1.85–1.81 (multiple peaks, 2H), 1.64–1.58 (multiple peaks, 2H), 1.32 (s, 3H), 1.27 (m, 1H), 0.90 (s, 3H), 0.84 (s, 3H). <sup>13</sup>C{<sup>1</sup>H} NMR (176 MHz, CDCl<sub>3</sub>): δ 166.1, 134.8, 116.3, 74.2, 55.0, 48.7, 43.9, 36.6, 32.8, 27.3, 20.4, 18.2, 14.2. IR (thin film, neat): 2956, 1453 cm<sup>-1</sup>. HRMS electrospray ( $m/z$ ): [M+H]<sup>+</sup> calcd for C<sub>13</sub>H<sub>22</sub>NO, 208.1696; found, 208.1698.



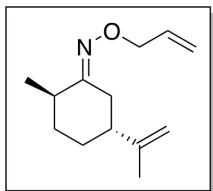
**Oxime Ether 29.** The general procedure was followed using (*R*)-(+)-2-(2'-carbomethoxyethyl)-2-methylcyclohexanone (500 mg, 2.52 mmol, 1 equiv), *O*-allyl hydroxylamine hydrochloride (414 mg, 3.78 mmol, 1.5 equiv), and pyridine (1.1 mL) affording **29** as a colorless oil consisting of a single (*E*) stereoisomer (529 mg, 83% yield). <sup>1</sup>H NMR (700 MHz, CDCl<sub>3</sub>): δ 5.98 (ddt,  $J = 17.3, 10.6, 5.6$  Hz, 1H), 5.25 (d,  $J = 17.3$  Hz, 1H), 5.17 (d,  $J = 10.6$  Hz, 1H), 4.51 (d,  $J = 5.6$  Hz, 2H), 3.65 (s, 3H), 2.77 (ddd,  $J = 14.5, 5.4, 5.4$  Hz, 1H), 2.34 (ddd,  $J = 16.4, 11.2, 5.4$  Hz, 1H), 2.22–2.15 (multiple peaks, 2H), 2.07 (ddd,  $J = 13.8, 11.2, 5.1$  Hz, 1H), 1.67–1.57 (multiple peaks, 5H), 1.46 (m, 2H), 1.06 (s, 3H). <sup>13</sup>C{<sup>1</sup>H} NMR (176 MHz, CDCl<sub>3</sub>): δ 174.7, 163.0,



134.7, 116.9, 74.2, 51.5, 39.8, 39.7, 32.9, 29.1, 25.8, 24.0, 21.5, 21.1. IR (thin film, neat): 2936, 1737, 1436  $\text{cm}^{-1}$ . HRMS electrospray ( $m/z$ ):  $[\text{M}+\text{H}]^+$  calcd for  $\text{C}_{14}\text{H}_{24}\text{NO}_3$ , 254.1751; found, 254.1753.

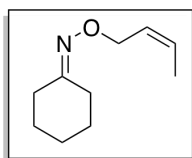


**Oxime Ether 30.** The general procedure was followed using (-)-menthone (1.23 g, 8.00 mmol, 1 equiv), *O*-allyl hydroxylamine hydrochloride (1.32 g, 12.00 mmol, 1.5 equiv), and pyridine (3.5 mL) affording **30** as a colorless oil consisting of a single (*E*) stereoisomer (1.31 g, 78% yield).  $^1\text{H}$  NMR (400 MHz,  $\text{CDCl}_3$ ):  $\delta$  5.99 (ddt,  $J = 17.3, 10.5, 5.6$  Hz, 1H), 5.26 (ddt,  $J = 17.3, 1.6, 1.6$  Hz, 1H), 5.16 (ddt,  $J = 10.5, 1.3, 1.3$  Hz, 1H), 4.52 (ddd,  $J = 5.6, 1.6, 1.3$  Hz, 2H), 2.84 (ddd,  $J = 13.3, 4.3, 1.3$  Hz, 1H), 2.12 (app octet,  $J = 6.7$  Hz, 1H), 1.87–1.73 (multiple peaks, 5H), 1.40 (m, 1H), 1.14 (m, 1H), 0.95 (d,  $J = 6.6$  Hz, 3H), 0.90 (d,  $J = 6.7$  Hz, 6H).  $^{13}\text{C}\{^1\text{H}\}$  NMR (100.7 MHz,  $\text{CDCl}_3$ ):  $\delta$  161.0, 135.1, 116.6, 74.0, 48.5, 32.1, 32.05, 32.04, 26.6, 26.5, 21.5, 21.0, 19.4. IR (thin film, neat): 2955, 1457  $\text{cm}^{-1}$ . HRMS electrospray ( $m/z$ ):  $[\text{M}+\text{H}]^+$  calcd for  $\text{C}_{13}\text{H}_{24}\text{NO}$ , 210.1852; found, 210.1852.



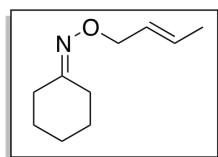
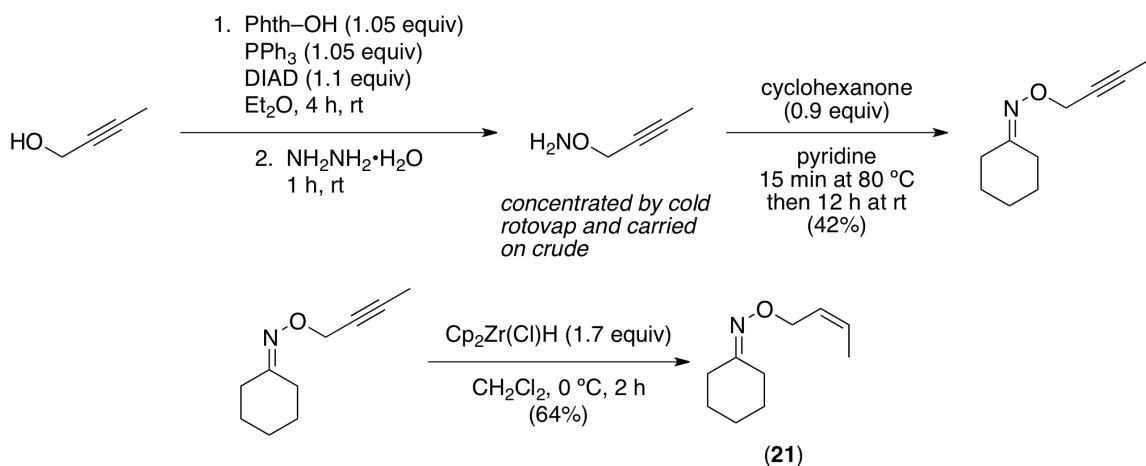
**Oxime Ether 60.** The general procedure was followed using (2*R*,5*R*)-dihydrocarvone (300 mg, 1.97 mmol, 1.0 equiv), *O*-allyl hydroxylamine hydrochloride (324 mg, 2.96 mmol, 1.5 equiv), and pyridine (0.85 mL). Oxime ether **60** was obtained as a colorless oil consisting of a single (*E*) stereoisomer (403 mg, 99% yield).  $^1\text{H}$  NMR (700 MHz,  $\text{CDCl}_3$ ):  $\delta$  6.02 (ddt,  $J = 17.3, 10.5, 5.6$  Hz, 1H), 5.29 (ddt,  $J = 17.3, 1.7, 1.7$  Hz, 1H), 5.19 (ddt,  $J = 10.5, 1.7, 1.3$  Hz, 1H), 4.75 (app s, 2H), 4.55 (ddd,  $J = 5.6, 1.7, 1.3$  Hz, 2H), 3.38 (ddd,  $J = 13.6, 3.9, 2.1$  Hz, 1H), 2.20 (m, 1H), 2.08 (app tt,  $J = 12.1, 3.6$  Hz, 1H), 1.96 (app dq,  $J = 12.9, 3.6$  Hz, 1H), 1.86 (m, 1H), 1.75 (s, 3H), 1.63 (dd,  $J = 13.4, 12.7$  Hz, 1H), 1.43 (app qd,  $J = 12.9, 3.6$  Hz, 1H), 1.26 (app qd,  $J = 12.6, 3.4$  Hz, 1H), 1.11 (d,  $J = 6.6$  Hz, 3H).  $^{13}\text{C}\{^1\text{H}\}$  NMR (176 MHz,  $\text{CDCl}_3$ ):  $\delta$  161.9, 148.7, 134.8, 116.8, 109.2, 74.2, 44.8, 37.3, 35.4, 30.9, 30.0, 20.7, 16.4. IR (thin film, neat) 2968, 2928, 2857, 1448  $\text{cm}^{-1}$ . HRMS  $[\text{M}+\text{H}]^+$  Calcd for  $\text{C}_{13}\text{H}_{22}\text{NO}$ : 208.1696; Found: 208.1685.

*Synthesis and Characterization of Crotyl Oxime Ether Substrates in Schemes 4.16 and 4.17*



**Oxime Ether 21.** Substrate **21** was prepared by the reaction sequence depicted in Scheme 4.26 involving (1) conversion of 2-butyn-1-ol to the corresponding hydroxylamine via the intermediate propargyloxy phthalimide (2) condensation of the hydroxylamine with cyclohexanone, and (3) alkyne reduction to the *cis* alkene with Schwartz' reagent. The final product **21** was isolated as a colorless oil (33% from cyclohexanone,  $R_f = 0.21$  in 95% hexane/5% Et<sub>2</sub>O). <sup>1</sup>H NMR (700 MHz, CDCl<sub>3</sub>): δ 5.68 (m, 1H), 5.63 (m, 1H), 4.59 (d,  $J = 6.3$  Hz, 2H), 2.46 (t,  $J = 6.3$  Hz, 2H), 2.20 (t,  $J = 6.3$  Hz, 2H), 1.69 (d,  $J = 6.4$  Hz, 3H), 1.67 (m, 2H), 1.61–1.57 (multiple peaks, 4H). <sup>13</sup>C{<sup>1</sup>H} NMR (176 MHz, CDCl<sub>3</sub>): δ 160.4, 127.9, 126.3, 68.8, 32.2, 27.0, 25.8, 25.7, 25.2, 13.3. IR (thin film, neat) 2929, 2858, 1448 cm<sup>-1</sup>. HRMS [M+H]<sup>+</sup> Calcd for C<sub>10</sub>H<sub>18</sub>NO: 168.1383; Found: 168.1382.

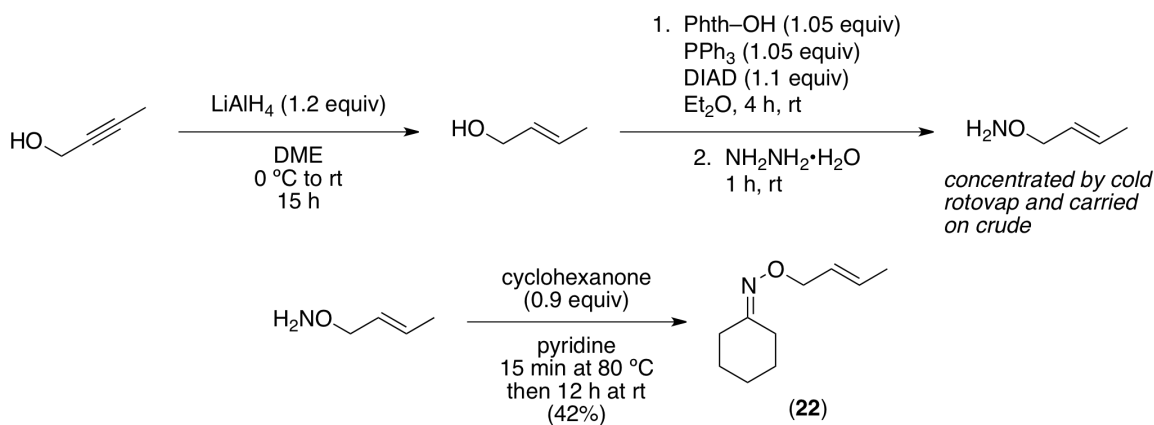
**Scheme 4.26.** Synthesis of *cis*-Crotyl Oxime Ether **21**



**Oxime Ether 22.** Substrate **22** was prepared by the reaction sequence depicted in Scheme 4.27 involving (1) LAH reduction of 2-butyn-1-ol, (2) conversion of the *trans*-crotyl alcohol to the corresponding hydroxylamine via the intermediate allyloxy phthalimide, and (3) condensation of the hydroxylamine with cyclohexanone. The final product **22** was isolated as a colorless oil (42% from cyclohexanone,  $R_f = 0.21$  in 95% hexane/5% Et<sub>2</sub>O).

$^1\text{H}$  NMR (700 MHz,  $\text{CDCl}_3$ ):  $\delta$  5.75 (m, 1H), 5.66 (m, 1H), 4.45 (dd,  $J = 6.2, 1.1$  Hz, 2H), 2.47 (t,  $J = 6.3$  Hz, 2H), 2.20 (t,  $J = 6.3$  Hz, 2H), 1.72 (dd,  $J = 6.5, 1.1$  Hz, 3H), 1.67 (m, 2H), 1.63–1.58 (multiple peaks, 4H).  $^{13}\text{C}\{^1\text{H}\}$  NMR (176 MHz,  $\text{CDCl}_3$ ):  $\delta$  160.2, 129.6, 127.2, 73.9, 32.2, 27.0, 25.8, 25.7, 25.4, 17.9. IR (thin film, neat) 2929, 2858, 1449  $\text{cm}^{-1}$ . HRMS  $[\text{M}+\text{H}]^+$  Calcd for  $\text{C}_{10}\text{H}_{18}\text{NO}$ : 168.1383; Found: 168.1381.

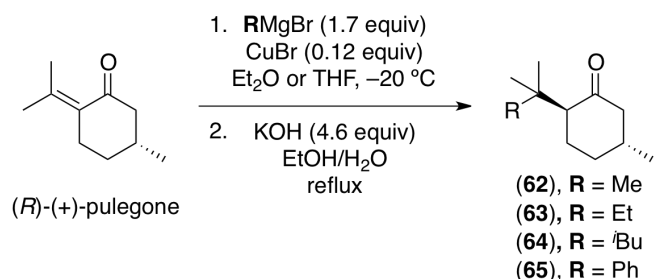
**Scheme 4.27.** Synthesis of *trans*-Crotyl Oxime Ether **22**



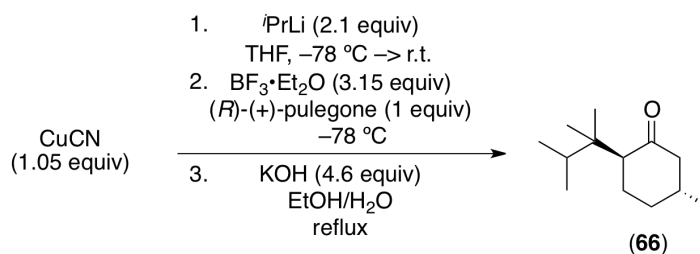
*Synthesis and Characterization of Allyl Oxime Ether Substrates in Table 4.4*

**General Procedure.** 8-Substituted menthone derivatives **62**, **63**, **64**, and **65** were prepared by a literature prep involving the conjugate addition of methyl, ethyl, isobutyl, or phenyl Grignard to (*R*)-(+)-pulegone in the presence of cat. CuBr (Scheme 4.28).<sup>29</sup> 8-Isopropyl menthone **66** was prepared by the conjugate addition of <sup>*t*</sup>PrLi (2 equiv) to (*R*)-(+)-pulegone (1 equiv) in the presence of CuCN (1 equiv) and BF<sub>3</sub>·Et<sub>2</sub>O (3 equiv) at -78 °C (Scheme 4.29). The resulting 8-substituted menthone derivatives were then refluxed in H<sub>2</sub>O/EtOH with KOH to enhance the ratio of the desired thermodynamic *trans* (*2S,5R*) ketone relative to the undesired *cis* (*2R,5R*) isomer, and were then purified by column chromatography.

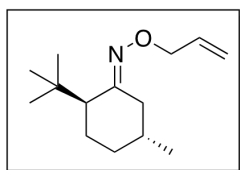
**Scheme 4.28.** Synthesis of 8-Substituted Menthone Derivatives **62**, **63**, **64**, and **65**



**Scheme 4.29.** Synthesis 8-Isopropyl Menthone **66**

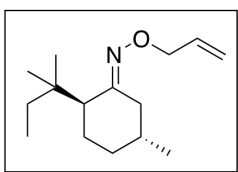


The enantiomerically pure (*2S,5R*) ketones **62–66** and *O*-allyl hydroxylamine hydrochloride were combined in pyridine in a scintillation vial. The vial was sealed with a Teflon-lined cap, and the mixture was heated to  $80\text{ }^\circ\text{C}$  for 30 min and then stirred at room temperature overnight. The reaction mixture was diluted by 5-fold with EtOAc or Et<sub>2</sub>O and washed with 20% aqueous AcOH (5 x equal volume to the organic layer) to remove pyridine. The organic layer was then neutralized with aqueous NaHCO<sub>3</sub>, washed with brine, dried over MgSO<sub>4</sub>, and concentrated to yield the oxime ether, which was further purified by column chromatography to remove residual impurities from the ketone synthesis steps. In all cases, the oxime ether products were isolated as a single oxime stereoisomer (*E*).

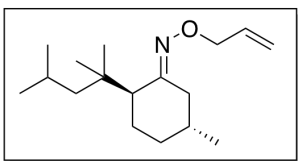


**Oxime Ether 38.** The general procedure was followed using 8-methylmenthone **62** (500 mg, 2.97 mmol, 1.0 equiv), *O*-allyl hydroxylamine hydrochloride (456 mg, 4.16 mmol, 1.4 equiv), and pyridine (1.3 mL). Oxime ether **38** was obtained as a colorless oil (545 mg, 82% yield,  $R_f = 0.47$  in 99% hexanes/1% Et<sub>2</sub>O). <sup>1</sup>H NMR (700 MHz, CDCl<sub>3</sub>):  $\delta$

6.00 (ddt,  $J = 17.3, 10.5, 5.6$  Hz, 1H), 5.25 (ddt,  $J = 17.3, 3.2, 1.0$  Hz, 1H), 5.16 (ddt,  $J = 10.5, 3.2, 1.0$  Hz, 1H), 4.52 (ddd,  $J = 5.6, 1.0, 1.0$  Hz, 2H), 3.15 (ddd,  $J = 12.9, 4.5, 1.7$  Hz, 1H), 1.98 (app dq,  $J = 12.9, 4.0$  Hz, 1H), 1.84 (dd,  $J = 11.6, 4.3$  Hz, 1H), 1.80 (m, 1H), 1.64 (m, 1H), 1.41 (dd,  $J = 12.9, 11.3$  Hz, 1H), 1.35 (app qd,  $J = 12.5, 3.6$  Hz, 1H), 1.06 (m, 1H), 1.03 (s, 9H), 0.95 (d,  $J = 6.5$  Hz, 3H).  $^{13}\text{C}\{^1\text{H}\}$  NMR (176 MHz,  $\text{CDCl}_3$ ):  $\delta$  160.5, 135.3, 116.7, 74.1, 53.1, 34.6, 34.2, 33.4, 32.8, 28.4, 28.3, 22.2. IR (thin film, neat): 2952, 1457  $\text{cm}^{-1}$ . HRMS electrospray ( $m/z$ ):  $[\text{M}+\text{H}]^+$  calcd for  $\text{C}_{14}\text{H}_{26}\text{NO}$ , 224.2009; found, 224.2006.

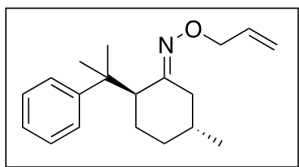


**Oxime Ether 39.** The general procedure was followed using 8-ethylmenthone **63** (300 mg, 1.65 mmol, 1.0 equiv), *O*-allyl hydroxylamine hydrochloride (270 mg, 2.47 mmol, 1.5 equiv), and pyridine (0.72 mL). Oxime ether **39** was obtained as a colorless oil (230 mg, 59% yield,  $R_f = 0.47$  in 99% hexanes/1%  $\text{Et}_2\text{O}$ ).  $^1\text{H}$  NMR (700 MHz,  $\text{CDCl}_3$ ):  $\delta$  6.00 (ddt,  $J = 17.3, 10.4, 5.6$  Hz, 1H), 5.25 (ddt,  $J = 17.3, 2.1, 1.3$  Hz, 1H); 5.16 (ddt,  $J = 10.4, 2.1, 1.3$  Hz, 1H), 4.51 (ddd,  $J = 5.6, 1.3, 1.3$  Hz, 2H), 3.16 (ddd,  $J = 12.9, 4.6, 1.7$  Hz, 1H), 1.93–1.90 (multiple peaks, 2H), 1.80 (m, 1H), 1.68–1.61 (multiple peaks, 2H), 1.41 (dd,  $J = 12.9, 11.3$  Hz, 1H), 1.39–1.30 (multiple peaks, 2H), 1.06 (m, 1H), 1.01 (s, 3H), 0.95 (d,  $J = 7.0$  Hz, 3H), 0.94 (s, 3H), 0.76 (t,  $J = 7.5$  Hz, 3H).  $^{13}\text{C}\{^1\text{H}\}$  NMR (176 MHz,  $\text{CDCl}_3$ ):  $\delta$  160.6, 135.4, 116.6, 74.1, 50.3, 35.2, 34.8, 34.3, 33.5, 33.1, 28.0, 25.4, 24.5, 22.3, 8.2. IR (thin film, neat): 2954, 2918, 1457  $\text{cm}^{-1}$ . HRMS electrospray ( $m/z$ ):  $[\text{M}+\text{H}]^+$  calcd for  $\text{C}_{15}\text{H}_{28}\text{NO}$ , 238.2165; found, 238.2163.

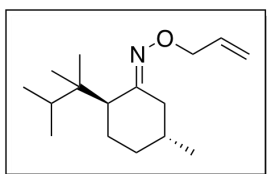


**Oxime Ether 40.** The general procedure was followed using 8-*iso*-butylmenthone **64** (175 mg, 0.83 mmol, 1.0 equiv), *O*-allyl hydroxylamine hydrochloride (109 mg, 1.00 mmol, 1.2 equiv), and pyridine (0.36 mL). Oxime ether **40** was obtained as a colorless oil (134 mg, 61% yield,  $R_f = 0.40$  in 99% hexanes/1%  $\text{Et}_2\text{O}$ ).  $^1\text{H}$  NMR (700 MHz,  $\text{CDCl}_3$ ):  $\delta$  6.00 (ddt,  $J = 17.3, 10.5, 5.6$  Hz, 1H), 5.25 (ddt,  $J = 17.3, 3.3, 1.7$  Hz, 1H), 5.16 (ddt,  $J = 10.5, 3.3, 1.2$  Hz, 1H), 4.51 (ddd,  $J = 5.6, 1.7, 1.2$  Hz, 2H), 3.17 (ddd,  $J = 12.8, 4.5, 1.2$  Hz, 1H), 1.95 (app. dq,  $J = 12.7, 3.7$  Hz, 1H), 1.92 (dd,  $J = 11.3, 4.0$  Hz,

1H), 1.80 (m, 1H), 1.66–1.58 (multiple peaks, 3H), 1.37 (dd,  $J = 12.8, 11.6$  Hz, 1H), 1.36 (m, 1H), 1.24 (dd,  $J = 13.8, 5.2$  Hz, 1H), 1.06 (m, 1H), 1.04 (s, 3H), 0.99 (s, 3H), 0.95 (d,  $J = 6.5$  Hz, 3H), 0.90 (d,  $J = 6.6$  Hz, 3H), 0.88 (d,  $J = 6.6$ , 1H).  $^{13}\text{C}\{1\text{H}\}$  NMR (176 MHz,  $\text{CDCl}_3$ ):  $\delta$  160.6, 135.4, 116.7, 74.1, 51.8, 49.1, 35.9, 34.9, 34.5, 33.6, 28.2, 26.6, 25.6, 25.5, 24.0, 22.3. Two  $^{13}\text{C}$  resonances are coincidentally overlapping. IR (thin film, neat): 2953, 2926, 1457  $\text{cm}^{-1}$ . HRMS electrospray ( $m/z$ ):  $[\text{M}+\text{H}]^+$  calcd for  $\text{C}_{17}\text{H}_{32}\text{NO}$ , 266.2478; found, 266.2471.



**Oxime Ether 41.** The general procedure was followed using 8-phenylmenthone **65** (515 mg, 2.2 mmol, 1.0 equiv), *O*-allyl hydroxylamine hydrochloride (368 mg, 3.36 mmol, 1.5 equiv), and pyridine (1 mL). Oxime ether **41** was obtained as a colorless oil (359 mg, 56% yield,  $R_f = 0.62$  in 95% hexanes/5%  $\text{Et}_2\text{O}$ ).  $^1\text{H}$  NMR (700 MHz,  $\text{CDCl}_3$ ):  $\delta$  7.36 (dd,  $J = 8.5, 1.1$  Hz, 2H), 7.27 (dd,  $J = 8.5, 7.3$  Hz, 2H), 7.25 (tt,  $J = 7.3, 1.1$  Hz, 1H), 5.90 (ddt,  $J = 17.3, 10.5, 5.7$  Hz, 1H), 5.22 (ddt,  $J = 17.3, 3.0, 1.3$  Hz, 1H), 5.14 (ddt,  $J = 10.5, 3.0, 1.3$  Hz, 1H), 4.43 (ddd,  $J = 5.7, 1.3, 1.3$  Hz, 2H), 3.11 (ddd,  $J = 13.3, 4.5, 1.8$  Hz, 1H), 2.44 (dd,  $J = 11.8, 4.2$  Hz, 1H), 1.70 (m, 1H), 1.65 (app. dq,  $J = 13.0, 3.8$  Hz, 1H), 1.58 (m, 1H), 1.51 (s, 3H), 1.43 (s, 3H), 1.37 (dd,  $J = 13.3, 11.4$  Hz, 1H), 1.34 (m, 1H), 0.99 (m, 1H), 0.92 (d,  $J = 6.5$  Hz, 3H).  $^{13}\text{C}\{1\text{H}\}$  NMR (176 MHz,  $\text{CDCl}_3$ ):  $\delta$  159.5, 150.6, 135.3, 127.7, 126.0, 125.1, 116.7, 74.1, 53.0, 40.1, 34.6, 34.2, 33.3, 28.7, 26.5, 25.2, 22.2. IR (thin film, neat): 2950, 2924, 1457  $\text{cm}^{-1}$ . HRMS electrospray ( $m/z$ ):  $[\text{M}+\text{H}]^+$  calcd for  $\text{C}_{19}\text{H}_{28}\text{NO}$ , 286.2165; found, 286.2172.

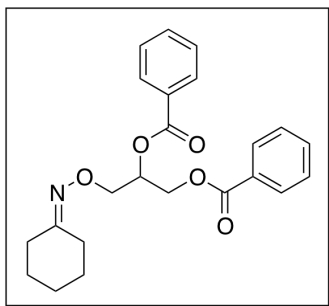


**Oxime ether 42.** The general procedure was followed using 8-*iso*-propylmenthone **66** (500 mg, 2.55 mmol, 1.0 equiv), *O*-allyl hydroxylamine hydrochloride (419 mg, 3.82 mmol, 1.5 equiv), and pyridine (1.1 mL). Oxime ether **42** was obtained as a colorless oil (283 mg, 44% yield,  $R_f = 0.38$  in 99% hexanes/1%  $\text{Et}_2\text{O}$ ).  $^1\text{H}$  NMR (700 MHz,  $\text{CDCl}_3$ ):  $\delta$  5.99 (ddt,  $J = 17.3, 10.5, 5.6$  Hz, 1H), 5.24 (ddt,  $J = 17.3, 3.4, 1.7$  Hz, 1H), 5.16 (ddt,  $J = 10.5, 3.4, 1.2$  Hz, 1H), 4.51 (ddd,  $J = 5.6, 1.7, 1.2$  Hz, 2H), 3.18 (ddd,  $J = 12.8, 4.7, 1.7$  Hz, 1H), 2.23 (app septet,  $J = 6.9$  Hz, 1H), 2.04 (dd,  $J = 11.8, 4.0$  Hz,

1H), 1.94 (app dq,  $J = 13.0, 3.7$  Hz, 1H), 1.81 (m, 1H), 1.66 (m, 1H), 1.40 (dd,  $J = 12.2, 11.3$  Hz, 1H), 1.36 (dddd,  $J = 12.6, 12.6, 12.6, 4.1$  Hz, 1H), 1.06 (dddd,  $J = 12.6, 12.6, 12.6, 3.6$  Hz, 1H), 0.97 (s, 3H), 0.96 (d,  $J = 6.5$  Hz, 3H), 0.81 (s, 3H), 0.80 (d,  $J = 6.8$  Hz, 3H), 0.74 (d,  $J = 6.8$  Hz, 3H).  $^{13}\text{C}\{^1\text{H}\}$  NMR (176 MHz,  $\text{CDCl}_3$ ):  $\delta$  160.9, 135.4, 116.6, 74.1, 50.1, 37.5, 35.0, 34.6, 33.9, 32.4, 28.5, 22.3, 20.4, 20.1, 17.34, 17.30. IR (thin film, neat): 2960, 1925, 1457  $\text{cm}^{-1}$ . HRMS electrospray ( $m/z$ ):  $[\text{M}+\text{H}]^+$  calcd for  $\text{C}_{16}\text{H}_{30}\text{NO}$ , 252.2322; found, 252.2313.

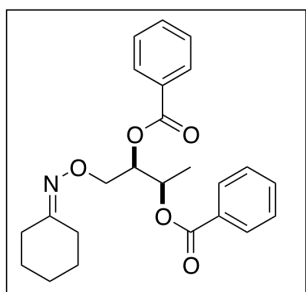
*Synthesis and Characterization of Dioxygenated Products in Schemes 4.12 and 4.25 and Tables 4.3 and 4.4*

**General Procedure.** Substrate (1 equiv),  $\text{PdCl}_2(\text{PhCN})_2$  (0.05 equiv), and  $\text{PhI}(\text{OBz})_2$  (2 or 3 equiv) were combined in dry toluene in a 4 mL or 20 mL scintillation vial and sealed with a Teflon-lined cap. Reactions were stirred at 50 °C for 8 h, then diluted with EtOAc and washed with 10% aqueous  $\text{Na}_2\text{SO}_3$  and brine. The combined aqueous layers were extracted with EtOAc, and the organic layers were then combined, dried over  $\text{MgSO}_4$ , filtered, concentrated, and purified by column chromatography on silica gel to afford the products as a mixture of diastereomers (indistinguishable by TLC; all product-containing column fractions were combined for final yields and dr determination). The ratio of diastereomers was determined by  $^{13}\text{C}$  NMR integrations and, when possible, confirmed by  $^1\text{H}$  NMR. In all cases, complete  $^1\text{H}$  and  $^{13}\text{C}$  NMR data are reported for the major product isomer. In addition, the distinct resonances associated with the minor isomer are reported for both the  $^1\text{H}$  and  $^{13}\text{C}$  NMR spectra (many of the peaks for the minor isomer are overlapping with those of the major isomer).

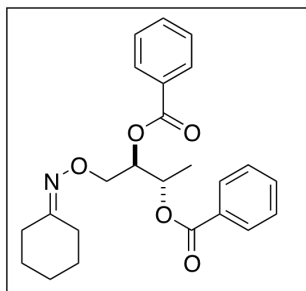


**Oxime Ether 17.** The general procedure was followed using substrate **16** (76.6 mg, 0.50 mmol, 1 equiv),  $\text{PdCl}_2(\text{PhCN})_2$  (9.6 mg, 0.025 mmol, 0.05 equiv),  $\text{PhI}(\text{OBz})_2$  (446 mg, 1.00 mmol, 2 equiv), and dry toluene (4.2 mL). Compound **17** was isolated in 59% yield as a colorless oil ( $R_f = 0.14$  in 79% hexanes/20%  $\text{Et}_2\text{O}$ /1%  $\text{Et}_3\text{N}$ ).  $^1\text{H}$  NMR (700 MHz,  $\text{CDCl}_3$ ):  $\delta$  8.06 (d,  $J = 7.9$  Hz, 2H), 8.03 (d,  $J = 7.9$  Hz, 2H), 7.56 (t,  $J = 7.3$  Hz, 1H), 7.55

(t,  $J = 7.3$  Hz, 1H), 7.44 (dd,  $J = 7.9, 7.3$  Hz, 2H), 7.42 (dd,  $J = 7.9, 7.3$  Hz, 2H), 5.73 (dtd,  $J = 6.2, 5.6, 3.6$  Hz, 1H), 4.67 (dd,  $J = 12.0, 3.6$  Hz, 1H), 4.58 (dd,  $J = 12.0, 6.2$  Hz, 1H), 4.38 (d,  $J = 5.6$  Hz, 2H), 2.42 (m, 2H), 2.15 (m, 2H), 1.63 (m, 2H) 1.57–1.55 (multiple peaks, 4H).  $^{13}\text{C}\{^1\text{H}\}$  NMR (176 MHz,  $\text{CDCl}_3$ ):  $\delta$  166.2, 165.8, 161.5, 133.09, 133.06, 130.0, 129.9, 129.8, 129.7, 128.4, 128.3, 71.3, 70.7, 63.6, 32.0, 26.9, 25.7, 25.6, 25.3. IR (thin film, neat): 2934, 1722, 1451  $\text{cm}^{-1}$ . HRMS electrospray ( $m/z$ ):  $[\text{M}+\text{H}]^+$  calcd for  $\text{C}_{23}\text{H}_{26}\text{NO}_5$ , 396.1805; found, 396.1808.



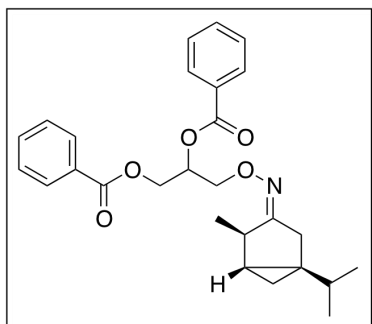
**Oxime Ether 20.** The general procedure was followed using substrate **22** (83.6 mg, 0.50 mmol, 1 equiv),  $\text{PdCl}_2(\text{PhCN})_2$  (9.6 mg, 0.025 mmol, 0.05 equiv),  $\text{PhI}(\text{OBz})_2$  (446 mg, 1.00 mmol, 2 equiv), and dry toluene (4.2 mL). Compound **20** was isolated in 53% yield as a colorless oil ( $R_f = 0.15$  in 84% hexanes/15%  $\text{Et}_2\text{O}$ /1%  $\text{Et}_3\text{N}$ ) with diastereomeric ratio threo:erythro  $\sim 10 : 1$  as measured by  $^{13}\text{C}$  NMR. Major (Threo) Isomer:  $^1\text{H}$  NMR (700 MHz,  $\text{CDCl}_3$ ):  $\delta$  8.08 (d,  $J = 7.9$  Hz, 2H), 8.05 (d,  $J = 7.9$  Hz, 2H), 7.55 (t,  $J = 7.2$  Hz, 1H), 7.54 (t,  $J = 7.2$  Hz, 1H), 7.43 (dd,  $J = 7.9, 7.2$  Hz, 2H), 7.42 (dd,  $J = 7.9, 7.2$  Hz, 2H), 5.61 (ddd,  $J = 6.7, 4.8, 4.6$  Hz, 1H), 5.51 (qd,  $J = 6.6, 4.8$  Hz, 1H), 4.35 (dd,  $J = 12.0, 4.6$  Hz, 1H), 4.32 (dd,  $J = 12.0, 6.7$  Hz, 1H), 2.37 (m, 2H), 2.12 (m, 2H), 1.63–1.52 (multiple peaks, 6H), 1.44 (d,  $J = 6.6$  Hz, 3H).  $^{13}\text{C}\{^1\text{H}\}$  NMR (176 MHz,  $\text{CDCl}_3$ ):  $\delta$  165.8, 165.7, 161.4, 132.98, 132.95, 130.1, 130.0, 129.7, 129.6, 128.31, 128.30, 73.9, 71.5, 69.7, 32.0, 26.8, 25.7, 25.5, 25.3, 16.5. IR (thin film, neat, mixture of isomers): 2936, 1716, 1451  $\text{cm}^{-1}$ . HRMS electrospray ( $m/z$ ):  $[\text{M}+\text{H}]^+$  calcd for  $\text{C}_{24}\text{H}_{28}\text{NO}_5$ , 410.1962; found, 410.1949.



**Oxime Ether 21.** The general procedure was followed using substrate **19** (83.6 mg, 0.50 mmol, 1 equiv),  $\text{PdCl}_2(\text{PhCN})_2$  (9.6 mg, 0.025 mmol, 0.05 equiv),  $\text{PhI}(\text{OBz})_2$  (446 mg, 1.00 mmol, 2 equiv), and dry toluene (4.2 mL). Compound **21** was isolated in 65% yield as a colorless oil ( $R_f = 0.15$  in 84% hexanes/15%  $\text{Et}_2\text{O}$ /1%  $\text{Et}_3\text{N}$ ) with diastereomeric ratio



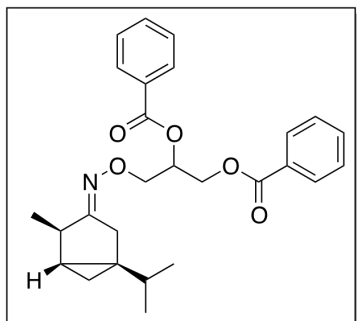
threo:erythro ~ 1 : 13 as measured by  $^{13}\text{C}$  NMR. Major (Erythro) Isomer:  $^1\text{H}$  NMR (700 MHz,  $\text{CDCl}_3$ ):  $\delta$  8.06 (d,  $J = 7.9$  Hz, 2H), 8.02 (d,  $J = 7.9$  Hz, 2H), 7.56 (t,  $J = 7.8$  Hz, 1H), 7.55 (t,  $J = 7.8$  Hz, 1H), 7.43 (dd,  $J = 7.9, 7.8$  Hz, 2H), 7.42 (dd,  $J = 7.9, 7.8$  Hz, 2H), 5.64 (ddd,  $J = 7.0, 4.1, 4.1$  Hz, 1H), 5.50 (qd,  $J = 6.6, 4.4$  Hz, 1H), 4.42 (dd,  $J = 11.9, 4.1$  Hz, 1H), 4.37 (dd,  $J = 11.9, 7.0$  Hz, 1H), 2.37 (m, 2H), 2.12 (m, 2H), 1.63–1.51 (multiple peaks, 6H), 1.49 (d,  $J = 6.6$  Hz, 3H).  $^{13}\text{C}\{^1\text{H}\}$  NMR (176 MHz,  $\text{CDCl}_3$ ):  $\delta$  165.62, 165.55, 163.4, 133.0, 132.9, 130.13, 130.11, 129.7, 129.6, 128.3, 73.8, 71.2, 70.0, 32.0, 26.8, 25.7, 25.5, 25.3, 15.8. Two  $^{13}\text{C}$  resonances are coincidentally overlapping. IR (thin film, neat, mixture of isomers): 2937, 1716, 1450  $\text{cm}^{-1}$ . HRMS electrospray ( $m/z$ ):  $[\text{M}+\text{H}]^+$  calcd for  $\text{C}_{24}\text{H}_{28}\text{NO}_5$ , 410.1962; found, 410.1953.



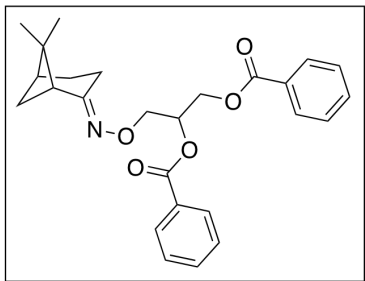
**Oxime Ether 31.** The general procedure was followed using substrate **24** (19.7 mg, 0.095 mmol, 1 equiv),  $\text{PdCl}_2(\text{PhCN})_2$  (1.8 mg, 0.0047 mmol, 0.05 equiv),  $\text{PhI}(\text{OBz})_2$  (84.8 mg, 0.19 mmol, 2 equiv), and dry toluene (0.79 mL). Compound **31** was isolated in 63% yield as a colorless oil ( $R_f = 0.09$  in 91% hexanes/8%  $\text{Et}_2\text{O}$ /1%  $\text{Et}_3\text{N}$ ) with diastereomeric ratio 52:48 as

measured by  $^1\text{H}$  NMR. Major Isomer:  $^1\text{H}$  NMR (700 MHz,  $\text{C}_6\text{D}_6$ ):  $\delta$  8.16 (d,  $J = 7.9$  Hz, 2H), 8.10 (d,  $J = 7.9$  Hz, 2H), 7.07 (t,  $J = 7.7$  Hz, 1H), 7.05 (t,  $J = 7.7$  Hz, 1H), 7.007 (dd,  $J = 7.9, 7.7$  Hz, 2H), 6.97 (dd,  $J = 7.9, 7.7$  Hz, 2H), 5.940 (m, 1H), 4.60 (dd,  $J = 12.0, 4.0$  Hz, 1H), 4.48 (dd,  $J = 11.8, 6.5$  Hz, 1H), 4.35–4.32 (multiple peaks, 2H), 3.18 (q,  $J = 7.0$  Hz, 1H), 2.44 (dd,  $J = 16.6, 1.2$  Hz, 1H), 2.23 (d,  $J = 16.6$  Hz, 1H), 1.054 (d,  $J = 7.0$  Hz, 3H), 1.04 (m, 1H), 0.764 (d,  $J = 6.9$  Hz, 3H), 0.754 (d,  $J = 6.9$  Hz, 3H), 0.604 (m, 1H), 0.27 (dd,  $J = 8.3, 4.3, 1.2$  Hz, 1H),  $-0.02$  (dd,  $J = 4.3, 4.3$  Hz, 1H).  $^{13}\text{C}\{^1\text{H}\}$  NMR (176 MHz,  $\text{C}_6\text{D}_6$ ):  $\delta$  167.7, 166.0, 165.81, 132.98, 132.95, 130.8, 130.5, 130.2, 130.0, 128.6, 128.5, 72.12, 71.4, 63.8, 37.8, 32.37, 31.99, 30.43, 27.28, 19.81, 19.80, 17.5, 16.1. Minor Isomer (distinct resonances):  $^1\text{H}$  NMR (700 MHz,  $\text{C}_6\text{D}_6$ ):  $\delta$  8.17 (d,  $J = 7.9$  Hz, 2H), 7.012 (dd,  $J = 7.9, 7.7$  Hz, 2H), 4.57 (dd,  $J = 12.0, 3.7$  Hz, 1H), 4.47 (dd,  $J = 12.0, 6.4$  Hz, 1H), 3.15 (q,  $J = 7.0$  Hz, 1H), 2.43 (dd,  $J = 16.6, 1.2$  Hz, 1H), 2.29 (d,  $J = 16.6$  Hz, 1H), 1.048 (d,  $J = 7.0$  Hz, 3H), 1.03 (m, 1H), 0.750 (d,  $J = 6.9$  Hz, 3H), 0.732 (d,  $J = 6.9$  Hz, 3H),

0.604 (m, 1H), 0.30 (ddd,  $J = 8.3, 4.3, 1.2$  Hz, 1H), 0.15 (dd,  $J = 4.3, 4.3$  Hz, 1H).  $^{13}\text{C}\{^1\text{H}\}$  NMR (176 MHz,  $\text{C}_6\text{D}_6$ ):  $\delta$  167.8, 165.75, 72.11, 71.2, 37.7, 32.39, 32.01, 30.38, 27.26, 20.1, 20.0, 17.6, 16.0. IR (thin film, neat, mixture of isomers): 2959, 1718, 1452  $\text{cm}^{-1}$ . HRMS electrospray ( $m/z$ ):  $[\text{M}+\text{H}]^+$  calcd for  $\text{C}_{27}\text{H}_{32}\text{NO}_5$ , 450.2275; found, 450.2280.

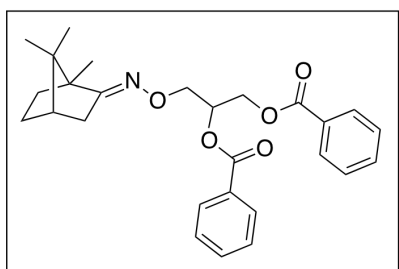


**Oxime Ether 32.** The general procedure was followed using substrate **25** (20.7 mg, 0.10 mmol, 1 equiv),  $\text{PdCl}_2(\text{PhCN})_2$  (1.9 mg, 0.0050 mmol, 0.05 equiv),  $\text{PhI}(\text{OBz})_2$  (89.2 mg, 0.200 mmol, 2 equiv), and dry toluene (0.83 mL). Compound **32** was isolated in 64% yield as a colorless oil ( $R_f = 0.09$  in 91% hexanes/8%  $\text{Et}_2\text{O}$ /1%  $\text{Et}_3\text{N}$ ) with diastereomeric ratio 63:37 as measured by  $^{13}\text{C}$  NMR. Major Isomer:  $^1\text{H}$  NMR (700 MHz,  $\text{CDCl}_3$ ):  $\delta$  8.06 (d,  $J = 7.9$  Hz, 2H), 8.02 (d,  $J = 7.9$  Hz, 2H), 7.56 (t,  $J = 7.2$  Hz, 1H), 7.55 (t,  $J = 7.2$  Hz, 1H), 7.43 (dd,  $J = 7.9, 7.2$  Hz, 2H), 7.42 (dd,  $J = 7.9, 7.2$  Hz, 2H), 5.70 (m, 1H), 4.66 (m, 1H), 4.55 (dd,  $J = 12.1, 6.1$  Hz, 1H), 4.38–4.33 (multiple peaks, 2H), 2.63 (m, 1H), 2.54 (d,  $J = 17.8$  Hz, 1H), 2.30 (br d,  $J = 17.8$  Hz, 1H), 1.30 (sept,  $J = 7.0$  Hz, 1H), 1.11 (d,  $J = 7.2$  Hz, 3H), 0.926 (d,  $J = 7.0$  Hz, 3H), 0.88 (m, 1H), 0.85 (d,  $J = 7.0$  Hz, 3H), 0.50 (m, 1H), 0.06 (app t,  $J = 4.6$  Hz, 1H).  $^{13}\text{C}\{^1\text{H}\}$  NMR (176 MHz,  $\text{CDCl}_3$ ):  $\delta$  169.5, 166.2, 165.7, 133.09, 133.06, 129.94, 129.76, 129.71, 129.67, 128.4, 128.3, 71.7, 70.6, 63.5, 40.70, 32.19, 31.3, 28.8, 26.6, 21.38, 19.9, 19.6, 16.6. Minor Isomer (distinct resonances):  $^1\text{H}$  NMR (700 MHz,  $\text{CDCl}_3$ ):  $\delta$  2.59 (d,  $J = 17.8$  Hz, 1H), 2.32 (br d,  $J = 17.8$  Hz, 1H), 1.14 (d,  $J = 7.2$  Hz, 3H), 0.931 (d,  $J = 7.0$  Hz, 3H), 0.89 (d,  $J = 7.0$  Hz, 3H),  $-0.04$ , (app t,  $J = 4.6$  Hz, 1H).  $^{13}\text{C}\{^1\text{H}\}$  NMR (176 MHz,  $\text{CDCl}_3$ ):  $\delta$  169.3, 165.8, 133.08, 133.07, 129.93, 129.77, 129.72, 71.6, 70.7, 40.73, 32.17, 31.4, 29.0, 26.8, 21.41, 20.0, 16.8. IR (thin film, neat, mixture of isomers): 2958, 1718, 1456  $\text{cm}^{-1}$ . HRMS electrospray ( $m/z$ ):  $[\text{M}+\text{H}]^+$  calcd for  $\text{C}_{27}\text{H}_{32}\text{NO}_5$  450.2275; found, 450.2280.



**Oxime Ether 33.** The general procedure was followed using substrate **27** (96.6 mg, 0.50 mmol, 1 equiv), PdCl<sub>2</sub>(PhCN)<sub>2</sub> (9.6 mg, 0.035 mmol, 0.05 equiv), PhI(OBz)<sub>2</sub> (446 mg, 1.00 mmol, 2 equiv), and dry toluene (4.2 mL). Compound **33** was isolated in 68% yield as a colorless oil ( $R_f = 0.18$  in 84% hexanes/15% Et<sub>2</sub>O/1%

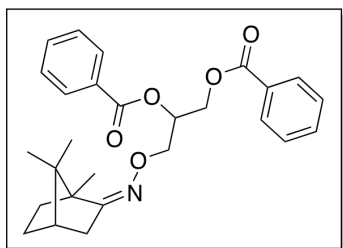
Et<sub>3</sub>N) with diastereomeric ratio 59:41 as measured by <sup>13</sup>C NMR. Major Isomer: <sup>1</sup>H NMR (700 MHz, CDCl<sub>3</sub>): δ 8.06 (d,  $J = 7.9$  Hz, 2H), 8.02 (d,  $J = 7.9$  Hz, 2H), 7.55 (t,  $J = 7.2$  Hz, 1H), 7.54 (t,  $J = 7.2$  Hz, 1H), 7.43 (dd,  $J = 7.9, 7.2$  Hz, 2H), 7.41 (dd,  $J = 7.9, 7.2$  Hz, 2H), 5.73 (m, 1H), 4.68 (m, 1H), 4.58 (m, 1H), 4.38 (app d,  $J = 6.1$  Hz, 2H), 2.70 (m, 1H), 2.54 (m, 1H), 2.46–2.36 (multiple peaks, 2H), 2.04 (m, 1H), 1.88 (m, 1H), 1.83 (m, 1H), 1.29 (d,  $J = 10.5$  Hz, 1H), 1.253 (s, 3H), 0.78 (s, 3H). <sup>13</sup>C{<sup>1</sup>H} NMR (176 MHz, CDCl<sub>3</sub>): δ 166.2, 165.77, 165.75, 133.1, 133.01, 130.0, 129.74, 129.716, 129.66, 128.34, 128.29, 71.5, 70.7, 63.6, 47.9, 40.5, 40.40, 27.09, 25.52, 22.06, 21.99, 18.51. Minor Isomer (distinct resonances): <sup>1</sup>H NMR (700 MHz, CDCl<sub>3</sub>): δ 1.35 (d,  $J = 10.5$  Hz, 1H), 1.248 (s, 3H), 0.76 (s, 3H). <sup>13</sup>C{<sup>1</sup>H} NMR (176 MHz, CDCl<sub>3</sub>): δ 165.74, 133.03, 129.75, 129.722, 128.30, 71.4, 70.8, 63.5, 40.37, 27.14, 25.49, 22.05, 22.01, 18.53. IR (thin film, neat, mixture of isomers): 2948, 1718, 1452 cm<sup>-1</sup>. HRMS electrospray ( $m/z$ ): [M+H]<sup>+</sup> calcd for C<sub>26</sub>H<sub>30</sub>NO<sub>5</sub>, 436.2118; found, 436.2126.



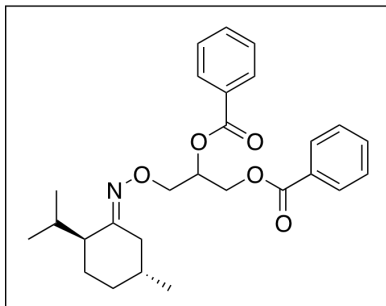
**Oxime ether 34.** The general procedure was followed using substrate **27** (104 mg, 0.50 mmol, 1 equiv), PdCl<sub>2</sub>(PhCN)<sub>2</sub> (9.6 mg, 0.025 mmol, 0.05 equiv), PhI(OBz)<sub>2</sub> (446 mg, 1.00 mmol, 2 equiv), and dry toluene (4.2 mL). Compound **34** was isolated in 25% yield as a colorless oil ( $R_f = 0.12$  in 84% hexanes/15%

Et<sub>2</sub>O/1% Et<sub>3</sub>N) with diastereomeric ratio 75:25 as measured by <sup>13</sup>C NMR. Major Isomer: <sup>1</sup>H NMR (700 MHz, CDCl<sub>3</sub>): δ 8.07 (d,  $J = 7.8$  Hz, 2H), 8.03 (d,  $J = 7.8$  Hz, 2H), 7.55 (t,  $J = 7.8$  Hz, 1H), 7.54 (t,  $J = 7.8$  Hz, 1H), 7.43 (t,  $J = 7.8$  Hz, 2H), 7.42 (t,  $J = 7.8$  Hz, 2H), 5.73 (m, 1H), 4.66 (dd,  $J = 12.0, 3.5$  Hz, 1H), 4.57 (dd,  $J = 12.0, 6.3$  Hz, 1H), 4.42–4.36 (multiple peaks, 2H), 2.45 (m, 1H), 1.92 (d,  $J = 18.0$  Hz, 1H), 1.83 (m, 1H), 1.79 (m,

1H), 1.67 (m, 1H), 1.45 (m, 1H), 1.17 (m, 1H), 0.95 (s, 3H), 0.88 (s, 3H), 0.74 (s, 3H).  $^{13}\text{C}\{^1\text{H}\}$  NMR (176 MHz,  $\text{CDCl}_3$ ):  $\delta$  170.5, 166.2, 165.7, 133.05, 133.02, 130.01, 129.76, 129.75, 129.66, 128.35, 128.30, 71.3, 70.90, 63.59, 51.83, 48.15, 43.6, 33.75, 32.72, 27.2, 19.38, 18.4, 11.0. Minor Isomer (distinct resonances):  $^1\text{H}$  NMR (700 MHz,  $\text{CDCl}_3$ ):  $\delta$  2.43 (m, 1H), 1.96 (d,  $J = 18.0$  Hz, 1H), 1.38 (m, 1H), 0.76 (s, 3H).  $^{13}\text{C}\{^1\text{H}\}$  NMR (176 MHz,  $\text{CDCl}_3$ ):  $\delta$  170.4, 165.8, 133.01, 130.02, 129.77, 128.29, 71.4, 70.92, 63.61, 51.81, 48.11, 33.70, 32.69, 19.35, 18.5. IR (thin film, neat, mixture of isomers): 2956, 1718, 1452  $\text{cm}^{-1}$ . HRMS electrospray (m/z):  $[\text{M}+\text{H}]^+$  calcd for  $\text{C}_{27}\text{H}_{32}\text{NO}_5$ , 450.2275; found, 450.2281.

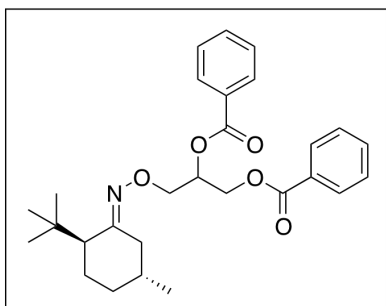


**Oxime Ether 35.** The general procedure was followed using substrate **28** (104 mg, 0.50 mmol, 1 equiv),  $\text{PdCl}_2(\text{PhCN})_2$  (9.6 mg, 0.025 mmol, 0.05 equiv),  $\text{PhI}(\text{OBz})_2$  (446 mg, 1.00 mmol, 2 equiv), and dry toluene (4.2 mL). Compound **35** was isolated in 68% yield as a colorless oil ( $R_f = 0.24$  in 84% hexanes/15%  $\text{Et}_2\text{O}$ /1%  $\text{Et}_3\text{N}$ ) with diastereomeric ratio 66:34 as measured by  $^{13}\text{C}$  NMR. Major Isomer:  $^1\text{H}$  NMR (700 MHz,  $\text{CDCl}_3$ ):  $\delta$  8.06 (d,  $J = 8.1$  Hz, 2H), 8.02 (d,  $J = 8.1$  Hz, 2H), 7.55 (t,  $J = 8.1$  Hz, 1H), 7.54 (t,  $J = 8.1$  Hz, 1H), 7.43 (t,  $J = 8.1$  Hz, 2H), 7.41 (t,  $J = 8.1$  Hz, 2H), 5.72 (m, 1H), 4.67 (dd,  $J = 12.3, 3.9$  Hz, 1H), 4.58 (dd,  $J = 12.3, 6.4$  Hz, 1H), 4.32–4.30 (multiple peaks, 2H), 2.45 (m, 1H), 1.85 (d,  $J = 16.3$  Hz, 1H), 1.81–1.78 (multiple peaks, 2H), 1.61–1.54 (multiple peaks, 2H), 1.24 (s, 3H), 1.20 (m, 1H), 0.86 (s, 3H), 0.80 (s, 3H).  $^{13}\text{C}\{^1\text{H}\}$  NMR (176 MHz,  $\text{CDCl}_3$ ):  $\delta$  166.8, 166.1, 165.7, 133.04, 133.00, 130.0, 129.8, 129.73, 129.66, 128.34, 128.29, 71.8, 70.7, 63.6, 55.16, 48.8, 43.8, 36.5, 32.7, 27.3, 20.2, 18.2, 14.0. Minor Isomer (distinct resonances):  $^1\text{H}$  NMR (700 MHz,  $\text{CDCl}_3$ ):  $\delta$  1.86 (d,  $J = 16.3$  Hz, 1H), 1.26 (s, 3H), 0.85 (s, 3H), 0.81 (s, 3H).  $^{13}\text{C}\{^1\text{H}\}$  NMR (176 MHz,  $\text{CDCl}_3$ ):  $\delta$  165.8, 70.8, 55.18, 43.9, 32.6, 14.1. IR (thin film, neat, mixture of isomers): 2956, 1718, 1452  $\text{cm}^{-1}$ . HRMS electrospray (m/z):  $[\text{M}+\text{H}]^+$  calcd for  $\text{C}_{27}\text{H}_{32}\text{NO}_5$ , 450.2275; found, 450.2287.



**Oxime Ether 37.** The general procedure was followed using substrate **30** (104.7 mg, 0.50 mmol, 1 equiv), PdCl<sub>2</sub>(PhCN)<sub>2</sub> (9.6 mg, 0.025 mmol, 0.05 equiv), PhI(OBz)<sub>2</sub> (446 mg, 1.00 mmol, 2 equiv), and dry toluene (4.2 mL). Compound **37** was isolated in 75% yield as a colorless oil ( $R_f = 0.18$  in 91% hexanes/8%

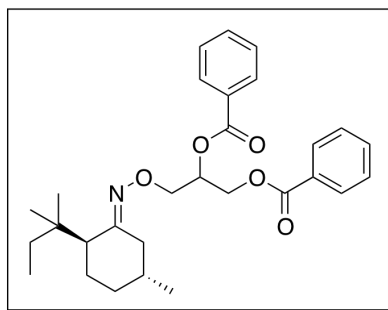
Et<sub>2</sub>O/1% Et<sub>3</sub>N) with diastereomeric ratio 74:26 as measured by <sup>13</sup>C NMR. Major Isomer: <sup>1</sup>H NMR (700 MHz, CDCl<sub>3</sub>): δ 8.06 (d,  $J = 7.8$  Hz, 2H), 8.03 (d,  $J = 7.8$  Hz, 2H), 7.56–7.53 (multiple peaks, 2H), 7.44–7.40 (multiple peaks, 4H), 5.72 (m, 1H), 4.69 (dd,  $J = 11.9, 3.7$  Hz, 1H) 4.59 (dd,  $J = 11.9, 6.2$  Hz, 1H), 4.40 (app d,  $J = 5.9$  Hz, 2H), 2.83 (dd,  $J = 12.8, 3.5$  Hz, 1H), 2.09 (m, 1H), 1.85–1.82 (multiple peaks, 2H), 1.78 (m, 1H), 1.74–1.67 (multiple peaks, 2H), 1.36 (m, 1H), 1.11 (m, 1H), 0.91 (d,  $J = 6.3$  Hz, 3H), 0.89 (d,  $J = 7.0$  Hz, 6H). <sup>13</sup>C{<sup>1</sup>H} NMR (176 MHz, CDCl<sub>3</sub>): δ 166.2, 165.78, 162.1, 133.02, 132.99, 130.1, 129.8, 129.74, 129.66, 128.34, 128.28, 71.2, 71.0, 63.6, 48.59, 32.30, 32.20, 32.18, 26.7, 26.37, 21.5, 21.1, 19.3. Minor Isomer (distinct resonances): <sup>13</sup>C{<sup>1</sup>H} NMR (176 MHz, CDCl<sub>3</sub>): δ 165.76, 161.2, 71.3, 70.9, 48.61, 32.34, 32.24, 32.16, 26.35, 19.2. IR (thin film, neat, mixture of isomers): 2956, 1718, 1452 cm<sup>-1</sup>. HRMS electrospray ( $m/z$ ): [M+H]<sup>+</sup> calcd for C<sub>27</sub>H<sub>34</sub>NO<sub>5</sub>, 452.2431; found, 452.2434.



**Oxime Ether 43.** The general procedure was followed using substrate **38** (50 mg, 0.0112 mmol, 1 equiv), PdCl<sub>2</sub>(PhCN)<sub>2</sub> (4.3 mg, 0.0112 mmol, 0.05 equiv), PhI(OBz)<sub>2</sub> (300 mg, 0.672 mmol, 3 equiv), and dry toluene (1.9 mL). Compound **43** was isolated in 69% yield as a colorless oil ( $R_f = 0.22$  in 91% hexanes/8%

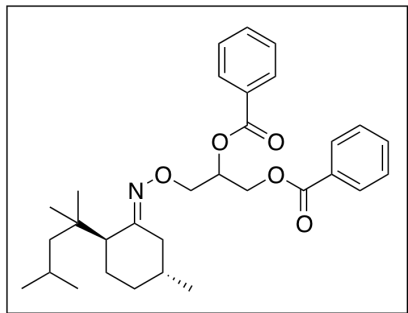
Et<sub>2</sub>O/1% Et<sub>3</sub>N) with diastereomeric ratio 86:14 as measured by <sup>13</sup>C NMR. Major Isomer: <sup>1</sup>H NMR (700 MHz, CDCl<sub>3</sub>): δ 8.06 (dd,  $J = 8.4, 1.3$  Hz, 2H), 8.03 (dd,  $J = 8.4, 1.3$  Hz, 2H), 7.56–7.53 (multiple peaks, 2H), 7.44–7.41 (multiple peaks, 4H), 5.72 (m, 1H), 4.68 (dd,  $J = 12.0, 3.6$  Hz, 1H), 4.58 (dd,  $J = 12.0, 6.1$  Hz, 1H), 4.42–4.37 (multiple peaks, 2H), 3.10 (ddd,  $J = 12.8, 4.5, 1.8$  Hz, 1H), 1.98 (m, 1H), 1.84 (dd,  $J = 11.5, 4.2$  Hz, 1H), 1.78 (m, 1H), 1.61 (m, 1H), 1.38 (dd,  $J = 12.9, 11.3$  Hz, 1H), 1.34 (m, 1H), 1.06 (m, 1H),

1.026 (s, 9H), 0.91 (d,  $J = 6.5$  Hz, 3H).  $^{13}\text{C}\{^1\text{H}\}$  NMR (176 MHz,  $\text{CDCl}_3$ ):  $\delta$  166.2, 165.75, 162.1, 133.02, 132.99, 130.0, 129.8, 129.74, 129.65, 128.33, 128.27, 71.27, 70.96, 63.6, 53.3, 34.56, 34.38, 33.6, 32.7, 28.5, 28.3, 22.11. Minor Isomer (distinct resonances):  $^1\text{H}$  NMR (700 MHz,  $\text{CDCl}_3$ ):  $\delta$  1.031 (s, 3H), 0.87 (d,  $J = 6.6$  Hz, 3H).  $^{13}\text{C}\{^1\text{H}\}$  NMR (176 MHz,  $\text{CDCl}_3$ ):  $\delta$  165.74, 129.73, 71.23, 70.86, 53.4, 34.58, 34.36, 33.5, 22.06. IR (thin film,  $\text{CH}_2\text{Cl}_2$ , mixture of isomers): 2951, 1719, 1452  $\text{cm}^{-1}$ . HRMS electrospray (m/z):  $[\text{M}+\text{H}]^+$  calcd for  $\text{C}_{28}\text{H}_{36}\text{NO}_5$ , 466.2588; found, 466.2591.



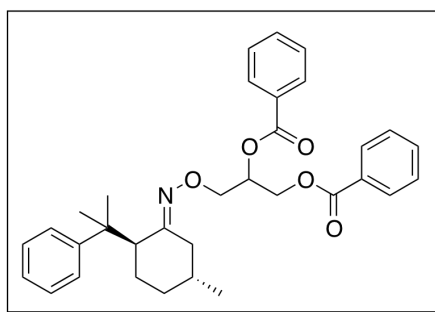
**Oxime Ether 44.** The general procedure was followed using substrate **39** (50 mg, 0.211 mmol, 1 equiv),  $\text{PdCl}_2(\text{PhCN})_2$  (4.0 mg, 0.0105 mmol, 0.05 equiv),  $\text{PhI}(\text{OBz})_2$  (282 mg, 0.633 mmol, 3 equiv), and dry toluene (1.8 mL). Compound **44** was isolated in 70% yield as a colorless oil ( $R_f = 0.23$  in 91% hexanes/8%

$\text{Et}_2\text{O}/1\% \text{Et}_3\text{N}$ ) with diastereomeric ratio 86:14 as measured by  $^{13}\text{C}$  NMR. Major Isomer:  $^1\text{H}$  NMR (700 MHz,  $\text{C}_6\text{D}_6$ ):  $\delta$  8.16 (d,  $J = 7.8$  Hz, 2H), 8.11 (d,  $J = 7.8$  Hz, 2H), 7.06 (t,  $J = 7.6$  Hz, 1H), 7.04 (t,  $J = 7.6$  Hz, 1H), 6.99 (dd,  $J = 7.8, 7.6$  Hz, 2H), 6.96 (dd,  $J = 7.8, 7.6$  Hz, 2H), 5.94 (m, 1H), 4.61 (dd,  $J = 12.0, 3.8$  Hz, 1H), 4.51 (dd,  $J = 12.0, 6.5$  Hz, 1H), 4.35 (multiple peaks, 2H), 3.31 (ddd,  $J = 12.7, 4.2, 1.9$  Hz, 1H), 1.87–1.80 (multiple peaks, 2H), 1.72 (m, 1H), 1.53–1.49 (multiple peaks, 2H), 1.40 (m, 1H), 1.23 (m, 1H), 1.19 (s, 3H), 1.18 (m, 1H), 1.04 (s, 3H), 0.86 (t,  $J = 7.8$  Hz, 3H), 0.80–0.73 (multiple peaks, 4H).  $^{13}\text{C}\{^1\text{H}\}$  NMR (176 MHz,  $\text{CDCl}_3$ ):  $\delta$  166.1, 165.7, 162.1, 133.00, 132.98, 129.98, 129.8, 129.7, 129.6, 128.31, 128.25, 71.23, 70.93, 63.59, 50.48, 35.06, 34.66, 34.44, 33.7, 33.1, 28.09, 25.32, 24.5, 22.2, 8.1. Minor Isomer (distinct resonances):  $^{13}\text{C}\{^1\text{H}\}$  NMR (176 MHz,  $\text{CDCl}_3$ ):  $\delta$  71.15, 70.85, 63.56, 50.55, 35.05, 34.69, 34.42, 33.6, 28.11, 25.35, 22.1. IR (thin film, neat, mixture of isomers): 2956, 2872, 1722, 1452  $\text{cm}^{-1}$ . HRMS electrospray (m/z):  $[\text{M}+\text{H}]^+$  calcd for  $\text{C}_{29}\text{H}_{38}\text{NO}_5$ , 480.2744; found, 480.2749.



**Oxime Ether 45.** The general procedure was followed using substrate **40** (50 mg, 0.188 mmol, 1 equiv), PdCl<sub>2</sub>(PhCN)<sub>2</sub> (3.6 mg, 0.0094 mmol, 0.05 equiv), PhI(OBz)<sub>2</sub> (252 mg, 0.564 mmol, 3 equiv), and dry toluene (1.6 mL). Compound **45** was isolated in 54% yield as a colorless oil ( $R_f = 0.24$  in 91% hexanes/8%

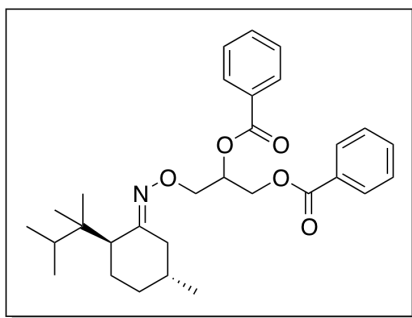
Et<sub>2</sub>O/1% Et<sub>3</sub>N) with diastereomeric ratio 86:14 as measured by <sup>13</sup>C NMR. Major Isomer: <sup>1</sup>H NMR (700 MHz, C<sub>6</sub>D<sub>6</sub>): δ 8.15 (d,  $J = 7.9$  Hz, 2H), 8.11 (d,  $J = 7.9$  Hz, 2H), 7.07 (t,  $J = 7.4$  Hz, 1H), 7.05 (t,  $J = 7.4$  Hz, 1H), 7.00 (dd,  $J = 7.9, 7.4$  Hz, 2H), 6.97 (dd,  $J = 7.9, 7.4$  Hz, 2H), 5.95 (m, 1H), 4.63 (dd,  $J = 12.0, 3.7$  Hz, 1H), 4.52 (dd,  $J = 12.0, 6.4$  Hz, 1H), 4.39–4.34 (multiple peaks, 2H), 3.33 (ddd,  $J = 12.6, 4.1, 1.9$  Hz, 1H), 1.84 (dd,  $J = 12.1, 4.1$  Hz, 1H), 1.79–1.73 (multiple peaks, 2H), 1.68 (app sept,  $J = 6.3$  Hz, 1H), 1.54–1.52 (multiple peaks, 2H), 1.34 (dd,  $J = 14.4, 5.4$  Hz, 1H), 1.24 (m, 1H), 1.21 (s, 3H), 1.16 (dd,  $J = 13.1, 11.8$  Hz, 1H), 1.10 (s, 3H), 1.02 (d,  $J = 6.6$  Hz, 3H), 1.00 (d,  $J = 6.6$  Hz, 3H), 0.80 (m, 1H), 0.77 (d,  $J = 6.4$  Hz, 3H). <sup>13</sup>C{<sup>1</sup>H} NMR (176 MHz, C<sub>6</sub>D<sub>6</sub>): δ 166.0, 165.74, 162.13, 133.0, 132.9, 130.8, 130.5, 130.1, 130.0, 128.6, 128.5, 71.9, 71.5, 63.83, 52.4, 49.6, 36.1, 35.06, 35.01, 34.14, 28.9, 26.8, 26.0, 25.9, 25.8, 24.4, 22.33. Minor Isomer (distinct resonances): <sup>1</sup>H NMR (700 MHz, C<sub>6</sub>D<sub>6</sub>): δ 1.23 (s, 3H), 0.74 (d,  $J = 6.4$  Hz, 3H). <sup>13</sup>C{<sup>1</sup>H} NMR (176 MHz, C<sub>6</sub>D<sub>6</sub>): δ 165.71, 162.11, 71.7, 71.3, 63.79, 49.7, 35.10, 34.97, 34.05, 26.9, 22.29. IR (thin film, neat, mixture of isomers): 2952, 1723, 1452 cm<sup>-1</sup>. HRMS electrospray ( $m/z$ ): [M+H]<sup>+</sup> calcd for C<sub>31</sub>H<sub>42</sub>NO<sub>5</sub>, 508.3057; found, 508.3064.



**Oxime Ether 46.** The general procedure was followed using substrate **41** (143 mg, 0.50 mmol, 1 equiv), PdCl<sub>2</sub>(PhCN)<sub>2</sub> (9.6 mg, 0.025 mmol, 0.05 equiv), PhI(OBz)<sub>2</sub> (446 mg, 1.00 mmol, 2 equiv), and dry toluene (4.2 mL). Compound **46** was isolated in 44% yield as a colorless oil ( $R_f = 0.16$  in

91% hexanes/8% Et<sub>2</sub>O/1% Et<sub>3</sub>N) with diastereomeric ratio 85:15 as measured by <sup>13</sup>C NMR. Major Isomer: <sup>1</sup>H NMR (700 MHz, CDCl<sub>3</sub>): δ 8.06 (d,  $J = 7.5$  Hz, 2H), 8.04 (d,  $J$

= 7.5 Hz, 2H), 7.558 (t,  $J = 7.5$  Hz, 1H), 7.556 (t,  $J = 7.5$  Hz, 1H), 7.44 (app t,  $J = 7.5$  Hz, 4H), 7.36 (d,  $J = 8.0$  Hz, 2H), 7.27 (t,  $J = 8.0$  Hz, 2H), 7.13 (t,  $J = 8.0$  Hz, 1H), 5.49 (dddd,  $J = 6.2, 6.0, 5.2, 3.4$  Hz, 1H), 4.59 (dd,  $J = 12.0, 3.4$  Hz, 1H), 4.49 (d,  $J = 12.0, 6.2$  Hz, 1H), 4.29 (dd,  $J = 12.0, 6.0$  Hz, 1H), 4.25 ( $J = 12.0, 5.2$  Hz, 1H), 3.05 (dd,  $J = 13.4, 4.5$  Hz, 1H), 2.48 (dd,  $J = 11.8, 3.7$  Hz, 1H), 1.76–1.69 (multiple peaks, 2H), 1.55 (m, 1H), 1.51 (s, 3H), 1.41 (s, 3H), 1.38–1.33 (multiple peaks, 2H), 1.00 (m, 1H), 0.89 (d,  $J = 6.5$  Hz, 3H).  $^{13}\text{C}\{^1\text{H}\}$  NMR (176 MHz,  $\text{CDCl}_3$ ):  $\delta$  166.2, 165.7, 161.2, 150.5, 133.1, 133.00, 130.0, 129.8, 129.72, 129.65, 128.4, 128.3, 127.70, 125.8, 125.2, 71.4, 70.83, 63.6, 52.9, 39.9, 34.6, 34.27, 33.39, 28.67, 26.0, 25.9, 22.1 Minor Isomer (distinct resonances):  $^1\text{H}$  NMR (700 MHz,  $\text{CDCl}_3$ ):  $\delta$  5.57 (m, 1H), 4.40 (dd,  $J = 12.0, 6.2$  Hz, 1H), 1.53 (s, 3H), 1.40 (s, 3H).  $^{13}\text{C}\{^1\text{H}\}$  NMR (176 MHz,  $\text{CDCl}_3$ ):  $\delta$  161.0, 150.6, 133.03, 127.74, 125.7, 125.1, 70.79, 70.7, 63.4, 53.1, 39.8, 34.7, 34.30, 33.44, 28.75, 26.6, 25.6. IR (thin film,  $\text{CH}_2\text{Cl}_2$ , mixture of isomers): 3062, 2953, 2927, 1718, 1452  $\text{cm}^{-1}$ . HRMS electrospray ( $m/z$ ):  $[\text{M}+\text{H}]^+$  calcd for  $\text{C}_{33}\text{H}_{38}\text{NO}_5$ , 528.2744; found, 528.2745.

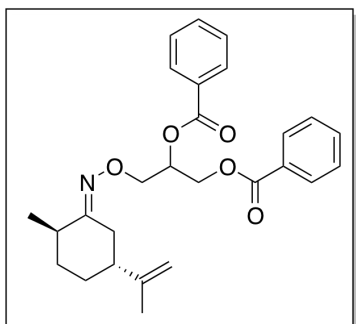


**Oxime Ether 47.** The general procedure was followed using substrate **42** (50 mg, 0.199 mmol, 1 equiv),  $\text{PdCl}_2(\text{PhCN})_2$  (3.8 mg, 0.01 mmol, 0.05 equiv),  $\text{PhI}(\text{OBz})_2$  (266 mg, 0.597 mmol, 3 equiv), and dry toluene (1.6 mL). Compound **47** was isolated in 37% yield as a colorless oil ( $R_f = 0.24$  in 91%

hexanes/8%  $\text{Et}_2\text{O}$ /1%  $\text{Et}_3\text{N}$ ) with diastereomeric ratio 90:10 as measured by  $^{13}\text{C}$  NMR. Major Isomer:  $^1\text{H}$  NMR (700 MHz,  $\text{C}_6\text{D}_6$ ):  $\delta$  8.15 (dd,  $J = 8.1, 1.3$  Hz, 2H), 8.10 (dd,  $J = 8.1, 1.3$  Hz, 2H), 7.07 (tt,  $J = 7.5, 1.3$  Hz, 1H), 7.04 (tt,  $J = 7.5, 1.3$  Hz, 1H), 7.00 (dd,  $J = 8.1, 7.5$  Hz, 2H), 6.97 (dd,  $J = 8.1, 7.5$  Hz, 2H), 5.92 (dddd,  $J = 6.5, 5.6, 5.6, 3.8$  Hz, 1H), 4.61 (dd,  $J = 11.8, 3.8$  Hz, 1H), 4.50 (dd,  $J = 11.8, 6.5$  Hz, 1H), 4.35 (app d,  $J = 5.6$  Hz, 2H), 3.32 (ddd,  $J = 12.6, 4.4, 2.0$  Hz, 1H), 2.44 (app sept,  $J = 7.0$  Hz, 1H), 1.96 (dd,  $J = 11.9, 3.9$  Hz, 1H), 1.75 (app dq,  $J = 13.1, 4.0$  Hz, 1H), 1.58–1.52 (multiple peaks, 2H), 1.25 (app qd,  $J = 13.0, 3.6$  Hz, 1H), 1.19 (s, 3H), 1.18 (dd,  $J = 12.3, 11.6$  Hz, 1H), 0.89 (d,  $J = 7.0$  Hz, 3H), 0.85 (s, 3H), 0.84 (d,  $J = 7.0$  Hz, 3H), 0.78 (m, 1H), 0.77 (d,  $J = 6.4$  Hz, 3H).  $^{13}\text{C}\{^1\text{H}\}$  NMR ( $\text{C}_6\text{D}_6$ ):  $\delta$  166.0, 165.7, 162.4, 133.0, 132.9, 130.8, 130.5, 130.1,



130.0, 128.6, 128.5, 71.80, 71.44, 63.84, 50.7, 37.8, 35.17, 35.08, 34.4, 32.9, 29.1, 22.35, 20.8, 20.7, 17.7, 17.61. Minor Isomer (distinct resonances):  $^1\text{H}$  NMR (700 MHz,  $\text{C}_6\text{D}_6$ ):  $\delta$  1.21 (s, 3H).  $^{13}\text{C}\{^1\text{H}\}$  NMR ( $\text{C}_6\text{D}_6$ ):  $\delta$  162.3, 71.76, 71.36, 63.82, 50.8, 35.20, 35.03, 34.3, 22.31, 17.58. IR (thin film, neat, mixture of isomers): 2962, 1722, 1452  $\text{cm}^{-1}$ . HRMS electrospray (m/z):  $[\text{M}+\text{H}]^+$  calcd for  $\text{C}_{30}\text{H}_{40}\text{NO}_5$ , 494.2901; found, 494.2903.



**Oxime Ether 61.** The general procedure was followed using substrate **60** (83.6 mg, 0.50 mmol, 1 equiv),  $\text{PdCl}_2(\text{PhCN})_2$  (9.6 mg, 0.025 mmol, 0.05 equiv),  $\text{PhI}(\text{OBz})_2$  (446 mg, 1.00 mmol, 2 equiv), and dry toluene (4.2 mL). Compound **61** was isolated in 53% yield as a colorless oil ( $R_f = 0.10$  in 91% hexanes/8%  $\text{Et}_2\text{O}$ /1%  $\text{Et}_3\text{N}$ ) with diastereomeric ratio 55:45 as measured by  $^{13}\text{C}$  NMR.

Major Isomer:  $^1\text{H}$  NMR (700 MHz,  $\text{CDCl}_3$ ):  $\delta$  8.06 (d,  $J = 7.8$  Hz, 2H), 8.03 (d,  $J = 7.8$  Hz, 2H), 7.56–7.54 (multiple peaks, 2H), 7.44–7.41 (multiple peaks, 4H), 5.72 (m, 1H), 4.71–4.64 (multiple peaks, 3H), 4.59 (dd,  $J = 11.9, 6.2$  Hz, 2H), 3.31 (m, 1H), 2.15 (m, 1H), 2.00 (m, 1H), 1.92 (m, 1H), 1.81 (m, 1H), 1.69 (s, 3H), 1.54 (m, 1H), 1.39 (m, 1H), 1.18 (m, 1H), 1.05 (d,  $J = 6.5$  Hz, 3H).  $^{13}\text{C}\{^1\text{H}\}$  NMR (176 MHz,  $\text{CDCl}_3$ ):  $\delta$  166.18, 165.8, 162.98, 148.5, 133.1, 130.0, 129.78, 129.76, 129.74, 129.66, 128.4, 128.3, 109.2, 71.33, 71.0, 63.68, 44.9, 37.3, 35.39, 30.81, 30.13, 20.7, 16.17. Minor Isomer (distinct resonances):  $^1\text{H}$  NMR (700 MHz,  $\text{CDCl}_3$ ):  $\delta$  5.72 (m, 1H), 4.58 (dd,  $J = 11.9, 6.2$  Hz, 1H), 1.65 (s, 3H), 1.24 (m, 1H), 1.06 (d,  $J = 6.5$  Hz, 3H).  $^{13}\text{C}\{^1\text{H}\}$  NMR (176 MHz,  $\text{CDCl}_3$ ):  $\delta$  166.19, 165.7, 163.01, 133.0, 109.1, 71.28, 70.7, 63.67, 44.8, 37.4, 35.42, 30.83, 30.10, 20.6, 16.18. IR (thin film, neat, mixture of isomers): 2965, 2929, 1721, 1451  $\text{cm}^{-1}$ .  $[\text{M}+\text{H}]^+$  calcd for  $\text{C}_{27}\text{H}_{31}\text{NO}_5$ , 450.2275; found, 450.2265.

*Details for Control Reactions in Table 4.2 and Scheme 4.14, and Additional Studies with Added Acid*

**Table 4.2, Entry 2.** Substrate **16** (7.7 mg, 0.05 mmol, 1 equiv) and  $\text{PhI}(\text{OBz})_2$  (44.6 mg, 0.10 mmol, 2 equiv) were combined in toluene- $d_8$  (0.42 mL) in a 4 mL scintillation vial and sealed with a Teflon-lined cap. Reaction was stirred at 50  $^\circ\text{C}$  for 8 h, then the reaction

mixture was transferred into an NMR tube along with 1,3-dinitrobenzene as an internal standard (8.4 mg, 0.05 mmol, 1 equiv). No characteristic peaks corresponding to dioxygenated products were observed by  $^1\text{H}$  NMR, and 99% starting material remained.

**Table 4.2, Entries 3 and 4.** Substrate **16** (7.7 mg, 0.05 mmol, 1 equiv),  $\text{PhI}(\text{OBz})_2$  (44.6 mg, 0.10 mmol, 2 equiv), and 0.42 mL of a 0.00595 M or 0.131 M stock solution of TfOH in toluene (0.0025 or 0.055 mmol, 0.05 or 1.10 equiv) were combined in a 4 mL scintillation vial and sealed with a Teflon-lined cap. Reactions were stirred at 50 °C for 8 h, then 1,3-dinitrobenzene was added as an internal standard (8.4 mg, 0.05 mmol, 1 equiv). A 0.1 mL aliquot was transferred to an NMR tube and diluted with  $\text{CDCl}_3$ . No characteristic peaks corresponding to dibenzoylated products were observed by  $^1\text{H}$  NMR in either case, and 83% and 89% starting material remained in entries 3 and 4, respectively.

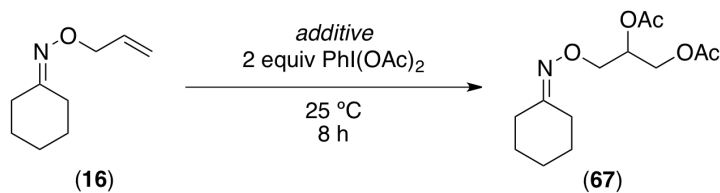
**Scheme 4.14.** Allyl propyl ether (5.0 mg, 0.05 mmol, 1 equiv),  $\text{PdCl}_2(\text{PhCN})_2$  (1.0 mg, 0.0025 mmol, 0.05 equiv), and  $\text{PhI}(\text{OBz})_2$  (44.6 mg, 0.10 mmol, 2 equiv) were combined in toluene- $d_8$  (0.42 mL) in a 4 mL scintillation vial and sealed with a Teflon-lined cap. Reaction was stirred at 50 °C for 8 h, then the reaction mixture was transferred into an NMR tube along with 1,3-dinitrobenzene as an internal standard (8.4 mg, 0.05 mmol, 1 equiv). No characteristic peaks corresponding to dioxygenated products were observed by  $^1\text{H}$  NMR, and 71% starting material remained.

**Additional Experiment: Superstoichiometric Acid.** We hypothesized that an acid-catalyzed reaction pathway was not feasible using substoichiometric quantities of acid because of the presence of a basic nitrogen in the oxime ether substrate. Thus, we were interested in the outcome of using superstoichiometric acid (> 1 equiv). Entries 3 and 4 in Table 4.2 were repeated using 110 or 120 mol% of TfOH or  $\text{BF}_3\cdot\text{OEt}_2$ , respectively. With superstoichiometric TfOH, 20% of the starting material remained at the end of the reaction, and numerous small peaks in the 4.5–6.5 ppm region of the  $^1\text{H}$  NMR spectrum (not corresponding to dibenzoylated products) were observed. No products were observable by gas chromatographic analysis, and we believe that substantial degradation

of the oxime ether substrate (including auxiliary cleavage) occurs under these relatively harsh conditions. Similarly, with superstoichiometric  $\text{BF}_3 \cdot \text{OEt}_2$ , only a small amount of starting material remained by  $^1\text{H}$  NMR (20%), although no other peaks were observed in the 4.5–6.5 ppm region of the  $^1\text{H}$  NMR spectrum.

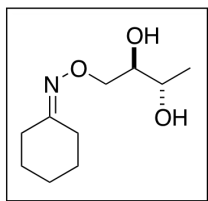
**Additional Experiment: Duplicating Published Reaction Conditions.** The dibenzoylation experiments involving TfOH or  $\text{BF}_3 \cdot \text{OEt}_2$  in Table 4.2 were designed to imitate published reaction conditions for TfOH-<sup>20</sup> or  $\text{BF}_3 \cdot \text{OEt}_2$ -<sup>21</sup>-catalyzed alkene diacetoxylation, but using our solvent (toluene) and our dioxygenating reagent [ $\text{PhI}(\text{OBz})_2$ ]. However, we also duplicated the published acid-catalyzed reaction conditions more exactly (using  $\text{PhI}(\text{OAc})_2$  and the alternative solvent systems), and achieved results very similar to those described in Table 4.2. Reactions were analyzed by gas chromatography, and the amounts of remaining starting material given below in Table 4.7 are GC calibrated yield based on a hexadecane standard.

**Table 4.7.** Subjection of **16** to TfOH or  $\text{BF}_3 \cdot \text{OEt}_2$  with  $\text{PhI}(\text{OAc})_2$



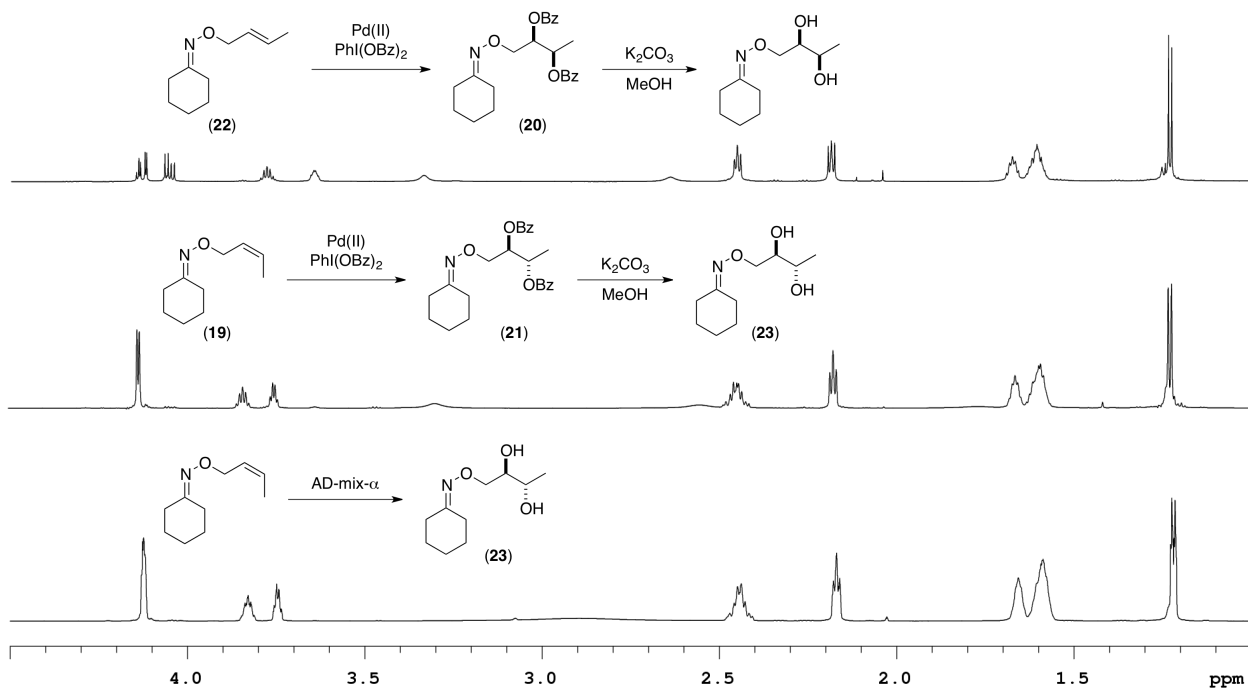
entry	additive	solvent	<b>67</b> (% yield)	<b>16</b> (% remaining)
1	5 mol % TfOH	$\text{CH}_2\text{Cl}_2$	<i>not detected</i>	67
2	110 mol % TfOH	$\text{CH}_2\text{Cl}_2$	<i>not detected</i>	<i>not detected</i>
3	10 mol % $\text{BF}_3 \cdot \text{OEt}_2$	$\text{AcOH}/\text{Ac}_2\text{O}$	<i>not detected</i>	77
4	120 mol % $\text{BF}_3 \cdot \text{OEt}_2$	$\text{AcOH}/\text{Ac}_2\text{O}$	<i>not detected</i>	<i>not detected</i>

*Synthesis and Characterization of Authentic Diol 23 (Scheme 4.19) and Comparison to 23 Derived from 21 (Scheme 4.18)*

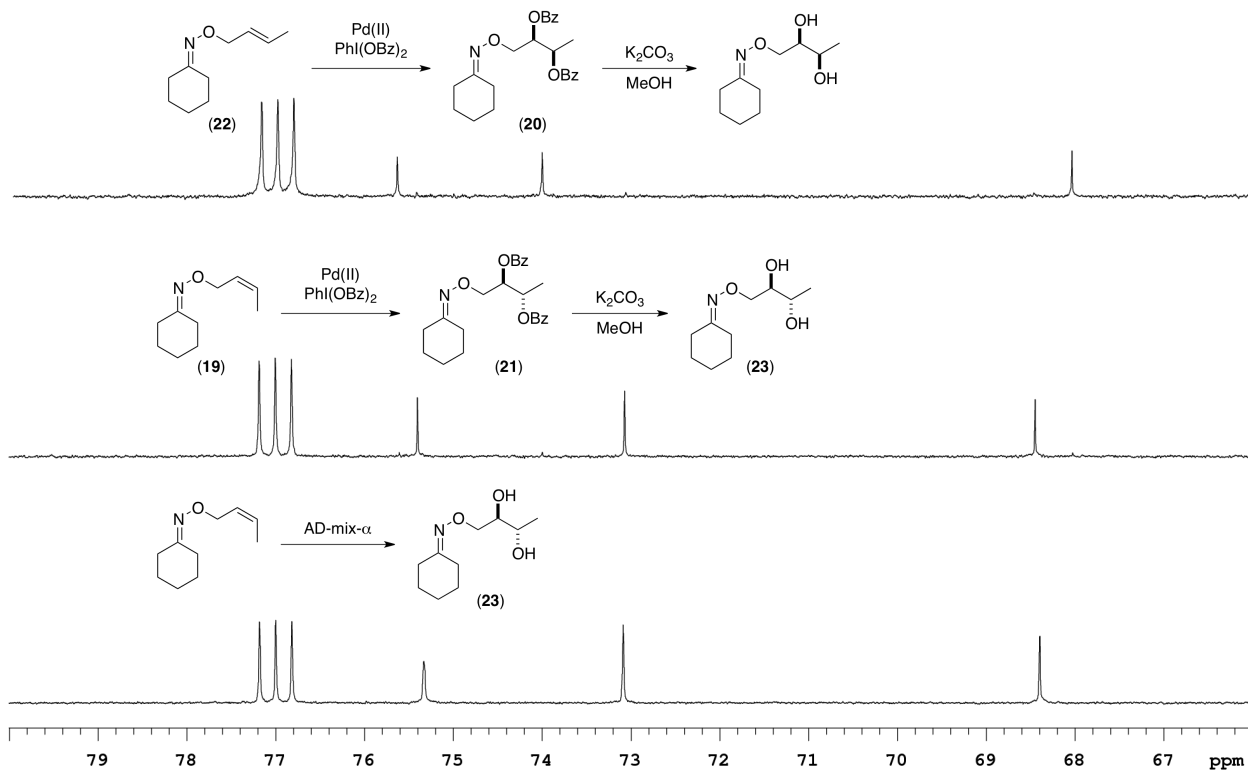


**Authentic Diol 23.** Substrate **19** (46 mg, 0.30 mmol, 1 equiv), AD-mix- $\alpha$  (420 mg), and  $\text{CH}_3\text{SO}_2\text{NH}_2$  (28.5 mg, 0.300 mmol, 1 equiv) were combined in *t*BuOH (1.5 mL) and  $\text{H}_2\text{O}$  (1.5 mL) and stirred at 0 °C for 6 h, then at room temperature for 1 h. To the mixture was added  $\text{Na}_2\text{SO}_3$  (460 mg) and KOH (168 mg), and stirring was continued at room temperature for 1 h. Reaction mixture was diluted with EtOAc, washed with brine, dried over  $\text{MgSO}_4$ , filtered, concentrated, and purified by column chromatography to afford **23** in 82% yield as a colorless oil ( $R_f = 0.19$  in 50% hexanes/50% EtOAc).  $^1\text{H}$  NMR (700 MHz,  $\text{CDCl}_3$ ):  $\delta$  4.13–4.12 (multiple peaks, 2H), 3.83 (m, 1H), 3.75 (m, 1H), 2.90 (br s, 2H), 2.44 (m, 2H), 2.17 (m, 2H), 1.66 (m, 2H), 1.61–1.57 (multiple peaks, 4H), 1.22 (d,  $J = 6.7$  Hz, 3H).  $^{13}\text{C}\{^1\text{H}\}$  NMR (176 MHz,  $\text{CDCl}_3$ ):  $\delta$  161.6, 75.3, 73.1, 68.4, 32.2, 26.9, 25.64, 25.62, 25.2, 18.3. IR (thin film, neat): 3378 (br), 2929, 2857, 1449  $\text{cm}^{-1}$ .  $[\text{M}+\text{H}]^+$  calcd for  $\text{C}_{10}\text{H}_{20}\text{NO}_3$ , 202.1438; found, 202.1438.

Comparison of  $^1\text{H}$  NMR spectra to assign *threo* vs *erythro* relative stereochemistry:



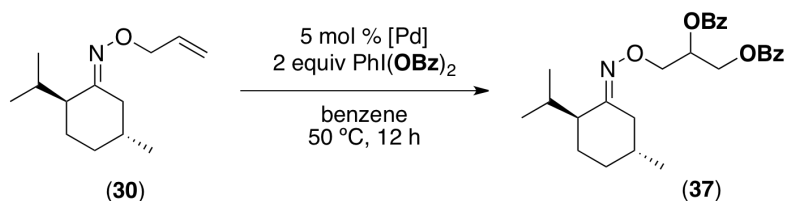
Comparison of  $^{13}\text{C}$  NMR spectra to assign *threo* vs *erythro* relative stereochemistry:



### Stereoselectivity for Dibenzoylation of **30** with Different Pd Catalysts

A number of different Pd<sup>II</sup> salts were screened for the dibenzoylation reaction of chiral substrate **30**. Table 4.8 summarizes the results. Although some catalysts [Pd(OTf)<sub>2</sub> and Pd(TFA)<sub>2</sub>] provided better stereoselectivity than PdCl<sub>2</sub>(PhCN)<sub>2</sub>, the yield of the reaction was substantially better with PdCl<sub>2</sub>(PhCN)<sub>2</sub>.

**Table 4.8.** Stereoselectivity of Dioxygenation of **30** as a Function of Pd Catalyst



entry	catalyst	%yield <sup>a</sup>	dr <sup>b</sup>
1	Pd(OAc) <sub>2</sub>	66	68:32
2	Pd(OBz) <sub>2</sub>	78	70:30
3	PdCl <sub>2</sub> (MeCN) <sub>2</sub>	73	73:27
4	PdCl <sub>2</sub> (PhCN) <sub>2</sub>	78	74:26
5	PdCl <sub>2</sub>	55	70:30
6	PdBr <sub>2</sub>	56	60:40
7	PdI <sub>2</sub>	59	62:38
8	Pd(TFA) <sub>2</sub>	55	76:24
9	Pd(OTf) <sub>2</sub>	36	82:18

<sup>a</sup>Crude NMR yield relative to dinitrobenzene.

<sup>b</sup>Determined by chiral HPLC of product purified by column chromatography.

#### 4.14 References

1. Woodward, R. B.; Brutcher, F. V. *cis*-Hydroxylation of a Synthetic Steroid Intermediate with Iodine, Silver Acetate and Wet Acetic Acid. *J. Am. Chem. Soc.* **1958**, *80*, 209.
2. Review: Wilson, C. V. The Reaction of Halogens with Silver Salts of Carboxylic Acids. *Org. React.* **1957**, *9*, 332.
3. Johnson, R. A.; Sharpless, K. B. Catalytic Asymmetric Epoxidation of Allylic Alcohols. In *Catalytic Asymmetric Synthesis*, 2nd ed.; Ojima, I., Ed.; Wiley-VCH: New York, 2000; p 229.
4. (a) Kolb, H. C.; VanNieuwenhze, M. S.; Sharpless, K. B. Catalytic Asymmetric Dihydroxylation *Chem. Rev.* **1994**, *94*, 2483. (b) Johnson, R. A.; Sharpless, K. B. Catalytic Asymmetric Dihydroxylation – Discovery and Development. In *Catalytic Asymmetric Synthesis*, 2nd ed.; Ojima, I., Ed.; Wiley-VCH: New York, 2000; p 357. (c) Bolm, C.; Hildebrand, J. P.; Muñiz, K. Recent Advances in Asymmetric Dihydroxylation and Aminohydroxylation. In *Catalytic Asymmetric Synthesis*, 2nd ed.; Ojima, I., Ed.; Wiley-VCH: New York, 2000; p 399. (d) Donohoe, T. J.; Bataille, C. J. R.; Innocenti, P. Hydrogen-Bonding-Mediated Directed Osmium Dihydroxylation. *Org. React.* **2011**, *76*, 1.
5. Bataille, C. J. R.; Donohoe, T. J. Osmium-Free Direct *Syn*-Dihydroxylation of Alkenes. *Chem. Soc. Rev.* **2011**, *40*, 114.
6. (a) Han, H.; Cho, C.-W.; Janda, K. D. A Substrate-Based Methodology that Allows the Regioselective Control of the Catalytic Aminohydroxylation Reaction. *Chem. Eur. J.* **1999**, *5*, 1565. (b) Bodkin, J. A.; McLeod, M. D. The Sharpless Asymmetric Aminohydroxylation. *J. Chem. Soc., Perkin Trans. 1* **2002**, 2733.
7. Reviews: (a) Muñiz, K. High-Oxidation-State Palladium Catalysis: New Reactivity for Organic Synthesis. *Angew. Chem., Int. Ed.* **2009**, *48*, 9412. (b) Canty, A. J. Organopalladium and Platinum Chemistry in Oxidizing Milieu as Models for Organic Synthesis Involving the Higher Oxidation States of Palladium. *Dalton. Trans.* **2009**, *47*, 10409. (c) Xu, L.-M.; Li, B.-J.; Yang, Z.; Shi, Z.-J. Organopalladium(IV) Chemistry. *Chem. Soc. Rev.* **2010**, *39*, 712. (d) Hickman, A. J.; Sanford, M. S. High-Valent Organometallic Copper and Palladium in Catalysis. *Nature* **2012**, *484*, 177.
8. Reviews: (a) Jensen, K. H.; Sigman, M. S. Mechanistic Approaches to Palladium-Catalyzed Alkene Difunctionalization Reactions. *Org. Biomol. Chem.* **2008**, *6*, 4083. (b) Jacques, B.; Muñiz, K. Palladium Catalysis for Oxidative 1,2-Difunctionalization of Alkenes. In *Catalyzed Carbon-Heteroatom Bond Formation*; Yudin, A. K., Ed.; Wiley-VCH: Weinheim, Germany, **2010**, 119 (c) McDonald, R. I.; Liu, G.; Stahl, S. S. Palladium(II)-Catalyzed Alkene Functionalization via Nucleopalladation: Stereochemical Pathways and Enantioselective Catalytic Applications. *Chem. Rev.* **2011**, *111*, 2981.

9. (a) Li, Y.; Song, D.; Dong, V. M. Palladium-Catalyzed Olefin Dioxygenation. *J. Am. Chem. Soc.* **2008**, *130*, 2962. (b) Wang, A.; Jiang, H.; Chen, H. Palladium-Catalyzed Diacetoxylation of Alkenes with Molecular Oxygen as Sole Oxidant. *J. Am. Chem. Soc.* **2009**, *131*, 3846. (c) Wang, W.; Wang, F.; Shi, M. Bis(NHC)-Palladium(II) Complex-Catalyzed Dioxygenation of Alkenes. *Organometallics* **2010**, *29*, 928. (d) Park, C. P.; Lee, J. H.; Yoo, K. S.; Jung, K. W. Efficient Diacetoxylation of Alkenes via Pd(II)/Pd(IV) Process with Peracetic Acid and Acetic Anhydride. *Org. Lett.* **2010**, *12*, 2450.
10. (a) Alexanian, E. J.; Lee, C.; Sorensen, E. J. Palladium-Catalyzed Ring-Forming Aminoacetoxylation of Alkenes. *J. Am. Chem. Soc.* **2005**, *127*, 7690. (b) Liu, G.; Stahl, S. S. Highly Regioselective Pd-Catalyzed Intermolecular Aminoacetoxylation of Alkenes and Evidence for *cis*-Aminopalladation and SN2 C–O Bond Formation. *J. Am. Chem. Soc.* **2006**, *128*, 7179. (c) Desai, L. V.; Sanford, M. S. Construction of Tetrahydrofurans by Pd<sup>II</sup>/Pd<sup>IV</sup>-Catalyzed Aminoxylation of Alkenes. *Angew. Chem., Int. Ed.* **2007**, *46*, 5737.
11. (a) Rosewall, C. F.; Sibbald, P. A.; Liskin, D. V.; Michael, F. E. Palladium-Catalyzed Carboamination of Alkenes Promoted by *N*-Fluorobenzenesulfonimide via C–H Activation of Arenes. *J. Am. Chem. Soc.* **2009**, *131*, 9488. (b) Sibbald, P. A.; Rosewall, C. F.; Swartz, R. D.; Michael, F. E. Mechanism of *N*-Fluorobenzenesulfonimide Promoted Diamination and Carboamination Reactions: Divergent Reactivity of a Pd(IV) Species. *J. Am. Chem. Soc.* **2009**, *131*, 15945.
12. (a) Streuff, J.; Hövelmann, C. H.; Nieger, M.; Muñoz, K. Palladium(II)-Catalyzed Intramolecular Diamination of Unfunctionalized Alkenes. *J. Am. Chem. Soc.* **2005**, *127*, 14586. (b) Muñoz, K. Advancing Palladium-Catalyzed C–N Bond Formation: Bisindoline Construction from Successive Amide Transfer to Internal Alkenes. *J. Am. Chem. Soc.* **2007**, *129*, 14542. (c) Muñoz, K.; Hövelmann, C. H.; Streuff, J. Oxidative Diamination of Alkenes with Ureas as Nitrogen Sources: Mechanistic Pathways in the Presence of a High Oxidation State Palladium Catalyst. *J. Am. Chem. Soc.* **2008**, *130*, 763. (d) Sibbald, P. A.; Michael, F. E. Palladium-Catalyzed Diamination of Unactivated Alkenes Using *N*-Fluorobenzenesulfonimide as Source of Electrophilic Nitrogen. *Org. Lett.* **2009**, *11*, 1147. (e) Iglesias, Á.; Pérez, E. G.; Muñoz, K. An Intermolecular Palladium-Catalyzed Diamination of Unactivated Alkenes. *Angew. Chem., Int. Ed.* **2010**, *49*, 8109. (f) Muñoz, K.; Kirsch, J.; Chávez, P. Intermolecular Regioselective 1,2-Diamination of Allylic Ethers. *Adv. Synth. Catal.* **2011**, *353*, 689. (g) Martínez, C.; Muñoz, K. Palladium-Catalyzed Vicinal Difunctionalization of Internal Alkenes: Diastereoselective Synthesis of Diamines. *Angew. Chem., Int. Ed.* **2012**, *51*, 7031.
13. (a) Wu, T.; Yin, G.; Liu, G. Palladium-Catalyzed Intramolecular Aminofluorination of Unactivated Alkenes. *J. Am. Chem. Soc.* **2009**, *131*, 16354. (b) Qiu, S.; Xu, T.; Zhou, J.; Guo, Y.; Liu, G. Palladium-Catalyzed Intermolecular Aminofluorination of Styrenes. *J. Am. Chem. Soc.* **2010**, *132*, 2856.



14. Michael, F. E.; Sibbald, P. A.; Cochran, B. M. Palladium-Catalyzed Intramolecular Chloroamination of Alkenes. *Org. Lett.* **2008**, *10*, 793.
15. (a) Kalyani, D.; Sanford, M. S. Oxidatively Intercepting Heck Intermediates: Pd-Catalyzed 1,2- and 1,1-Arylhalogenation of Alkenes. *J. Am. Chem. Soc.* **2008**, *130*, 2150. (b) Kalyani, D.; Satterfield, A. D.; Sanford, M. S. Palladium-Catalyzed Oxidative Arylhalogenation of Alkenes: Synthetic Scope and Mechanistic Insights. *J. Am. Chem. Soc.* **2010**, *132*, 8419.
16. (a) Tong, X.; Beller, M.; Tse, M. K. A Palladium-Catalyzed Cyclization–Oxidation Sequence: Synthesis of Bicyclo[3.1.0]hexanes and Evidence for SN2 C–O Bond Formation. *J. Am. Chem. Soc.* **2007**, *129*, 4906. (b) Welbes, L. L.; Lyons, T. W.; Cychosz, K. A.; Sanford, M. S. Synthesis of Cyclopropanes via Pd(II/IV)-Catalyzed Reactions of Enynes. *J. Am. Chem. Soc.* **2007**, *129*, 5836. (c) Lyons, T. W.; Sanford, M. S. Palladium (II/IV) Catalyzed Cyclopropanation Reactions: Scope and Mechanism. *Tetrahedron* **2009**, *65*, 3211. (d) Tsujihara, T.; Takenaka, K.; Onitsuka, K.; Hatanaka, M.; Sasai, H. PdII/PdIV Catalytic Enantioselective Synthesis of Bicyclo[3.1.0]hexanes via Oxidative Cyclization of Enynes. *J. Am. Chem. Soc.* **2009**, *131*, 3452.
17. (a) Giri, R.; Chen, X.; Yu, J.-Q. Palladium-Catalyzed Asymmetric Iodination of Unactivated C–H Bonds Under Mild Conditions. *Angew. Chem., Int. Ed.* **2005**, *44*, 2112. (b) Giri, R.; Liang, J.; Lei, J.-G.; Li, J.-J.; Wang, D.-H.; Chen, X.; Naggar, I. C.; Guo, C.; Foxman, B. M.; Yu, J.-Q. Pd-Catalyzed Stereoselective Oxidation of Methyl Groups by Inexpensive Oxidants under Mild Conditions: A Dual Role for Carboxylic Anhydrides in Catalytic C–H Bond Oxidation. *Angew. Chem., Int. Ed.* **2005**, *44*, 7420. (c) Giri, R.; Chen, X.; Hao, X.-S.; Li, J.-J.; Liang, J.; Fan, Z.-P.; Yu, J.-Q. Catalytic and Stereoselective Iodination of Prochiral C–H Bonds. *Tetrahedron: Asymmetry* **2005**, *16*, 3502. (d) Giri, R.; Lan, Y.; Liu, P.; Houk, K. N.; Yu, J.-Q. Understanding Reactivity and Stereoselectivity in Palladium-Catalyzed Diastereoselective  $sp^3$  C–H Bond Activation: Intermediate Characterization and Computational Studies. *J. Am. Chem. Soc.* **2012**, *134*, 14118.
18. For examples of enantioselective C–H functionalization using chiral ancillary ligands, see: (a) Shi, B.-F.; Maugel, N.; Zhang, Y.-H.; Yu, J.-Q. Pd<sup>II</sup>-Catalyzed Enantioselective Activation of C(sp<sup>2</sup>)–H and C(sp<sup>3</sup>)–H Bonds Using Monoprotected Amino Acids as Chiral Ligands. *Angew. Chem., Int. Ed.* **2008**, *47*, 4882. (b) Shi, B.-F.; Zhang, Y.-H.; Lam, J. K.; Wang, D.-H.; Yu, J.-Q. Pd(II)-Catalyzed Enantioselective C–H Olefination of Diphenylacetic Acids. *J. Am. Chem. Soc.* **2010**, *132*, 460. (c) Musaev, D. G.; Kaledin, A.; Shi, B.-F.; Yu, J.-Q. Key Mechanistic Features of Enantioselective C–H Bond Activation Reactions Catalyzed by [(Chiral Mono-*N*-Protected Amino Acid)–Pd(II)] Complexes. *J. Am. Chem. Soc.* **2012**, *134*, 1690.
19. (a) Desai, L. V.; Hull, K. L.; Sanford, M. S. Palladium-Catalyzed Oxygenation of Unactivated  $sp^3$  C–H Bonds. *J. Am. Chem. Soc.* **2004**, *126*, 9542. (b) Desai, L. V.; Malik, H. A.; Sanford, M. S. Oxone as an Inexpensive, Safe, and Environmentally

- Benign Oxidant for C–H Bond Oxygenation. *Org. Lett.* **2006**, *8*, 1141. (c) Kalyani, D.; Dick, A. R.; Anani, W. Q.; Sanford, M. S. Scope and Selectivity in Palladium-Catalyzed Directed C–H Bond Halogenation Reactions. *Tetrahedron* **2006**, *62*, 11483. (d) Thu, H.-Y.; Yu, W.-Y.; Che, C.-M. Intermolecular Amidation of Unactivated  $sp^2$  and  $sp^3$  C–H Bonds via Palladium-Catalyzed Cascade C–H Activation/Nitrene Insertion. *J. Am. Chem. Soc.* **2006**, *128*, 9048. (e) Desai, L. V.; Stowers, K. J.; Sanford, M. S. Insights in Directing Group Ability in Palladium-Catalyzed C–H Bond Functionalization. *J. Am. Chem. Soc.* **2008**, *130*, 13285. (f) Thirunavukkarasu, V. S.; Parthasarathy, K.; Cheng, C.-H. Synthesis of Fluorenones from Aromatic Aldoxime Ethers and Aryl Halides by Palladium-Catalyzed Dual C–H Activation and Heck Cyclization. *Angew. Chem., Int. Ed.* **2008**, *47*, 9462. (g) Yu, W.-Y.; Sit, W. N.; Lai, K.-M.; Zhou, Z.; Chan, A. S. C. Palladium-Catalyzed Oxidative Ethoxycarbonylation of Aromatic C–H Bond with Diethyl Azodicarboxylate. *J. Am. Chem. Soc.* **2008**, *130*, 3304. (h) Zhao, X.; Dimitrijevic, E.; Dong, V. M. Palladium-Catalyzed C–H Bond Functionalization with Arylsulfonyl Chlorides. *J. Am. Chem. Soc.* **2009**, *131*, 3466. (i) Chan, C.-W.; Zhou, Z.; Chan, A. S. C.; Yu, W.-Y. Pd-Catalyzed *Ortho*-C–H Acylation/Cross Coupling of Aryl Ketone *O*-Methyl Oximes with Aldehydes Using *tert*-Butyl Hydroperoxide as Oxidant. *Org. Lett.* **2010**, *12*, 3926. (j) Neufeldt, S. R.; Sanford, M. S. *O*-Acetyl Oximes as Transformable Directing Groups for Pd-Catalyzed C–H Bond Functionalization. *Org. Lett.* **2010**, *12*, 532. (k) Kalyani, D.; McMurtrey, K. B.; Neufeldt, S. R.; Sanford, M. S. Room-Temperature C–H Arylation: Merger of Pd-Catalyzed C–H Functionalization and Visible-Light Photocatalysis. *J. Am. Chem. Soc.* **2011**, *133*, 18566.
20. Kang, Y.-B.; Gade, L. H. The Nature of the Catalytically Active Species in Olefin Dioxygenation with  $\text{PhI}(\text{OAc})_2$ : Metal or Proton? *J. Am. Chem. Soc.* **2011**, *133*, 3658.
21. An analogous metal-free transformation has also been shown using  $\text{BF}_3 \cdot \text{OEt}_2$  as a Lewis acid catalyst: Zhong, W.; Yang, J.; Meng, X.; Li, Z.  $\text{BF}_3 \cdot \text{OEt}_2$ -Promoted Diastereoselective Diacetoxylation of Alkenes by  $\text{PhI}(\text{OAc})_2$ . *J. Org. Chem.* **2011**, *76*, 9997.
22. Seayad, J.; Seayad, A. M.; Chai, C. L. L. Copper-Catalyzed Diacetoxylation of Olefins Using  $\text{PhI}(\text{OAc})_2$  as Oxidant. *Org. Lett.* **2010**, *12*, 1412.
23. Takano, S.; Yoshimitsu, T.; Ogasawara, K. Asymmetric Dihydroxylation of a *Meso*-Symmetric Cyclic Diene Using AD-Mix Reagents: A New Enantiocontrolled Route to Conduritol E. *J. Org. Chem.* **1994**, *59*, 54.
24. (a) Levy, G. C.; Nelson, G. L. Carbon-13 NMR Study of Aliphatic Amides and Oximes. Spin-Lattice Relaxation Times and Fast Internal Motions. *J. Am. Chem. Soc.* **1972**, *94*, 4897. (b) Hawkes, G. E.; Herwig, K.; Roberts, J. D. Nuclear Magnetic Resonance Spectroscopy: Use of  $^{13}\text{C}$  Spectra to Establish Configurations of Oximes. *J. Org. Chem.* **1974**, *39*, 1017.

25. Karabatsos, G. J.; Hsi, N. Structural Studies by Nuclear Magnetic Resonance–XI: Conformations and Configurations of Oxime *O*-Methyl Ethers. *Tetrahedron* **1967**, *23*, 1079.
26. Lu, W.-J.; Chen, Y.-W.; Hou, X.-L. Iridium-Catalyzed Highly Enantioselective Hydrogenation of the C=C Bond of  $\alpha,\beta$ -Unsaturated Ketones. *Angew. Chem., Int. Ed.* **2008**, *47*, 10133.
27. Doyle, J. R.; Slade, P. E.; Jonassen, H. B. Metal-Diolefin Coordination Compounds. *Inorg. Synth.* **1960**, *6*, 216.
28. Stang, P. J.; Boehshar, M.; Wingert, H.; Kitamura, T. Acetylenic Esters: Preparation and Characterization of Alkynyl Carboxylates via Polyvalent Iodonium Species. *J. Am. Chem. Soc.* **1988**, *110*, 3272.
29. Ort, O. *Org. Synth.* (–)-8-Phenylmenthol. **1987**, *65*, 203.

## CHAPTER 5

### A Transformable Directing Group for Pd-Catalyzed C–H Oxygenation

#### 5.1 Background and Significance

The use of a directing group for palladium-catalyzed C–H functionalization is an effective strategy for achieving rate acceleration and control over site-selectivity (Chapter 1).<sup>1</sup> However, limitations of this strategy are apparent in situations when a directing group moiety is undesired in the final target molecule. In such cases, this substrate-control strategy for selective C–H functionalization is only advantageous if the directing group can be *temporarily* installed and subsequently removed or transformed. The majority of directing groups for Pd-catalyzed C–H functionalization, however, are nitrogen-containing heterocycles or other functional groups that are not easily manipulated following the C–H functionalization event (*e.g.*, Figure 5.1).<sup>1c</sup>

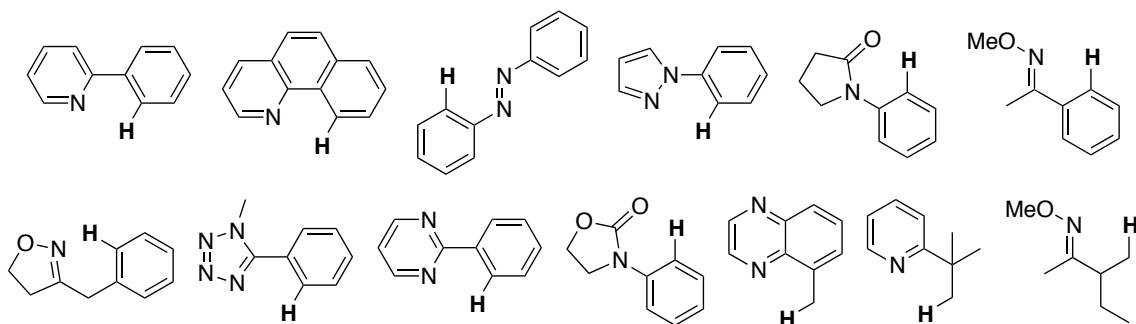
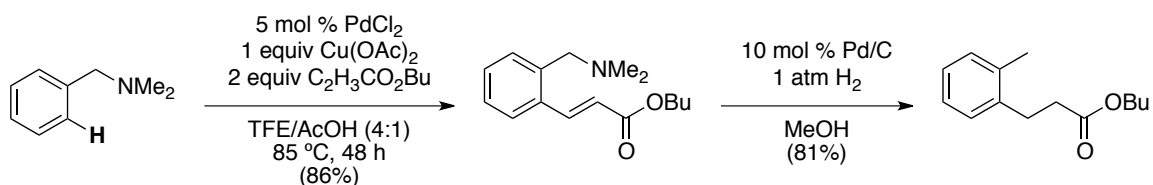


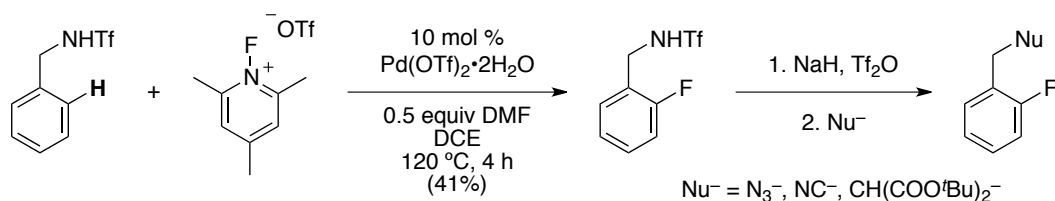
**Figure 5.1.** Examples of Substrates With Nitrogen-Containing Directing Groups for Pd-Catalyzed C–H Functionalization

An ideal directing ligand would be sufficiently robust to tolerate C–H activation/functionalization conditions, but could subsequently be converted into diverse functional groups. Instances of such directing groups in Pd-catalyzed reactions are still relatively rare, and at the time the work in this chapter was published<sup>2</sup> only a few examples were known (Schemes 5.1–5.5). Indirect C–H alkylation of substituted toluenes has been shown *via* a sequence involving (1) *N,N*-dimethylbenzylamine-directed C–H olefination and (2) reduction of both the dimethylbenzylamine and the installed olefin (Scheme 5.1).<sup>3</sup> Benzyl amines protected by trifluoromethylsulfonyl groups have been used to direct C–H fluorination, followed by nucleophilic displacement of the amine directing group (Scheme 5.2).<sup>4</sup>

**Scheme 5.1.** Indirect *ortho*-C–H Alkylation of Toluenes via Alkenylation of *N,N*-Dimethylbenzylamines<sup>3</sup>



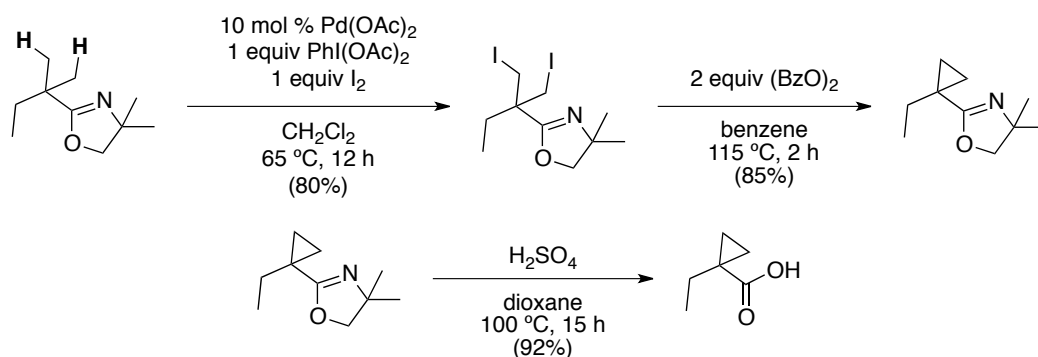
**Scheme 5.2.** Triflamide-Directed C–H Fluorination Followed by Nucleophilic Displacement of Directing Group<sup>4</sup>



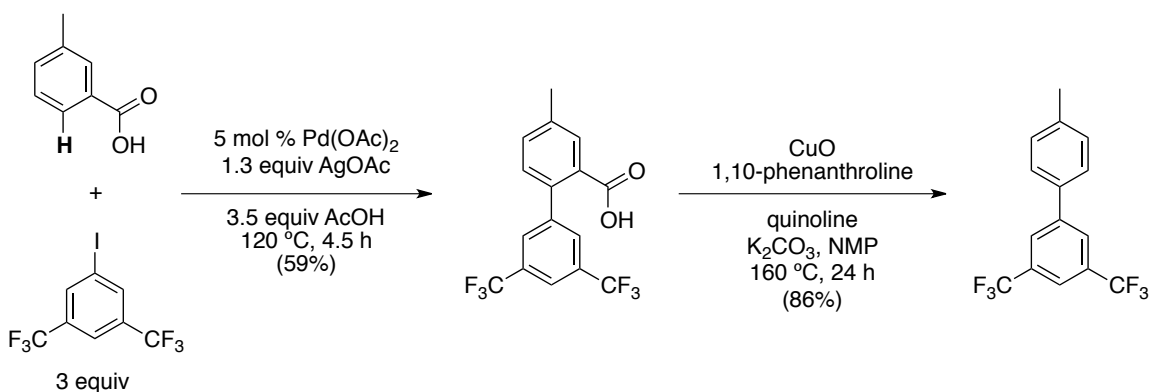
Oxazolines have been utilized for Pd-catalyzed C–H iodination reactions followed by H<sub>2</sub>SO<sub>4</sub>-catalyzed hydrolysis to afford carboxylic acids (Scheme 5.3).<sup>5</sup> Carboxylic acids have also been employed to direct Pd-catalyzed C–H arylations, and have then been removed by decarboxylation (Scheme 5.4).<sup>6</sup> Amides have proven effective for directing Pd-catalyzed C–C and C–halogen bond formation and have been subsequently

transformed into nitriles (Scheme 5.5)<sup>7a</sup>, fluorenones<sup>7a</sup>, or carboxylic acids<sup>7b,c</sup> (Scheme 5.6). In addition to these examples, a number of other transformable directing groups have been disclosed since the publication of the work described in this chapter. These reports are reviewed in sections 5.7 and 5.8 below.

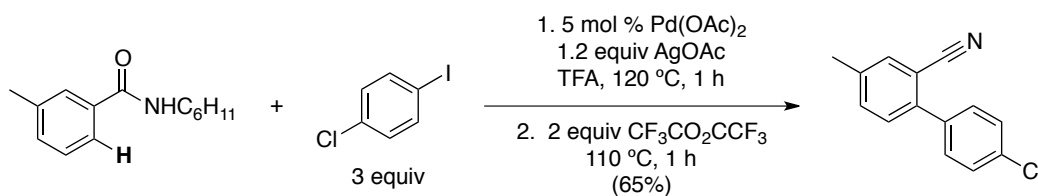
**Scheme 5.3.** Oxazoline-Directed C–H Iodination Followed by Directing Group Hydrolysis<sup>5</sup>



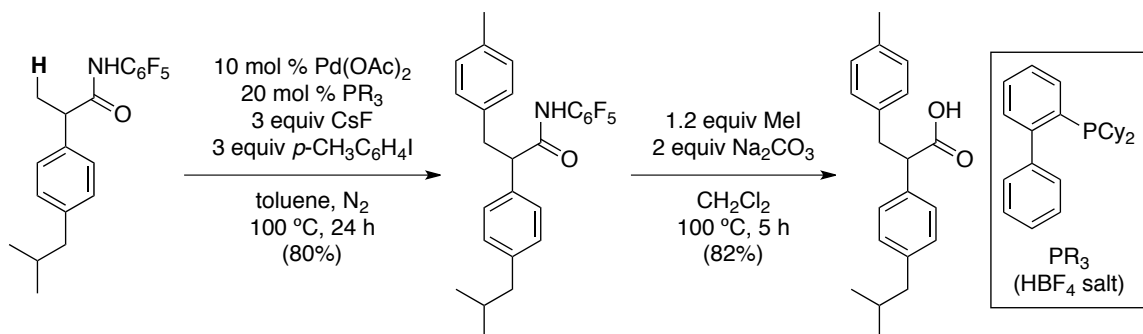
**Scheme 5.4.** Carboxylic Acid-Directed C–H Arylation Followed by Decarboxylation<sup>6</sup>



**Scheme 5.5.** Amide-Directed C–H Arylation Followed by Conversion to a Nitrile<sup>7a</sup>

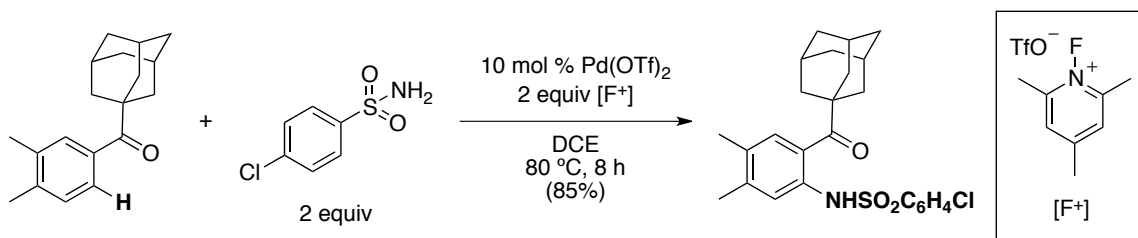


**Scheme 5.6.** Amide-Directed C–H Arylation Followed by Conversion to a Carboxylic Acid<sup>7b</sup>



Ketones would be particularly attractive directing groups because they are versatile and widely-used synthetic intermediates.<sup>8</sup> However, they are poor ligands for Pd<sup>II</sup>, and thus are usually ineffective directing groups for Pd-catalyzed C–H functionalization. Ketone-directed C–H arylation reactions catalyzed by Ru have been shown, but metals such as these are typically ineffective for converting C–H into C–heteroatom bonds.<sup>9</sup> Two examples of ketone-directed C–H arylation have been demonstrated under basic<sup>10a</sup> or strongly acidic conditions.<sup>10b</sup> Recently, a ketone-directed C–H amidation was reported using an electron-deficient Pd complex in conjunction with K<sub>2</sub>S<sub>2</sub>O<sub>8</sub> or [F<sup>+</sup>] oxidants (Scheme 5.7).<sup>10c</sup> This transformation is limited to the functionalization of sp<sup>2</sup> C–H bonds.

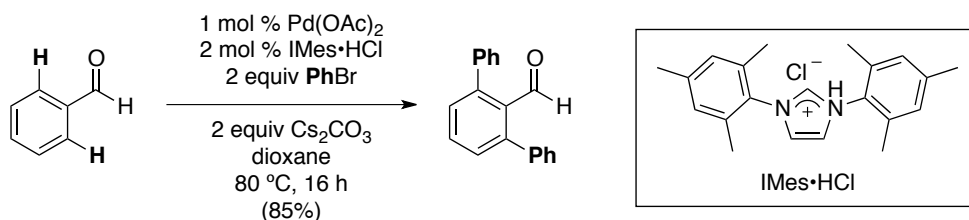
**Scheme 5.7.** Ketone-Directed C–H Amidation<sup>10c</sup>



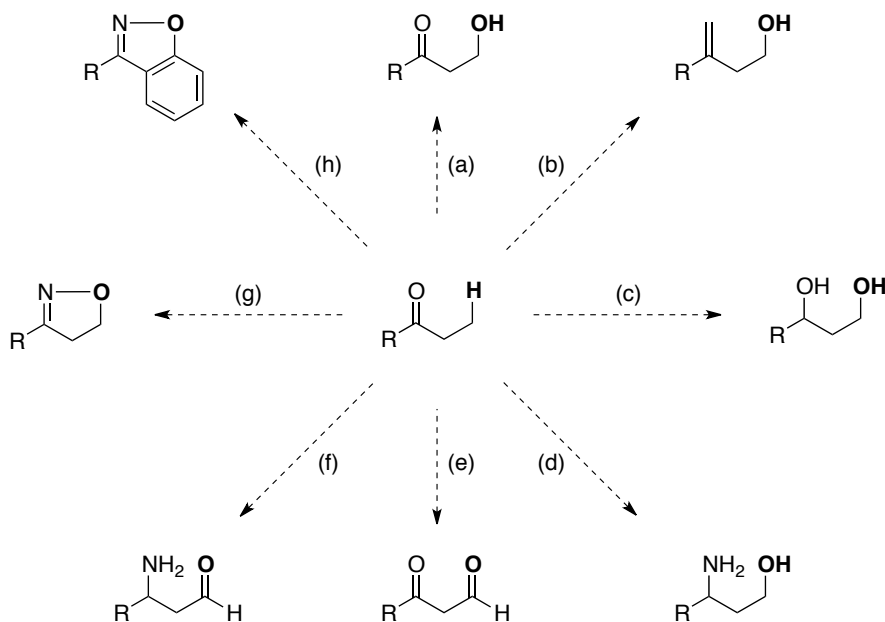
*Ortho*-C–H arylation of benzaldehydes has been shown in the presence of an *N*-heterocyclic carbene ligand (Scheme 5.8),<sup>11</sup> but ketone- or aldehyde-directed functionalization of unactivated sp<sup>3</sup> C–H bonds has not been demonstrated. A general

ketone-directed C–H activation/C–heteroatom bond forming reaction would enable access to compounds with valuable substitution patterns; for example, C–H oxygenation directed by a ketone or ketone surrogate could serve as a route to (a)  $\beta$ -hydroxy ketones, (b) homoallyl alcohols, (c) 1,3-diols, (d) 1,3-aminoalcohols, (e) 3-oxoaldehydes, (f)  $\beta$ -amino aldehydes, (g) isoxazolines, and (h) benzisoxazoles (Scheme 5.9).

**Scheme 5.8.** *Ortho*-C–H Arylation of Benzaldehydes<sup>11</sup>



**Scheme 5.9.** Ketones as Synthons for Diverse  $\beta$ -Oxygenated Motifs

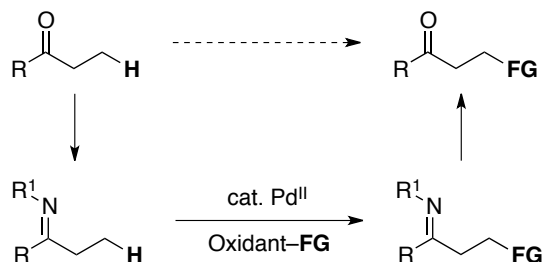


In contrast to ketones, nitrogen-containing groups have proven to be effective directing ligands for Pd-catalyzed C–H functionalization reactions (see Figure 5.1). As such, we sought to *temporarily* mask ketones as more coordinating imine or oxime derivatives during C–H functionalization and subsequently remove the masking group



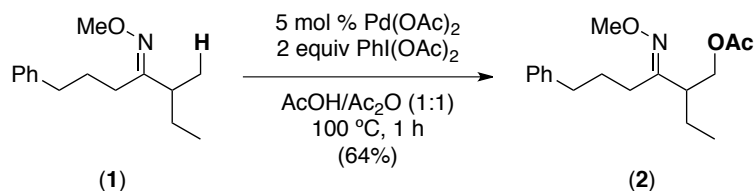
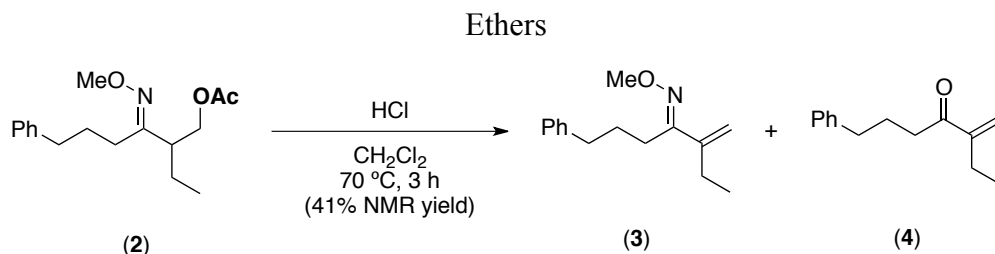
(Scheme 5.10). This strategy would enable the formal  $\beta$  or *ortho*-C–H functionalization of ketones.

**Scheme 5.10.** Approach to  $\beta$ -C–H Functionalization of Ketones

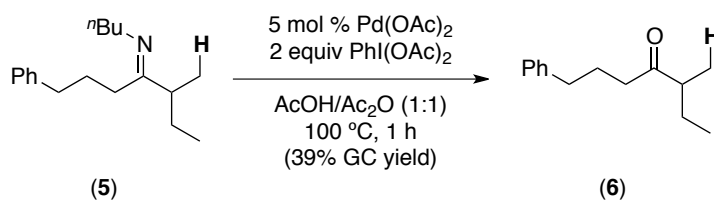


## 5.2 Directing Group Optimization

Two key challenges exist in the design of a ketone surrogate for Pd-catalyzed C–H functionalization. First, the protecting group must be stable to the catalytic reaction conditions. Second, the group must be readily removed in high yield without affecting the newly installed functional group. Our prior studies have shown that oxime ethers such as **1** are highly effective directing groups for Pd-catalyzed  $sp^2$ - and  $sp^3$ -C–H bond acetoxylation reactions with  $\text{PhI}(\text{OAc})_2$  (Scheme 5.11).<sup>12,13</sup> However, removal of the oxime ether protecting group from the  $\beta$ -functionalized products is problematic. As summarized in Scheme 5.12 for substrate **2**, acid-catalyzed hydrolysis<sup>14</sup> is sluggish and produces significant quantities of elimination products **3** and **4**. Alternatively, conversion of oxime ethers to ketones has been reported using Amberlyst 15 at temperatures ranging from 25 to 110 °C.<sup>15</sup> In our hands, however, **2** and derivatives were unreactive under these conditions at room temperature, and at elevated temperatures (80 °C), **2** reacted to form a complex mixture of products that did not include the expected  $\beta$ -acetoxy or  $\beta$ -hydroxy ketone. The use of superstoichiometric  $\text{TiCl}_3$  is effective in some cases,<sup>16</sup> but this expensive, air-sensitive reagent is not practical for general application.

**Scheme 5.11.** Methyl Oxime Ether-Directed C–H Acetoxylation**Scheme 5.12.** Elimination During Acid-Catalyzed Hydrolysis of  $\beta$ -Acetoxyated Oxime

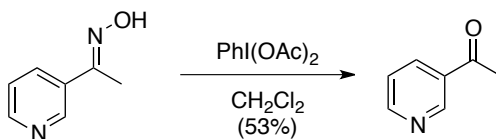
Imines would be a versatile alternative to oxime ethers, as they are readily hydrolyzed under mild conditions. Pd-catalyzed imine-directed acetoxylation of an sp<sup>2</sup> C–H bond has been reported;<sup>13a</sup> however, in our hands imines have proven too labile for analogous sp<sup>3</sup> C–H functionalizations. For example, the reaction of **5** under standard acetoxylation conditions affords the hydrolyzed ketone **6** as the major identifiable product (39% yield, Scheme 5.13).

**Scheme 5.13.** Lability of Alkyl Imines Under C–H Acetoxylation Conditions

Simple hydroxyl (OH) oximes are another attractive ketone surrogate. These readily available, stable, often crystalline starting materials are known to direct stoichiometric cyclopalladation at both sp<sup>2</sup>- and sp<sup>3</sup>- C–H sites<sup>17</sup> and are much more readily cleaved than their oxime ether counterparts.<sup>18</sup> In addition, they can be prepared from NH<sub>2</sub>OH•HCl, which is about 100-fold less expensive than NH<sub>2</sub>OMe•HCl.<sup>19</sup> Despite

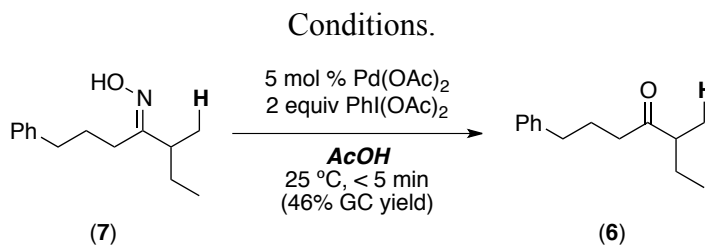
these advantages, oximes are known to undergo rapid oxidative cleavage in the presence of oxidants like  $\text{PhI}(\text{OAc})_2$  (Scheme 5.14).<sup>20</sup>

**Scheme 5.14.** Oxidative Cleavage of Hydroxyl Oximes by  $\text{PhI}(\text{OAc})_2$ <sup>20</sup>

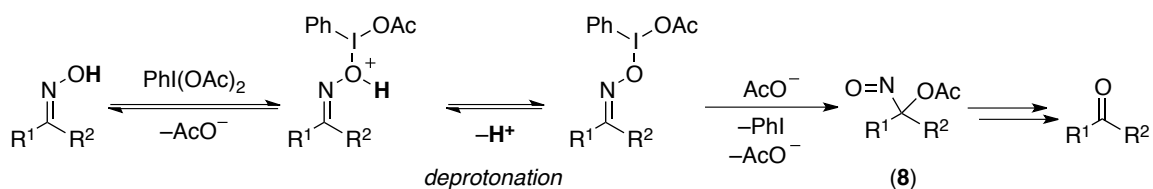


For example, combining oxime **7** with  $\text{Pd}(\text{OAc})_2$  and  $\text{PhI}(\text{OAc})_2$  in  $\text{AcOH}$  results in a nearly instantaneous color change from colorless to blue-green, concomitant with regeneration of the parent ketone **6** (Scheme 5.15). This color change is consistent with prior observations by Moriarty and coworkers<sup>20</sup> and can be attributed to rapid formation of a nitroso species **8** which decomposes to produce the corresponding ketone (Scheme 5.16). Importantly, the mechanism of this oxidative cleavage involves an O–H deprotonation step and therefore is expected to be specific to hydroxyl oximes.

**Scheme 5.15.** Oxidative Cleavage of Hydroxyl Oxime **7** Under C–H Acetoxylation



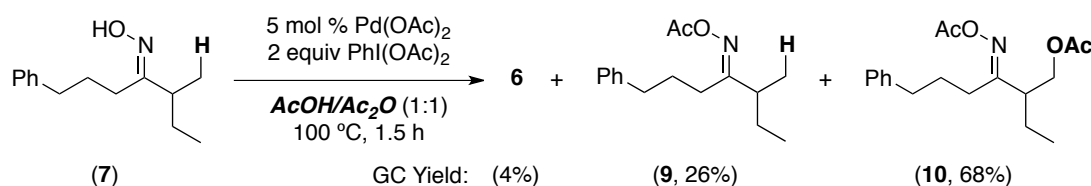
**Scheme 5.16.** Mechanism of Oxidative Cleavage of Hydroxyl Oximes by  $\text{PhI}(\text{OAc})_2$ <sup>20</sup>



Encouragingly, a similar color change is *not* observed when the reaction solvent is changed from  $\text{AcOH}$  to  $\text{AcOH}/\text{Ac}_2\text{O}$  (1:1). Under these conditions, only traces of ketone

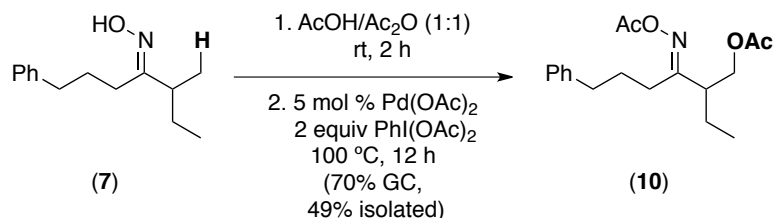
**6** (4% by GC) are formed; instead the major product (68% by GC) is the *O*-acetylated/ $\beta$ -H acetoxylation compound **10** (Scheme 5.17). This initial result suggested that the *in situ* reaction of **7** with Ac<sub>2</sub>O affords a stable *O*-acetyl oxime (**9**) capable of directing C–H acetoxylation.

**Scheme 5.17.** *O*-Acetylation and C–H Acetoxylation of Hydroxyl Oximes in the Presence of Ac<sub>2</sub>O



Further study led to the development of the following protocol that is general for a range of hydroxyl oxime substrates: (1) stirring the oxime starting material in AcOH/Ac<sub>2</sub>O for 2 h at 25 °C to effect quantitative *in situ* *O*-acetylation, (2) addition of Pd catalyst and oxidant, and (3) heating the reaction mixture at 80 °C (sp<sup>2</sup>-C–H acetoxylation) or 100 °C (sp<sup>3</sup>-C–H acetoxylation) for 4–24 h. This protocol affords **10** in 70% GC yield from **7** (Scheme 5.18).

**Scheme 5.18.** *O*-Acetyl Oxime-Directed Acetoxylation from Hydroxyl Oxime **7**



### 5.3 Scope of *O*-Acetyl Oxime-Directed Acetoxylation

As summarized in Table 5.1, a number of dialkyl oximes underwent *in situ* acetylation/ $\beta$ -acetoxylation in modest to good yields using the optimized reaction conditions. The observed trends in reactivity and selectivity were similar to those in sp<sup>3</sup>-C–H functionalization reactions of related oxime ethers.<sup>12a</sup> For example, oxidation

occurred selectively at 1°  $\beta$ -sp<sup>3</sup> C–H bonds over the analogous 2° sites (entries 1–4). Acetoxylation of a 2° C–H group could be achieved in modest yield in the rigid *trans*-decalone system (entry 6). The reaction conditions were compatible with a number of functional groups including alkyl chlorides (entry 4) and protected amines (entry 3); furthermore, remote benzylic C–H bonds were well tolerated under the oxidizing reaction conditions (entry 1). The acetoxyated products were typically isolated as mixtures of *E/Z* oxime stereoisomers, which rapidly interconvert under the catalytic reaction conditions.

**Table 5.1.** *O*-Acetyl Oxime-Directed Acetoxylation of  $sp^3$  C–H Bonds<sup>a</sup>

1. AcOH/Ac<sub>2</sub>O (1:1)  
rt, 2 h

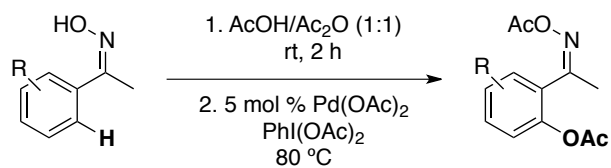
2. cat. Pd(OAc)<sub>2</sub>  
PhI(OAc)<sub>2</sub>  
100 °C

entry	substrate	product	isolated yield <sup>b</sup>
1 <sup>c</sup>	 (7)	 (10)	49% (70%) <sup>d</sup>
2 <sup>c</sup>	 (11)	 (12)	61%
3 <sup>c</sup>	 (13)	 (14)	65%
4 <sup>c</sup>	 (15)	 (16)	33%
5 <sup>c</sup>	 (17)	 (18)	66%
6	 (19)	 (20)	41%

<sup>a</sup>General conditions: substrate (1 equiv), AcOH/Ac<sub>2</sub>O (1:1, 0.12 M in substrate), 2 h, rt; then Pd(OAc)<sub>2</sub> (0.05 equiv), PhI(OAc)<sub>2</sub> (1.5–3 equiv), 100 °C, 12 h. <sup>b</sup>The remaining mass balance (as determined by GC of the crude reaction mixtures) was generally unreacted *O*-acetyloxime (analogous to **9** in Scheme 17). <sup>c</sup>Starting material and product consisted of a mixture of oxime *E/Z* stereoisomers. <sup>d</sup>GC yield.

*O*-Acetyl ketoximes are also effective directing groups for Pd-catalyzed acetoxylation at sp<sup>2</sup>-C–H sites (Table 5.2). Both electron poor and electron rich aryl rings underwent mono-*ortho*-oxygenation in high yields (entries 1 and 4). Further, aryl bromides (entry 2) and silyl-protected phenols (entry 5) were compatible with the reaction conditions.

**Table 5.2.** *O*-Acetyl Oxime-Directed Acetoxylation of  $sp^2$  C–H Bonds<sup>a</sup>



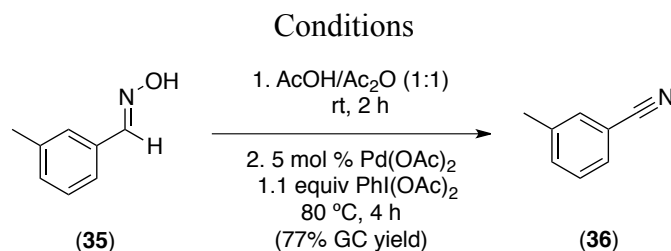
entry	substrate	product	isolated yield <sup>b</sup>
1 <sup>c</sup>	 (21)	 (22)	61%
2 <sup>c</sup>	 (23)	 (24)	86%
3 <sup>c</sup>	 (25)	 (26)	72%
4 <sup>c</sup>	 (27)	 (28)	77%
5 <sup>c</sup>	 (29)	 (30)	79%
6 <sup>c</sup>	 (31)	 (32)	80%
7	 (33)	 (34)	55%

<sup>a</sup>General conditions: substrate (1 equiv), AcOH/Ac<sub>2</sub>O (1:1, 0.12 M in substrate), 2 h, rt; then Pd(OAc)<sub>2</sub> (0.05 equiv), PhI(OAc)<sub>2</sub> (1–2 equiv), 80 °C, 4–24 h. <sup>b</sup>The remaining mass balance (as determined by GC of the crude reaction mixtures) was generally unreacted *O*-acetyloxime (analogous to **9** in Scheme 17). <sup>c</sup>Product consisted of a mixture of oxime *E/Z* stereoisomers.

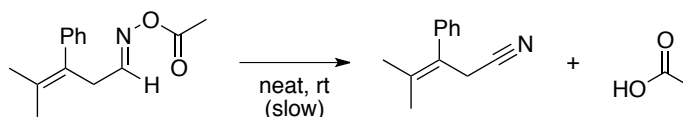


One notable limitation of this method is that *O*-acetyl aldoximes such as **35** were susceptible to rapid elimination of AcOH to generate nitriles (**36**, Scheme 5.19). Similar reactivity of *O*-acetyl aldoximes has been previously reported (Scheme 5.20).<sup>21</sup>

**Scheme 5.19.** Nitrile Formation From an *O*-Acetyl Aldoxime Under C–H Acetoxylation



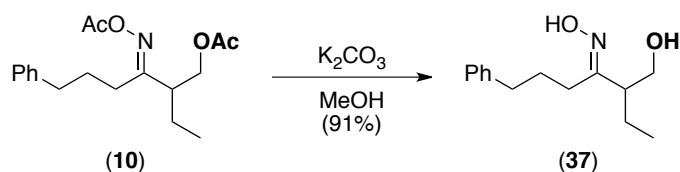
**Scheme 5.20.** Nitrile Formation via Elimination of AcOH from an *O*-Acetyl Aldoxime<sup>21b</sup>



#### 5.4 Deprotection to $\beta$ - and *ortho*-Hydroxyketones

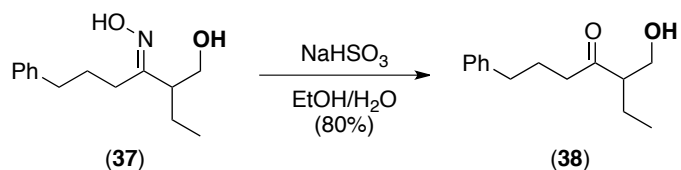
The C–H acetoxylation products in Tables 5.1 and 5.2 were obtained in yields comparable to those previously reported with oxime ethers as directing groups.<sup>12a,c</sup> Importantly, however, the *O*-acetyl oxime directing group is significantly more readily deprotected. For example,  $\beta$ -hydroxy ketones can be accessed in high yield via an operationally simple two-step procedure involving initial methanolysis of both acetate groups (to afford  $\beta$ -hydroxy oximes) followed by removal of the oxime functionality. The first step can be accomplished *via* treatment of starting materials like **10** with  $\text{K}_2\text{CO}_3$  in MeOH to afford **37** in 91% isolated yield (Scheme 5.21).

**Scheme 5.21.** Methanolysis of Acetate Groups in **10**



While numerous methods exist for the second step (conversion of an oxime to a ketone), many of our substrates are susceptible to competing formation of side products (*e.g.*, via alcohol oxidation, isoxazoline formation, or elimination). After extensive experimentation, we identified the use of  $NaHSO_3$  in  $EtOH/H_2O$ <sup>22</sup> as the most general and high yielding method to transform our oximes into  $\beta$ -hydroxy ketones, while circumventing undesired side reactions and persistent byproducts. Under these conditions, substrate **37** could be converted cleanly to **38** in 80% yield (Scheme 5.22). Compound **38** was obtained in pure form after a simple extraction, obviating the need for chromatography.

**Scheme 5.22.** Cleavage of Oxime **37** by  $NaHSO_3$  to Afford  $\beta$ -Hydroxy Ketone **38**



The two deprotection steps could also be combined to provide an operationally simple, high yielding, one-pot route from *O*-acetyl oxime C–H oxidation products to  $\beta$ -hydroxy ketones. For example, treatment of **10** with  $K_2CO_3$  in MeOH, followed by addition of  $NaHSO_3$  and  $H_2O$  provided **38** in 80% yield after a simple extractive work-up (Scheme 5.23). As shown in Table 5.3, this one-pot deprotection could also be achieved with other substrates. Under these conditions, elimination products were not observed, and isoxazoline formation was limited to  $\leq 5\%$  (for characterization of the isoxazoline contaminant see section 5.9).

**Scheme 5.23.** One Pot Deprotection of  $\beta$ -Acetoxy Acetyl Oxime **10** to  $\beta$ -Hydroxy

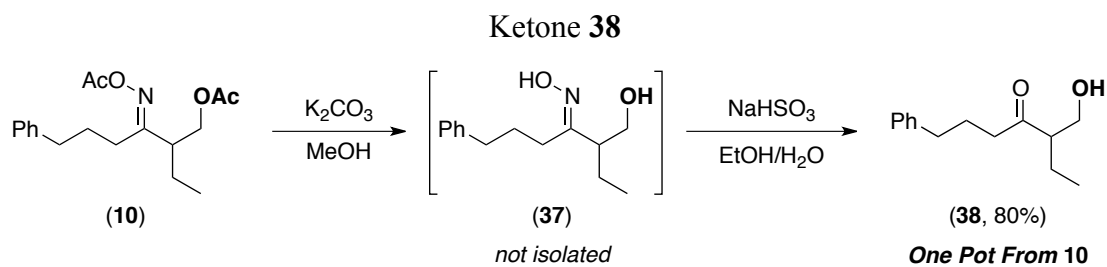


**Table 5.3.** Deprotection of  $\beta$ - and *ortho*-Acetoxy Acetyl Oximes to  $\beta$ - and *ortho*-Hydroxy Ketones

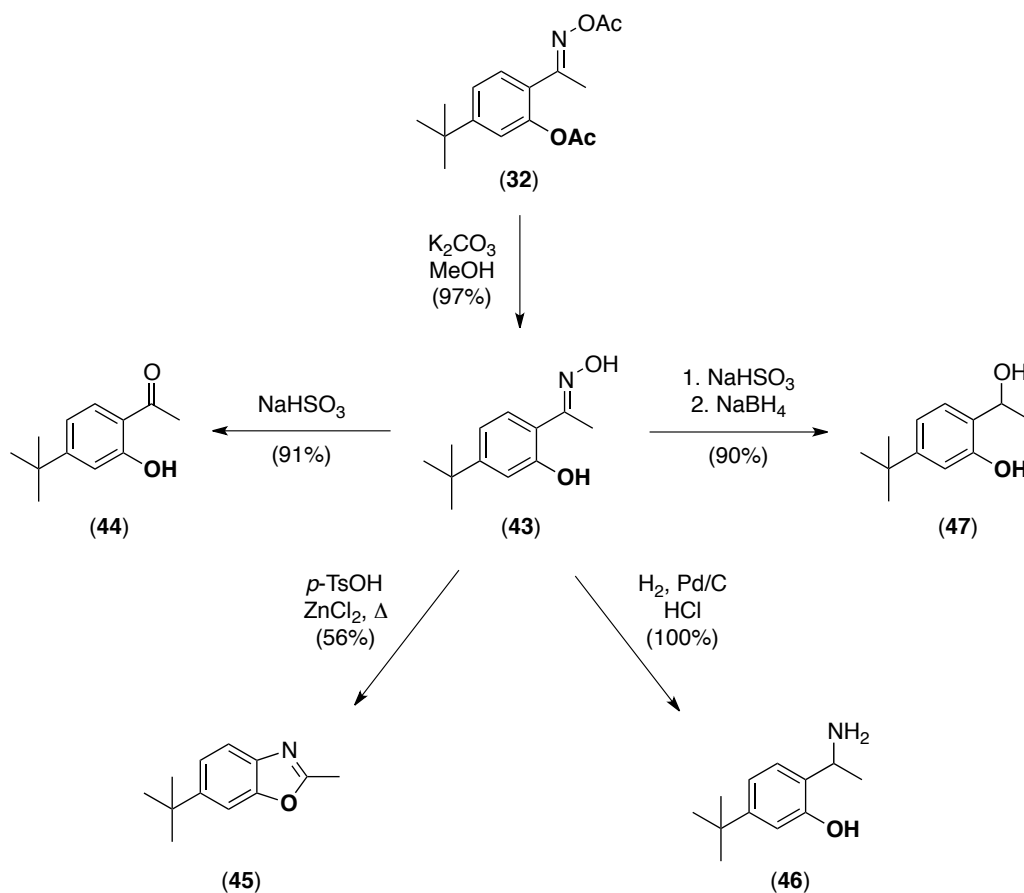
entry	substrate	product	isolated yield <sup>b</sup>
1			80%
2			56%
3			83%
4			89%

<sup>a</sup>Conditions in entries 1–3 (one pot):  $\text{K}_2\text{CO}_3$  (3 x 0.15 equiv/2.5 h), MeOH, 25 °C, then 3.5 equiv of  $\text{NaHSO}_3$ ,  $\text{H}_2\text{O}$ , 80 °C, 3 h. Conditions in entry 4 (two steps): (i) 0.15 equiv of  $\text{K}_2\text{CO}_3$ , MeOH, 25 °C, 1 h, then (ii) 3.5 equiv of  $\text{NaHSO}_3$ ,  $\text{H}_2\text{O}$ , EtOH, 90 °C, 12 h.

## 5.5 Diverse Transformations of the *O*-Acetyl Oxime Directing Group

An important characteristic of the *O*-acetyl oxime directing group is that it enables access to diverse motifs from a single synthetic intermediate. As exemplified with **32** in Scheme 5.24,  $K_2CO_3$ -catalyzed methanolysis of the acetyl groups provided oxime **43** in quantitative yield. Product **43** could then be converted to the corresponding acetophenone **44**, to benzoxazole **45** (via Beckmann rearrangement followed by intramolecular condensation), to amino phenol **46** (via reduction), and to diol **47** (via oxime hydrolysis followed by reduction).

**Scheme 5.24.** Diverse Transformations of C–H Functionalization Product **32**

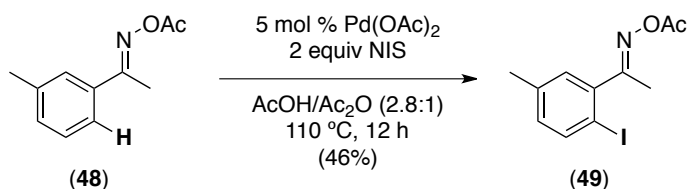


## 5.6 Other C–H Functionalizations of *O*-Acetyl Oximes

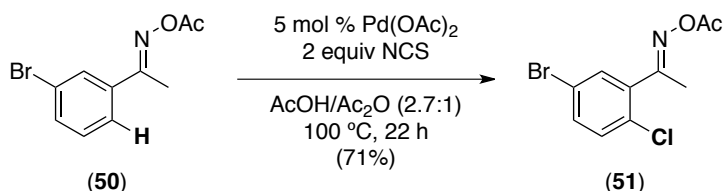
Preliminary results indicate that these *O*-acetyl oximes are also effective directing

groups for other Pd-catalyzed C–H functionalization reactions. For example, as shown in Schemes 5.25 and 5.26, the Pd-catalyzed iodination of **48** and chlorination of **50** proceed to form aryl halides **49** and **51** in modest to good yields.<sup>23</sup> Interestingly, under standard Pd-catalyzed C–H arylation conditions with PhI and AgOAc in trifluoroacetic acid (TFA),<sup>24</sup> **50** underwent an *in situ* Beckmann rearrangement/C–H phenylation to afford acetamide **52** (Scheme 5.27).

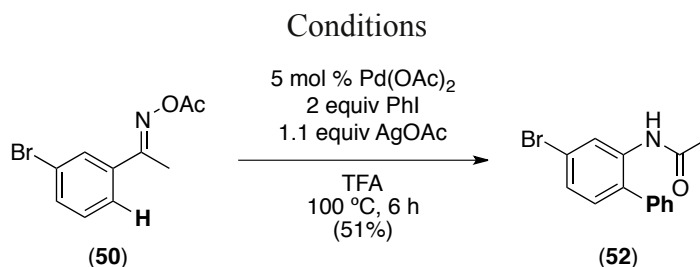
**Scheme 5.25.** *O*-Acetyl Oxime-Directed C–H Iodination



**Scheme 5.26.** *O*-Acetyl Oxime-Directed C–H Chlorination



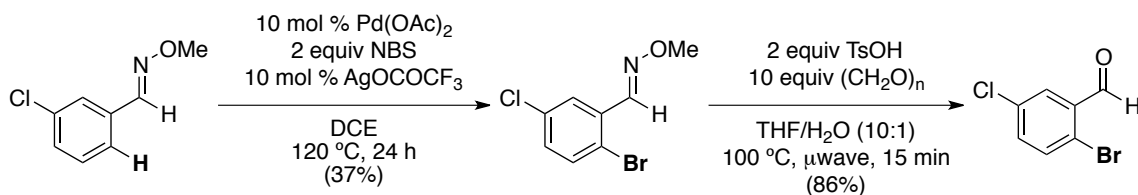
**Scheme 5.27.** Rearrangement of an *O*-Acetyl Oxime to an Anilide Under C–H Arylation



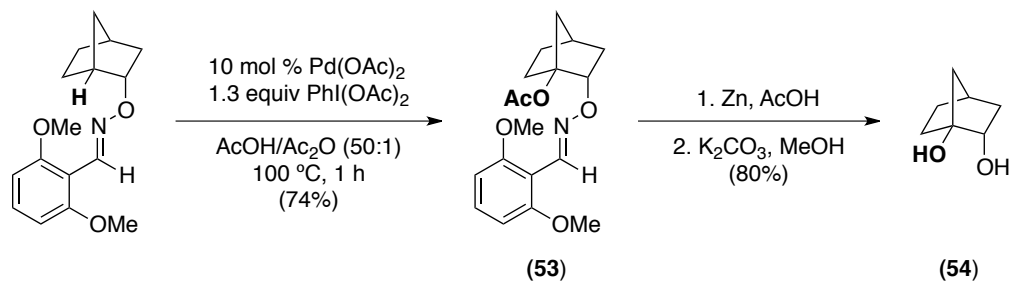
## 5.7 Subsequent Examples of Transformable Directing Groups

Since the publication of the work described in this chapter,<sup>2</sup> a number of other transformable directing groups for Pd-catalyzed C–H functionalization have been disclosed<sup>25</sup>, including two examples of transformable aldoxime ethers.<sup>26,27</sup> Methyl aldoxime ether-directed *ortho* bromination with subsequent deprotection using superstoichiometric TsOH under microwave conditions affords *ortho*-brominated benzaldehydes (Scheme 5.28).<sup>26</sup> Acetoxylation of sp<sup>3</sup> C–H bonds at the *exo* position of aldoxime ethers has also been shown, and subsequent deprotection of products like **53** with Zn/AcOH affords 1,2-diols (**54**, Scheme 5.29).<sup>27</sup>

**Scheme 5.28.** *Ortho* Bromination and Hydrolysis of Methyl Benzaldoxime Ethers<sup>26</sup>



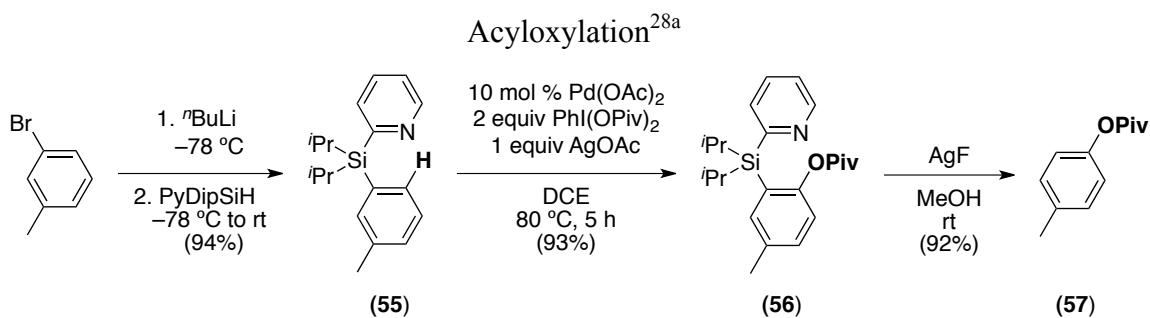
**Scheme 5.29.** *Exo*-Aldoxime Ether-Directed C–H Acetoxylation Followed by Conversion to a Diol<sup>27</sup>



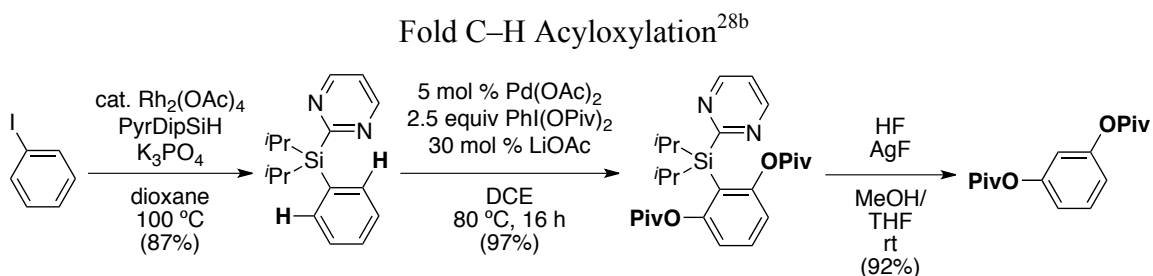
Several other types of transformable directing groups feature a coordinating pyridine moiety tethered to a substrate by a cleavable silyl,<sup>28</sup> sulfone,<sup>29</sup> aminal,<sup>30a</sup> amide,<sup>30b</sup> or sulfoximine<sup>31</sup> linkage. For example, Gevorgyan has demonstrated *ortho* acyloxylation of arenes using the pyridyldiisopropylsilyl (PyDipSi) directing group (**55**, Scheme 5.30).<sup>28a</sup> This group can act as a ‘traceless’ ligand that can be completely removed by AgF to afford products like **57** from **56**. Conversion of a PyDipSi-directed

C–H functionalization product like **56** into an aryl iodide, aryl boronate, catechol, and a biaryl has also been demonstrated. Arene acyloxylation with the PyDipSi directing group is highly mono-selective; however, double-fold acyloxylation can be achieved with the related pyrimidinyldiisopropylsilyl (PyrDipSi) moiety (Scheme 5.31).<sup>28b</sup>

**Scheme 5.30.** Pyridyldiisopropylsilyl as a Traceless Directing Group for C–H

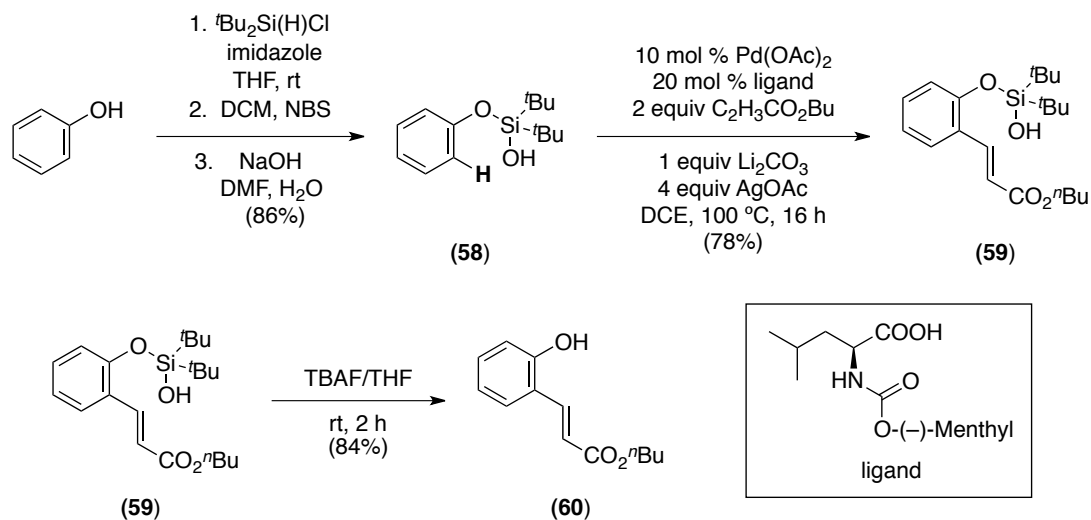


**Scheme 5.31.** Pyrimidinyldiisopropylsilyl as a Traceless Directing Group for Double-



The lability of silyl linkages has also been exploited for C–H olefination<sup>32a,b</sup> and oxygenation<sup>32c</sup> of aryl substrates that employ silanol as a transformable directing ligand (e.g., **58**, Scheme 5.32). When tethered by an oxygen atom, removal of the silanol directing group from **59** reveals phenol **60** (Scheme 5.32).<sup>32a,c</sup> Alternatively, silanols linked by a methylene have been deprotected to provide substituted toluenes.<sup>32b</sup>

**Scheme 5.32.** Silanol-Directed *ortho* C–H Olefination of Arenes with Subsequent Deprotection to a Phenol<sup>32a</sup>



Finally, a number of other recent examples of transformable directing groups for acetoxylation<sup>33</sup>, arylation<sup>34</sup>, and olefination<sup>35</sup> rely on amide-type linkages that can be hydrolyzed to carboxylic acids or amines.

## 5.8 Conclusions and Outlook

This chapter describes the use of *in situ* generated *O*-acetyl oximes as effective directing groups in Pd-catalyzed C–H functionalization reactions. These directing groups are stable under the catalytic reaction conditions but can then be readily manipulated to afford ketones, alcohols, amines, and heterocycles. At present, this work represents the only instance of a ketone-derived transformable directing group for Pd-catalyzed C–H functionalization. Over the past 5 years, the search for effective, convenient, and versatile transformable directing groups has gained momentum. Nevertheless, numerous challenges remain to be addressed.

Table 5.4 summarizes the current state-of-the-art for transformable directing groups for Pd-catalyzed C–H functionalization. Clearly, a broad range of substrate classes can serve as synthons for C–H functionalized products. These synthons include phenols (entry 1), thiophenols (entry 2), aryl halides (entries 3 and 4), anilines (entry 5), benzaldehydes (entries 6 and 7), benzoic acids (entries 8–11), phenyl ketones (entry 12),



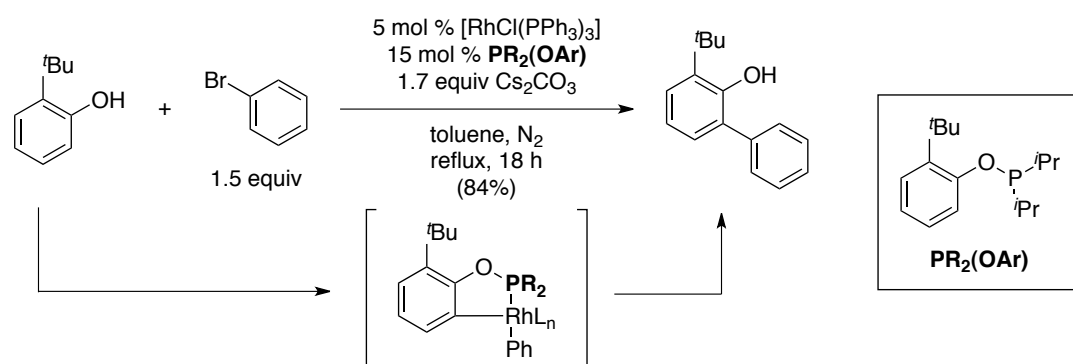
benzylamines (entries 13 and 14), benzyl chlorides (entry 15), 3-aryl carboxylic acids (entry 16), aliphatic alcohols (entry 17), aliphatic amines (entry 18), alkyl ketones (entry 19), and alkyl carboxylic acids (entries 20–22). Although much progress has been made over the past few years, most of the groups represented in Table 5.4 have limited generality, and have only been developed for a single type of C–H functionalization reaction. Furthermore, deprotection usually requires relatively high temperatures and/or the use of strong acids or bases. Silyl-tethered directing groups (entries 1 and 14) can be removed under relatively mild conditions (room temperature with a fluoride source, Schemes 5.30–5.32), but the use of these ligands has not been demonstrated for  $sp^3$ -C–H functionalization.

**Table 5.4.** Transformable Directing Groups for Pd-Catalyzed C–H Functionalization

entry	synthon	substrate-DG	C–H functionalization	entry	synthon	substrate-DG	C–H functionalization
1			olefination <sup>32a</sup> oxygenation <sup>32c</sup>	12			acetoxylation <sup>2</sup>
2			acetoxylation <sup>29</sup>	13			olefination <sup>3</sup>
3			mono-acyloxylation <sup>28a</sup>	14			fluorination <sup>4</sup>
4			di-acyloxylation <sup>28b</sup>	15			olefination <sup>32b</sup>
5			arylation <sup>34a</sup>	16			olefination <sup>35</sup>
6			bromination <sup>26</sup>	17			acetoxylation <sup>27</sup>
7			acetoxylation <sup>30a</sup>	18			oxygenation <sup>30b</sup>
8			arylation <sup>6,7c</sup>	19			acetoxylation <sup>2</sup>
9			acetoxylation <sup>33</sup>	20			iodination <sup>5</sup>
10			arylation <sup>34b</sup>	21			arylation <sup>7b</sup>
11			arylation <sup>7a</sup>	22			acyloxylation <sup>31</sup>

Moreover, a major drawback to the directing group strategy is the requirement for stoichiometric quantities of a directing ligand. Instead, the ability to use a directing ligand *catalytically* would be more atom economical and would eliminate the need for separate deprotection steps. Examples of catalytic directing groups exist for transformations mediated by other metals. For instance, rhodium-catalyzed *ortho* arylation of phenols can be achieved using only 15 mol % of an arylphosphinite ligand, which binds to the substrate (and to Rh) reversibly *in situ* (Scheme 5.33).<sup>36</sup>

**Scheme 5.33.** Rh-Catalyzed *ortho* Arylation of Phenols Using a Catalytic Directing Group<sup>36</sup>



It is expected that maturation of the field of ligand-directed Pd-catalyzed C–H functionalization will result in the development of directing groups that are general for diverse transformations and can be used catalytically.

## 5.9 Experimental Procedures and Characterization Data

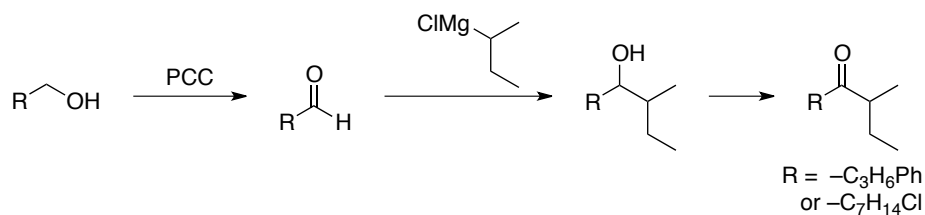
### General Procedures

NMR spectra were obtained on a Varian Inova 500 (499.90 MHz for  $^1\text{H}$ ; 125.70 MHz for  $^{13}\text{C}$ ), a Varian Inova 400 (399.96 MHz for  $^1\text{H}$ ; 100.57 MHz for  $^{13}\text{C}$ ), or a Varian MR400 (399.54 or 400.52 MHz for  $^1\text{H}$ ; 100.71 MHz for  $^{13}\text{C}$ ; 376.88 MHz for  $^{19}\text{F}$ ) spectrometer.  $^1\text{H}$  and  $^{13}\text{C}$  NMR chemical shifts are reported in parts per million (ppm) relative to TMS, with the residual solvent peak used as an internal reference. Multiplicities are reported as follows: singlet (s), doublet (d), doublet of doublets (dd), doublet of doublets of doublets

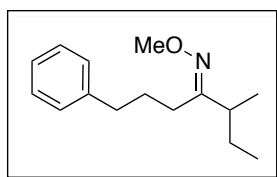
(ddd), doublet of doublets of doublets of doublets (dddd), triplet (t), quartet (q), quintet (quin), sextet (sext), doublet of triplets (dt), triplet of doublets (td), quartet of triplets (qt), multiplet (m), and broad resonance (br). IR spectra were obtained on a Perkin-Elmer Spectrum BX FT-IR spectrometer. Melting points were determined with a Mel-Temp 3.0, a Laboratory Devices Inc, USA instrument, and are uncorrected. HRMS data were obtained on a Micromass AutoSpec Ultima Magnetic Sector mass spectrometer. Gas chromatography was carried out on a Shimadzu 17A using a Restek Rtx®-5 (Crossbond 5% diphenyl – 95% dimethyl polysiloxane; 15 m, 0.25 mm ID, 0.25  $\mu$ m df) column.

**Materials and Methods.** All commercial reagents and solvents were used as received without further purification. Pd(OAc)<sub>2</sub> and PhI(OAc)<sub>2</sub> were obtained from Pressure Chemical and TCI America, respectively. Ac<sub>2</sub>O was obtained from EMD Chemicals, and all other solvents were obtained from Fisher Chemical. Flash chromatography was performed on EM Science silica gel 60 (0.040-0.063 mm particle size, 230-400 mesh) and thin layer chromatography was performed on Merck TLC plates pre-coated with silica gel 60 F254. Ketone **6** and the ketone used to prepare oxime substrate **15** were prepared by the sequential oxidation of a commercial alcohol to an aldehyde, treatment with *sec*-butyl Grignard, and oxidation of the resulting alcohol to the ketone (below). The parent ketone of oxime **13** was prepared by further treatment of the alkyl chloride parent ketone of **15** with potassium phthalimide.

**Scheme 5.34.** Synthetic Route to Ketone **6** and Related Ketones

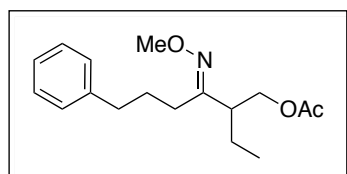


*Synthesis and Characterization of Compounds in Schemes 5.11–5.13*



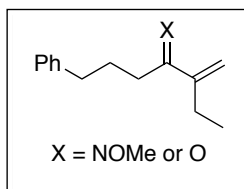
**Oxime Ether 1.** Ketone **6** (500 mg, 2.45 mmol, 1 equiv) was combined with  $\text{NH}_2\text{OMe}\cdot\text{HCl}$  (256 mg, 2.94 mmol, 1.2 equiv) in pyridine (1.06 mL) in a 20 mL scintillation vial. The vial was sealed with a Teflon-lined cap and heated to 80 °C for 15 min.

The reaction mixture was then diluted with EtOAc (5 mL) and washed with 20% aqueous AcOH (5 x 5 mL) to remove pyridine. The organic layer was then neutralized with aqueous  $\text{NaHCO}_3$ , washed with brine, dried over  $\text{MgSO}_4$ , and concentrated to yield methyl oxime **1** as a colorless oil consisting of ~1.6:1 ratio of major and minor *E/Z* isomers (556 mg, 97% yield). Major Isomer:  $^1\text{H}$  NMR (400 MHz,  $\text{CDCl}_3$ ):  $\delta$  7.29 (m, 2H), 7.21–7.19 (multiple peaks, 3H), 3.813 (s, 3H), 2.66 (m, 2H), 2.30–2.14 (multiple peaks, 3H), 1.92–1.79 (multiple peaks, 2H), 1.50 (m, 1H), 1.36 (m, 1H), 1.05 (d,  $J = 6.8$  Hz, 3H), 0.872 (t,  $J = 7.2$  Hz, 3H).  $^{13}\text{C}\{^1\text{H}\}$  NMR ( $\text{CDCl}_3$ ):  $\delta$  164.13, 141.94, 128.35, 128.27, 125.80, 61.01, 40.71, 36.37, 27.92, 27.06, 26.43, 17.88, 11.92. Minor Isomer (distinct resonances):  $^1\text{H}$  NMR (400 MHz,  $\text{CDCl}_3$ ):  $\delta$  3.809 (s, 3H), 3.08 (m, 1H), 1.02 (d,  $J = 7.2$  Hz, 3H), 0.867 (t,  $J = 7.2$  Hz, 3H).  $^{13}\text{C}\{^1\text{H}\}$  NMR ( $\text{CDCl}_3$ ):  $\delta$  163.63, 142.22, 128.43, 125.72, 61.03, 35.77, 34.17, 29.97, 28.53, 26.54, 16.74, 12.15. IR (thin film, mixture of *E/Z* isomers): 2962, 2935, 1454  $\text{cm}^{-1}$ . HRMS electrospray ( $m/z$ ):  $[\text{M}+\text{H}]^+$  calcd for  $\text{C}_{15}\text{H}_{24}\text{NO}$  (mixed isomers), 234.1858; found, 234.1866.



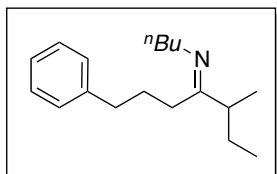
**$\beta$ -Acetoxy Oxime Ether 2.** Methyl oxime **1** (14.6 mg, 0.050 mmol, 1 equiv) was combined with  $\text{Pd}(\text{OAc})_2$  (0.6 mg, 0.0025 mmol, 0.05 equiv) and  $\text{PhI}(\text{OAc})_2$  (32.2 mg, 0.100 mmol, 2 equiv) in AcOH/ $\text{Ac}_2\text{O}$  (1:1, 416  $\mu\text{L}$ ) in a 4 mL scintillation vial. The vial was sealed with a Teflon-lined cap and heated to 100 °C for 12 h to afford **2** as a pale yellow oil (64% calibrated GC yield).  $^1\text{H}$  NMR (400 MHz,  $\text{CDCl}_3$ ):  $\delta$  7.28 (m, 2H), 7.21–7.17 (multiple peaks, 3H), 4.11 (m, 2H), 3.81 (s, 3H), 2.64 (t,  $J = 7.6$  Hz, 2H), 2.48 (quin,  $J = 7.2$  Hz, 1H), 2.31–2.15 (multiple peaks, 2H), 2.02 (s, 3H), 1.81 (m, 2H), 1.52 (m, 2H), 0.89 (t,  $J = 7.6$  Hz, 3H).  $^{13}\text{C}\{^1\text{H}\}$  NMR ( $\text{CDCl}_3$ ):  $\delta$  170.92, 159.89, 141.77, 128.32, 128.30, 125.85, 65.18, 61.30, 45.01, 36.16, 27.40, 27.32,

22.34, 20.90, 11.31. IR (thin film): 2963, 2936, 1740  $\text{cm}^{-1}$ . HRMS electrospray ( $m/z$ ):  $[\text{M}+\text{Na}]^+$  calcd for  $\text{NaC}_{17}\text{H}_{25}\text{NO}_3$ , 314.1732; found, 314.1731.



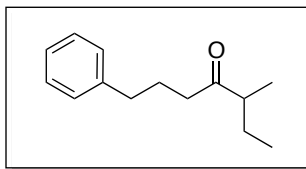
**Elimination Products 3 and 4.**  $\beta$ -Acetoxyated oxime ether **2** (12.7 mg, 0.0436 mmol, 1 equiv) was dissolved in 0.5 M HCl/ $\text{CH}_2\text{Cl}_2$  (436  $\mu\text{L}$ ) in a 4 mL scintillation vial. The vial was sealed with a Teflon-lined cap and heated to 70  $^\circ\text{C}$  for 3 h.

Reaction solvent was removed by rotary evaporator and crude residue was analyzed by  $^1\text{H}$  NMR. Elimination was identified by the presence of two sets of olefin peaks (see NMR spectrum in Supporting Information of reference 2). Integration of these peaks relative to an internal standard ( $\text{PhNO}_2$ ) indicates a total of 41% yield of elimination products.



**Butyl Imine 5.** Ketone **6** (250 mg, 1.22 mmol, 1 equiv) was combined with *n*-butylamine (2.42 mL, 24.48 mmol, 20 equiv), *p*-TsOH monohydrate (4.6 mg, 0.0244 mmol, 0.02 equiv), and 4  $\text{\AA}$  molecular sieves (2 g) in toluene (1.9 mL) in a 20 mL scintillation vial. The vial was sealed with a Teflon-lined cap and heated to 110  $^\circ\text{C}$  for 16 h. Solid  $\text{NaHCO}_3$  was added (30 mg); reaction was then diluted with hexanes, filtered through celite, and concentrated to afford imine **5** as a yellow oil consisting of  $\sim$ 3:1 ratio of major to minor *E/Z* isomers (300 mg, 95% yield). Major Isomer:  $^1\text{H}$  NMR (400 MHz,  $\text{CDCl}_3$ ):  $\delta$  7.31–7.17 (multiple peaks, 5H), 3.25 (t,  $J = 7.2$  Hz, 2H), 2.64 (t,  $J = 7.6$  Hz, 2H), 2.26–2.15 (multiple peaks, 3H), 1.75 (m, 2H), 1.60–1.55 (multiple peaks, 2H), 1.44–1.24 (multiple peaks, 4H), 1.02 (d,  $J = 6.8$  Hz, 3H), 0.90 (t,  $J = 7.2$  Hz, 3H), 0.84 (t,  $J = 7.4$  Hz, 3H).  $^{13}\text{C}\{^1\text{H}\}$  NMR ( $\text{CDCl}_3$ ):  $\delta$  175.71, 141.55, 128.37, 128.34, 125.98, 50.44, 45.56, 36.29, 33.33, 29.45, 28.41, 27.48, 20.66, 18.22, 14.02, 12.08. Minor Isomer (distinct resonances):  $^1\text{H}$  NMR (400 MHz,  $\text{CDCl}_3$ ):  $\delta$  3.34 (t,  $J = 7.2$  Hz, 2H), 2.79 (m, 1H), 1.89 (m, 2H), 0.98 (d,  $J = 7.0$  Hz, 3H), 0.93 (t,  $J = 7.4$  Hz, 3H).  $^{13}\text{C}\{^1\text{H}\}$  NMR ( $\text{CDCl}_3$ ):  $\delta$  175.29, 142.64, 128.46, 128.18, 125.57, 49.65, 36.44, 35.95, 33.48, 33.04, 29.03, 27.09, 20.70, 17.43, 12.27. IR (thin film, mixture of *E/Z* isomers): 2959, 2930,

2872, 1711, 1657  $\text{cm}^{-1}$ . HRMS electrospray ( $m/z$ ):  $[\text{M}+\text{H}]^+$  calcd for  $\text{C}_{18}\text{H}_{30}\text{N}$  (mixture of *E/Z* isomers), 260.2378; found, 260.2380.

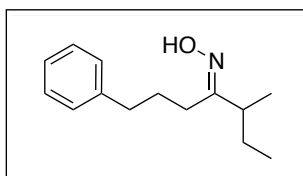


**Ketone 6.** Ketone **6** was synthesized as described in the Materials and Methods section. Additionally, **6** was formed as the major product from the reaction depicted in Scheme 5.13.

From reaction of imine 5: Imine **5** (10 mg, 0.0385 mmol, 1 equiv) was combined with  $\text{Pd}(\text{OAc})_2$  (0.4 mg, 0.0019 mmol, 0.05 equiv) and  $\text{PhI}(\text{OAc})_2$  (24.8 mg, 0.077 mmol, 2 equiv) in  $\text{AcOH}/\text{Ac}_2\text{O}$  (1:1, 320  $\mu\text{L}$ ) in a 4 mL scintillation vial. The vial was sealed with a Teflon-lined cap and heated to 100  $^\circ\text{C}$  for 1 h to afford ketone **6** as the major product observable by GC (39% calibrated GC yield).  $^1\text{H}$  NMR (400 MHz,  $\text{CDCl}_3$ ):  $\delta$  7.28 (m, 2H), 7.21–7.17 (multiple peaks, 3H), 2.62 (t,  $J = 7.4$  Hz, 2H), 2.46–2.38 (multiple peaks, 3H), 1.91 (quin,  $J = 7.4$  Hz, 2H), 1.66 (sept,  $J = 7.4$  Hz, 1H), 1.36 (sept,  $J = 7.4$  Hz, 1H), 1.04 (d,  $J = 7.0$  Hz, 3H), 0.86 (t,  $J = 7.4$  Hz, 3H).  $^{13}\text{C}\{^1\text{H}\}$  NMR ( $\text{CDCl}_3$ ):  $\delta$  214.59, 141.72, 128.43, 128.33, 125.87, 47.85, 40.31, 35.14, 25.90, 25.08, 15.90, 11.69. IR (thin film, mixture of *E/Z* isomers): 2964, 2933, 2876, 1707  $\text{cm}^{-1}$ . HRMS electrospray ( $m/z$ ):  $[\text{M}+\text{Na}]^+$  calcd for  $\text{C}_{14}\text{H}_{20}\text{O}$  (mixture of *E/Z* isomers), 227.1412; found, 227.1411.

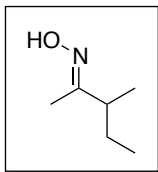
### Synthesis and Characterization of Oxime Substrates

**General Procedure:** Ketone (1 equiv) and  $\text{NH}_2\text{OH}\cdot\text{HCl}$  (1.35 equiv) were combined in pyridine (0.385 mL/mmol ketone) in a scintillation vial. The vial was sealed with a Teflon-lined cap, and the mixture was heated to 80 °C for 15 min or until the starting material had disappeared (as determined by TLC) after which time an aqueous layer was observable in the reaction mixture. The reaction mixture was diluted by 5-fold with EtOAc or  $\text{Et}_2\text{O}$  and washed with 20% aqueous AcOH (5 x equal volume to the organic layer) to remove pyridine. The organic layer was then neutralized with aqueous  $\text{NaHCO}_3$ , washed with brine, dried over  $\text{MgSO}_4$ , and concentrated to yield the oxime. Where noted, the oximes were obtained as mixtures of *E* and *Z* stereoisomers. In these cases, the ratio is reported based on  $^1\text{H}$  NMR integration. In all cases, complete  $^1\text{H}$  and  $^{13}\text{C}$  NMR data are reported for the major isomer. In addition, all of the distinct resonances associated with the minor isomer are reported for both the  $^1\text{H}$  and  $^{13}\text{C}$  NMR spectra (many of the peaks for the minor isomer are coincidentally overlapping with those of the major isomer).

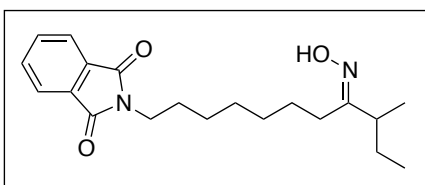


**Oxime 7.** The general procedure was followed utilizing ketone **6** (4.68 g, 22.9 mmol). The product was obtained as a pale yellow oil consisting of a ~3.3:1 mixture of major and minor oxime stereoisomers (4.99 g, 99% yield). Major Isomer:  $^1\text{H}$  NMR (400 MHz,  $\text{CDCl}_3$ ):  $\delta$  8.05 (br s, 1H), 7.28 (m, 2H), 7.21–7.18 (multiple peaks, 3H), 2.68 (t,  $J = 7.6$  Hz, 2H), 2.37–2.21 (multiple peaks, 3H), 1.88 (m, 2H), 1.52 (m, 1H), 1.37 (m, 1H), 1.06 (d,  $J = 7.2$  Hz, 3H), 0.87 (t,  $J = 7.6$  Hz, 3H).  $^{13}\text{C}\{^1\text{H}\}$  NMR ( $\text{CDCl}_3$ ):  $\delta$  164.43, 141.90, 128.35, 128.26, 125.78, 40.55, 36.33, 27.51, 26.96, 26.46, 17.61, 11.81. Minor Isomer (distinct resonances):  $^1\text{H}$  NMR (400 MHz,  $\text{CDCl}_3$ ):  $\delta$  3.21 (sextet,  $J = 7.2$  Hz, 1H), 2.18 (m, 2H), 1.04 (d,  $J = 7.2$  Hz, 3H), 0.88 (t,  $J = 7.2$  Hz, 3H).  $^{13}\text{C}\{^1\text{H}\}$  NMR ( $\text{CDCl}_3$ ):  $\delta$  163.95, 141.91, 128.41, 125.74, 35.55, 33.36, 29.67, 27.56, 26.40, 16.51, 12.13. IR (thin film, mixture of *E/Z* isomers): 3251, 2962, 2931, 2874, 1453  $\text{cm}^{-1}$ . HRMS electrospray ( $m/z$ ):  $[\text{M}+\text{H}]^+$  calcd for  $\text{C}_{14}\text{H}_{22}\text{NO}$  (mixture of *E/Z* isomers), 220.1701; found, 220.1698.

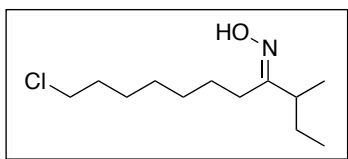




**Oxime 11.** The general procedure was followed utilizing 3-methyl-2-pentanone (2.00 g, 20.0 mmol). The product was obtained as a colorless oil consisting of an ~8:1 mixture of major and minor oxime stereoisomers (1.90 g, 83% yield). Major Isomer:  $^1\text{H}$  NMR (400 MHz,  $\text{CDCl}_3$ ):  $\delta$  8.20 (br s, 1H), 2.28 (sext,  $J = 7.2$  Hz, 1H), 1.81 (s, 3H), 1.52 (m, 1H), 1.40 (m, 1H), 1.07 (d,  $J = 7.2$  Hz, 3H), 0.86 (t,  $J = 7.6$  Hz, 3H).  $^{13}\text{C}\{^1\text{H}\}$  NMR ( $\text{CDCl}_3$ ):  $\delta$  161.97, 41.20, 26.80, 17.49, 11.76, 10.36. Minor Isomer (distinct resonances):  $^1\text{H}$  NMR (400 MHz,  $\text{CDCl}_3$ ):  $\delta$  3.30 (m, 1H), 1.78 (s, 3H), 1.03 (d,  $J = 6.8$  Hz, 3H), 0.89 (t,  $J = 7.4$  Hz, 3H).  $^{13}\text{C}\{^1\text{H}\}$  NMR ( $\text{CDCl}_3$ ):  $\delta$  32.53, 26.46, 16.60, 15.32, 11.93. IR (thin film, mixture of *E/Z* isomers): 3230, 2963, 2932, 2876, 1460  $\text{cm}^{-1}$ . HRMS electron impact ( $m/z$ ):  $[\text{M}]^+$  calcd for  $\text{C}_6\text{H}_{13}\text{NO}$  (mixture of *E/Z* isomers), 115.0997; found, 115.1001.

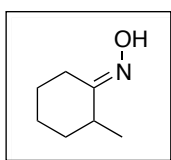


**Oxime 13.** The general procedure was followed utilizing 2-(9-methyl-8-oxoundecyl)isoindoline-1,3-dione (4.00 g, 12.1 mmol). The product was obtained as a pale yellow solid consisting of a ~3.4:1 mixture of major and minor oxime stereoisomers (3.68 g, 88% yield, mp = 39–43 °C). Major Isomer:  $^1\text{H}$  NMR (400 MHz,  $\text{CDCl}_3$ ):  $\delta$  8.90 (br s, 1H), 7.76 (dd,  $J = 5.6, 3.2$  Hz, 2H), 7.68 (dd,  $J = 5.6, 3.2$  Hz, 2H), 3.65 (t,  $J = 7.6$  Hz, 2H), 2.28–2.18 (multiple peaks, 3H), 1.65 (m, 2H), 1.57–1.45 (multiple peaks, 3H), 1.33 (br s, 7H), 1.04 (d,  $J = 7.2$  Hz, 3H), 0.85 (t,  $J = 7.2$  Hz, 3H).  $^{13}\text{C}\{^1\text{H}\}$  NMR ( $\text{CDCl}_3$ ):  $\delta$  168.41, 164.76, 133.77, 132.10, 123.09, 40.48, 37.96, 29.98, 28.80, 28.48, 26.98, 26.68, 26.59, 25.82, 17.60, 11.77. Minor Isomer (distinct resonances):  $^1\text{H}$  NMR (400 MHz,  $\text{CDCl}_3$ ):  $\delta$  3.18 (sext,  $J = 7.2$  Hz, 1H), 2.09 (m, 2H), 1.02 (d,  $J = 7.2, 3\text{H}$ ), 0.86 (t,  $J = 7.2$  Hz, 3H).  $^{13}\text{C}\{^1\text{H}\}$  NMR ( $\text{CDCl}_3$ ):  $\delta$  164.19, 33.27, 29.30, 28.85, 28.45, 26.59, 26.40, 26.02, 16.53, 12.10. IR (KBr, mixture of *E/Z* isomers): 3252, 2931, 2858, 1768, 1716, 1394  $\text{cm}^{-1}$ . HRMS electrospray ( $m/z$ ):  $[\text{M}+\text{Na}]^+$  calcd for  $\text{NaC}_{20}\text{H}_{28}\text{N}_2\text{O}_3$  (mixture of *E/Z* isomers), 367.1998; found, 367.2007.



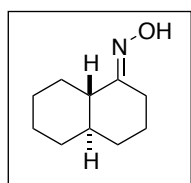
**Oxime 15.** The general procedure was followed utilizing 11-chloro-3-methylundecan-4-one (2.11 g, 9.64 mmol). The product was obtained as a colorless oil consisting of a ~6:1 mixture of major and minor oxime stereoisomers

(612 mg, 27% yield). Major Isomer:  $^1\text{H}$  NMR (400 MHz,  $\text{CDCl}_3$ ):  $\delta$  3.53 (t,  $J = 6.8$  Hz, 2H), 2.29–2.22 (multiple peaks, 3H), 1.77 (quin,  $J = 6.8$  Hz, 2H), 1.62–1.50 (multiple peaks, 3H), 1.48–1.31 (multiple peaks, 7H), 1.07 (d,  $J = 6.8$  Hz, 3H), 0.88 ( $J = 7.6$  Hz, 3H). Exchangeable proton (OH) was not observed.  $^{13}\text{C}\{^1\text{H}\}$  NMR ( $\text{CDCl}_3$ ):  $\delta$  165.12, 45.10, 40.55, 32.57, 29.99, 28.54, 27.03, 26.74, 26.57, 25.86, 17.67, 11.83. Minor Isomer (distinct resonances):  $^1\text{H}$  NMR (400 MHz,  $\text{CDCl}_3$ ):  $\delta$  3.21 (sext,  $J = 7.2$  Hz, 1H), 2.13 (m, 2H), 1.05 (d,  $J = 7.2$  Hz, 3H), 0.89 (t,  $J = 7.6$  Hz, 3H).  $^{13}\text{C}\{^1\text{H}\}$  NMR ( $\text{CDCl}_3$ ):  $\delta$  33.36, 30.05, 29.35, 28.65, 26.77, 26.47, 26.12, 12.15. IR (thin film, mixture of *E/Z* isomers): 3250, 2961, 2931, 2858, 1457  $\text{cm}^{-1}$ . HRMS electrospray ( $m/z$ ):  $[\text{M}+\text{H}]^+$  calcd for  $\text{C}_{12}\text{H}_{25}\text{ClNO}$  (mixture of *E/Z* isomers), 234.1625; found, 234.1624.



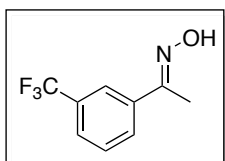
**Oxime 17.** The general procedure was followed utilizing 2-methylcyclohexanone (1.35 g, 12.0 mmol). The product was obtained as a pale yellow oil consisting of a ~5:1 mixture of major and minor oxime stereoisomers (1.37 g, 90% yield). Major Isomer:  $^1\text{H}$  NMR (500 MHz,  $\text{CDCl}_3$ ):  $\delta$  8.82 (br s, 1H), 3.09 (m, 1H), 2.31 (m, 1H), 1.94–1.84 (multiple peaks, 2H), 1.78 (m, 2H), 1.48 (m, 2H), 1.31 (m, 1H), 1.12 (d,  $J = 7.0$  Hz, 3H).  $^{13}\text{C}\{^1\text{H}\}$  NMR ( $\text{CDCl}_3$ ):  $\delta$  163.49, 37.16, 35.57, 26.02, 24.67, 23.82, 16.82. Minor Isomer (distinct resonances):  $^1\text{H}$  NMR (500 MHz,  $\text{CDCl}_3$ ):  $\delta$  9.12 (br s, 1H), 3.58 (m, 1H), 2.22 (m, 2H).

$^{13}\text{C}\{^1\text{H}\}$  NMR ( $\text{CDCl}_3$ ):  $\delta$  31.57, 28.27, 26.63, 20.33, 16.21. IR (thin film, mixture of *E/Z* isomers): 3270, 2963, 2927, 2856, 1444  $\text{cm}^{-1}$ . HRMS electron impact ( $m/z$ ):  $[\text{M}]^+$  calcd for  $\text{C}_7\text{H}_{13}\text{NO}$  (mixture of *E/Z* isomers), 127.0997; found, 127.1001.

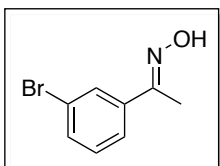


**Oxime 19.** The general procedure was followed utilizing *trans*-1-decalone (4.58 g, 30.1 mmol). The product was obtained as a white fluffy solid consisting of a single oxime isomer (4.77 g, 95% yield, mp

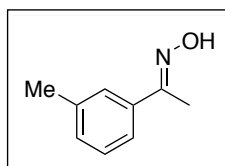
= 157–158 °C).  $^1\text{H}$  NMR (500 MHz,  $\text{CDCl}_3$ ):  $\delta$  3.42 (dddd,  $J = 13.8, 4.4, 2.7, 2.0$  Hz, 1H), 1.94 (m, 1H), 1.88 (m, 1H), 1.82–1.74 (multiple peaks, 2H), 1.72–1.67 (multiple peaks, 3H), 1.61 (td,  $J = 13.8, 5.0$  Hz, 1H), 1.43 (qt,  $J = 13.0, 4.0$  Hz, 1H), 1.35–1.16 (multiple peaks, 5H), 1.08 (m, 1H). Exchangeable proton (OH) was not observed.  $^{13}\text{C}\{^1\text{H}\}$  NMR ( $\text{CDCl}_3$ ):  $\delta$  162.22, 47.63, 44.20, 34.26, 33.59, 26.63, 25.95, 25.90, 25.33, 24.77. IR (KBr): 3226, 2161, 2923, 2847, 1439  $\text{cm}^{-1}$ . HRMS electrospray ( $m/z$ ):  $[\text{M}]^+$  calcd for  $\text{C}_{10}\text{H}_{17}\text{NO}$ , 167.1310; found, 167.1310.



**Oxime 21.** The general procedure was followed utilizing 3'-(trifluoromethyl)acetophenone (759 mg, 4.03 mmol). The product was obtained as a white solid consisting of a single oxime isomer (789 mg, 96% yield, mp = 58–60 °C).  $^1\text{H}$  NMR (500 MHz,  $\text{CDCl}_3$ ):  $\delta$  9.41 (s, 1H), 7.89 (s, 1H), 7.82 (d,  $J = 8.0$  Hz, 1H), 7.64 (d,  $J = 8.0$  Hz, 1H), 7.51 (t,  $J = 8.0$  Hz, 1H), 2.33 (s, 3H).  $^{13}\text{C}\{^1\text{H}\}$  NMR ( $\text{CDCl}_3$ ):  $\delta$  155.09, 137.27, 130.99 (q,  $J = 32.7$  Hz), 129.24 (q,  $J = 1.1$  Hz), 129.02, 125.83 (q,  $J = 3.8$  Hz), 123.94 (q,  $J = 272.5$  Hz), 122.95 (q,  $J = 3.8$  Hz), 12.22.  $^{19}\text{F}$  NMR ( $\text{CDCl}_3$ ):  $\delta$  -62.8. IR (KBr): 3256, 3086, 2924, 1465  $\text{cm}^{-1}$ . HRMS electrospray ( $m/z$ ):  $[\text{M}+\text{H}]^+$  calcd for  $\text{C}_9\text{H}_8\text{F}_3\text{NO}$ , 204.0636; found, 204.0636.

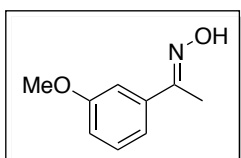


**Oxime 23.** The general procedure was followed utilizing 3'-bromoacetophenone (2.99 g, 15.0 mmol). The product was obtained as a white solid consisting of a single oxime isomer (3.17 g, 99% yield, mp = 92–93 °C).  $^1\text{H}$  NMR (500 MHz,  $\text{CDCl}_3$ ):  $\delta$  8.69 (s, 1H), 7.77 (t,  $J = 1.7$  Hz, 1H), 7.56 (m, 1H), 7.51 (ddd,  $J = 7.8, 1.7, 1.0$  Hz, 1H), 7.257 (t,  $J = 7.8$  Hz, 1H), 2.28 (s, 3H).  $^{13}\text{C}\{^1\text{H}\}$  NMR ( $\text{CDCl}_3$ ):  $\delta$  154.98, 138.42, 132.19, 130.00, 129.16, 124.61, 122.68, 12.27. IR (KBr): 3239, 2912, 1418  $\text{cm}^{-1}$ . HRMS electron impact ( $m/z$ ):  $[\text{M}]^+$  calcd for  $\text{C}_8\text{H}_8\text{BrNO}$  212.9789; found, 212.9790.

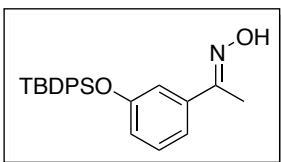


**Oxime 25.** The general procedure was followed utilizing 3'-methylacetophenone (2.01 g, 15.0 mmol). The product was obtained

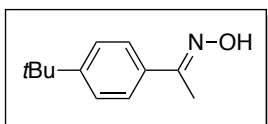
as a white solid consisting of a single oxime isomer (1.71 g, 76% yield, mp = 51–52 °C).  $^1\text{H}$  NMR (500 MHz,  $\text{CDCl}_3$ ):  $\delta$  8.09 (s, 1H), 7.45 (br s, 1H), 7.42 (br d,  $J$  = 8 Hz, 1H), 7.27 (t,  $J$  = 8 Hz, 1H), 7.19 (br d,  $J$  = 8 Hz, 1H), 2.38 (s, 3H), 2.28 (s, 3H).  $^{13}\text{C}\{^1\text{H}\}$  NMR ( $\text{CDCl}_3$ ):  $\delta$  156.15, 138.12, 136.44, 130.00, 128.39, 126.70, 123.21, 21.44, 12.44. IR (KBr): 3215, 2041, 2920, 1490, 1456  $\text{cm}^{-1}$ . HRMS electron impact ( $m/z$ ):  $[\text{M}]^+$  calcd for  $\text{C}_9\text{H}_{11}\text{NO}$ , 149.0841; found, 149.0837.



**Oxime 27.** The general procedure was followed utilizing 3'-methoxyacetophenone (2.25 g, 15.0 mmol). The product was obtained as a colorless oil consisting of a single oxime isomer (2.26 g, 91% yield).  $^1\text{H}$  NMR (500 MHz, DMSO):  $\delta$  11.21 (s, 1H), 7.30 (t,  $J$  = 8.1 Hz, 1H), 7.21 (m, 1H), 7.18 (m, 1H), 6.94 (ddd,  $J$  = 8.1, 2.4, 1.0 Hz, 1H), 3.77 (s, 3H), 2.14 (s, 3H).  $^{13}\text{C}\{^1\text{H}\}$  NMR ( $\text{CDCl}_3$ ):  $\delta$  159.62, 156.02, 137.90, 129.48, 118.61, 115.09, 111.31, 55.29, 12.26. IR (thin film): 3228, 2938, 2836, 1578, 1427  $\text{cm}^{-1}$ . HRMS electron impact ( $m/z$ ):  $[\text{M}]^+$  calcd for  $\text{C}_9\text{H}_{11}\text{NO}_2$ , 165.0790; found, 165.0790.

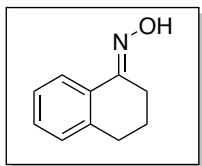


**Oxime 29.** The general procedure was followed utilizing TBDPSO-protected 3'-hydroxyacetophenone (4.39 g, 11.7 mmol). The product was obtained as a white solid consisting of a single oxime isomer (4.30 g, 94% yield, mp = 89–93 °C).  $^1\text{H}$  NMR (400 MHz,  $\text{CDCl}_3$ ):  $\delta$  8.55 (br s, 1H), 7.75–7.72 (multiple peaks, 4H), 7.46–7.36 (multiple peaks, 6H), 7.16 (dt,  $J$  = 8.0, 1.2 Hz, 1H), 7.08–7.04 (multiple peaks, 2H), 6.72 (ddd,  $J$  = 8.0, 2.4, 1.2 Hz, 1H), 2.09 (s, 3H), 1.13 (s, 9H).  $^{13}\text{C}\{^1\text{H}\}$  NMR ( $\text{CDCl}_3$ ):  $\delta$  155.77, 155.65, 137.70, 135.51, 132.76, 129.94, 129.18, 127.80, 120.44, 118.69, 117.68, 26.53, 19.47, 12.02. IR (KBr): 3214, 3070, 2934, 2859, 1580, 1427  $\text{cm}^{-1}$ . HRMS electrospray ( $m/z$ ):  $[\text{M}+\text{Na}]^+$  calcd for  $\text{C}_{24}\text{H}_{27}\text{NO}_2\text{Si}$ , 412.1709; found, 412.1699.

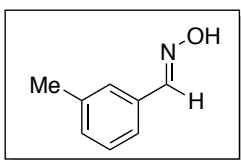


**Oxime 31.** The general procedure was followed utilizing 4'-*tert*-butylacetophenone (3.00 g, 17.0 mmol). The product was obtained as a white solid consisting of a single oxime isomer (3.20 g, 98% yield, mp = 100–101 °C).  $^1\text{H}$  NMR (500 MHz,  $\text{CDCl}_3$ ):  $\delta$  7.81 (s, 1H), 7.57

(d,  $J = 6.8$  Hz, 2H), 7.40 (d,  $J = 6.8$  Hz, 2H), 2.28 (s, 3H), 1.33 (s, 9H).  $^{13}\text{C}\{^1\text{H}\}$  NMR ( $\text{CDCl}_3$ ):  $\delta$  155.83, 152.43, 133.66, 125.75, 125.44, 34.67, 31.20, 12.18. IR (KBr): 3243, 2965, 1457  $\text{cm}^{-1}$ . HRMS electrospray ( $m/z$ ):  $[\text{M}+\text{H}]^+$  calcd for  $\text{C}_{12}\text{H}_{18}\text{NO}$ , 192.1388; found, 192.1381.



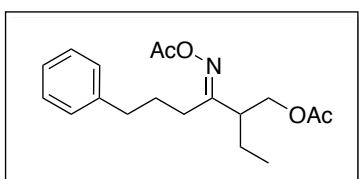
**Oxime 33.** The general procedure was followed utilizing  $\alpha$ -tetralone (2.00 g, 13.7 mmol). The product was obtained as a red-brown solid consisting of a single oxime isomer (1.99 g, 90% yield, mp = 95–96  $^{\circ}\text{C}$ ).  $^1\text{H}$  NMR (400 MHz,  $\text{CDCl}_3$ ):  $\delta$  8.06 (br s, 1H), 7.89 (dd,  $J = 7.4$ , 1.2 Hz, 1H), 7.27 (ddd,  $J = 7.4$ , 7.4, 1.2 Hz, 1H), 7.23–7.14 (multiple peaks, 2H), 2.82 (t,  $J = 6.7$  Hz, 2H), 2.77 (t,  $J = 5.3$  Hz, 2H), 1.88 (m, 2H).  $^{13}\text{C}\{^1\text{H}\}$  NMR ( $\text{CDCl}_3$ ):  $\delta$  155.38, 139.81, 130.40, 129.21, 128.66, 126.47, 124.02, 29.78, 23.84, 21.27. IR (KBr): 3194, 3063, 2935, 1486, 1450  $\text{cm}^{-1}$ . HRMS electron impact ( $m/z$ ):  $[\text{M}]^+$  calcd for  $\text{C}_{10}\text{H}_{11}\text{NO}$ , 161.0841; found, 161.0835.



**Oxime 35.** The general procedure was followed utilizing *m*-tolualdehyde (1.80 g, 15.0 mmol). The product was obtained as a pale yellow solid consisting of a single oxime isomer (1.88 g, 93% yield, mp = 51–53  $^{\circ}\text{C}$ ).  $^1\text{H}$  NMR (500 MHz,  $\text{CDCl}_3$ ):  $\delta$  8.13 (s, 1H), 8.08 (s, 1H), 7.41 (br s, 1H), 7.38 (br d,  $J = 7.6$  Hz, 1H), 7.28 (t,  $J = 7.6$  Hz, 1H), 7.21 (br d,  $J = 7.6$  Hz, 1H), 2.38 (s, 3H).  $^{13}\text{C}\{^1\text{H}\}$  NMR ( $\text{CDCl}_3$ ):  $\delta$  150.47, 138.49, 131.76, 130.90, 128.66, 127.53, 124.30, 21.28. IR (KBr): 3167, 3087, 2986, 2872, 2777, 1492, 1477  $\text{cm}^{-1}$ . HRMS electron impact ( $m/z$ ):  $[\text{M}]^+$  calcd for  $\text{CHNO}$ , 135.0684; found, 135.0679.

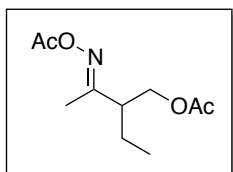
### Synthesis and Characterization of Acetoxyated Products

**General Procedure:** The oxime substrate was dissolved in 1:1 AcOH/Ac<sub>2</sub>O in a loosely capped 20 mL scintillation vial or a larger pressure vessel. This solution was stirred at room temperature for 2 h. Pd(OAc)<sub>2</sub> and PhI(OAc)<sub>2</sub> were added, and the reaction vessel was sealed with a Teflon-lined cap or a Teflon bushing. The reaction was then heated at 80 or 100 °C for 12 h (unless otherwise noted). The resulting mixture was filtered through glass wool, diluted with EtOAc (2 x volume of reaction solvent), and washed several times with equal volumes of saturated NaHCO<sub>3</sub> until the aqueous solution was no longer acidic. The organic layer was then washed with brine, dried over MgSO<sub>4</sub>, and concentrated to give the crude product, which was purified by chromatography on silica gel. Where noted, the oximes were obtained as mixtures of *E* and *Z* stereoisomers. In these cases, the ratio is reported based on <sup>1</sup>H NMR integration. In all cases, complete <sup>1</sup>H and <sup>13</sup>C NMR data are reported for the major isomer. In addition, all of the distinct resonances associated with the minor isomer are shown for both the <sup>1</sup>H and <sup>13</sup>C NMR spectra (many of the peaks for the minor isomer are coincident with those of the major isomer). All other characterization (HRMS, IR, melting point) was carried out on a mixture of the oxime *E/Z* isomers.



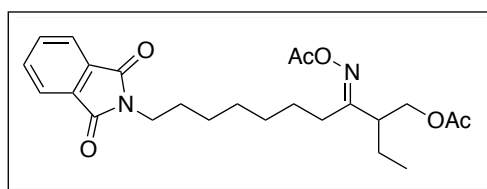
**Acetoxyated Product 10.** The general procedure was followed utilizing substrate **7** (2.00 g, 9.12 mmol, 1 equiv), Pd(OAc)<sub>2</sub> (102 mg, 0.456 mmol, 0.05 equiv), PhI(OAc)<sub>2</sub> (6.06 g, 18.2 mmol, 2 equiv), AcOH (38 mL), and Ac<sub>2</sub>O (38 mL), with heating at 100 °C. Product **10** was obtained as a pale yellow oil consisting of a ~3:1 mixture of major and minor oxime stereoisomers (1.44 g, 49% yield, R<sub>f</sub> = 0.20 in 80% hexanes/20% EtOAc). Major Isomer: <sup>1</sup>H NMR (500 MHz, CDCl<sub>3</sub>): δ 7.30 (m, 2H), 7.22–7.17 (multiple peaks, 3H), 4.21 (dd, *J* = 11.2, 5.6 Hz, 1H), 4.12 (dd, *J* = 11.2, 8.3 Hz, 1H), 2.70–2.66 (multiple peaks, 3H), 2.32 (t, *J* = 8.3 Hz, 2H), 2.09 (s, 3H), 2.01 (s, 3H), 1.88–1.82 (multiple peaks, 2H), 1.62–1.53 (multiple peaks, 2H), 0.92 (t, *J* = 7.3 Hz, 3H). <sup>13</sup>C {<sup>1</sup>H} NMR (CDCl<sub>3</sub>): δ 170.70, 168.88, 168.64, 140.94, 128.40, 128.30, 126.09, 64.39, 45.51, 35.85, 27.84, 27.43, 22.15, 20.77, 19.60, 11.39. Minor Isomer (distinct resonances): <sup>1</sup>H NMR (500 MHz, CDCl<sub>3</sub>): δ 3.32 (m, 1H), 2.17 (s, 3H),

1.99 (s, 3H).  $^{13}\text{C}\{^1\text{H}\}$  NMR ( $\text{CDCl}_3$ ):  $\delta$  128.36, 125.88, 64.04, 41.43, 35.40, 31.25, 27.58, 21.77, 19.68, 11.89. IR (thin film, mixture of *E/Z* isomers): 2966, 1740  $\text{cm}^{-1}$ . HRMS electrospray ( $m/z$ ):  $[\text{M}+\text{Na}]^+$  calcd for  $\text{NaC}_{18}\text{H}_{25}\text{NO}_4$  (mixture of *E/Z* isomers), 342.1681; found, 342.1674.



**Acetoxyated Product 12.** The general procedure was followed utilizing substrate **11** (1.90 g, 16.5 mmol, 1 equiv),  $\text{Pd}(\text{OAc})_2$  (185 mg, 0.825 mmol, 0.05 equiv),  $\text{PhI}(\text{OAc})_2$  (7.97 g, 24.75 mmol, 1.5 equiv),  $\text{AcOH}$  (60 mL), and  $\text{Ac}_2\text{O}$  (60 mL), with heating at 100  $^\circ\text{C}$ .

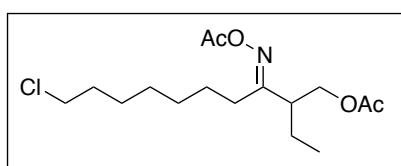
Product **12** was obtained as a pale yellow oil consisting of an  $\sim$ 11:1 mixture of major and minor oxime stereoisomers (2.17 g, 61% yield,  $R_f = 0.28$  in 70% hexanes/30% EtOAc). Major Isomer:  $^1\text{H}$  NMR (500 MHz,  $\text{CDCl}_3$ ):  $\delta$  4.22–4.06 (multiple peaks, 2H), 2.76 (dddd,  $J = 7.9, 7.9, 6.2, 6.2$  Hz, 1H), 2.17 (s, 3H), 2.03 (s, 3H), 1.92 (s, 3H), 1.64–1.47 (multiple peaks, 2H), 0.92 (t,  $J = 7.6$  Hz, 3H).  $^{13}\text{C}\{^1\text{H}\}$  NMR ( $\text{CDCl}_3$ ):  $\delta$  170.79, 168.68, 166.00, 64.14, 45.97, 21.73, 20.80, 19.68, 12.39, 11.33. Minor Isomer (distinct resonances):  $^1\text{H}$  NMR (500 MHz,  $\text{CDCl}_3$ ):  $\delta$  3.54 (m, 1H), 2.15 (s, 3H), 2.03 (s, 3H), 1.98 (s, 3H).  $^{13}\text{C}\{^1\text{H}\}$  NMR ( $\text{CDCl}_3$ ):  $\delta$  63.94, 40.17, 21.51, 19.57, 16.31, 11.58. IR (thin film, mixture of *E/Z* isomers): 2967, 2938, 2880, 1739, 1366  $\text{cm}^{-1}$ . HRMS electrospray ( $m/z$ ):  $[\text{M}+\text{Na}]^+$  calcd for  $\text{NaC}_{10}\text{H}_{17}\text{NO}_4$  (mixture of *E/Z* isomers), 238.1055; found, 238.1059.



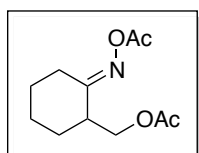
**Acetoxyated Product 14.** The general procedure was followed utilizing substrate **13** (325 mg, 0.944 mmol, 1 equiv),  $\text{Pd}(\text{OAc})_2$  (10.6 mg, 0.047 mmol, 0.05 equiv),  $\text{PhI}(\text{OAc})_2$  (608

mg, 1.89 mmol, 2 equiv),  $\text{AcOH}$  (3.9 mL), and  $\text{Ac}_2\text{O}$  (3.9 mL), with heating at 100  $^\circ\text{C}$ . Product **14** was obtained as an orange oil consisting of a  $\sim$ 3.6:1 mixture of major and minor oxime stereoisomers (272 mg, 65% yield,  $R_f = 0.29$  in 65% hexanes/35% EtOAc). Major Isomer:  $^1\text{H}$  NMR (400 MHz,  $\text{CDCl}_3$ ):  $\delta$  7.79 (dd,  $J = 5.6, 3.2$  Hz, 2H), 7.67 (dd,  $J = 5.6, 3.2$  Hz, 2H), 4.17 (dd,  $J = 11.2, 6.0$  Hz, 1H), 4.17 (dd,  $J = 11.2, 8.0$  Hz, 1H), 3.63 (t,  $J = 7.2$  Hz, 2H), 2.64 (dddd,  $J = 7.6, 7.6, 6.4, 6.4$  Hz, 1H), 2.31–2.18 (multiple peaks, 2H), 2.12 (s, 3H), 1.98 (s, 3H), 1.67–1.42 (multiple peaks, 6H), 1.31 (br s, 6H), 0.883 (t,

$J = 7.6$  Hz, 3H).  $^{13}\text{C}\{^1\text{H}\}$  NMR ( $\text{CDCl}_3$ ):  $\delta$  170.62, 168.98, 168.70, 168.27, 133.77, 131.97, 123.00, 64.38, 45.39, 37.73, 29.62, 28.53, 28.41, 28.34, 26.47, 25.78, 22.16, 20.71, 19.66, 11.32. Minor Isomer (distinct resonances):  $^1\text{H}$  NMR (400 MHz,  $\text{CDCl}_3$ ):  $\delta$  3.31 (dddd,  $J = 8.8, 8.8, 6.2, 6.2$  Hz, 1H), 2.15 (s, 3H), 2.04 (s, 3H).  $^{13}\text{C}\{^1\text{H}\}$  NMR ( $\text{CDCl}_3$ ):  $\delta$  170.56, 168.48, 168.32, 133.72, 64.02, 41.42, 37.78, 31.84, 29.22, 28.73, 26.57, 25.88, 21.75, 20.69, 19.62. IR (thin film, mixture of *E/Z* isomers): 2934, 2860, 1766, 1742, 1708  $\text{cm}^{-1}$ . HRMS electrospray ( $m/z$ ):  $[\text{M}+\text{Na}]^+$  calcd for  $\text{NaC}_{24}\text{H}_{32}\text{N}_2\text{O}_6$  (mixture of *E/Z* isomers), 467.2158; found, 467.2163.



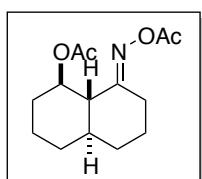
**Acetoxyated Product 16.** The general procedure was followed utilizing substrate **15** (500 mg, 1.80 mmol, 1 equiv),  $\text{Pd}(\text{OAc})_2$  (20.2 mg, 0.090 mmol, 0.05 equiv),  $\text{PhI}(\text{OAc})_2$  (1.16 g, 3.60 mmol, 2 equiv),  $\text{AcOH}$  (7.5 mL), and  $\text{Ac}_2\text{O}$  (7.5 mL), with heating at 100 °C. Product **16** was obtained as a pale yellow oil consisting of a ~3:1 mixture of major and minor oxime stereoisomers (330 mg, 48% yield,  $R_f = 0.27$  in 77% hexanes/23% EtOAc). Major Isomer:  $^1\text{H}$  NMR (500 MHz,  $\text{CDCl}_3$ ):  $\delta$  4.22 (dd,  $J = 11.2, 5.9$  Hz, 1H), 4.17 (dd,  $J = 11.2, 8.1$  Hz, 1H), 3.53 (t,  $J = 6.8$  Hz, 2H), 2.69 (m, 1H), 2.35–2.26 (multiple peaks, 2H), 2.18 (s, 3H), 2.03 (s, 3H), 1.80–1.73 (multiple peaks, 2H), 1.65–1.57 (multiple peaks, 2H), 1.55–1.48 (multiple peaks, 2H), 1.47–1.40 (multiple peaks, 2H), 1.40–1.32 (multiple peaks, 4H), 0.94 (t,  $J = 7.3$  Hz, 3H).  $^{13}\text{C}\{^1\text{H}\}$  NMR ( $\text{CDCl}_3$ ):  $\delta$  170.78, 168.98, 168.93, 64.53, 45.55, 45.00, 32.46, 29.75, 28.57, 28.41, 26.64, 25.88, 22.34, 20.86, 19.81, 11.45. Minor Isomer (distinct resonances):  $^1\text{H}$  NMR (500 MHz,  $\text{CDCl}_3$ ):  $\delta$  3.32 (dddd,  $J = 8.8, 6.1$  Hz, 1H), 2.16 (s, 3H), 2.03 (s, 3H).  $^{13}\text{C}\{^1\text{H}\}$  NMR ( $\text{CDCl}_3$ ):  $\delta$  64.17, 49.98, 45.06, 41.56, 31.93, 29.31, 26.71, 25.98, 21.91, 20.83, 19.74, 11.98. IR (thin film, mixture of *E/Z* isomers): 2934, 2859, 1741  $\text{cm}^{-1}$ . HRMS electrospray ( $m/z$ ):  $[\text{M}+\text{Na}]^+$  calcd for  $\text{NaC}_{16}\text{H}_{28}\text{ClNO}_4$  (mixture of *E/Z* isomers), 356.1605; found, 356.1610.



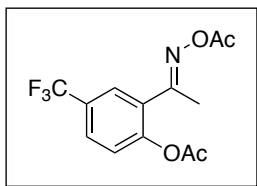
**Acetoxyated Product 18.** The general procedure was followed utilizing substrate **17** (150 mg, 1.18 mmol, 1 equiv),  $\text{Pd}(\text{OAc})_2$  (13.2



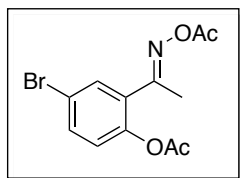
mg, 0.059 mmol, 0.05 equiv),  $\text{PhI}(\text{OAc})_2$  (570 mg, 1.77 mmol, 1.5 equiv),  $\text{AcOH}$  (4.9 mL), and  $\text{Ac}_2\text{O}$  (4.9 mL), with heating at 100 °C. Product **18** was obtained as a pale orange oil consisting of a ~4:1 mixture of major and minor oxime stereoisomers (177 mg, 66% yield,  $R_f = 0.21$  (major) and 0.29 (minor) in 72% hexanes/28% EtOAc). Major Isomer:  $^1\text{H}$  NMR (500 MHz,  $\text{CDCl}_3$ ):  $\delta$  4.49 (dd,  $J = 11.0, 6.6$  Hz, 1H), 4.13 (dd,  $J = 11.0, 7.3$  Hz, 1H), 2.79–2.72 (multiple peaks, 2H), 2.34 (ddd,  $J = 13.9, 9.0, 4.6$  Hz, 1H), 2.16 (s, 3H), 2.05 (s, 3H), 1.98 (m, 1H), 1.74–1.53 (multiple peaks, 5H).  $^{13}\text{C}\{^1\text{H}\}$  NMR ( $\text{CDCl}_3$ ):  $\delta$  170.93, 169.27, 167.57, 63.92, 41.40, 29.89, 25.92, 25.63, 23.19, 20.87, 19.77. Minor Isomer (distinct resonances):  $^1\text{H}$  NMR (500 MHz,  $\text{CDCl}_3$ ):  $\delta$  4.26–4.18 (multiple peaks, 2H), 3.76 (br m, 1H), 2.59 (br d,  $J = 15.0$  Hz, 1H), 2.14 (s, 3H).  $^{13}\text{C}\{^1\text{H}\}$  NMR ( $\text{CDCl}_3$ ):  $\delta$  170.72, 168.61, 167.83, 63.05, 34.25, 27.05, 26.34, 20.79, 20.69, 19.56. IR (thin film, mixture of *E/Z* isomers): 2939, 2863, 1762, 1736  $\text{cm}^{-1}$ . HRMS electrospray ( $m/z$ ):  $[\text{M}+\text{Na}]^+$  calcd for  $\text{NaC}_{11}\text{H}_{17}\text{NO}_4$  (mixture of *E/Z* isomers), 250.1055; found, 250.1044.



**Acetoxyated Product 20.** The general procedure was followed utilizing substrate **19** (1.32 g, 7.87 mmol, 1 equiv),  $\text{Pd}(\text{OAc})_2$  (88.3 mg, 0.394 mmol, 0.05 equiv),  $\text{PhI}(\text{OAc})_2$  (7.60 g, 23.6 mmol, 3 equiv),  $\text{AcOH}$  (33 mL), and  $\text{Ac}_2\text{O}$  (33 mL), with heating at 100 °C. Product **20** was obtained as a pale orange waxy solid consisting of a single oxime isomer (922 mg, 44% yield,  $R_f = 0.25$  in 77% hexanes/23% EtOAc, mp = 69–74 °C).  $^1\text{H}$  NMR (400 MHz,  $\text{CDCl}_3$ ):  $\delta$  5.14 (ddd,  $J = 10.9, 10.9, 4.7$  Hz, 1H), 3.32 (br d,  $J = 13.1$  Hz, 1H), 2.14 (s, 3H), 2.02 (s, 3H), 1.96–1.65 (multiple peaks, 6H), 1.52–1.22 (multiple peaks, 6H), 1.10 (m, 1H).  $^{13}\text{C}\{^1\text{H}\}$  NMR ( $\text{CDCl}_3$ ):  $\delta$  170.45, 166.25, 69.92, 52.20, 43.66, 33.08, 33.00, 31.53, 27.41, 25.87, 23.02, 21.20, 19.98. Two  $^{13}\text{C}$  resonances are coincidentally overlapping. IR (KBr): 2939, 2863, 1760, 1742, 1637, 1448  $\text{cm}^{-1}$ . HRMS electrospray ( $m/z$ ):  $[\text{M}+\text{Na}]^+$  calcd for  $\text{NaC}_{14}\text{H}_{21}\text{NO}_4$ , 290.1368; found, 290.1379.

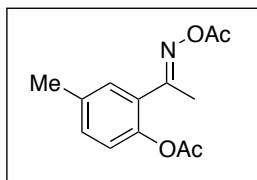


**Acetoxyated Product 22.** The general procedure was followed utilizing substrate **21** (250 mg, 1.23 mmol, 1 equiv), Pd(OAc)<sub>2</sub> (27.6 mg, 0.123 mmol, 0.10 equiv), PhI(OAc)<sub>2</sub> (792 mg, 2.46 mmol, 2 equiv), AcOH (5.1 mL), and Ac<sub>2</sub>O (5.1 mL), with heating at 80 °C for 24 h. Product **22** was obtained as a pale yellow oil consisting of a ~16:1 mixture of major and minor oxime stereoisomers (227 mg, 61% yield, R<sub>f</sub> = 0.21 in 80% hexanes/20% EtOAc). The minor isomer was assigned as a stereoisomer (not a regioisomer) by analogy to compounds **26** and **28** as well as based on the previously reported analogous reactions of oxime ether<sup>12b</sup> and 2-phenylpyridine-based substrates<sup>13b</sup>. Major Isomer: <sup>1</sup>H NMR (400 MHz, CDCl<sub>3</sub>): δ 7.73 (d, *J* = 2.0 Hz, 1H), 7.69 (dd, *J* = 8.4, 2.0 Hz, 1H), 7.30 (d, *J* = 8.4 Hz, 1H), 2.34 (s, 3H), 2.33 (s, 3H), 2.24 (s, 3H). <sup>13</sup>C{<sup>1</sup>H} NMR (CDCl<sub>3</sub>): δ 168.72, 168.02, 160.63, 150.63 (q, *J* = 1.1 Hz), 129.45, 128.45 (q, *J* = 33.4 Hz), 127.81 (q, *J* = 3.5 Hz), 126.95 (q, *J* = 3.5 Hz), 124.05, 123.39 (q, *J* = 272.4 Hz), 21.01, 19.57, 16.57. <sup>19</sup>F NMR (CDCl<sub>3</sub>): δ -62.41. Minor Isomer (distinct resonances): <sup>1</sup>H NMR (400 MHz, CDCl<sub>3</sub>): δ 2.39 (s, 3H), 2.04 (s, 3H). <sup>13</sup>C{<sup>1</sup>H} NMR (CDCl<sub>3</sub>): δ 128.62, 126.36, 21.85, 19.36. IR (thin film, mixture of *E/Z* isomers): 3075, 2940, 1766 cm<sup>-1</sup>. HRMS electrospray (*m/z*): [M+Na]<sup>+</sup> calcd for NaC<sub>13</sub>H<sub>12</sub>F<sub>3</sub>NO<sub>4</sub> (mixture of *E/Z* isomers), 326.0616; found, 326.0614.

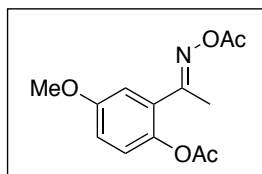


**Acetoxyated Product 24.** The general procedure was followed utilizing substrate **23** (1.50 g, 7.01 mmol, 1 equiv), Pd(OAc)<sub>2</sub> (78.7 mg, 0.351 mmol, 0.05 equiv), PhI(OAc)<sub>2</sub> (2.48 g, 7.71 mmol, 1.1 equiv), AcOH (29 mL), and Ac<sub>2</sub>O (29 mL), with heating at 80 °C. Product **24** was obtained as a pale yellow oil consisting of a ~12:1 mixture of major and minor oxime stereoisomers (1.89 g, 86% yield, R<sub>f</sub> = 0.29 in 77% hexanes/23% EtOAc). The minor isomer was assigned as a stereoisomer (not a regioisomer) by analogy to compounds **26** and **28** (in the current paper) as well as based on the previously reported analogous reactions of oxime ether<sup>12b</sup> and 2-phenylpyridine-based substrates<sup>13b</sup>. Major Isomer: <sup>1</sup>H NMR (400 MHz, CDCl<sub>3</sub>): δ 7.61 (d, *J* = 2.8 Hz, 1H), 7.54 (dd, *J* = 8.6, 2.8 Hz, 1H), 7.04 (d, *J* = 8.6 Hz, 1H), 2.30 (app. s, 6H), 2.24 (s, 3H). <sup>13</sup>C{<sup>1</sup>H} NMR (CDCl<sub>3</sub>): δ 168.90, 168.06, 160.49, 147.13, 133.68, 132.31, 130.41, 124.96, 119.00,

20.97, 19.57, 16.48. Minor Isomer (distinct resonances): 2.31 (s, 3H), 2.22 (s, 3H), 1.98 (s, 3H). IR (thin film, mixture of *E/Z* isomers): 2932, 1762  $\text{cm}^{-1}$ . HRMS electrospray ( $m/z$ ):  $[\text{M}+\text{Na}]^+$  calcd for  $\text{NaC}_{12}\text{H}_{12}\text{BrNO}_4$  (mixture of *E/Z* isomers), 335.9847; found, 335.9847.

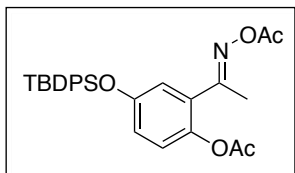


**Acetoxyated Product 26.** The general procedure was followed utilizing substrate **25** (800 mg, 5.36 mmol, 1 equiv),  $\text{Pd}(\text{OAc})_2$  (60.2 mg, 0.268 mmol, 0.05 equiv),  $\text{PhI}(\text{OAc})_2$  (1.90 g, 5.90 mmol, 1.1 equiv),  $\text{AcOH}$  (22 mL), and  $\text{Ac}_2\text{O}$  (22 mL), with heating at 80  $^\circ\text{C}$ . Product **26** was obtained as a pale orange waxy solid consisting of an ~8:1 mixture of major and minor oxime stereoisomers (962 mg, 72% yield,  $R_f = 0.24$  in 77% hexanes/23% EtOAc, mp = 57–65  $^\circ\text{C}$ ). The minor isomer was assigned as a stereoisomer (not a regioisomer) on the basis of the fact that hydrolysis led to a single ketone product **42**. Major Isomer:  $^1\text{H}$  NMR (500 MHz,  $\text{CDCl}_3$ ):  $\delta$  7.27 (s, 1H), 7.22 (d,  $J = 8.0$  Hz, 1H), 7.02 (d,  $J = 8.0$  Hz, 1H), 2.36 (s, 3H), 2.30 (s, 3H), 2.29 (s, 3H), 2.23 (s, 3H).  $^{13}\text{C}\{^1\text{H}\}$  NMR ( $\text{CDCl}_3$ ):  $\delta$  169.53, 168.45, 161.89, 145.88, 135.87, 131.48, 130.01, 128.23, 122.96, 21.08, 20.79, 19.71, 16.67. Minor Isomer (distinct resonances): 2.38 (s, 3H), 2.22 (s, 3H), 1.99 (s, 3H). IR (KBr, mixture of *E/Z* isomers): 2942 1758  $\text{cm}^{-1}$ . HRMS electrospray ( $m/z$ ):  $[\text{M}+\text{Na}]^+$  calcd for  $\text{NaC}_{13}\text{H}_{15}\text{NO}_4$  (mixture of *E/Z* isomers), 272.0899; found, 272.0892.

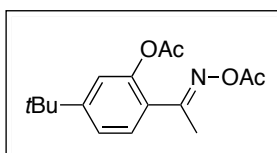


**Acetoxyated Product 28.** The general procedure was followed utilizing substrate **27** (1.50 g, 9.08 mmol, 1 equiv),  $\text{Pd}(\text{OAc})_2$  (102 mg, 0.454 mmol, 0.05 equiv),  $\text{PhI}(\text{OAc})_2$  (3.22 g, 9.99 mmol, 1.1 equiv),  $\text{AcOH}$  (38 mL), and  $\text{Ac}_2\text{O}$  (38 mL), with heating at 80  $^\circ\text{C}$  for 4 h. Product **28** was obtained as an orange oil consisting of a ~20:1 mixture of major and minor oxime stereoisomers (1.78 g, 74% yield,  $R_f = 0.23$  in 70% hexanes/30% EtOAc). The minor isomer was assigned as a stereoisomer (not a regioisomer) on the basis of the fact that hydrolysis led to a single ketone product. Major Isomer:  $^1\text{H}$  NMR (400 MHz,  $\text{CDCl}_3$ ):  $\delta$  7.04 (d,  $J = 8.8$  Hz, 1H), 6.97–6.92 (multiple peaks, 2H), 3.80 (s, 3H), 2.30 (s, 3H), 2.28 (s, 3H), 2.23 (s, 3H).  $^{13}\text{C}\{^1\text{H}\}$  NMR ( $\text{CDCl}_3$ ):

$\delta$  169.70, 168.36, 161.58, 157.12, 141.50, 129.27, 124.07, 115.97, 114.59, 55.70, 20.98, 19.66, 16.58. Minor Isomer (distinct resonances):  $^1\text{H}$  NMR (400 MHz,  $\text{CDCl}_3$ ):  $\delta$  3.83 (s, 3H), 2.31 (s, 3H), 2.20 (s, 3H), 1.97 (s, 3H). IR (thin film, mixture of *E/Z* isomers): 2938, 1760  $\text{cm}^{-1}$ . HRMS electrospray ( $m/z$ ):  $[\text{M}+\text{Na}]^+$  calcd for  $\text{NaC}_{13}\text{H}_{15}\text{NO}_5$  (mixture of *E/Z* isomers), 288.0848; found, 288.0851.

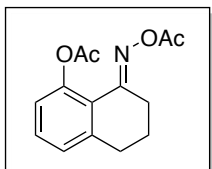


**Acetoxy Product 30.** The general procedure was followed utilizing substrate **29** (200 mg, 0.513 mmol, 1 equiv),  $\text{Pd}(\text{OAc})_2$  (5.8 mg, 0.026 mmol, 0.05 equiv),  $\text{PhI}(\text{OAc})_2$  (182 mg, 0.564 mmol, 1.1 equiv),  $\text{AcOH}$  (2.1 mL), and  $\text{Ac}_2\text{O}$  (2.1 mL), with heating at 80  $^\circ\text{C}$  for 10 h. Product **30** was obtained as pale yellow viscous oil consisting of a ~19:1 mixture of major and minor oxime stereoisomers (198 mg, 79% yield,  $R_f = 0.25$  in 80% hexanes/20% EtOAc). The minor isomer was assigned as a stereoisomer (not a regioisomer) by analogy to compounds **26** and **28** (in the current paper). Major Isomer:  $^1\text{H}$  NMR (400 MHz,  $\text{CDCl}_3$ ):  $\delta$  7.70–7.68 (multiple peaks, 4H), 7.45–7.35 (multiple peaks, 6H), 6.82–6.80 (multiple peaks, 2H), 6.72 (dd,  $J = 8.8, 2.8$  Hz, 1H), 2.23 (s, 3H), 2.18 (s, 3H), 2.07 (s, 3H), 1.10 (s, 9H).  $^{13}\text{C}\{^1\text{H}\}$  NMR ( $\text{CDCl}_3$ ):  $\delta$  169.74, 168.40, 161.18, 153.15, 141.55, 135.46, 132.26, 130.09, 128.94, 127.90, 123.78, 121.49, 120.21, 26.41, 21.00, 19.66, 19.39, 16.24. Minor Isomer (distinct resonances):  $^1\text{H}$  NMR (400 MHz,  $\text{CDCl}_3$ ):  $\delta$  2.15 (s, 3H), 2.04 (s, 3H), 1.92 (s, 3H), 1.11 (s, 9H). IR (thin film, mixture of *E/Z* isomers): 3074, 2933, 2859, 1765  $\text{cm}^{-1}$ . HRMS electrospray ( $m/z$ ):  $[\text{M}+\text{Na}]^+$  calcd for  $\text{NaC}_{28}\text{H}_{31}\text{NO}_5\text{Si}$  (mixture of *E/Z* isomers), 512.1869; found, 512.1865.

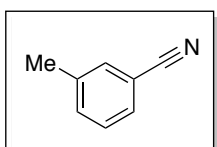


**Acetoxy Product 32.** The general procedure was followed utilizing substrate **31** (1.91 g, 10.0 mmol, 1 equiv),  $\text{Pd}(\text{OAc})_2$  (112 mg, 0.500 mmol, 0.05 equiv),  $\text{PhI}(\text{OAc})_2$  (3.22 g, 10.0 mmol, 1 equiv),  $\text{AcOH}$  (42 mL), and  $\text{Ac}_2\text{O}$  (42 mL), with heating at 80  $^\circ\text{C}$ . Product **32** was obtained as a pale orange solid consisting of an ~11:1 mixture of major and minor oxime stereoisomers (2.32 g, 80% yield,  $R_f = 0.29$  in 77% hexanes/23% EtOAc, mp = 43–51  $^\circ\text{C}$ ). Major Isomer:  $^1\text{H}$  NMR (500 MHz,  $\text{CDCl}_3$ ):  $\delta$  7.41 (d,  $J = 8.1$  Hz, 1H), 7.29 (dd,  $J = 8.1, 2.0$  Hz, 1H), 7.11 (d,  $J = 2.0$  Hz, 1H), 2.312 (s, 3H), 2.310 (s, 3H), 2.23 (s,

3H), 1.31 (s, 9H).  $^{13}\text{C}\{^1\text{H}\}$  NMR ( $\text{CDCl}_3$ ):  $\delta$  169.56, 168.46, 161.50, 154.96, 147.87, 129.12, 125.55, 123.14, 120.35, 34.84, 31.01, 21.14, 19.71, 16.37. Minor Isomer (distinct resonances):  $^1\text{H}$  NMR (500 MHz,  $\text{CDCl}_3$ ):  $\delta$  2.30 (s, 3H), 2.22 (s, 3H), 2.01 (s, 3H), 1.34 (s, 9H). IR (KBr, mixture of *E/Z* isomers): 2961, 1772  $\text{cm}^{-1}$ . HRMS electrospray ( $m/z$ ):  $[\text{M}+\text{Na}]^+$  calcd for  $\text{NaC}_{16}\text{H}_{21}\text{NO}_4$  (mixture of *E/Z* isomers), 314.1368; found, 314.1362.



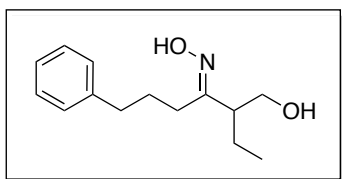
**Acetoxy Product 34.** The general procedure was followed utilizing substrate **33** (1.5 g, 9.30 mmol, 1 equiv),  $\text{Pd}(\text{OAc})_2$  (104 mg, 0.465 mmol, 0.05 equiv),  $\text{PhI}(\text{OAc})_2$  (3.30 g, 10.2 mmol, 1.1 equiv),  $\text{AcOH}$  (39 mL), and  $\text{Ac}_2\text{O}$  (39 mL), with heating at 80  $^\circ\text{C}$ . Product **34** was obtained as a tan powder consisting of a single oxime isomer (1.34 g, 55% yield,  $R_f = 0.26$  in 77% hexanes/23% EtOAc, mp = 127–128  $^\circ\text{C}$ ).  $^1\text{H}$  NMR (400 MHz,  $\text{CDCl}_3$ ):  $\delta$  7.33 (t,  $J = 7.8$  Hz, 1H), 7.10 (dd,  $J = 7.8, 1.2$  Hz, 1H), 6.96 (dd,  $J = 8.2, 1.2$  Hz, 1H), 2.88 (t,  $J = 6.4$  Hz, 2H), 2.78 (t,  $J = 6.4$  Hz, 2H), 2.40 (s, 3H), 2.19 (s, 3H), 1.84 (m, 2H).  $^{13}\text{C}\{^1\text{H}\}$  NMR ( $\text{CDCl}_3$ ):  $\delta$  170.58, 167.58, 160.15, 148.92, 143.67, 130.84, 126.48, 122.39, 122.15, 30.31, 26.15, 21.37, 20.78, 19.65. IR (KBr): 2942, 1764  $\text{cm}^{-1}$ . HRMS electrospray ( $m/z$ ):  $[\text{M}+\text{Na}]^+$  calcd for  $\text{NaC}_{14}\text{H}_{15}\text{NO}_4$ , 284.0899; found, 284.0898.



**Benzonitrile Product 36.** The general procedure was followed utilizing substrate **35** (30 mg, 0.222 mmol, 1 equiv),  $\text{Pd}(\text{OAc})_2$  (2.5 mg, 0.011 mmol, 0.05 equiv),  $\text{PhI}(\text{OAc})_2$  (78.7 mg, 0.244 mmol, 1.1 equiv),  $\text{AcOH}$  (920  $\mu\text{L}$ ), and  $\text{Ac}_2\text{O}$  (920  $\mu\text{L}$ ), with heating at 80  $^\circ\text{C}$  for 4 h. The calibrated GC yield (77%) was obtained by comparing to an authentic sample of commercially available **36**.

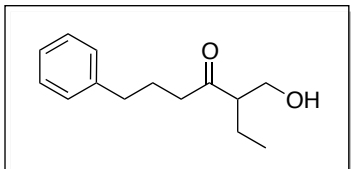
## Synthesis and Characterization of $\beta$ - and ortho-Hydroxy Ketones

**General Procedure For One Pot Deprotection:** To a solution of the *O*-acetyl oxime in MeOH (0.46 mL/mmol oxime) in a loosely capped scintillation vial at room temperature was added finely ground  $K_2CO_3$  (0.15 equiv every 2 h over the course of 6 h, 0.45 equiv total).  $NaHSO_3$  (3.5 equiv) and  $H_2O$  (equal amount as MeOH) were then added, and the vial was sealed with a Teflon-lined cap and heated at 80 °C for 3 h.<sup>22</sup> The reaction mixture was concentrated by rotary evaporation to remove methanol. The remaining primarily aqueous reaction mixture was diluted with  $CHCl_3$  (4 x volume of reaction solvent) and rinsed briefly with 1 M HCl (2 x volume of reaction solvent). The layers were separated, and the aqueous layer was extracted several times with  $CHCl_3$ . The combined organic extracts were neutralized with aqueous  $NaHCO_3$ , washed once with brine, dried over  $MgSO_4$ , filtered through a plug of silica, and concentrated to afford the  $\beta$ -hydroxyketone.



**$\beta$ -Hydroxy Oxime 37.** To a solution of acetyl oxime **10** (170 mg, 0.532 mmol, 1 equiv) in MeOH (1.16 mL) in a loosely capped scintillation vial at room temperature was added finely ground  $K_2CO_3$  (11 mg, 0.0798 mmol, 0.15 equiv). After stirring at room temperature for 12 h, the MeOH was removed by rotary evaporation, and the crude product was purified by column chromatography to yield the unprotected  $\beta$ -hydroxy oxime **37** as pale yellow solid consisting of a 4:1 mixture of major and minor oxime isomers (113.4 mg, 91% yield,  $R_f$  = 0.27 and 0.19 in 60% hexanes/40% EtOAc, mp = 68–74 °C). Major Isomer:  $^1H$  NMR (400 MHz,  $CDCl_3$ ):  $\delta$  7.95 (br s, 1H), 7.28 (m, 2H), 7.20–7.17 (multiple peaks, 3H), 3.70 (m, 2H), 2.67 (t,  $J$  = 7.8 Hz, 2H), 2.48 (m, 1H), 2.31–2.19 (multiple peaks, 2H), 1.87 (m, 2H), 1.53 (quint,  $J$  = 7.4 Hz, 2H), 0.91 (t,  $J$  = 7.4 Hz, 3H). One exchangeable proton (OH) is not observed.  $^{13}C\{^1H\}$  NMR ( $CDCl_3$ ):  $\delta$  163.56, 141.71, 128.36, 128.33, 125.89, 62.76, 47.74, 36.16, 27.30, 27.26, 22.13, 11.77. Minor Isomer:  $^1H$  NMR (400 MHz,  $CDCl_3$ ):  $\delta$  7.28 (m, 2H), 7.20–7.16 (multiple peaks, 3H), 3.74 (dd,  $J$  = 10.8, 5.6 Hz, 1H), 3.67 (dd,  $J$  = 10.8, 8.4 Hz, 1H), 3.27 (dddd,  $J$  = 8.4, 8.4, 6.2, 6.2 Hz, 1H), 2.67 (t,  $J$  = 7.6 Hz, 2H), 2.22 (td,  $J$  = 7.4, 4.1

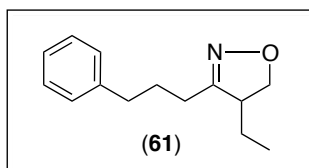
Hz, 2H), 1.90 (m, 2H), 1.52 (m, 2H), 0.92 (t,  $J = 7.4$  Hz, 3H). Both exchangeable protons (OH) are not observed.  $^{13}\text{C}\{^1\text{H}\}$  NMR ( $\text{CDCl}_3$ ):  $\delta$  161.82, 141.87, 128.42, 128.32, 125.82, 63.72, 43.29, 35.47, 30.97, 27.54, 21.02, 12.22. IR (KBr, mixture of *E/Z* isomers): 3203, 2963, 2923, 1496, 1453  $\text{cm}^{-1}$ . HRMS electrospray ( $m/z$ ):  $[\text{M}+\text{Na}]^+$  calcd for  $\text{NaC}_{14}\text{H}_{21}\text{NO}_2$  (mixture of *E/Z* isomers), 258.1470; found, 258.1471.



**$\beta$ -Hydroxy Ketone 38.** From Hydroxyl Oxime: Oxime

**37** (150 mg, 0.637 mmol, 1 equiv) was combined with  $\text{NaHSO}_3$  (232.2 mg, 2.231 mmol, 3.5 equiv) in  $\text{EtOH}/\text{H}_2\text{O}$  (1:1, 1.28 mL) in a scintillation vial. The vial was sealed

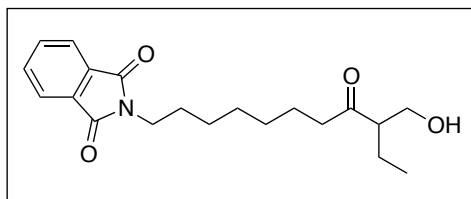
with a Teflon-lined cap and heated to 80 °C for 3 h. The resulting solution was concentrated by rotary evaporation to remove ethanol. The remaining primarily aqueous reaction mixture was diluted with  $\text{CHCl}_3$  (8 mL), and rinsed briefly with 1 *M* HCl (5 mL). The layers were separated, and the aqueous layer was extracted several times with  $\text{CHCl}_3$ . The combined organic extracts were neutralized with aqueous  $\text{NaHCO}_3$ , washed once with brine, dried over  $\text{MgSO}_4$ , filtered through Celite, and concentrated to afford **38** as a colorless oil (113 mg, 80% yield). From acetyl oxime: The one pot deprotection procedure was followed utilizing **10** (50 mg, 0.156 mmol), to yield **38** as a colorless oil (28 mg, 80% yield) contaminated with ~3% of the corresponding isoxazoline.  $^1\text{H}$  NMR (400 MHz,  $\text{CDCl}_3$ ):  $\delta$  7.28 (m, 2H), 7.21–7.17 (multiple peaks, 3H), 3.78 (m, 1H), 3.69 (m, 1H), 2.65–2.57 (multiple peaks, 3H), 2.51 (td,  $J = 7.0, 2.0$ , 2H), 2.03 (br t,  $J = 5.9$  Hz, 1H), 1.93 (quin,  $J = 7.4$  Hz, 2H), 1.69–1.46 (multiple peaks, 2H), 0.91 (t,  $J = 7.4$  Hz, 3H).  $^{13}\text{C}\{^1\text{H}\}$  NMR ( $\text{CDCl}_3$ ):  $\delta$  214.70, 141.55, 128.43, 128.37, 125.94, 62.44, 55.00, 41.98, 35.03, 24.78, 21.28, 11.78. IR (thin film): 3423, 2926  $\text{cm}^{-1}$ . HRMS electrospray ( $m/z$ ):  $[\text{M}+\text{Na}]^+$  calcd for  $\text{NaC}_{14}\text{H}_{20}\text{O}_2$ , 243.1361; found, 243.1360.



**Isoxazoline 61.** To confirm the identity of the contaminant in the one-pot deprotection of **10**, isoxazoline **61** was isolated as a colorless oil ( $R_f = 0.47$  in 80% hexanes/20% EtOAc) and characterized as follows:  $^1\text{H}$  NMR (400 MHz,  $\text{CDCl}_3$ ):  $\delta$  7.28

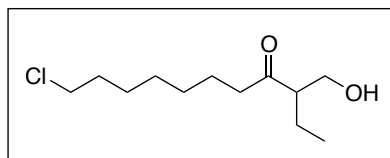
(m, 2H), 7.21–7.18 (multiple peaks, 3H), 4.33 (dd,  $J = 10.0, 8.0$  Hz, 1H), 3.98 (dd,  $J =$

8.0, 8.0 Hz, 1H), 3.10 (m, 1H), 2.74–2.63 (multiple peaks, 2H), 2.42 (m, 1H), 2.22 (ddd,  $J = 14.8, 8.8, 6.0$  Hz, 1H), 2.00–1.88 (multiple peaks, 2H), 1.65 (m, 1H), 1.40 (m, 1H), 0.91 (t,  $J = 8.0$  Hz, 3H).  $^{13}\text{C}\{^1\text{H}\}$  NMR ( $\text{CDCl}_3$ ):  $\delta$  161.21, 141.46, 128.45, 128.38, 125.96, 72.70, 51.26, 35.32, 27.66, 25.56, 23.34, 11.43. IR (thin film): 2962, 2932, 2864  $\text{cm}^{-1}$ . HRMS electrospray ( $m/z$ ):  $[\text{M}+\text{H}]^+$  calcd for  $\text{C}_{14}\text{H}_{20}\text{NO}$ , 218.1545; found, 218.1546.



**$\beta$ -Hydroxy Ketone 39.** The one pot deprotection procedure was followed utilizing **14** (50 mg, 0.112 mmol), to yield **39** as a colorless oil (31 mg, 79% yield) contaminated with ~5% of the

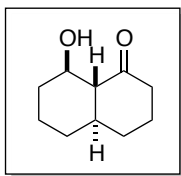
corresponding isoxazoline.  $^1\text{H}$  NMR (500 MHz,  $\text{CDCl}_3$ ):  $\delta$  7.82 (dd,  $J = 5.5, 3.0$  Hz, 2H), 7.69 (dd,  $J = 5.5, 3.0$  Hz, 2H), 3.76 (br t,  $J = 7.5$  Hz, 1H), 3.69–3.60 (multiple peaks, 3H), 2.61 (m, 1H), 2.46 (t,  $J = 7.5$  Hz, 2H), 2.16 (m, 1H), 1.66–1.46 (multiple peaks, 6H), 1.32–1.23 (multiple peaks, 6H), 0.90 (t,  $J = 7.5$  Hz, 3H).  $^{13}\text{C}\{^1\text{H}\}$  NMR ( $\text{CDCl}_3$ ):  $\delta$  215.06, 168.46, 133.84, 132.14, 123.14, 62.44, 54.93, 42.76, 37.92, 28.96, 28.85, 28.45, 26.58, 23.21, 21.30, 11.81. IR (thin film): 3472, 2932, 2858, 1770, 1702  $\text{cm}^{-1}$  HRMS electrospray ( $m/z$ ):  $[\text{M}+\text{Na}]^+$  calcd for  $\text{NaC}_{20}\text{H}_{27}\text{NO}_4$ , 368.1838; found, 368.1826.



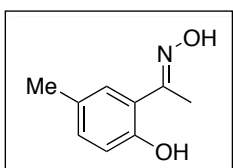
**$\beta$ -Hydroxy Ketone 40.** The one pot deprotection procedure was followed utilizing **16** (50 mg, 0.159 mmol), to yield **40** as a colorless oil (21 mg, 56% yield) contaminated with ~5% of the corresponding

isoxazoline.  $^1\text{H}$  NMR (400 MHz,  $\text{CDCl}_3$ ):  $\delta$  3.80 (dd,  $J = 10.8, 7.6$  Hz, 1H), 3.70 (dd,  $J = 11.2, 4.0$  Hz, 1H), 3.52 (t,  $J = 6.8$  Hz, 2H), 2.63 (dddd,  $J = 7.2, 7.2, 7.2, 4.0$  Hz, 1H), 2.49 (td,  $J = 7.2, 1.2$  Hz, 2H), 2.30–2.20 (br s, 1H), 1.76 (quin,  $J = 6.8$  Hz, 2H), 1.69–1.49 (multiple peaks, 4H), 1.42 (m, 2H), 1.36–1.26 (multiple peaks, 4H), 0.92 (t,  $J = 7.3$  Hz, 3H).  $^{13}\text{C}\{^1\text{H}\}$  NMR ( $\text{CDCl}_3$ ):  $\delta$  215.05, 62.45, 54.94, 45.07, 42.78, 32.51, 29.00, 28.67, 26.66, 23.21, 21.31, 11.82. IR (thin film): 3412, 2932, 2857, 1703  $\text{cm}^{-1}$  HRMS electrospray ( $m/z$ ):  $[\text{M}+\text{Na}]^+$  calcd for  $\text{NaC}_{12}\text{H}_{23}\text{O}_2\text{Cl}$ , 257.1284; found, 257.1278.

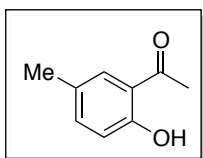




**$\beta$ -Hydroxy Ketone 41.** The one pot deprotection procedure was followed utilizing **20** (300 mg, 1.122 mmol), to yield **41** as a white solid (157 mg, 83% yield, mp = 43–44 °C).  $^1\text{H}$  NMR (400 MHz,  $\text{CDCl}_3$ ):  $\delta$  3.81 (m, 1H), 3.61 (d,  $J = 2.0$ , 1H), 2.42–2.27 (multiple peaks, 2H), 2.06 (m, 1H), 1.98 (m, 2H), 1.84–1.61 (multiple peaks, 4H), 1.46 (m, 2H), 1.29 (m, 2H), 1.18 (m, 1H).  $^{13}\text{C}\{^1\text{H}\}$  NMR ( $\text{CDCl}_3$ ):  $\delta$  214.82, 69.15, 61.79, 42.82, 41.90, 33.50, 32.68, 32.04, 26.09, 23.35. IR (KBr): 3446, 2927, 2862, 1701  $\text{cm}^{-1}$ . HRMS electrospray ( $m/z$ ):  $[\text{M}+\text{Na}]^+$  calcd for  $\text{NaC}_{10}\text{H}_{16}\text{O}_2$  191.1048; found, 191.1045.

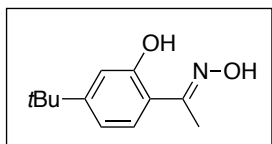


***ortho*-Hydroxy Oxime 62.** To a solution of acetyl oxime **26** (100 mg, 0.402 mmol, 1 equiv) in MeOH (870  $\mu\text{L}$ ) in a loosely capped scintillation vial was added finely ground  $\text{K}_2\text{CO}_3$  (8.3 mg, 0.060 mmol, 0.15 equiv). After stirring at room temperature for 0.5 h, the MeOH was removed by rotary evaporation, and the crude reaction mixture was diluted with  $\text{CH}_2\text{Cl}_2$  (4 mL) and neutralized with dilute aqueous AcOH. The organic layer was concentrated to afford **62** as a white solid (62 mg, 93% yield, mp = 136–138 °C).  $^1\text{H}$  NMR (400 MHz,  $\text{CDCl}_3$ ):  $\delta$  10.91 (s, 1H), 7.22 (s, 1H), 7.14 (br s, 1H), 7.07 (dd,  $J = 8.4$ , 2.0 Hz, 1H), 6.87 (d,  $J = 8.4$  Hz, 1H), 2.35 (s, 3H), 2.30 (s, 3H).  $^{13}\text{C}\{^1\text{H}\}$  NMR ( $\text{CDCl}_3$ ):  $\delta$  159.68, 155.32, 131.53, 128.10, 127.86, 118.06, 117.05, 20.64, 10.78. IR (KBr): 3335, 2918, 2861, 1636, 1504  $\text{cm}^{-1}$ . HRMS electrospray ( $m/z$ ):  $[\text{M}]^+$  calcd for  $\text{C}_9\text{H}_{11}\text{NO}_2$  165.0790; found, 165.0790.

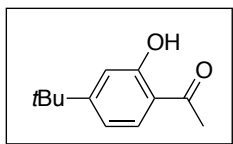


***ortho*-Hydroxy Ketone 42.** Oxime **62** (50 mg, 0.303 mmol, 1 equiv) was combined with  $\text{NaHSO}_3$  (110.3 mg, 1.06 mmol, 3.5 equiv) in EtOH/ $\text{H}_2\text{O}$  (1:1, 380  $\mu\text{L}$ ) in a scintillation vial. The vial was sealed with a Teflon-lined cap and heated to 90 °C for 12 h. The reaction mixture was concentrated by rotary evaporation to remove ethanol. The remaining primarily aqueous reaction mixture was diluted with  $\text{CHCl}_3$  (1.5 mL) and rinsed briefly with 1 M HCl (~1 mL). The layers were separated and the aqueous layer was extracted several times with  $\text{CHCl}_3$ . The combined organic extracts were neutralized with aqueous  $\text{NaHCO}_3$ , washed once with brine, dried over  $\text{MgSO}_4$ , and concentrated to afford **42** as a

white solid (42 mg, 91% yield). The spectroscopic data for **42** matched those reported in the literature.<sup>37</sup>

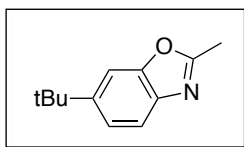


**ortho-Hydroxy Oxime 43.** To a solution of acetyl oxime **32** (400 mg, 1.373 mmol, 1 equiv) in MeOH (3 mL) in a loosely capped scintillation vial was added finely ground K<sub>2</sub>CO<sub>3</sub> (29 mg, 0.206 mmol, 0.15 equiv). After stirring at room temperature for 1 h, the MeOH was removed by rotary evaporation. The crude product was purified by column chromatography to afford **43** as a pale yellow solid (276 mg, 97% yield, R<sub>f</sub> = 0.8 in 65% hexanes/35% EtOAc, mp = 82–92 °C). <sup>1</sup>H NMR (500 MHz, CDCl<sub>3</sub>): δ 7.37 (d, *J* = 8.3 Hz, 1H), 7.01 (d, *J* = 2.0 Hz, 1H), 6.94 (dd, *J* = 8.3, 2.0 Hz, 1H), 2.35 (s, 3H), 1.31 (s, 9H). Extremely broad OH peaks were visible in the baseline. <sup>13</sup>C{<sup>1</sup>H} NMR (CDCl<sub>3</sub>): δ 159.43, 157.22, 154.80, 127.29, 116.51, 115.77, 114.31, 34.71, 31.03, 10.74. IR (KBr): 3380, 2956, 2869, 1563 cm<sup>-1</sup>. HRMS electron impact (*m/z*): [M]<sup>+</sup> calcd for C<sub>12</sub>H<sub>17</sub>NO<sub>2</sub>, 207.1259; found, 207.1255.

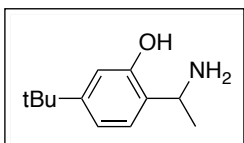


**ortho-Hydroxy Ketone 14.** Oxime **43** (50 mg, 0.241 mmol, 1 equiv) was combined with NaHSO<sub>3</sub> (87.8 mg, 0.844 mmol, 3.5 equiv) in EtOH/H<sub>2</sub>O (1:1, 300 μL) in a scintillation vial. The vial was sealed with a Teflon-lined cap and heated to 90 °C for 13 h. The reaction mixture was concentrated by rotary evaporation to remove ethanol. The remaining primarily aqueous reaction mixture was diluted with Et<sub>2</sub>O (1.5 mL) and rinsed briefly with 1 M HCl (~1 mL). The layers were separated and the aqueous layer was extracted several times with Et<sub>2</sub>O. The combined organic extracts were neutralized with aqueous NaHCO<sub>3</sub>, washed once with brine, dried over MgSO<sub>4</sub>, and filtered through a plug of silica to afford **44** as a colorless oil (42 mg, 91% yield). <sup>1</sup>H NMR (400 MHz, CDCl<sub>3</sub>): δ 12.25 (s, 1H), 7.66 (d, *J* = 8.2 Hz, 1H), 6.99 (d, *J* = 2.0 Hz, 1H), 6.94 (dd, *J* = 8.2, 2.0, 1H), 2.60 (s, 3H), 1.31 (s, 9H). <sup>13</sup>C{<sup>1</sup>H} NMR (CDCl<sub>3</sub>): δ 203.79, 162.31, 161.05, 130.37, 117.40, 116.62, 115.02, 35.31, 30.76, 26.46. IR (thin film): 3249, 2964, 1639 cm<sup>-1</sup>. HRMS electrospray (*m/z*): [M+Na]<sup>+</sup> calcd for NaC<sub>12</sub>H<sub>16</sub>O<sub>2</sub>, 193.1229; found, 193.1221.

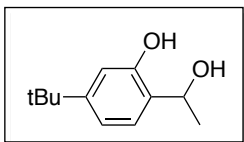
*Synthesis and Characterization of Remaining Compounds in Schemes 5.24–5.27*



**Benzoxazole 45.** Oxime **43** (41 mg, 0.198 mmol, 1 equiv), *p*-TsOH monohydrate (3.8 mg, 0.0198 mmol, 0.1 equiv), and ZnCl<sub>2</sub> (31.1 mg, 0.228 mmol, 1.15 equiv) were dissolved in MeCN (1 mL), and the resulting solution was heated to 90 °C for 5 h.<sup>38</sup> The reaction mixture was concentrated by rotary evaporation, and the crude product was taken up in Et<sub>2</sub>O, washed with aqueous NaHCO<sub>3</sub> and brine, dried over MgSO<sub>4</sub>, and concentrated to afford **45** as a colorless oil (23 mg, 56% yield, R<sub>f</sub> = 0.38 in 80% hexanes/20% EtOAc). <sup>1</sup>H NMR (400 MHz, CDCl<sub>3</sub>): δ 7.55 (d, *J* = 8.4 Hz, 1H), 7.49 (d, *J* = 1.7 Hz, 1H), 7.35 (dd, *J* = 8.4, 1.7 Hz, 1H), 2.61 (s, 3H), 1.37 (s, 9H). <sup>13</sup>C{<sup>1</sup>H} NMR (CDCl<sub>3</sub>): δ 163.52, 151.20, 148.43, 139.08, 121.63, 118.43, 106.90, 35.01, 31.68, 14.49. IR (thin film): 3224, 3062, 2959, 1614 cm<sup>-1</sup>. HRMS electrospray (*m/z*): [M+H]<sup>+</sup> calcd for C<sub>12</sub>H<sub>15</sub>NO 190.1232; found, 190.1226.

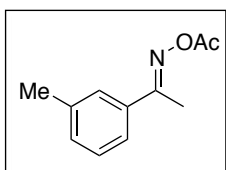


**Amine 46.** Oxime **43** (60 mg, 0.289 mmol, 1 equiv) was combined with 2 drops of conc. HCl and 10 wt % Pd/C (31 mg, 0.0289 mmol Pd, 0.1 equiv) in MeOH (1.5 mL). A H<sub>2</sub> balloon was attached to the reaction vessel, and the reaction was stirred at 25 °C for 12 h.<sup>39</sup> Solid NaHCO<sub>3</sub> (30 mg, 0.360 mmol, 1.2 equiv) was added, and the reaction mixture was then filtered through glass wool and concentrated. The crude product was taken up in CH<sub>2</sub>Cl<sub>2</sub>, filtered through Celite, and concentrated to yield **46** as a tan crystalline solid (56 mg, 100% yield, mp = 123–128 °C). <sup>1</sup>H NMR (500 MHz, CD<sub>3</sub>OD): δ 7.18 (d, *J* = 7.8 Hz, 1H), 6.95–6.93 (multiple peaks, 2H), 4.56 (q, *J* = 7.0 Hz, 1H), 1.63 (d, *J* = 7.0 Hz, 3H), 1.29 (s, 9H). Exchangeable protons (OH and NH<sub>2</sub>) are not observed. <sup>13</sup>C{<sup>1</sup>H} NMR (CD<sub>3</sub>OD): δ 156.04, 155.06, 128.09, 122.22, 118.01, 113.80, 48.70, 35.44, 31.62, 18.92. IR (KBr): 3229, 3034, 2964 cm<sup>-1</sup>. HRMS electrospray (*m/z*): [M+H]<sup>+</sup> calcd for C<sub>12</sub>H<sub>20</sub>NO 194.1545; found, 194.1544.

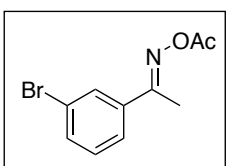


**Alcohol 47.** Ketone **44** (42.7 mg, 0.222 mmol, 1 equiv) and NaBH<sub>4</sub> (12.6 mg, 0.333 mmol, 1.5 equiv) were stirred in MeOH

(340  $\mu$ L) at 25  $^{\circ}$ C for 3.5 h.<sup>40</sup> The reaction mixture was concentrated by rotary evaporation, and the crude residue was taken up in Et<sub>2</sub>O (2.5 mL) and washed with 2 M HCl (400  $\mu$ L). The aqueous layer was extracted with Et<sub>2</sub>O (5 x 500  $\mu$ L). The combined organic layers were washed with water (2 x 500  $\mu$ L), dried over MgSO<sub>4</sub>, and concentrated to afford **47** as a pale yellow wax (38.6 mg, 90% yield). <sup>1</sup>H NMR (500 MHz, CD<sub>3</sub>OD):  $\delta$  7.17 (d,  $J$  = 8.0 Hz, 1H), 6.85 (dd,  $J$  = 8.0, 2 Hz, 1H), 6.80 (d,  $J$  = 2 Hz, 1H), 5.09 (q,  $J$  = 6.5 Hz, 1H), 1.42 (d,  $J$  = 6.5 Hz, 3H), 1.27 (s, 9H). Exchangeable protons (OH) are not observed. <sup>13</sup>C{<sup>1</sup>H} NMR (CD<sub>3</sub>OD):  $\delta$  155.04, 152.35, 129.85, 126.49, 117.43, 113.47, 67.03, 35.16, 31.78, 24.11. IR (KBr): 3417, 2965, 2904, 2868 cm<sup>-1</sup>. HRMS electron impact (m/z): [M]<sup>+</sup> calcd for C<sub>12</sub>H<sub>18</sub>O<sub>2</sub>, 194.1307; found, 194.1311.

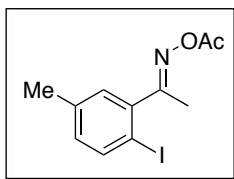


**Acetyl Oxime 48.** Oxime **25** (500 mg, 3.35 mmol) was stirred at room temperature in AcOH/Ac<sub>2</sub>O (1:1, 7.2 mL) for 3 h. The reaction mixture was diluted with EtOAc (50 mL) and quenched with aqueous NaHCO<sub>3</sub>. The organic layer was washed with brine (10 mL), dried over MgSO<sub>4</sub>, and concentrated to yield **48** as a white crystalline solid (635 mg, 99% yield, mp 41–43  $^{\circ}$ C). <sup>1</sup>H NMR (400 MHz, CDCl<sub>3</sub>):  $\delta$  7.58 (m, 1H), 7.51 (m, 1H), 7.31–7.24 (multiple peaks, 2H), 2.38 (s, 3H), 2.37 (s, 3H), 2.27 (s, 3H). <sup>13</sup>C{<sup>1</sup>H} NMR (CDCl<sub>3</sub>):  $\delta$  168.85, 162.57, 128.19, 134.69, 131.25, 128.34, 127.42, 124.08, 21.27, 19.74, 14.38. HRMS electrospray (m/z): [M+Na]<sup>+</sup> calcd for NaC<sub>11</sub>H<sub>13</sub>NO<sub>2</sub> 214.0844; found, 214.0844.

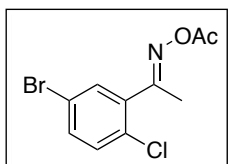


**Acetyl Oxime 50.** Oxime **23** (1.00 g, 4.67 mmol) was stirred at room temperature in AcOH/Ac<sub>2</sub>O (1:1, 10 mL) for 3 h. The reaction mixture was diluted with EtOAc (65 mL) and quenched with aqueous NaHCO<sub>3</sub>. The organic layer was washed with brine (1 x 25 mL), dried over MgSO<sub>4</sub>, and concentrated to yield **50** as a white crystalline solid (1.18 g, 99% yield, mp 31–34  $^{\circ}$ C). <sup>1</sup>H NMR (500 MHz, CDCl<sub>3</sub>):  $\delta$  7.89 (t,  $J$  = 2 Hz, 1H), 7.67 (ddd,  $J$  = 7.8, 2, 1.0 Hz, 1H), 7.57 (ddd,  $J$  = 7.8, 2, 1.0 Hz, 1H), 7.28 (t,  $J$  = 7.8 Hz, 1H), 2.36 (s, 3H), 2.27 (s, 3H). <sup>13</sup>C{<sup>1</sup>H} NMR (CDCl<sub>3</sub>):  $\delta$  168.59, 161.09, 136.79, 133.46,

130.03, 129.87, 125.54, 122.69, 19.72, 14.29. IR (KBr): 3068, 1769  $\text{cm}^{-1}$ . HRMS electrospray (m/z):  $[\text{M}+\text{Na}]^+$  calcd for  $\text{NaC}_{10}\text{H}_{10}\text{BrNO}_2$ , 277.9793; found, 277.9784.

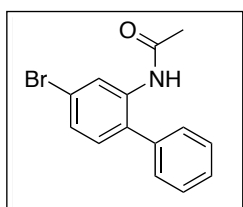


**Iodinated Product 49.** Acetyl oxime **48** (100 mg, 0.523 mmol, 1 equiv), *N*-iodosuccinimide (235 mg, 1.046 mmol, 2 equiv),  $\text{Pd}(\text{OAc})_2$  (5.9 mg, 0.0261 mmol, 5 mol %), AcOH (8 mL), and  $\text{Ac}_2\text{O}$  (2.8 mL) were combined in a 20 mL scintillation vial, and the vial was sealed with a Teflon-lined cap. The reaction was heated to 110  $^\circ\text{C}$  for 12 h. The resulting mixture was filtered through glass wool and concentrated to give the crude product, which was purified by chromatography on silica gel to yield iodinated product **49** as a pale yellow oil consisting of a single oxime isomer (77 mg, 46% yield,  $R_f = 0.19$  in 90% hexanes/10% EtOAc).  $^1\text{H}$  NMR (400 MHz,  $\text{CDCl}_3$ ):  $\delta$  7.71 (d,  $J = 8.0$  Hz, 1H), 7.10 (d,  $J = 1.8$  Hz, 1H), 6.91 (m, 1H), 2.34 (s, 3H), 2.30 (s, 3H), 2.26 (s, 3H).  $^{13}\text{C}\{^1\text{H}\}$  NMR ( $\text{CDCl}_3$ ):  $\delta$  168.70, 166.37, 140.87, 139.28, 138.40, 131.60, 130.42, 90.72, 20.78, 19.79, 18.41. IR (thin film): 2923, 1762  $\text{cm}^{-1}$ . HRMS electrospray (m/z):  $[\text{M}+\text{Na}]^+$  calcd for  $\text{NaC}_{11}\text{H}_{12}\text{INO}_2$ , 339.9811; found, 339.9800.



**Chlorinated Product 51.** Acetyl oxime **50** (105 mg, 0.410 mmol, 1 equiv), *N*-chlorosuccinimide (104 mg, 0.820 mmol, 2 equiv),  $\text{Pd}(\text{OAc})_2$  (4.6 mg, 0.0205 mmol, 5 mol %), AcOH (8.0 mL), and  $\text{Ac}_2\text{O}$  (3.0 mL) were combined in a 20 mL scintillation vial, and the vial was sealed with a Teflon-lined cap. The reaction was heated to 100  $^\circ\text{C}$  for 22 h. The resulting mixture was filtered through glass wool, diluted with EtOAc (30 mL), and washed several times with saturated  $\text{NaHCO}_3$ , until the aqueous solution was no longer acidic. The organic layer was then washed with brine, dried over  $\text{MgSO}_4$ , and concentrated to give the crude material, which was purified by chromatography on silica gel to yield chlorinated product **51** as a pale yellow solid consisting of an  $\sim 3:1$  mixture of major:minor oxime *E/Z* isomers (85 mg, 71% yield,  $R_f = 0.36, 0.30$  in 84% hexanes/16%EtOAc, mp of major isomer = 80–83  $^\circ\text{C}$ ). The minor isomer was assigned as a stereoisomer (not a regioisomer) by analysis of the splitting pattern in the aromatic region of the  $^1\text{H}$  NMR spectrum. Major Isomer:  $^1\text{H}$  NMR (500 MHz,  $\text{CDCl}_3$ ):  $\delta$  7.53 (d,  $J$

= 2.4 Hz, 1H), 7.47 (dd,  $J = 8.5, 2.4$  Hz, 1H), 7.28 (d,  $J = 8.5$  Hz, 1H), 2.36 (s, 3H), 2.26 (s, 3H).  $^{13}\text{C}\{^1\text{H}\}$  NMR ( $\text{CDCl}_3$ ):  $\delta$  168.24, 162.70, 136.80, 133.66, 133.04, 131.49, 131.36, 120.59, 19.61, 17.65. Minor Isomer:  $^1\text{H}$  NMR (500 MHz,  $\text{CDCl}_3$ ):  $\delta$  7.46 (dd,  $J = 8.6, 2.4$  Hz, 1H), 7.31 (d,  $J = 8.6$  Hz, 1H), 7.25 (d,  $J = 2.4$  Hz, 1H), 2.33 (s, 3H), 2.00 (s, 3H).  $^{13}\text{C}\{^1\text{H}\}$  NMR ( $\text{CDCl}_3$ ):  $\delta$  168.05, 160.39, 136.00, 133.152, 131.12, 129.95, 129.42, 120.44, 21.37, 19.36. IR (thin film, major isomer): 2936, 1783, 1768  $\text{cm}^{-1}$ . HRMS electrospray ( $m/z$ ):  $[\text{M}+\text{Na}]^+$  calcd for  $\text{NaC}_{10}\text{H}_9\text{ClNO}_2$  (major isomer) 311.9403; found, 311.9397.



**Rearranged Acetanilide 55.** Acetyl oxime **50** (200 mg, 0.754 mmol, 1 equiv),  $\text{AgOAc}$  (138 mg, 0.829 mmol, 1.1 equiv),  $\text{Pd}(\text{OAc})_2$  (8.5 mg, 0.038 mmol, 0.05 equiv), iodobenzene (227  $\mu\text{L}$ , 2.037 mmol, 2.7 equiv), and trifluoroacetic acid (750  $\mu\text{L}$ ) were combined in a 4 mL scintillation vial, and the vial was sealed with a Teflon-lined cap.<sup>24</sup> The reaction was heated to 100  $^\circ\text{C}$  for 6 h, then concentrated. The resulting crude reaction mixture was purified by column chromatography to yield **55** as a pale yellow solid (111.7 mg, 51% yield,  $R_f = 0.29$  in 70% hexanes/30% EtOAc, mp = 111–114  $^\circ\text{C}$ ). Compound **55** was also prepared from *N*-(3-bromophenyl)acetamide using the same arylating conditions to confirm the identity of **55**.<sup>24</sup>  $^1\text{H}$  NMR (500 MHz,  $\text{CDCl}_3$ ):  $\delta$  8.55 (br s, 1H), 7.50 (t,  $J = 7.5$  Hz, 2H), 7.44 (m, 1H), 7.35–7.29 (multiple peaks, 3H), 7.10 (m, 2H), 2.02 (s, 3H).  $^{13}\text{C}\{^1\text{H}\}$  NMR ( $\text{CDCl}_3$ ):  $\delta$  168.10, 137.08, 135.86, 131.15, 130.58, 129.29, 129.06, 128.36, 127.21, 124.00, 122.09, 24.62. IR (KBr): 3262, 3027, 2796, 1658  $\text{cm}^{-1}$ . HRMS electrospray ( $m/z$ ):  $[\text{M}+\text{Na}]^+$  calcd for  $\text{NaC}_{14}\text{H}_{12}\text{BrNO}$ , 312.0000; found, 311.9990.

## 5.10 References

1. (a) Daugulis, O.; Zaitsev, V. G.; Shabashov, D.; Pham, Q.-N.; Lazareva, A. Regioselective Functionalization of Unreactive Carbon–Hydrogen Bonds. *Synlett* **2006**, 3382. (b) Kalyani, D.; Sanford, M. S. Chelate-Directed Oxidative Functionalization of Carbon–Hydrogen Bonds: Synthetic Applications and Mechanistic Insights. In *Topics in Organometallic Chemistry: Directed Metalation*; Chatani, N., Ed.; Springer: Berlin, Heidelberg, New York, 2007; Vol. 24, pp 85–116. (c) Lyons, T. W.; Sanford, M. S. Palladium-Catalyzed Ligand-Directed C–H Functionalization Reactions. *Chem. Rev.* **2010**, *110*, 1147. (d) Neufeldt, S. R.; Sanford, M. S. Controlling Site Selectivity in Palladium Catalyzed C–H Bond Functionalization. *Acc. Chem. Res.* **2012**, *45*, 936.
2. Neufeldt, S. R.; Sanford, M. S. *O*-Acetyl Oximes as Transformable Directing Groups for Pd-Catalyzed C–H Bond Functionalization. *Org. Lett.* **2010**, *12*, 532.
3. Cai, G.; Fu, Y.; Li, Y.; Wan, X.; Shi, Z. Indirect *ortho* Functionalization of Substituted Toluenes through *ortho* Olefination of *N,N*-Dimethylbenzylamines Tuned by the Acidity of Reaction Conditions. *J. Am. Chem. Soc.* **2007**, *129*, 7666.
4. Wang, X.; Mei, T.-S.; Yu, J.-Q. Versatile Pd(OTf)<sub>2</sub>•2H<sub>2</sub>O-Catalyzed *ortho*-Fluorination Using NMP as a Promoter. *J. Am. Chem. Soc.* **2009**, *131*, 7520.
5. Giri, R.; Wasa, M.; Breazzano, S. P.; Yu, J.-Q. Converting *gem*-Dimethyl Groups into Cyclopropanes via Pd-Catalyzed Sequential C–H Activation and Radical Cyclization. *Org. Lett.* **2006**, *8*, 5685.
6. Chiong, H. A.; Pham, Q.-N.; Daugulis, O. Two Methods for Direct *ortho*-Arylation of Benzoic Acids. *J. Am. Chem. Soc.* **2007**, *129*, 9879.
7. (a) Shabashov, D.; Maldonado, J. R. M.; Daugulis, O. Carbon–Hydrogen Bond Functionalization Approach for the Synthesis of Fluorenones and *ortho*-Arylated Benzonitriles. *J. Org. Chem.* **2008**, *73*, 7818. (b) Wasa, M.; Engle, K. M.; Yu, J.-Q. Pd(0)/PR<sub>3</sub>-Catalyzed Intermolecular Arylation of sp<sup>3</sup> C–H Bonds. *J. Am. Chem. Soc.* **2009**, *131*, 9886. (c) Cornella, J.; Righi, M.; Larrosa, I. Carboxylic Acids as Traceless Directing Groups for Formal *meta*-Selective Direct Arylation. *Angew. Chem., Int. Ed.* **2011**, *50*, 9429.
8. Larock, R. C. *Comprehensive Organic Transformations*, 2nd ed.; John Wiley & Sons, Inc.: New York, 1999; pp 1197–1620.
9. For reviews on ketone-directed C–H alkylation and arylation reactions catalyzed by metals other than Pd, see: (a) Alberico, D.; Scott, M. E.; Lautens, M. Aryl–Aryl Bond Formation by Transition-Metal-Catalyzed Direct Arylation. *Chem. Rev.* **2007**, *107*, 174. (b) Colby, D. A.; Bergman, R. G.; Ellman, J. A. Rhodium-Catalyzed C–C Bond Formation via Heteroatom-Directed C–H Bond Activation. *Chem. Rev.* **2010**, *110*, 624.
10. (a) Terao, Y.; Kametani, Y.; Wakui, H.; Satoh, T.; Miura, M.; Nomura, M. Multiple Arylation of Alkyl Aryl Ketones and  $\alpha,\beta$ -Unsaturated Carbonyl

- Compounds via Palladium Catalysis. *Tetrahedron* **2001**, *57*, 5967. (b) Gandeepan, P.; Parthasarathy, K.; Cheng, C.-H. Synthesis of Phenanthrone Derivatives from *sec*-Alkyl Aryl Ketones and Aryl Halides via a Palladium-Catalyzed Dual C–H Bond Activation and Enolate Cyclization. *J. Am. Chem. Soc.* **2010**, *132*, 8569. (c) Xiao, B.; Gong, T.-J.; Xu, J.; Liu, Z.-J.; Liu, L. Palladium-Catalyzed Intermolecular Directed C–H Amidation of Aromatic Ketones. *J. Am. Chem. Soc.* **2011**, *133*, 1466.
11. Gürbüz, N.; Özdemir, I.; Çetinkaya, B. Selective Palladium-Catalyzed Arylation(s) of Benzaldehyde Derivatives by *N*-Heterocarbene Ligands. *Tetrahedron Lett.* **2005**, *46*, 2273.
  12. (a) Desai, L. V.; Hull, K. L.; Sanford, M. S. Palladium-Catalyzed Oxygenation of Unactivated  $sp^3$  C–H Bonds. *J. Am. Chem. Soc.* **2004**, *126*, 9542. (b) Desai, L. V.; Malik, H. A.; Sanford, M. S. Oxone as an Inexpensive, Safe, and Environmentally Benign Oxidant for C–H Bond Oxygenation. *Org. Lett.* **2006**, *8*, 1141. (c) Desai, L. V.; Stowers, K. J.; Sanford, M. S. Insights into Directing Group Ability in Palladium-Catalyzed C–H Bond Functionalization. *J. Am. Chem. Soc.* **2008**, *130*, 13285.
  13. For related C–H acetoxylation reactions of other substrates, see: (a) Dick, A. R.; Hull, K. L.; Sanford, M. S. A Highly Selective Catalytic Method for the Oxidative Functionalization of C–H Bonds. *J. Am. Chem. Soc.* **2004**, *126*, 2300. (b) Kalyani, D.; Sanford, M. S. Regioselectivity in Palladium-Catalyzed C–H Activation/Oxygenation Reactions. *Org. Lett.* **2005**, *7*, 4149. (c) Giri, R.; Liang, J.; Lei, J.-G.; Li, J.-J.; Wang, D.-H.; Chen, X.; Naggar, I. C.; Guo, C.; Foxman, B. M.; Yu, J.-Q. Pd-Catalyzed Stereoselective Oxidation of Methyl Groups by Inexpensive Oxidants under Mild Conditions: A Dual Role for Carboxylic Anhydrides in Catalytic C–H Bond Oxidation. *Angew. Chem., Int. Ed.* **2005**, *44*, 7420. (d) Wang, D.-H.; Hao, X.-S.; Wu, D.-F.; Yu, J.-Q. Palladium-Catalyzed Oxidation of *Boc*-Protected *N*-Methylamines with IOAc as the Oxidant: A *Boc*-Directed  $sp^3$  C–H Bond Activation. *Org. Lett.* **2006**, *8*, 3387. (e) Reddy, B. V. S.; Reddy, L. R.; Corey, E. J. Novel Acetoxylation and C–C Coupling Reactions at Unactivated Positions in  $\alpha$ -Amino Acid Derivatives. *Org. Lett.* **2006**, *8*, 3391. (f) Wang, G.-W.; Yuan, T.-T.; Wu, X.-L. Direct Ortho-Acetoxylation of Anilides via Palladium-Catalyzed  $sp^2$  C–H Bond Oxidative Activation. *J. Org. Chem.* **2008**, *73*, 4717. (g) Zhang, J.; Khaskin, E.; Anderson, N. P.; Zavalij, P. Y.; Vedernikov, A. N. Catalytic Aerobic Oxidation of Substituted 8-Methylquinolines in Pd<sup>II</sup>-2,6-Pyridinedicarboxylic Acid Systems. *Chem. Commun.* **2008**, 3625. (h) Stowers, K. J.; Sanford, M. S. Mechanistic Comparison between Pd-Catalyzed Ligand-Directed C–H Chlorination and C–H Acetoxylation. *Org. Lett.* **2009**, *11*, 4584. (i) Gou, F.-R.; Wang, X.-C.; Huo, P.-F.; Bi, H.-P.; Guan, Z.-H.; Liang, Y.-M. Palladium-Catalyzed Aryl C–H Bonds Activation/Acetoxylation Utilizing a Bidentate System. *Org. Lett.* **2009**, *11*, 5726. (j) Jiang, H.; Chen, H.; Wang, A.; Liu, X. Palladium-Catalyzed Acetoxylation of  $sp^3$  C–H Bonds Using Molecular Oxygen. *Chem. Commun.* **2010**, *46*, 7259. (k) Vickers, C. J.; Mei, T.-S.; Yu, J.-Q.



- Pd(II)-Catalyzed *o*-C–H Acetoxylation of Phenylalanine and Ephedrine Derivatives with MeCOOO*t*Bu/Ac<sub>2</sub>O. *Org. Lett.* **2010**, *12*, 2511. (l) Zhang, S.; Luo, F.; Wang, W.; Jia, X.; Hu, M.; Cheng, J. Chelation-Assisted Palladium-Catalyzed Acyloxylation of Benzyl sp<sup>2</sup> C–H Bonds Using PhI(OAc)<sub>2</sub> as Oxidant. *Tetrahedron Lett.* **2010**, *51*, 3317. (m) Wang, L.; Xia, X.-D.; Guo, W.; Chen, J.-R.; Xiao, W.-J. Palladium-Catalyzed C–H Acetoxylation of 2-Methoxyimino-2-Aryl-Acetates and Acetamides. *Org. Biomol. Chem.* **2011**, *9*, 6895. (n) Guo, H.-M.; Rao, W.-H.; Niu, H.-Y.; Jiang, L.-L.; Meng, G.; Jin, J.-J. Palladium-Catalyzed C–H Bond Functionalization of C6-Aryl Purines. *Chem. Commun.* **2011**, *47*, 5608. (o) Reddy, B. V. S.; Ramesh, K.; Yadav, J. S. First Example of Quinoxaline-Directed C–H Activation: A Novel Method for Acetoxylation of Arenes. *Synlett* **2011**, 169. (p) Pilarski, L. T.; Janson, P. G.; Szabó, K. J. Palladium-Catalyzed Selective Acyloxylation Using Sodium Perborate as Oxidant. *J. Org. Chem.* **2011**, *76*, 1503. (q) Sun, C.-L.; Liu, J.; Wang, Y.; Zhou, X.; Li, B.-J.; Shi, Z.-J. Direct Sequential C–O and C–C Formation via Double sp<sup>2</sup> C–H Bond Activations to Construct 6*H*-Benzo[*c*]chromen-6-ones. *Synlett* **2011**, 883. (r) Reddy, B. V. S.; Revathi, G.; Reddy, A. S.; Yadav, J. S. Regioselective *ortho*-Acetoxylation/Methoxylation of *N*-(2-Benzoylphenyl)benzamides via Substrate Directed C–H Activation. *Tetrahedron Lett.* **2011**, *52*, 5926. (s) Reddy, B. V. S.; Narasimhulu, G.; Umadevi, N.; Yadav, J. S. Quinazolinone-Directed C–H Activation: A Novel Strategy for the Acetoxylation-Methoxylation of the Arenes. *Synlett* **2012**, *23*, 1364.
14. For example, see Shipe, W. D.; Sorensen, E. J. A Convergent Synthesis of the Tricyclic Architecture of the Guanacastepenes Featuring a Selective Ring Fragmentation. *Org. Lett.* **2002**, *4*, 2063.
  15. (a) Sakamoto, T.; Kikugawa, Y. Synthesis of Aldehydes from Carboxylic Acids via *N*-Methoxyimidoyl Bromides: Deoxygenation of *O*-Methyloximes. *Synthesis* **1993**, 563. (b) Mears, R. J.; Sailes, H. E.; Watts, J. P.; Whiting, A. Synthesis, Structure and Comparative Stability of β-Hydrazono, Oximino Methyl Ether and Imino Boronates. *J. Chem. Soc., Perkin Trans. 1* **2000**, 3250.
  16. (a) Desai, L. V. Palladium-Catalyzed Functionalization of C–H Bonds and Alkenes. *Ph.D. Thesis*, University of Michigan, April 2008. (b) Corey, E. J.; Niimura, K.; Konishi, Y.; Hashimoto, S.; Hamada, Y. A New Synthetic Route to Prostaglandins. *Tetrahedron Lett.* **1986**, *27*, 2199.
  17. For selected examples, see (a) Baldwin, J. E.; Jones, R. H.; Nájera, C.; Yus, M. Functionalization of Unactivated Methyl Groups Through Cyclopalladation Reactions. *Tetrahedron* **1985**, *41*, 699. (b) Baldwin, J. E.; Nájera, C.; Yus, M. Oxidation of Unactivated Methyl Groups via a Cyclopalladation Reaction. *J. Chem. Soc., Chem. Commun.* **1985**, 126. (c) Carr, K.; Saxton, H. M.; Sutherland, J. K. The 4α-Demethylation of Lanostenone. *J. Chem. Soc. Perkin Trans. 1* **1988**, 1599.

18. Corsaro, A.; Chiacchio, U.; Pistarà, V. Regeneration of Carbonyl Compounds from the Corresponding Oximes. *Synthesis* **2001**, 1903.
19. Cost calculated on a molar basis using: *Aldrich Catalog Handbook of Fine Chemicals*; Aldrich Chemical: Milwaukee, WI, 2009.
20. Moriarty, R. M.; Prakash, O.; Vavilikolanu, P. R. Oxidative Cleavage of Ketoximes with Iodosobenzene Diacetate. *Synth. Commun.* **1986**, *16*, 1247.
21. (a) Waring, P. The Synthesis of 6-Aminomethyl-5,6,7,8-tetrahydropterin. *Aust. J. Chem.* **1988**, *41*, 667. (b) Armesto, D.I Agarrabeitia, A. R.; Horspool, W. M.; Gallego, M. G. Unexpected Influence of Mono-phenyl Substitution on the Photochemistry of  $\beta,\gamma$ -Unsaturated Oxime Acetates. *J. Chem. Soc., Chem. Commun.* **1990**, 934.
22. Pines, S. H.; Chemerda, J. M.; Kozlowski, M. A. Cleavage of Oximes with Bisulfite. A General Procedure. *J. Org. Chem.* **1966**, *31*, 3446.
23. (a) Kalyani, D.; Dick, A. R.; Anani, W. Q.; Sanford, M. S. A Simple Catalytic Method for the Regioselective Halogenation of Arenes. *Org. Lett.* **2006**, *8*, 2523. (b) Kalyani, D.; Dick, A. R.; Anani, W. Q.; Sanford, M. S. Scope and Selectivity in Palladium-Catalyzed Directed C–H Bond Halogenation Reactions. *Tetrahedron* **2006**, *62*, 11483.
24. Daugulis, O.; Zaitsev, V. G. Anilide *ortho*-Arylation by Using C–H Activation Methodology. *Angew. Chem., Int. Ed.* **2005**, *44*, 4046.
25. For a recent review, see Rousseau, G.; Breit, B. Removable Directing Groups in Organic Synthesis and Catalysis. *Angew. Chem., Int. Ed.* **2011**, *50*, 2450.
26. Dubost, E.; Fossey, C.; Cailly, T.; Rault, S.; Fabis, F. Selective *ortho*-Bromination of Substituted Benzaldoximes Using Pd-Catalyzed C–H Activation: Application to the Synthesis of Substituted 2-Bromobenzaldehydes. *J. Org. Chem.* **2011**, *76*, 6414.
27. Ren, Z.; Mo, F.; Dong, G. Catalytic Functionalization of Unactivated  $sp^3$  C–H Bonds via *exo*-Directing Groups: Synthesis of Chemically Differentiated 1,2-Diols. *J. Am. Chem. Soc.* **2012**, *Just Accepted Manuscript* (02 Oct 2012)
28. (a) Chemyak, N.; Dudnik, A. S.; Huang, C.; Gevorgyan, V. PyDipSi: A General and Easily Modifiable/Traceless Si-Tethered Directing Group for C–H Acyloxylation of Arenes. *J. Am. Chem. Soc.* **2010**, *132*, 8270. (b) Gulevich, A. V.; Melkonyan, F. S.; Sarkar, D.; Gevorgyan, V. Double-Fold C–H Oxygenation of Arenes Using PyrDipSi: a General and Efficient Traceless/Modifiable Silicon-Tethered Directing Group. *J. Am. Chem. Soc.* **2012**, *134*, 5528.
29. Richter, H.; Beckendorf, S.; Mancheño, O. G. Modifiable Sulfur Tethers as Directing Groups for Aromatic C–H Acetoxylation Reactions. *Adv. Synth. Catal.* **2011**, *353*, 295.

30. (a) Stache, E. E.; Seizert, C. A.; Ferreira, E. M. Molecular Scaffolds with Remote Directing Groups for Selective Palladium-Catalyzed C–H Bond Functionalizations. *Chem. Sci.* **2012**, *3*, 1623. (b) Zhang, S.-Y.; He, G.; Zhao, Y.; Wright, K.; Nack, W. A.; Chen, G. Efficient Alkyl Ether Synthesis via Palladium-Catalyzed, Picolinamide-Directed Alkoxylation of Unactivated C(sp<sup>3</sup>)–H and C(sp<sup>2</sup>)–H Bonds at Remote Positions. *J. Am. Chem. Soc.* **2012**, *134*, 7313.
31. Rit, R. K.; Yadav, M. R.; Sahoo, A. K. Pd(II)-Catalyzed Primary-C(sp<sup>3</sup>)–H Acyloxylation at Room Temperature. *Org. Lett.* **2012**, *14*, 3724.
32. (a) Huang, C.; Chattopadhyay, B.; Gevorgyan, V. Silanol: A Traceless Directing Group for Pd-Catalyzed *o*-Alkenylation of Phenols. *J. Am. Chem. Soc.* **2011**, *133*, 12406. (b) Wang, C.; Ge, H. Silanol as a Removable Directing Group for the Pd<sup>II</sup>-Catalyzed Direct Olefination of Arenes. *Chem. Eur. J.* **2011**, *17*, 14371. (c) Huang, C.; Ghavtadze, N.; Chattopadhyay, B.; Gevorgyan, V. Synthesis of Catechols from Phenols via Pd-Catalyzed Silanol-Directed C–H Oxygenation. *J. Am. Chem. Soc.* **2011**, *133*, 17630.
33. Yadav, M. R.; Rit, R. K.; Sahoo, A. K. Sulfoximines: A Reusable Directing Group for Chemo- and Regioselective *ortho* C–H Oxidation of Arenes. *Chem. Eur. J.* **2012**, *18*, 5541.
34. (a) Nishikata, T.; Abela, A. R.; Huang, S.; Lipshutz, B. H. Cationic Palladium(II) Catalysis: C–H Activation/Suzuki–Miyaura Couplings at Room Temperature. *J. Am. Chem. Soc.* **2010**, *132*, 4978. (b) Péron, F.; Fossey, C.; Cailly, T.; Fabis, F. *N*-Tosylcarboxamide as a Transformable Directing Group for Pd-Catalyzed C–H *Ortho*-Arylation. *Org. Lett.* **2012**, *14*, 1827.
35. Leow, D.; Li, G.; Mei, T.-S.; Yu, J.-Q. Activation of Remote *meta*-C–H Bonds Assisted by an End-On Template. *Nature* **2012**, *486*, 518.
36. Bedford, R. B.; Coles, S. J.; Hursthouse, M. B.; Limmert, M. E. The Catalytic Intermolecular Orthoarylation of Phenols. *Angew. Chem., Int. Ed.* **2003**, *42*, 112.
37. Mamat, C.; Büttner, S.; Trabhardt, T.; Fischer, C.; Langer, P. Regioselective Synthesis of 5-Alkylsalicylates, 5-Alkyl-2-hydroxy-acetophenones, and 5-Alkyl-2-hydroxy-benzophenones by [3 + 3] Cyclization of 1,3-Bis(silyl enol ethers) with 2-Alkyl-1,1,3,3-tetraethoxypropanes. *J. Org. Chem.* **2007**, *72*, 6273.
38. Procedure for Beckmann rearrangement adapted from Xiao, L.-f.; Xia, C.-g.; Chen, J. *p*-Toluenesulfonic Acid Mediated Zinc Chloride: Highly Effective Catalyst for the Beckmann Rearrangement. *Tetrahedron Lett.* **2007**, *48*, 7218.
39. Procedure for oxime reduction adapted from Chung, J. U.; Kim, S. Y.; Lim, J. O.; Choi, H. K.; Kang, S. U.; Yoon, H. S.; Ryu, H.; Kang, D. W.; Lee, J.; Kang, B.; Choi, S.; Toth, A.; Pearce, L. V.; Pavlyukovets, V. A.; Lundberg, D. J.; Blumberg, P. M.  $\alpha$ -Substituted *N*-(4-*tert*-butylbenzyl)-*N'*-[4-(methylsulfonylamino)-benzyl]thiourea Analogues as Potent and Stereospecific TRPV1 Antagonists. *Bioorg. Med. Chem.* **2007**, *15*, 6043.

40. Procedure for acetophenone reduction adapted from Prein, M.; Maurer, M.; Peters, E. M.; Peters, K.; von Schnering, H. G.; Adam, W. Diastereoselective Synthesis of 4-Hydroperoxy-3,5-cyclohexadienones in the Photooxygenation of Hydroxyethyl-Substituted Phenols. *Chem. Eur. J.* **1995**, *1*, 89.